

**Evaluation of tri-*iso*-amyl phosphate as an  
alternate extractant to tri-*n*-butyl phosphate  
for nuclear materials processing**

*by*

**BENADICT RAKESH K**  
(Enrollment No: CHEM02201004003)

**Indira Gandhi Centre for Atomic Research, Kalpakkam**

*A Thesis Submitted to the  
Board of Studies in Chemical Sciences  
In partial fulfillment of requirements  
For the Degree of*

**DOCTOR OF PHILOSOPHY**

*of*

**HOMI BHABHA NATIONAL INSTITUTE**



**November, 2015**

---

# Homi Bhabha National Institute

## Recommendations of the Viva Voce Committee

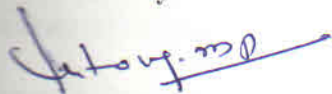
---

The members of the Viva Voce Committee, we certify that we have read the dissertation prepared by Mr. Benadict Rakesh K entitled "Evaluation of tri-*iso*-octyl phosphate as an alternate extractant to tri-*n*-butyl phosphate for nuclear materials processing" and recommend that it may be accepted as fulfilling the thesis requirement for the award of Degree of Doctor of Philosophy.

---

Chairman - Dr. M.P. Antony

Date:



13.10.2016

---

Guide - Convener - Dr. P.R. Vasudeva Rao

Date:



13 Oct 2016

---

Member 1 - Dr. U. Kamachi Mudali

Date:



13/10/16

---

Member 2 - Dr. N. Sivaraman

Date:



13/10/2016

---

Technology Advisor - Dr. A. Suresh

Date:



13/10/2016

---

Examiner - Prof. Bhalchandra M. Bhanage

Date:



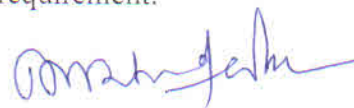
13/10/2016

---

Final approval and acceptance of this thesis is contingent upon the candidate's submission of the final copies of thesis to HBNI.

I hereby certify that I have read this thesis prepared under my direction and recommend that it may be accepted as fulfilling the thesis requirement.

Date: 13 Oct 2016



Place: IGCAR,  
Kalpakam

Dr. P.R. Vasudeva Rao  
Guide

---

## STATEMENT BY AUTHOR

---

This dissertation has been submitted in partial fulfillment of requirements for an advanced degree at Homi Bhabha National Institute (HBNI) and is deposited in the library to be made available to borrowers under rules of the HBNI.

Brief quotations from this dissertation are allowable without special permission, provided that accurate acknowledgement of source is made. Requests for permission for extended quotation from or reproduction of this manuscript in whole or in part may be granted by the Competent Authority of HBNI when in his or her judgment the proposed use of the material is in the interest of scholarship. In all other instances, however, permission must be obtained from the author.



**(Benadict Rakesh K)**

## DECLARATION

---

I, hereby declare that the investigation presented in the thesis entitled “**Evaluation of tri-*iso*-amyl phosphate as an alternate extractant to tri-*n*-butyl phosphate for nuclear materials processing**” submitted to **Homi Bhabha National Institute (HBNI)**, Mumbai, India for the award of **Doctor of Philosophy in Chemical Sciences** has been carried out by me under the guidance of **Dr. P.R. Vasudeva Rao**. The work is original and has not been submitted earlier as a whole or in part for a degree / diploma at this or any other Institution / University.



(**Benadict Rakesh K**)

# LIST OF PUBLICATIONS

---

## INTERNATIONAL JOURNAL PUBLICATIONS

1. **K. Benadict Rakesh**, A. Suresh, P.R. Vasudeva Rao; Studies on third phase formation in the extraction of  $\text{Th}(\text{NO}_3)_4$  by tri-*iso*-amyl phosphate in *n*-alkane diluents. *Separation Science and Technology*, **2013**, 48, 2761-2770.
2. **K. Benadict Rakesh**, A. Suresh, P.R. Vasudeva Rao; Third phase formation in the extraction of  $\text{Th}(\text{NO}_3)_4$  by tri-*n*-butyl phosphate and tri-*iso*-amyl phosphate in *n*-dodecane and *n*-tetradecane from nitric acid media. *Solvent Extraction and Ion Exchange*, **2014**, 32, 249-266.
3. **K. Benadict Rakesh**, A. Suresh, P.R. Vasudeva Rao; Extraction and stripping behaviour of tri-*iso*-amyl phosphate and tri-*n*-butyl phosphate in *n*-dodecane with U(VI) in nitric acid media. *Radiochimica Acta* **2014**, 102 (7), 619-628.
4. **K. Benadict Rakesh**, A. Suresh, P.R. Vasudeva Rao; Compositional characterization of organic phases after the phase splitting in the extraction of  $\text{Th}(\text{NO}_3)_4$  by 1.1 M tri-*n*-butyl phosphate/*n*-alkane. *Solvent Extraction and Ion Exchange*, **2014**, 32, 703-719.
5. **K. Benadict Rakesh**, A. Suresh, P.R. Vasudeva Rao; Separation of U(VI) and Th(IV) from Nd(III) by cross-current solvent extraction mode using tri-*iso*-amyl phosphate as the extractant. *Solvent Extraction and Ion Exchange*, **2015**, 33, 448-461.
6. **K. Benadict Rakesh**, A. Suresh, N. Sivaraman, V.K. Aswal, P.R. Vasudeva Rao; Extraction and third phase formation behaviour of tri-*iso*-amyl phosphate and tri-*n*-butyl phosphate with Zr(IV) and Hf(IV) – A

comparative study. *Journal of Radioanalytical and Nuclear Chemistry*, **2016**, 309 (3), 1037-1048.

### **NATIONAL/INTERNATIONAL CONFERENCES**

1. **K. Benadict Rakesh**, A. Suresh, P.R. Vasudeva Rao; Third phase formation in the extraction of  $\text{Th}(\text{NO}_3)_4$  by tri-*iso*-amyl phosphate (TiAP) in *n*-tetradecane. *Proceedings of biennial DAE – BRNS symposium on emerging trends in Separation Science and Technology (SESTEC-2012)*, Feb. 27 - March 1, 2012, Mithibai College, Vile Parle, Mumbai, Maharashtra, **India**, p 117.
2. **K. Benadict Rakesh**, A. Suresh, P.R. Vasudeva Rao; Extraction of U(VI) by 1.1 M tri-*iso*-amyl phosphate in *n*-dodecane from nitric acid media – Batch studies. *Proceedings of eleventh biennial DAE-BRNS symposium on Nuclear and Radiochemistry (NUCAR-2013)*, Feb. 19 - Feb. 23, 2013, Govt. Model Science College, R. D. University, Jabalpur, Madhya Pradesh, **India**, p 247.
3. **K. Benadict Rakesh**, A. Suresh, P.R. Vasudeva Rao; Comparison of third phase formation in the extraction of  $\text{Th}(\text{NO}_3)_4$  by 1.1 M solutions of tri-*iso*-amyl phosphate and tri-*n*-butyl phosphate in *n*-dodecane from nitric acid media. *Proceedings of eleventh biennial DAE-BRNS symposium on Nuclear and Radiochemistry (NUCAR-2013)*, Feb. 19 - 23, 2013, Govt. Model Science College, R. D. University, Jabalpur, Madhya Pradesh, **India**, p 249.
4. **K. Benadict Rakesh**, A. Suresh, P.R. Vasudeva Rao; Compositional characterization of organic phases after the phase splitting in the extraction of Th(IV) by 1.1 M tri-*n*-butyl phosphate/*n*-alkane. *Proceedings of biennial symposium on emerging trends in Separation Science and Technology*

- (SESTEC-2014), Feb. 25 - 28, 2014, BARC Training School, Anushakthi Nagar, Mumbai, Maharashtra, **India**, p 95.
5. **K. Benadict Rakesh**, A. Suresh, N. Sivaraman, K. Nagarajan, P.R. Vasudeva Rao; Separation of U(VI) and Th(IV) from Nd(III) using tri-*iso*-amyl phosphate (TiAP) as the extractant – Batch Studies. *Fourth international conference on Asian Nuclear Prospects (ANUP-2014)*, Nov. 9-12, 2014, Lotte City Hotel, Jeju, **Republic of Korea**.
  6. **K. Benadict Rakesh**, A. Suresh, P.R. Vasudeva Rao; Studies on third phase formation in the extraction of  $Zr(NO_3)_4$  by solutions of tri-*iso*-amyl phosphate and tri-*n*-butyl phosphate in *n*-dodecane. *Chemistry in Nuclear Technology (CHEMNUT-2015)*, July 30 - 31, 2015, Indira Gandhi Centre for Atomic Research, Kalpakkam, **India**.



**(Benadict Rakesh K)**



*Dedicated To  
My Beloved  
“Father, Mother & Brother”*



# ACKNOWLEDGEMENTS

---

First and foremost, I extend my sincere thanks to my research supervisor Dr. P.R. Vasudeva Rao, Former Director, Indira Gandhi Centre for Atomic Research (IGCAR) for his valuable guidance during my research tenure. His innovative ideas, immense knowledge and keen interest made my research work challenging and stimulating. His mentorship, support and consolidated review have lead to the successful completion of the thesis work.

I express my deep sense of gratitude to Dr. Arun Kumar Bhaduri, Director, IGCAR for the oppotunity to pursue research in this premier institute. My heartfelt thanks to Former Directors of IGCAR, Dr. Baldev Raj, Mr. S.C. Chetal and Dr. S.A.V. Satya Murty for their motivation and encouragement. I am pleased to thank Dr. S. Anthonysamy, Dean, Chemical Sciences, Homi Bhabha National Institute (HBNI) for his academic support. I wish to thank Former Deans of HBNI, Dr. K.S. Viswanathan and Dr. V. Ganesan for their valuable suggestions and unstinted encouragement during my course work. It gives me immense pleasure to acknowledge IGCAR and HBNI for their financial support.

It is a matter of great pleasure to thank Dr. M.P. Antony, Chairman, Doctoral Committee for the regular appraisal, kind advice and suggestions to improve the quality of the work. I am indebted to the helps bestowed by Former Doctoral Committee Chairmen, Dr. T.G. Srinivasan and Dr. K. Nagarajan. I take this opportunity to thank Dr. U. Kamachi Mudali and Dr. N. Sivaraman, Members, Doctoral Committee for their valuable suggestions and fruitful discussions.

I sincerely thank Dr. A. Suresh, Technology Advisor, Doctoral Committee for spending his time and resource with patience. His constructive suggestions and effective analytic approach helped for the meticulous execution of the experiments. His assistance and advice greatly helped to improvise my research work, diligently.

I am grateful to my section colleagues Dr. K.N. Sabharwal, Mr. N.L. Sreenivasan, Mr. S. Subramaniam, Dr. C.V.S.B. Rao, Mrs. Sujatha, Dr. Gopakumar, Mr. B. Sreenivasulu, Mr. C. Pitchaiah, Mrs. S. Jayalakshmi, Mrs. N. Navamani, Mrs. R. Ganga Devi and Mr. P. Amarendiren. Their co-operation in the lab helped me to plan and execute the experiments meticulously. I would express my sincere thanks to Dr. R. Kumaresan, Dr. Jayakumar, Dr. Deepika, Dr. Tarun Kumar Sahoo, Dr. Alok Rout, Dr. Jammu Ravi, Mrs. Rama and Miss. Aditi Chandrasekar for their timely help in crucial moments. I profoundly thank all the members of H-13 and H-14 labs for their assistance. I express my sincere thanks to Dr. K. Sankaran and Mrs. S. Annapoorani for the analysis of samples by ICP-OES and Dr. B. Prabhakara Reddy for water analysis. I am thankful to Mr. R. Raja Madhavan for providing hafnium oxide. I take this opportunity to thank the entire family of Chemistry Group for their help towards my research.

Special thanks to Dr. V.K. Aswal, Scientific Officer, Solid State Physics Division, Bhabha Atomic Research Centre, Mumbai for spending his time, knowledge and effort during scattering experiments. I immensely thank Dr. John Philip and Mr. Gopinath Shit for the fruitful discussions. I would like to acknowledge the support provided by Dr. Shyamrao Disale, Dr. Rupesh Gaikwad, Miss. Amrutha Manoj, Mr. Suresh Annam and Mr. Dhruvjyoti Das.

I thank Dr. M. Sai Baba for the excellent facilities in JRF enclave. Words are insufficient to thank my seniors especially, Dr. Srinivasan, Dr. Sri Maha Vishnu, Dr. Ilaiyaraja, Dr. Priyadarshini, Dr. Pradeep Kumar Samantaroy and Dr. D. Sharath for their motivation during my research. I extend my thanks to my fellow researchers Mr. T.R. Devidas, Mr. M. Kalyan Phani, Mr. G. Prasanna, Mr. Avinash Patsa, Dr. V. Mahendran, Miss A.V. Meera, Mrs. Rasmi, Mrs. Soja K. Vijay, Dr. Anbumozhi Angayarkanni and Dr. Leona J. Felicia for being with me in crucial and amusing moments. I am extremely thankful to Mr. D. Sanjay Kumar, Mr. R. Gopi, Mr. D. Karthickeyan, Mr. Radhikesh, Mr. Irshad, Mr. Srinivasan, Mr. Vairavel, Mr. Lakshmanan, Mr. Thangam, Mr. K.G. Raghavendra, Mr. Subrata Ghosh, Mr. Hari Prasad, Mr. Zaibudeen, Mr. Surojit Ranoo and all my juniors for the cheerful moments in enclave.

I extend my warm thanks to Mr. K. Senthil Kumar, Mrs. S. Sangeetha, Mr. Jibin, Mr. R. Suresh and all my school and college friends for their encouragement while doing research. I am delighted to thank my Father Mr. E. Kuzhanthai Swami, Mother Mrs. M. Mary Selvi, Brother Mr. K. Roosevelt, Cousin Mrs. Ancelin and relatives for their love, affection and moral support. Finally, I thank each and everyone who helped me in completing the research work successfully.



**(Benadict Rakesh K)**

# CONTENTS

---

Sl. No.	Title	Page No.
I.	Synopsis	i
II.	List of Figures	xiii
III.	List of Tables	xviii
IV.	Abbreviations	xxi

## CHAPTER 1

### INTRODUCTION

1.1	Significance of energy	1
1.2	Various sources of energy - Advantages and limitations	1
1.3	Potential of nuclear energy	2
1.4	India's three stage nuclear program	3
1.5	Nuclear fuel cycle	4
1.6	Properties of elements of interest to nuclear industry	6
1.6.1	Lanthanides	6
1.6.2	Actinides	7
1.6.2.1	Thorium	8
1.6.2.2	Uranium	9
1.6.2.3	Plutonium	10
1.6.3	Zirconium	11
1.6.4	Hafnium	13
1.6.5	Estimation of metal ions and free acidity	14
1.7	Solvent extraction	16
1.7.1	Fundamental aspects of solvent extraction	16
1.7.2	Advantages of solvent extraction	17

1.7.3	Characteristics of an ideal solvent	18
1.7.4	Requirement of diluents in solvent extraction	19
1.7.5	Classification of extractants	19
1.7.6	Solvent extraction in various nuclear processes	20
1.8	Tri- <i>n</i> -butyl phosphate - A unique extractant of nuclear industry	21
1.9	Applications of tri- <i>n</i> -butyl phosphate	22
1.9.1	Uranium ore processing	22
1.9.2	PUREX process	22
1.9.3	THOREX process	25
1.9.4	Monazite ore processing	26
1.9.5	Zirconium-Hafnium separation	27
1.9.6	Other applications	28
1.10	Limitations of tri- <i>n</i> -butyl phosphate	28
1.10.1	Red oil formation	28
1.10.2	Degradation	29
1.10.3	Third phase formation	30
1.11	Insights into third phase formation phenomenon	32
1.11.1	Interpretation of third phase formation - Particle growth model	34
1.11.2	Interpretation of third phase formation - Interparticle interaction Model	35
1.12	Alternate extractants for tri- <i>n</i> -butyl phosphate	37
1.13	Tri- <i>iso</i> -amyl Phosphate – A potential alternate extractant for tri- <i>n</i> -butyl phosphate	39
1.14	Literature survey on tri- <i>iso</i> -amyl phosphate	40
1.15	Scope of the present work	41

## CHAPTER 2

### EXPERIMENTAL

2.1	Chemicals	45
-----	-----------	----

2.2	Instruments	51
2.3	Preparation of solutions	54
2.3.1	Standard solutions	54
2.3.2	Indicator solutions	55
2.3.3	Complexing solutions	56
2.3.4	Buffer solutions	57
2.3.5	Stock solutions	58
2.3.6	Feed solutions	61
2.4	Experimental procedure	62
2.4.1	Extraction of U(VI) as a function of $[U(VI)]_{aq,eq}$	62
2.4.2	Extraction and stripping of U(VI) in cross-current mode	63
2.4.3	Stripping of U(VI) as a function of time	64
2.4.4	Extraction of Th(IV) as a function of $[Th(IV)]_{aq,eq}$ in biphasic and triphasic regions under near-zero free acid condition	64
2.4.5	Extraction of Th(IV) as a function of $[Th(IV)]_{aq,eq}$ in biphasic and triphasic regions in nitric acid media	65
2.4.6	Determination of LOC and CAC for the extraction of Th(IV) as a function of extractant concentration under near-zero free acid condition	66
2.4.7	Determination of LOC and CAC for the extraction of Th(IV) from Th(IV)-Nd(III) feed solution	67
2.4.8	Determination of LOC and CAC for the extraction of Zr(IV) as a function of $[HNO_3]_{aq,eq}$	67
2.4.9	Third phase formation experiments for the extraction of Zr(IV) in nitric acid media	67
2.4.10	Extraction of metal ion/s from U(VI)-Th(IV)-Nd(III) feed solution in nitric acid media	68
2.4.11	Measurement of distribution ratios of Zr(IV) and Hf(IV)	69
2.4.12	Estimation of extractant by nitric acid equilibration method	69
2.4.13	Preparation of samples for SANS experiments	69
2.5	Analytical methods	70

2.5.1	Determination of density and volume	70
2.5.2	Determination of concentration of Hf(IV)	70
	2.5.2.1 Complexometry	70
	2.5.2.2 Spectrophotometry	70
2.5.3	Determination of concentration of Nd(III)	71
2.5.4	Determination of concentration of nitric acid	71
2.5.5	Determination of concentration of Th(IV)	72
2.5.6	Determination of concentration of U(VI)	72
	2.5.6.1 Complexometry	72
	2.5.6.2 Davies-Gray method	72
	2.5.6.3 Spectrophotometry	72
2.5.7	Determination of zirconium	72
	2.5.7.1 Complexometry	72
	2.5.7.2 Spectrophotometry	73
2.5.8	Determination of concentration of water	73
2.5.9	Determination of viscosity	74
2.5.10	SANS - Data analysis	74

## **CHAPTER 3**

### **EXTRACTION AND STRIPPING BEHAVIOUR OF TiAP AND TBP WITH U(VI) IN NITRIC ACID MEDIA**

3.1	Introduction	76
3.2	Validation of the analytical method for free acidity determination	78
	3.2.1 Comparison of literature data on U(VI) and HNO <sub>3</sub> extraction with the present study	78
	3.2.2 Comparison of estimation of free acidity with oxalate and oxalate-fluoride mixture as complexing agents	79

3.2.3	Validation of HNO <sub>3</sub> estimation using oxalate-fluoride as dual complexing agent	80
3.3	Extraction of U(VI) by 1.1 M TiAP/ <i>n</i> -DD as a function of metal loading and aqueous phase acidity	81
3.4	Extraction, scrubbing and stripping of U(VI) in cross-current mode - 1.1 M TalP/ <i>n</i> -DD - U(VI)/HNO <sub>3</sub> systems	89
3.5	Stripping behaviour of U(VI) as a function of time	91
3.6	Conclusions	93

## **CHAPTER 4**

### **THIRD PHASE FORMATION BEHAVIOUR OF TiAP AND TBP IN THE EXTRACTION OF Th(NO<sub>3</sub>)<sub>4</sub>**

4.1	Introduction	94
4.2	Distribution of Th(IV) and HNO <sub>3</sub> in organic phases	95
4.2.1	Effects of parameters on the distribution ratio of Th(IV) in biphasic region	95
4.2.2	Effects of parameters on third phase formation in the extraction of Th(IV)	97
4.2.3	Effects of parameters on the extraction of HNO <sub>3</sub>	103
4.2.4	Effects of parameters on the ratio of concentration of Th(IV) in TP to DP	107
4.2.5	Effects of parameters on the ratio of concentration of HNO <sub>3</sub> in TP to DP	110
4.2.6	Effects of parameters on the concentration of solutes at CAC and SAC	111
4.3	Variation of density of organic phases	112
4.4	Variation of the ratio of the volume of DP to TP in triphasic region	118

4.5	Scope of third phase formation studies with TalP/ <i>n</i> -alkane - Pu(IV)/HNO <sub>3</sub> systems in triphasic regions	123
4.6	Conclusions	123

## **C** H A P T E R **5**

### **NOVEL METHODS FOR THE ESTIMATION OF EXTRACTANT CONCENTRATION AFTER ORGANIC PHASE SPLITTING**

5.1	Introduction	125
5.2	Estimation of TBP in the TP and the DP	127
5.2.1	By using density and refractive index	127
5.2.2	By using third phase formation limit (LOC)	132
5.2.3	By using nitric acid loading in the extraction from 8 M HNO <sub>3</sub>	133
5.2.4	Comparison of the methods for TBP estimation	135
5.2.5	Volume correction in the determination of TBP concentrations in organic phases	135
5.3	Estimation of extractant in the TP and the DP by model	139
5.3.1	Validation of the model to calculate extractant concentration in the TP and the DP	140
5.3.2	Estimation of extractant in the TP and the DP as a function of various parameters by the model	142
5.4	Applications of newly developed TBP estimation methods	143
5.5	Conclusions	144

# CHAPTER 6

## SEPARATION OF U(VI) AND Th(IV) FROM Nd(III) BY CROSS-CURRENT SOLVENT EXTRACTION MODE USING TiAP

6.1	Introduction	146
6.2	Validation of analytical methods	147
6.3	Third phase formation behaviour of 0.183 M solutions of TiAP and TBP in <i>n</i> -DD	148
6.4	Separation of U(VI) from Th(IV) and Nd(III) with 0.183 M TalP/ <i>n</i> -DD	151
6.5	Third phase formation limits for the extraction of Th(IV) by 1.47 M TalP/ <i>n</i> -DD	154
6.6	Separation of Th(IV) from Nd(III) under high solvent loading conditions with 1.47 M TiAP/ <i>n</i> -DD	156
6.7	Separation of Th(IV) from feed solution in 8 M HNO <sub>3</sub>	158
6.8	Conclusions	160

# CHAPTER 7

## EXTRACTION AND THIRD PHASE FORMATION BEHAVIOUR OF TiAP AND TBP WITH Zr(IV) AND Hf(IV)

7.1	Introduction	162
7.2	Distribution ratios for the extraction of Zr(IV) and Hf(IV) as a function of nitric acid concentration	163
7.3	Third Phase formation limits for Zr(IV) as a function of extractant and nitric acid concentrations	164

7.4	Composition of organic phases before and after third phase formation with Zr(IV)	166
7.5	SANS studies on 1.1 M <i>TiAP/n-DD</i> - Zr(NO <sub>3</sub> ) <sub>4</sub> /HNO <sub>3</sub> and 1.1 M <i>TBP/n-DD</i> - Zr(NO <sub>3</sub> ) <sub>4</sub> /HNO <sub>3</sub> extraction systems	172
7.6	Third phase formation of <i>TiAP</i> and <i>TBP</i> systems with Zr(IV)-Hf(IV) solution	176
7.7	Conclusions	177

## CHAPTER 8

### CONCLUSIONS

8.1	Extraction and stripping behaviour of <i>TiAP</i> and <i>TBP</i> with U(VI) in nitric acid media	179
8.2	Third phase formation behaviour of <i>TiAP</i> and <i>TBP</i> in the extraction of Th(NO <sub>3</sub> ) <sub>4</sub>	179
8.3	Methods for the estimation of extractant concentration after organic phase splitting	180
8.4	Separation of U(VI) and Th(IV) from Nd(III) by cross-current solvent extraction mode using <i>TiAP</i>	181
8.5	Extraction and third phase formation behaviour of <i>TiAP</i> and <i>TBP</i> with Zr(IV) and Hf(IV)	181
8.6	Future perspectives	182

<b>REFERENCES</b>	<b>187</b>
-------------------	------------

## **SYNOPSIS**

Energy is the vital source for the development, welfare and prosperity of mankind. Nature has provided enormous renewable and non-renewable resources to meet our energy requirements. India relies on its coal resources and uncertain oil imports to fulfill its energy demands and the technology to exploit energy from non-renewable resources is in developmental stage. Even though the process of exploiting energy from fossil fuels is worthwhile, the release of toxic and green house gases pose health hazards and global climate changes. These circumstances have created a situation to focus the attention on nuclear as one of the viable options to harness energy [1,2]. The energy produced by nuclear fission is considered to be clean [3]. Opting for nuclear as a key source of energy helps the developing countries like India to satisfy their energy demands [4].

Mining and processing of ores of elements like uranium, thorium and zirconium as well as reprocessing of spent nuclear fuels remain as integral parts of nuclear energy production. The reprocessing of spent nuclear fuel allows effective utilization of unused heavy metals and reduces the radioactivity discharged to the environment [5]. Currently, the reprocessing of spent nuclear fuel to recover uranium and plutonium is being performed by solvent extraction technique using tri-*n*-butyl phosphate (TBP) as the extractant. TBP is easily available, inexpensive, highly selective for the separation of uranium and plutonium from most of the fission products and trivalent actinides and regenerable which made it as the preferred extractant for thermal reactor fuel reprocessing [6,7]. Other applications of TBP include U-233 separation from irradiated thorium by THOREX/Interim-23 process [8,9]. It is also utilized for monazite processing, Zr/Hf and Nb/Ta separations [10-13].

However, TBP is susceptible to radiation and chemical degradation [14,15], more soluble in aqueous media than its higher homologues, poorly selective for uranium over thorium [16] and forms third phase [17,18] with tetravalent metal ions like Pu(IV), Th(IV), Zr(IV), etc. The degradation products of TBP have high affinity to complex with actinides and therefore the stripping of the extracted actinides becomes difficult. The high aqueous solubility of TBP leads to red oil formation during the concentration of aqueous solutions which can result in explosive thermal run away reactions [19].

Among the above drawbacks, third phase formation in particular, limits the applications of TBP in fast reactor spent fuel reprocessing, monazite processing, Zr/Hf separation etc. Third phase formation is a well known phenomenon in solvent extraction where the loading of certain metal ions and acid beyond a particular concentration known as limiting organic concentration (LOC) splits the homogenous loaded extractant-diluent solution into a third phase and a diluent-rich phase. Mixing of organic and aqueous phases as well as mass transfer between these phases becomes difficult due to the formation of highly viscous third phase. Third phase formation can also lead to flooding in solvent extraction equipment like mixer-settler and centrifugal extractor.

Earlier studies on third phase formation in the extraction of Th(IV) and Pu(IV) by using various symmetrical trialkyl phosphates showed that higher homologues of TBP are potential extractants for the processes involving the extraction of these metal ions [20,21]. The aqueous solubility of tri-*iso*-amyl phosphate (TiAP), an higher homologue of TBP is less as compared to TBP. Based on the earlier studies TiAP has been identified as an alternate extractant for the fast reactor spent fuel reprocessing, monazite processing and

Zr/Hf separation. Earlier, TiAP has been used for the processing of short cooled fast reactor fuels in Russia [22].

However, prior to the deployment of a new extractant in processing plants, its extraction and third phase formation behaviour has to be compared with the existing extractant under identical conditions. The objective of the present study is to compare the extraction and third phase formation behaviour of TiAP and TBP with metal ions such as U(VI), Th(IV), Nd(III), Zr(IV) and Hf(IV) to evaluate the possibility of using TiAP as an alternate extractant to TBP. As a part of the study new methods are developed to estimate the extractant concentration in the organic phase after organic phase splitting. A model developed to predict the extractant concentration in the third phase from the concentration of Th(IV) present in the third phase was validated. The thesis is organized into eight chapters and the details of each chapter are described as follows.

### **Chapter 1: Introduction**

Chapter 1 describes the resources, potential and importance of nuclear energy for energy production. The significance of three stage nuclear program adopted by India to effectively utilize the limited uranium reserves and abundant thorium reserves to produce electricity is discussed. The chemistry of the elements used in the present study is described in this chapter. The importance of solvent extraction processes and the mechanism of extraction of metal ions are elaborated. The advantages and limitations of using TBP as the extractant for the separation of U(VI) and Pu(IV) from fission products in the spent nuclear fuels, monazite ore processing and Zr(IV)/Hf(IV) separation by solvent extraction are discussed in detail. A brief description about the scattering and spectroscopic techniques used for third phase formation studies is also provided in this chapter. The

significance of using *TiAP* as an alternate extractant to TBP for spent nuclear fuel reprocessing, monazite ore processing and Zr(IV)/Hf(IV) separation is highlighted in this chapter. A survey of research work reported in the literature with respect to solvent extraction of metal ions using *TiAP*, overview and scope of the present work are explained in this chapter.

## **Chapter 2: Experimental**

Chapter 2 describes the details of the chemicals, instruments and experimental procedures used for the present study. The preparation of standard solutions, indicator solutions, buffer solutions and extractant solutions is discussed in this chapter. The procedure adopted for the dissolution of zirconium sponge and the preparation of Zr(IV) solution in nitric acid media are mentioned in chapter 2. The methods used for the quantitative determination of metal ions such as U(VI), Th(IV), Nd(III), Zr(IV) and Hf(IV), and free acidity in the presence of aforementioned metal ions are provided. The details about the measurements of physical parameters such as density, refractive index and viscosity, and the volume of organic phases are also described. The experimental procedures for the extraction of metal ions as a function of equilibrium aqueous phase metal ion as well as nitric acid concentrations and stripping of U(VI) as a function of time are explained in chapter 2. The details about the batch wise extraction, scrubbing and stripping of metal ions with trialkyl phosphates (*TalP*) in cross-current mode are discussed. This chapter describes the procedure for the formation and dissolution of third phase. The procedure for the determination of LOC and CAC for the metal ions in near-zero free acid and nitric acid media are also provided in this chapter.

### **Chapter 3: Extraction and stripping behaviour of TiAP and TBP with U(VI) in nitric acid media**

Chapter 3 explains the batch extraction of U(VI) by 1.1 M TiAP in *n*-dodecane (*n*-DD) from U(VI) solutions in nitric acid media as a function of metal loading and equilibrium aqueous phase acidity at 303 K. A method adopted for free acidity determination by using a mixture of potassium oxalate and sodium fluoride for complexing U(VI) was cross-checked by comparing the data generated in the present study with literature data available for TBP under identical conditions. This chapter compares the extraction, scrubbing and stripping behaviour of 1.1 M TiAP/*n*-DD - U(VI)/HNO<sub>3</sub> and 1.1 M TBP/*n*-DD - U(VI)/HNO<sub>3</sub> systems by carrying out extraction, scrubbing and a series of stripping experiments in cross-current mode. The stripping behaviour of both the solvents loaded with U(VI) and HNO<sub>3</sub> was investigated as a function of time to understand the effects of nitric acid induced degradation on stripping and the results are discussed in this chapter.

### **Chapter 4: Third phase formation behaviour of TiAP and TBP in the extraction of Th(NO<sub>3</sub>)<sub>4</sub>**

Chapter 4 deals with the studies on third phase formation in the extraction of Th(NO<sub>3</sub>)<sub>4</sub> from its solution with near-zero free acidity and in nitric acid media by 1.1 M solutions of TiAP and TBP in various linear hydrocarbon diluents as a function of equilibrium aqueous phase Th(IV) concentration ( $[Th(IV)]_{aq,eq}$ ) at 303 K. Distribution of Th(NO<sub>3</sub>)<sub>4</sub> and HNO<sub>3</sub> between organic and aqueous phases in biphasic and triphasic regions for its extraction by the above mentioned solvents from Th(NO<sub>3</sub>)<sub>4</sub> solutions with near-zero free acidity and in nitric acid media was investigated with respect to  $[Th(IV)]_{aq,eq}$  at 303 K.

Variation of densities of organic phases in biphasic and triphasic regions was also studied as a function of  $[\text{Th(IV)}]_{\text{aq,eq}}$  at 303K and the results are discussed in this chapter. Differences in density between the third phase and the diluent-rich phase as well as the diluent-rich phase and the pure diluent, ratio of volume of the diluent-rich phase to that of the third phase were also determined over a wide range of  $[\text{Th(IV)}]_{\text{aq,eq}}$  in the triphasic region. The results obtained for TiAP based solvents are compared with the literature data available for TBP systems.

### **Chapter 5: Novel methods for the estimation of extractant concentration after organic phase splitting**

This chapter presents the novel methods developed to estimate the extractant concentration after organic phase splitting based on the measurement of physical properties and LOC for Th(IV) extraction from its solution with near-zero free acidity of the organic solutions. A model was developed for the estimation of extractant concentration in third phase and diluent-rich phase after phase splitting and also validated with experimentally determined extractant concentration. The variation of extractant concentration as a function of  $[\text{Th(IV)}]_{\text{aq,eq}}$  and diluent chain length are presented in this chapter. The trend in the extractant concentrations in the third phase and the diluent-rich phase in the extraction of  $\text{Th(NO}_3)_4$  by 1.1 M TaIP/*n*-alkane from saturated  $\text{Th(NO}_3)_4$  solutions with 1 M and 5 M  $\text{HNO}_3$  was measured by using nitric acid equilibration method and the results are discussed in chapter 5.

## **Chapter 6: Separation of U(VI) and Th(IV) from Nd(III) by cross-current solvent extraction mode using TiAP**

The aim of the studies described in this chapter is to evaluate the feasibility of employing *TiAP* as an alternate extractant to TBP for the processing of monazite ore which contains rare earths along with thorium and uranium. In the present study, Nd(III) was chosen as the representative element for rare earth elements and the separation of U(VI) and Th(IV) from Nd(III) in nitric acid media was studied with solutions of *TiAP* in *n*-DD by batch extraction in cross-current mode. The interference of U(VI), Th(IV) and Nd(III) in the presence of each other during their analysis by complexometric titrations are also validated in this chapter. The third phase formation limits of both *TiAP* and TBP based solvents were compared for the extraction of Th(IV) from highly concentrated solution of U(VI), Th(IV) and Nd(III) in nitric acid media. Solvent extraction studies conducted with solutions of U(VI), Th(IV) and Nd(III) in nitric acid media by *TiAP* and TBP revealed the identical extraction, scrubbing and stripping behaviour of both the extractants with respect to U(VI), Th(IV) and Nd(III).

## **Chapter 7: Extraction and third phase formation behaviour of TiAP and TBP with Zr(IV) and Hf(IV)**

Chapter 7 provides the data on the third phase formation limits of *TiAP* and TBP for the extraction of Zr(IV) from nitric acid media as a function of equilibrium aqueous phase nitric acid and extractant concentrations at 303 K. Compositions of organic phases in biphasic and triphasic regions in the extraction of Zr(IV) from 4 M HNO<sub>3</sub> medium by 1.1 M solutions of *TiAP* and TBP in *n*-DD as well as *n*-tetradecane were estimated. The extraction behaviour of *TiAP* and TBP with respect to Zr(IV) and Hf(IV) under identical

conditions is highlighted in this chapter. The results on the separation of Zr(IV) from Hf(IV) from their highly concentrated solutions in 4 M HNO<sub>3</sub> by TiAP and TBP based solvents (1.1 M in *n*-DD) at 303 K are also discussed to explore the applications of TiAP for Zr(IV)/Hf(IV) separation.

## Chapter 8: Conclusions

The conclusions drawn from the studies and the scope for the future work are summarized in Chapter 8. Some of the highlights of the present study are listed below.

- ❖ A method adopted for free acidity determination in the presence of a large amount of U(VI) and less amount of HNO<sub>3</sub> was validated.
- ❖ TiAP and TBP based solvents possess comparable extraction, scrubbing and stripping behaviour with respect to various metal ions such as U(VI), Th(IV) and Nd(III).
- ❖ The study confirmed that the third phase formation tendency of TBP based solvents is much higher compared to TiAP based solvents.
- ❖ Organic phase splitting tendency for Th(IV) increases with increase in aqueous phase acidity, diluent chain length and [Th(IV)]<sub>aq,eq</sub>.
- ❖ During the organic phase splitting, the extractant, metal ions and HNO<sub>3</sub> have high tendency to accumulate in the third phase leaving behind the diluent-rich phase.
- ❖ Novel methods for the estimation of extractant concentration after organic phase splitting were developed and authenticated.
- ❖ The model developed for the estimation of extractant concentration in the third phase was cross-checked by experiments and showed good agreement at higher [Th(IV)]<sub>aq,eq</sub>.

- ❖ The separation factor for Th(IV) with respect to Nd(III) can be improved with *TiAP* as the extractant and by carrying out the extraction with feed solution in 8 M  $\text{HNO}_3$ .
- ❖ Separation of Th(IV) from rare earth elements in highly concentrated monazite feed solution is feasible with *TiAP* based solvents.
- ❖ The data generated in the present study can be exploited for the development of flow sheets using *TiAP* based solvents to separate U(VI) and Th(IV) from rare earths for the processing of monazite leach solutions.
- ❖ The results indicated that *TiAP* can be used as an alternate extractant to TBP for the separation of U(VI) and Th(IV) from monazite ores and also for the separation of Zr(IV) from Hf(IV).

#### **References:**

1. R.B. Grover; S. Chandra; Scenario for growth of electricity in India. *Energy Policy* 34, (2006) 2834–2847.
2. C. Karakosta; C. Pappas; V. Marinakis; J. Psarras; Renewable energy and nuclear power towards sustainable development: Characteristics and prospects. *Renewable and Sustainable Energy Rev.* 22, (2013) 187–197.
3. B. Zwaan; The role of nuclear power in mitigating emissions from electricity generation. *Energy Strategy Rev.* 1, (2013) 296-301.
4. J. Parikh; K. Parikh; India's energy needs and low carbon options. *Energy* 36, (2011) 3650-3658.
5. P.K. Dey; N.K. Bansal; Spent fuel reprocessing: A vital link in Indian nuclear power program. *Nucl. Eng. Des.* 236, (2006) 723–729.

6. D.D. Sood; S.K. Patil; Chemistry of nuclear fuel reprocessing: Current status. J. Radioanal. Nucl. Chem. Articles 203 (2), (1996) 547-573.
7. H.A.C. McKay; J.H. Miles; J.L. Swanson; The purex process; In *Science and technology of tributyl phosphate*; W.W. Schulz; L.L. Burger; J.D. Navratil; K.P. Bender; Eds., Vol. 3, pp. 1-9, 1990, CRC Press: Boca Raton, FL.
8. G.R. Balasubramaniam; R.T. Chitnis; A. Ramanujam; M. Venkatesan; Laboratory studies on the recovery of uranium-233 from irradiated thorium by solvent extraction using 5% TBP Shell Sol-T as Solvent. BARC, Mumbai, India, Rpt. BARC-940, 1977.
9. W.D. Bond; The thorex process; In *Science and technology of tributyl phosphate*; W.W. Schulz; L.L. Burger; J.D. Navratil; K.P. Bender; Eds., Vol. 3, pp. 225-247, 1990, CRC Press: Boca Raton, FL.
10. J.H. Cavendish; Recovery and purification of uranium and thorium from ore concentrates; In *Science and technology of tributyl phosphate (Selected technical and industrial use)*; W.W. Schulz; J.D. Navratil; T. Bess; Eds., Vol. 2, Part A, pp. 1-42, 1987, CRC Press: Boca Raton, FL.
11. D.D. Sood; Nuclear Materials. Indian Association of Nuclear Chemists and Allied Scientists, Mumbai, India, pp. 91, 1996.
12. G.M. Ritcey; Use of TBP of separate zirconium from hafnium; In *Science and technology of tributyl phosphate (Selected technical and industrial use)*; W.W. Schulz; J.D. Navratil; T. Bess; Eds., Vol. 2, Part A, pp. 43-64, 1987, CRC Press: Boca Raton, FL.
13. C.K. Gupta; Hydrometallurgy; In *Chemical Metallurgy-Principles and Practice*; pp. 459-580. Wiley-VCH: Weinheim, 2003.

14. S.C. Tripathi; A. Ramanujam; K.K. Gupta; P. Bindu; Studies on the identification of harmful radiolytic products of 30% TBP-N-Dodecane-HNO<sub>3</sub> by gas-liquid chromatography. II. Formation and characterization of high molecular weight organophosphates. *Sep. Sci. Technol.* 36 (13), (2001) 2863-2883.
15. T. Tsujino; T. Ishihara; Changes to plutonium behavior of TBP and alkyl amines through irradiation. *J. Nucl. Sci. Technol.* 3 (8), (1966) 320-325.
16. T.V. Healy; H.A.C. Mckay; The extraction of nitrates by tri-n-butyl phosphates (TBP). Part 2 - The nature of TBP Phase. *Trans. Faraday Soc.* 52, (1956) 633-642.
17. Z. Kolarik; The formation of a third phase in the extraction of Pu(IV), U(IV) and Th(IV) nitrates with Tributyl phosphate in alkane diluents. *Proc. Int. Solv. Extr. Conf. ISEC'77*; B.H. Lucas; G.M. Ritcey; H.W. Smith; Eds., *CIM Spec. Vol. 2* (21), pp. 178-182, 1979, Can. Inst. Mining Metallurgy.
18. T.G. Srinivasan; M.K. Ahmed; A.M. Shakila; R. Dhamodaran; P.R. Vasudeva Rao; C.K. Mathews; Third phase formation in the extraction of plutonium by tri-n-butyl phosphate. *Radiochim. Acta* 40, (1986) 151-154.
19. T.G. Srinivasan, P.R. Vasudeva Rao; Red oil excursions: A review. *Sep. Sci. Technol.* 49, (2014) 2315–2329.
20. A. Suresh; T.G. Srinivasan; P.R. Vasudeva Rao; Extraction of U(VI), Pu(IV) and Th(IV) by some trialkyl phosphates. *Solvent Extr. Ion Exch.* 12 (4), (1994) 727-744.
21. A. Suresh; T.G. Srinivasan; P.R. Vasudeva Rao; Parameters influencing third-phase formation in the extraction of Th(NO<sub>3</sub>)<sub>4</sub> by some trialkyl phosphates. *Solvent Extr. Ion Exch.* 27, (2009) 132-158.

22. A.S. Nikiforov; B.S. Zakharin; Eh.V. Renard; A.M. Rozen; Eh.Ya. Smetanin;  
Reprocessing of high burn-up (100 GWd/t) short cooled fuel. In *Proc. Int. Conf.*  
*Actinides-89*, Tashkent, USSR, September 24-29, 1989, pp 20-21.

## LIST OF FIGURES

FIGURE No.	TITLE	PAGE No.
1.1	Schematic representation of closed fuel cycle	5
1.2	Schematic representation of open fuel cycle	5
1.3	Chemical structure of some of the extractants commonly used for the solvent extraction of nuclear materials	21
1.4	Flow sheet for the PUREX process	24
1.5	Schematic representation of third phase formation phenomenon	31
1.6	Third phase formation in 1.1 M TBP/ <i>n</i> -DD - Th(NO <sub>3</sub> ) <sub>4</sub> /1 M HNO <sub>3</sub> system	31
1.7	Schematic representation of interaction between reverse micelles using interparticle interaction model [122]	35
1.8	Schematic representation of reverse micelles formed during third phase formation interpreted by (A) Interparticle interaction model (B) Particle growth model [122]	37
1.9	Chemical structure of TiAP and TBP molecules	39
2.1	Schematic representation of SANS diffractometer	52
2.2	UV-Visible-NIR spectrophotometer (SHIMADZU UV-3600 model)	53
2.3	Water baths used for the experiments - (A) Julabo (F25-EC) (B) Polyscience (9100)	54
2.4	Double walled vessel used for solvent extraction experiments	62
2.5	Schematic representation of extraction, scrubbing and stripping of U(VI) with 1.1 M TaIP/ <i>n</i> -DD	63
3.1	Variation of $D_{U(VI)}$ as a function of $[U(VI)]_{aq,eq}$ for its extraction by 1.1 M TiAP/ <i>n</i> -DD from U(VI) solutions in nitric acid media at 303 K	83
3.2	Variation of $D_{HNO_3}$ with $[U(VI)]_{aq,eq}$ for the extraction of U(VI) by 1.1 M TiAP/ <i>n</i> -DD from U(VI) solutions in nitric acid media at 303 K	83
3.3	Variation of U(VI) and HNO <sub>3</sub> concentrations in the organic phase with $[U(VI)]_{aq,eq}$ for their extraction by 1.1 M TiAP/ <i>n</i> -DD from U(VI) solutions in nitric acid media at 303 K. (A) 0.5 M HNO <sub>3</sub> system (B) 2 M HNO <sub>3</sub> system	87
3.4	Variation of U(VI) and HNO <sub>3</sub> concentrations in the organic phase with $[U(VI)]_{aq,eq}$ for their extraction by 1.1 M TiAP/ <i>n</i> -DD from U(VI) solutions in nitric acid media at 303 K. (A) 4 M HNO <sub>3</sub> system (B) 6 M HNO <sub>3</sub> system	87
3.5	Variation of the HNO <sub>3</sub> concentration in the organic phase as a function of $[U(VI)]_{org,eq}$ for the extraction by 1.1 M TiAP/ <i>n</i> -DD from U(VI) solutions in nitric acid media at 303 K	88

3.6	Extraction and stripping of U(VI) by 1.1 M TalP/ <i>n</i> -DD from U(VI) solutions in 4 M HNO <sub>3</sub> at 303 K. (A) TiAP system (B) TBP system	91
3.7	Variation of the U(VI) concentration retained in the organic phase (1.1 M TalP/ <i>n</i> -DD) after the stripping of U(VI) from loaded organic phase as a function of time at 303 K	92
4.1	Distribution ratio of Th(IV) for its extraction by 1.1 M TiAP/ <i>n</i> -alkane from Th(NO <sub>3</sub> ) <sub>4</sub> solution with near-zero free acidity at 303 K	95
4.2	Variation of the $D_{\text{Th(IV)}}$ for Th(IV) extraction by 1.1 M TiAP/ <i>n</i> -DD from Th(NO <sub>3</sub> ) <sub>4</sub> solutions with near-zero free acidity, 1 M and 5 M nitric acid as a function of [Th(IV)] <sub>aq,eq</sub> at 303 K	96
4.3	Variation of the $D_{\text{Th(IV)}}$ for Th(IV) extraction by 1.1 M TalP/ <i>n</i> -DD from Th(NO <sub>3</sub> ) <sub>4</sub> solutions with near-zero free acidity, 1 M and 5 M nitric acid as a function of [Th(IV)] <sub>aq,eq</sub> at 303 K	98
4.4	Extraction isotherms for the extraction of Th(IV) by 1.1 M TalP/ <i>n</i> -alkane from Th(NO <sub>3</sub> ) <sub>4</sub> solution with near-zero free acidity as a function of [Th(IV)] <sub>aq,eq</sub> at 303 K	99
4.5	Extraction isotherms for the extraction of Th(IV) by 1.1 M TBP/ <i>n</i> -alkane from Th(NO <sub>3</sub> ) <sub>4</sub> solutions with 1 M and 5 M nitric acid as a function of [Th(IV)] <sub>aq,eq</sub> at 303 K; (A) <i>n</i> -dodecane system (B) <i>n</i> -tetradecane system	100
4.6	Extraction isotherms for the extraction of Th(IV) by 1.1 M TiAP/ <i>n</i> -alkane from Th(NO <sub>3</sub> ) <sub>4</sub> solutions with 1 M and 5 M nitric acid as a function of [Th(IV)] <sub>aq,eq</sub> at 303 K	102
4.7	Extraction isotherms for the extraction of HNO <sub>3</sub> by 1.1 M TBP/ <i>n</i> -alkane from Th(NO <sub>3</sub> ) <sub>4</sub> solutions with 1 M and 5 M nitric acid as a function of [Th(IV)] <sub>aq,eq</sub> at 303 K; (A) <i>n</i> -dodecane system (B) <i>n</i> -tetradecane system	104
4.8	Extraction isotherms for the extraction of HNO <sub>3</sub> by 1.1 M TiAP/ <i>n</i> -alkane from Th(NO <sub>3</sub> ) <sub>4</sub> solutions with 1 M and 5 M nitric acid as a function of [Th(IV)] <sub>aq,eq</sub> at 303 K; (A) <i>n</i> -dodecane system (B) <i>n</i> -tetradecane system	105
4.9	Extraction isotherms for the extraction of Th(IV) and HNO <sub>3</sub> by 1.1 M TBP/ <i>n</i> -decane from Th(NO <sub>3</sub> ) <sub>4</sub> solution in 1 M HNO <sub>3</sub> at 303 K	106
4.10	Extraction isotherms for the extraction of Th(IV) and HNO <sub>3</sub> by 1.1 M TBP/ <i>n</i> -hexadecane from Th(NO <sub>3</sub> ) <sub>4</sub> solution in 1 M HNO <sub>3</sub> at 303 K	107
4.11	Variation of ratio of Th(IV) in TP to that of DP with [Th(IV)] <sub>aq,eq</sub> for the extraction of Th(IV) by 1.1 M TalP/ <i>n</i> -alkane from Th(NO <sub>3</sub> ) <sub>4</sub> solution with near-zero free acidity at 303 K	108
4.12	Variation of ratio of Th(IV) concentration between the TP and the DP in the extraction of Th(IV) by 1.1 M TBP/ <i>n</i> -alkane from Th(NO <sub>3</sub> ) <sub>4</sub> solutions with 1 M and 5 M nitric acid as a function of [Th(IV)] <sub>aq,eq</sub> at 303 K	108

4.13	Variation of ratio of Th(IV) concentration between the TP and the DP in the extraction of Th(IV) by 1.1 M <i>TiAP/n</i> -alkane from Th(NO <sub>3</sub> ) <sub>4</sub> solutions with 1 M and 5 M nitric acid as a function of [Th(IV)] <sub>aq,eq</sub> at 303 K	109
4.14	Variation of ratio of concentration of HNO <sub>3</sub> between TP and DP in the extraction of Th(IV) by 1.1 M TBP/ <i>n</i> -alkane from Th(NO <sub>3</sub> ) <sub>4</sub> solutions with 1 M and 5 M nitric acid as a function of [Th(IV)] <sub>aq,eq</sub> at 303 K	110
4.15	Variation of ratio of concentration of HNO <sub>3</sub> between TP and DP in the extraction of Th(IV) by 1.1 M <i>TiAP/n</i> -alkane from Th(NO <sub>3</sub> ) <sub>4</sub> solutions with 1 M and 5 M nitric acid as a function of [Th(IV)] <sub>aq,eq</sub> at 303 K	111
4.16	Density of organic phases in the extraction of Th(IV) by 1.1 M TalP/ <i>n</i> -alkane from Th(NO <sub>3</sub> ) <sub>4</sub> solution with near-zero free acidity as a function of [Th(IV)] <sub>aq,eq</sub> at 303 K	113
4.17	Density of organic phases in the extraction of Th(IV) by 1.1 M TBP/ <i>n</i> -alkane from Th(NO <sub>3</sub> ) <sub>4</sub> solutions with 1 M and 5 M nitric acid as a function of [Th(IV)] <sub>aq,eq</sub> at 303 K	114
4.18	Density of organic phases in the extraction of Th(IV) by 1.1 M <i>TiAP/n</i> -alkane from Th(NO <sub>3</sub> ) <sub>4</sub> solutions with 1 M and 5 M nitric acid as a function of [Th(IV)] <sub>aq,eq</sub> at 303 K	114
4.19	Difference in density between DP and the corresponding diluent in the extraction of Th(IV) by 1.1 M <i>TiAP/n</i> -alkane from Th(NO <sub>3</sub> ) <sub>4</sub> solution with near-zero free acidity as a function of [Th(IV)] <sub>aq,eq</sub> at 303 K	115
4.20	Difference in density between the DP and the corresponding diluent in the extraction of Th(IV) by 1.1 M TalP/ <i>n</i> -alkane from Th(NO <sub>3</sub> ) <sub>4</sub> solutions with 1 M and 5 M nitric acid as a function of [Th(IV)] <sub>aq,eq</sub> at 303 K; (A) TBP systems (B) <i>TiAP</i> systems	116
4.21	Density and concentration of Th(IV) in the organic phases for 1.1 M TBP/ <i>n</i> -decane - Th(NO <sub>3</sub> ) <sub>4</sub> /1 M HNO <sub>3</sub> and 1.1 M TBP/ <i>n</i> -hexadecane - Th(NO <sub>3</sub> ) <sub>4</sub> /1 M HNO <sub>3</sub> systems as a function of [Th(IV)] <sub>aq,eq</sub> at 303 K	117
4.22	V <sub>DP</sub> /V <sub>TP</sub> ratio in the extraction of Th(IV) by 1.1 M <i>TiAP/n</i> -alkane from Th(NO <sub>3</sub> ) <sub>4</sub> solution with near-zero free acidity as a function of [Th(IV)] <sub>aq,eq</sub> at 303 K	119
4.23	V <sub>DP</sub> /V <sub>TP</sub> ratio in the extraction of Th(IV) by 1.1 M <i>TiAP/n</i> -alkane from Th(NO <sub>3</sub> ) <sub>4</sub> solutions with near-zero free acidity, 1 M and 5 M nitric acid as a function of [Th(IV)] <sub>aq,eq</sub> at 303 K	120
4.24	V <sub>DP</sub> /V <sub>TP</sub> ratio in the extraction of Th(IV) by 1.1 M TBP/ <i>n</i> -alkane from Th(NO <sub>3</sub> ) <sub>4</sub> solutions with near-zero free acidity, 1 M and 5 M nitric acid as a function of [Th(IV)] <sub>aq,eq</sub> at 303K; (A) <i>n</i> -dodecane systems (B) <i>n</i> -tetradecane systems	120
4.25	V <sub>DP</sub> /V <sub>TP</sub> ratio for the extraction of Th(IV) by 1.1 M TBP/ <i>n</i> -alkane from Th(NO <sub>3</sub> ) <sub>4</sub> solution with 1 M HNO <sub>3</sub> at 303 K	122

5.1	Variation of density of solutions of TBP in <i>n</i> -alkane as a function of TBP concentration	128
5.2	Variation of refractive index of water saturated solutions of TBP in <i>n</i> -alkane as a function of TBP concentration at 303 K	129
5.3	Variation of refractive index of <i>n</i> -alkane as a function of carbon chain length and refractive index of <i>n</i> -dodecane as a function of temperature	130
5.4	Variation of viscosity of water saturated solutions of TBP in <i>n</i> -alkane as a function of TBP concentration at 303 K	131
5.5	Variation of LOC in the extraction of Th(IV) by TBP/ <i>n</i> -alkane solutions from Th(NO <sub>3</sub> ) <sub>4</sub> solution with near-zero free acidity at 303 K	133
5.6	Variation of HNO <sub>3</sub> loading in TBP/ <i>n</i> -alkane solutions in the extraction from 8 M HNO <sub>3</sub> solution as a function of TBP concentration at 303 K	134
5.7	Variation of concentration of TBP in the TP and the DP for the extraction of Th(IV) by 1.1 M TBP/ <i>n</i> -alkane from Th(NO <sub>3</sub> ) <sub>4</sub> solution with 1 M HNO <sub>3</sub> as a function of [Th(IV)] <sub>aq,eq</sub> at 303 K	141
6.1	Schematic representation of general trend in the concentration of Th(IV) in organic and diluent-rich phases in the extraction of Th(IV) by TalP/ <i>n</i> -alkane as a function of aqueous phase Th(IV) concentration	150
6.2	Separation of U(VI) from Th(IV) and Nd(III) in 4 M HNO <sub>3</sub> by 0.183 M TiAP/ <i>n</i> -DD in cross-current mode at 303 K	152
6.3	Separation of U(VI) from Th(IV) and Nd(III) in 4 M HNO <sub>3</sub> by 0.183 M TBP/ <i>n</i> -DD in cross-current mode at 303 K	153
6.4	Scrubbing and stripping of U(VI) from loaded 0.183 M TiAP/ <i>n</i> -DD in cross-current mode at 303 K	153
6.5	Scrubbing and stripping of U(VI) from loaded 0.183 M TBP/ <i>n</i> -DD in cross-current mode at 303 K	154
6.6	Third phase formation in the extraction of Th(IV) from Th(IV)-Nd(III) feed solution in 4 M HNO <sub>3</sub> by 1.47 M TalP/ <i>n</i> -DD. A. TBP system B. TiAP system	155
6.7	Separation of Th(IV) from Nd(III) in 4 M HNO <sub>3</sub> by 1.47 M TiAP/ <i>n</i> -DD in cross-current mode at 303 K	157
6.8	Scrubbing and stripping of Th(IV) from loaded 1.47 M TiAP/ <i>n</i> -DD in cross-current mode at 303 K	157
6.9	Data on the concentration of U(VI), Th(IV) and Nd(III) in various stages of extraction, scrubbing and stripping for U(VI) separation from Th(IV) and Nd(III) by 0.183 M TiAP/ <i>n</i> -DD in cross-current mode at 303 K	159
6.10	Data on the concentration of Th(IV) and Nd(III) in various stages of extraction, scrubbing and stripping during the separation of Th(IV) from Nd(III) by 1.47 M TiAP/ <i>n</i> -DD in cross-current mode at 303 K	160
7.1	Variation of distribution ratios for the extraction of Zr(IV) and Hf(IV) by 1.1 M TalP/diluent as a function of [HNO <sub>3</sub> ] <sub>aq,eq</sub> at 303 K	164

7.2	Variation of LOC, in the extraction of Zr(IV) by solutions of TiAP and TBP in <i>n</i> -DD from Zr(NO <sub>3</sub> ) <sub>4</sub> solutions in nitric acid media as a function of [HNO <sub>3</sub> ] <sub>aq,eq</sub> at 303 K	165
7.3	Variation of CAC, in the extraction of Zr(IV) by solutions of TiAP and TBP in <i>n</i> -DD from Zr(NO <sub>3</sub> ) <sub>4</sub> solutions in nitric acid media as a function of [HNO <sub>3</sub> ] <sub>aq,eq</sub> at 303 K	166
7.4	Schematic representation of samples taken for the estimation of constituents of organic phases (biphasic organic, third and diluent-rich phases) in the extraction of Zr(IV) from its solution in nitric acid media (nominal acidity = 4 M HNO <sub>3</sub> ) by 1.1 M solutions of TiAP and TBP in <i>n</i> -DD at 298 K	168
7.5	SANS data obtained from the 1.1 M TiAP/ <i>n</i> -C <sub>12</sub> D <sub>26</sub> - Zr(NO <sub>3</sub> ) <sub>4</sub> /HNO <sub>3</sub> system	173
7.6	SANS data obtained from the 1.1 M TBP/ <i>n</i> -C <sub>12</sub> D <sub>26</sub> - Zr(NO <sub>3</sub> ) <sub>4</sub> /HNO <sub>3</sub> system	174
7.7	SANS data of the third phase sample of the 1.1 M TalP/ <i>n</i> -C <sub>12</sub> D <sub>26</sub> - Zr(NO <sub>3</sub> ) <sub>4</sub> /HNO <sub>3</sub> systems	175

## LIST OF TABLES

TABLE No.	TITLE	PAGE No.
1.1	Properties of thorium	8
1.2	Properties of uranium	9
1.3	Properties of plutonium	11
1.4	Properties of zirconium	12
1.5	Properties of hafnium	13
1.6	Concentration of various components present in the Indian monazite ore	27
3.1	Comparison of experimental data for the extraction of U(VI) and HNO <sub>3</sub> by 1.1 M TBP/ <i>n</i> -DD from U(VI) solutions in nitric acid media with literature data (KfK – 2536)	78
3.2	Determination of HNO <sub>3</sub> concentration in samples with various U(VI):HNO <sub>3</sub> mole ratios by using potassium oxalate - sodium fluoride mixture as complexing agent	80
3.3	Mass balance data for the extraction of U(VI) and HNO <sub>3</sub> by 1.1 M TBP/ <i>n</i> -DD from U(VI) solutions in 0.2 M & 2 M HNO <sub>3</sub>	81
3.4	Data on extraction of U(VI) and HNO <sub>3</sub> by 1.1 M TiAP/ <i>n</i> -DD from U(VI) solutions in 0.1 M and 0.5 M nitric acid at 303 K	85
3.5	Data on extraction of U(VI) and HNO <sub>3</sub> by 1.1 M TiAP/ <i>n</i> -DD from U(VI) solutions in 2 M and 4 M nitric acid at 303 K	86
3.6	Data on extraction of U(VI) and HNO <sub>3</sub> by 1.1 M TiAP/ <i>n</i> -DD from U(VI) solution in 6 M nitric acid at 303 K	86
3.7	Comparison of $D_{U(VI)}$ for 1.1 M TiAP/ <i>n</i> -DD - UO <sub>2</sub> (NO <sub>3</sub> ) <sub>2</sub> /HNO <sub>3</sub> and 1.1 M TBP/OK - UO <sub>2</sub> (NO <sub>3</sub> ) <sub>2</sub> /HNO <sub>3</sub> systems under similar extraction conditions	89
3.8	Data on extraction and stripping of U(VI) with 1.1 M TiAP/ <i>n</i> -DD and 1.1 M TBP/ <i>n</i> -DD at 303 K	90
3.9	Data on extraction, scrubbing and stripping of U(VI) with 1.1 M TiAP/ <i>n</i> -DD and 1.1 M TBP/ <i>n</i> -DD at 303 K	90
4.1	Data on concentration of Th(IV) and HNO <sub>3</sub> in organic phases at CAC and SAC for the extraction of Th(IV) by 1.1 M TalP/ <i>n</i> -alkane from Th(NO <sub>3</sub> ) <sub>4</sub> solutions with 1 M and 5 M nitric acid as a function of [Th(IV)] <sub>aq,eq</sub> at 303 K	112
5.1	Data on the concentration of TBP in the TP obtained by various experimental methods and model for 1.1 M TBP/ <i>n</i> -decane - Th(NO <sub>3</sub> ) <sub>4</sub> /1 M HNO <sub>3</sub> system	136

5.2	Data on the concentration of TBP in the DP obtained by various experimental methods and model for 1.1 M TBP/ <i>n</i> -decane - Th(NO <sub>3</sub> ) <sub>4</sub> /1 M HNO <sub>3</sub> system	137
5.3	Data on the concentration of TBP in the TP obtained by various experimental methods and model for 1.1 M TBP/ <i>n</i> -hexadecane - Th(NO <sub>3</sub> ) <sub>4</sub> /1 M HNO <sub>3</sub> system	137
5.4	Data on the concentration of TBP in the DP obtained by various experimental methods and model for 1.1 M TBP/ <i>n</i> -hexadecane - Th(NO <sub>3</sub> ) <sub>4</sub> /1 M HNO <sub>3</sub> system	138
5.5	Mass Balance of TBP before and after the extraction of Th(IV) by 1.1 M TBP/ <i>n</i> -alkane from 1 M Th(IV) solution in 1 M HNO <sub>3</sub> at 303 K	139
5.6	The concentration of <i>TiAP</i> in the TP and the DP obtained by model for the extraction of Th(IV) by 1.1 M <i>TiAP</i> / <i>n</i> -alkane from saturated Th(NO <sub>3</sub> ) <sub>4</sub> solution with near-zero free acidity at 303 K	143
5.7	The concentration of extractant in the TP and the DP obtained by model in the extraction of Th(IV) by 1.1 M <i>TalP</i> / <i>n</i> -alkane from saturated Th(NO <sub>3</sub> ) <sub>4</sub> solutions with 1 M and 5 M HNO <sub>3</sub> at 303 K	143
6.1	Interference of U(VI), Th(IV) and Nd(III) in nitric acid media during their estimation by titration	148
6.2	Mass Balance of Th(IV) before and after the extraction by 0.183 M <i>TalP</i> / <i>n</i> -DD from solution containing U(VI), Th(IV) and Nd(III) in 4 M HNO <sub>3</sub>	149
6.3	Data on the concentration of metal ions in organic and aqueous phases at the point of dissolution of the third phase for their extraction from solution in 4 M HNO <sub>3</sub> by 1.47 M <i>TalP</i> / <i>n</i> -DD at 303 K	155
7.1	Equilibrium concentrations of Zr(IV), HNO <sub>3</sub> , <i>TalP</i> and H <sub>2</sub> O in organic (org) and aqueous (aq) phases in the extraction of Zr(IV) by 1.1 M <i>TalP</i> / <i>n</i> -DD from its solution in nitric acid media (nominal acidity = 4 M HNO <sub>3</sub> ) as a function of [Zr(IV)] <sub>aq,eq</sub> at 298 K	169
7.2	Equilibrium concentrations of Zr(IV), HNO <sub>3</sub> , <i>TalP</i> and H <sub>2</sub> O in organic (org) and aqueous (aq) phases in the extraction of Zr(IV) by 1.1 M <i>TalP</i> / <i>n</i> -TD from its solution in nitric acid media (nominal acidity = 4 M HNO <sub>3</sub> ) as a function of [Zr(IV)] <sub>aq,eq</sub> at 298 K	171
7.3	Equilibrium concentrations of Zr(IV) and HNO <sub>3</sub> in organic (org) and aqueous (aq) phases in the extraction of Zr(IV) by 1.1 M <i>TalP</i> / <i>n</i> -DD (Deuterated) from its solution in nitric acid media (nominal acidity = 4 M HNO <sub>3</sub> ) as a function of [Zr(IV)] <sub>aq,eq</sub> at 298 K	172
7.4	The fitted parameters of SANS data for the biphasic organic (BP-Org) and the diluent-rich phase (DP) samples of <i>TiAP</i> and TBP solvents	176

7.5	Concentrations of Zr(IV), Hf(IV) and HNO <sub>3</sub> in concentrated and dilute feed solutions used for their extraction by 1.1 M TalP/ <i>n</i> -DD at 303 K	177
-----	--	-----

## ABBREVIATIONS

---



---

ABBREVIATION	FULL NAME
Ac	Actinides
$\sigma$	Aggregate diameter
N	Aggregation number
Amex	Amine extraction
aq	Aqueous
BP-Org	Biphasic organic phase
HDEHP	Bis(2-ethylhexyl)phosphoric acid
$C_{DP}$	Concentration of TBP in the diluent-rich phase
$C_{TP}$	Concentration of TBP in the third phase
$[Th(IV)]_{DP}$	Concentration of Th(IV) in the diluent-rich phase
$[Th(IV)]_{TP}$	Concentration of Th(IV) in the third phase
$[Th(IV)]_{Vir\ Org}$	Concentration of Th(IV) in the virtual un-split organic phase
CAC	Critical aqueous concentration
DBP	Dibutyl phosphate
DTPA	Diethylene triamine pentaacetic acid
DHOA	N,N-Dihexyl octanamide
DP	Diluent-rich phase
$D_A, D_B, D_M, D_{U(VI)},$ $D_{Th(IV)}, D_{Zr(IV)}, D_{Hf(IV)}$ $D_{HNO_3}$	Distribution ratio of solute A, solute B, metal ion, U(VI), Th(IV), Zr(IV), Hf(IV) and HNO <sub>3</sub> , respectively
D2EHPA	Di-2-ethyl hexyl phosphoric acid
<i>n</i> -DD	<i>n</i> -Dodecane
DLS	Dynamic light scattering
EDTA	Ethylene diamine tetraacetic acid
$[HNO_3]_{aq,eq}$	Equilibrium aqueous phase nitric acid concentration

$[\text{Th(IV)}]_{\text{aq,eq}}$	Equilibrium aqueous phase Th(IV) concentration
$[\text{U(VI)}]_{\text{aq,eq}}$	Equilibrium aqueous phase U(VI) concentration
$[\text{Zr(IV)}]_{\text{aq,eq}}$	Equilibrium aqueous phase Zr(IV) concentration
$K_{\text{eq}}$	Equilibrium constant
$[\text{Th(IV)}]_{\text{org,eq}}$	Equilibrium organic phase Th(IV) concentration
$[\text{U(VI)}]_{\text{org,eq}}$	Equilibrium organic phase U(VI) concentration
$[\text{Zr(IV)}]_{\text{org,eq}}$	Equilibrium organic phase Zr(IV) concentration
FBR	Fast breeder reactors
$d_{\text{hs}}$	Hard sphere diameter
HNP	Heavy normal paraffins
HMTA	Hexamethylenetetramine
HLW	High level waste
IR	Infra red
Ln	Lanthanides
LOC	Limiting organic concentration
MIBK	Methyl isobutyl ketone
MBP	Monobutyl phosphate
NMR	Nuclear magnetic resonance
CMPO	Octyl(phenyl)-N,N-diisobutyl carbamoyl methyl phosphine oxide
OK	Odourless kerosene
org	Organic
KHP	Potassium hydrogen phthalate
$U(r)$	Potential energy of attraction
PHWR	Pressurized heavy water reactors
$V_{\text{DP}}/V_{\text{TP}}$	Ratio of the volume of diluent-rich phase to that of third phase
$\mu$	Refractive index
SAC	Saturated aqueous concentration
Q	Scattering vector
$\beta_{\text{Zr(IV)}/\text{Hf(IV)}}$	Separation factor of Zr(IV) from Hf(IV)

SANS	Small angle neutron scattering
SAXS	Small angle x-ray scattering
SNF	Spent nuclear fuel
$\tau^{-1}$	Stickiness parameter
$C_a$	TBP concentration after the stripping of solutes
$C_b$	TBP concentration before the stripping of solutes
$[TBP]_{Free}$	TBP uncomplexed with metal ion and nitric acid
<i>n</i> -TD	<i>n</i> -Tetradecane
TTA	Thenoyl trifluoroacetone
TP	Third phase
TalP	Trialkyl phosphate
TalPs	Trialkyl phosphates
TiAP	Tri- <i>iso</i> -amyl phosphate
TAP	Tri- <i>n</i> -amyl phosphate
TBP	Tri- <i>n</i> -butyl phosphate
TOPO	Tri- <i>n</i> -octyl phosphine oxide
T2MBP	Tri-2-methyl butyl phosphate
VPO	Vapour pressure osmometry
$\phi$	Volume fraction of aggregates
$V_{Org}$	Volume of TBP in the organic phase in the biphasic region
$V_a$	Volume of TBP solution after the stripping of solutes
$V_b$	Volume of TBP solution before the stripping of solutes
$V_{DP}$	Volume of the diluent-rich phase
$V_{TP}$	Volume of the third phase
Br-PADAP	2-(5-Bromo-2-pyridylazo)-5-(diethylamino) phenol
LIX 63	5,8-diethyl-7-hydroxy-6-dodecanone oxime
PC88A	2-ethylhexyl 2-ethylhexyl phosphonic acid
PDCA	2,6-pyridine dicarboxylic acid
PAN	1-(2-pyridylazo)-2-naphthol



# Chapter 1



**“Research is what I’m doing when I don’t know what I’m doing”**

*-Wernher von Braun*

## INTRODUCTION

---

---

### 1.1 Significance of energy

Sustainable development and self sufficiency of a country can be attained only when its energy demands are fulfilled or else it leads to stagnant economy. The security of a nation indirectly relies on its energy security. In developing countries like India, growing GDP and rapid urbanization proportionately increase the demand for energy [1]. India is one of the topmost energy consumers in the world [2]. Pervasive electricity deficits cause poor quality of power supply that leads to damage of industrial and household equipments. Though India imports 30% of its commercial energy, always demands surpass supply. Also, the gap between demand and supply of energy widens with India's growing population. The escalating energy needs have to be contented or else it leads to formidable lack of productivity, poor standard of living and insecurity in the nation. Even though nature has provided diverse forms of energy, the choice is based on the economy. The economics of energy production depends upon the abundance, diversity and supply of energy resources, and cost effective technologies available in a country to harness energy [3]. Based on the economics of energy production, each country follows its own strategy for energy production from several renewable and non-renewable resources.

### 1.2 Various sources of energy - Advantages and limitations

Our country is the third largest producer of coal in the world. In the global scenario, emission of green house gases into the atmosphere and disposal of fly ash are the dominant environmental concern when coal is used as the primary source of energy [4]. Literature reveals that the radioactivity introduced into the atmosphere by fossil fuels is higher compared to nuclear power plant of comparable power producing capacity [5]. Although our

demand for oil is huge, the uncertainty in the oil price in global market, emission of toxic gases into the atmosphere, sludge formation and oil spillage into aquatic ecosystem seldom entertain the use of oil for energy production [6,7]. The fossil fuel resources around the world are limited and diminishing at an alarming rate such that they remain for only hundred years [8].

In contrast to non-renewable resources, energy obtained from renewable resources such as hydroelectricity, solar energy, wind energy etc., are clean and green as they hardly ever contribute to global warming and provide energy with zero fuel cost [9]. The power generation from hydroelectric projects depends upon rainwater and therefore the extent of electricity production is unpredictable. Due to the complications involved in the relocation of people around the hydroelectric plants, eco-conservation restriction and high initial investments, hydroelectric projects with less storage capacity are taken up [10]. Geography of India on globe is in favour of producing solar energy as the solar radiation is available in most of the parts of India for major time in a year. However, low technological inputs and heavy initial costs are major setbacks for solar energy production. Even though wind energy is considered to be clean and renewable, it is unreliable as wind is uncertain and unpredictable [11]. In Indian perspective, other renewable energy resources such as geothermal energy and tidal energy are either expensive or the technology is in rudimentary stage.

### **1.3 Potential of nuclear energy**

Complications and drawbacks involved in extracting energy from above mentioned resources have made nuclear energy as an important choice for a long term outlook [12-15]. The operation of a nuclear reactor for power production involves negligible production of green house gases and hence considered to be clean energy. The land and water usage to operate a nuclear reactor is less. As the energy density of nuclear fuels is million times higher

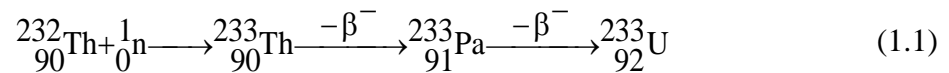
than fossil fuels, the fuel requirement for a nuclear reactor is very small and is in a concentrated form as compared to fossil fuels which in turn reduces the transport cost. Moreover, the fuel used in fast breeder reactors can be regained by breeding. The elements such as thorium, uranium, zirconium etc., required for the fabrication of nuclear fuels and structural materials are available in India. Currently there are twenty one nuclear reactors under operation in India which produce 5780 MWe energy. The contribution of nuclear energy towards India's electricity production is only 3% and it has been planned to increase it to 25% by the year 2050. Apart from electricity generation, various radioisotopes such as  $^{60}\text{Co}$ ,  $^{137}\text{Cs}$ ,  $^{131}\text{I}$ ,  $^{90}\text{Sr}$  and  $^{32}\text{P}$  produced in nuclear reactors are utilized for food storage, sterilization of equipments, waste or sludge treatment, irradiation of materials, research and medicine.

The accumulation of radioactive waste is a dominant concern on power production using nuclear energy. However, studies on the reduction of radiotoxicity by partitioning long-lived radioisotopes and transmuting them into short-lived radioisotopes in accelerator driven systems have been undertaken [16-19]. Moreover, research activities on the immobilisation of radioactive waste in a suitable matrix of glass or concrete in repository are under progress [20,21].

#### **1.4 India's three stage nuclear program**

The amount of uranium reserves existing in India is limited in terms of quality and quantity as compared to reserves available elsewhere in the world [22,23]. Exploiting uranium in thermal reactors for electricity production in open fuel cycle may exhaust the existing uranium in about forty years. Thorium reserves in India are abundant to the extent that utilization of thorium sustains the electricity production for some centuries. However, thorium is a fertile material and the production of electricity directly from thorium by fission

is not viable. Nevertheless, thorium can be converted to U-233 by neutron capture followed by  $\beta$ -decay as shown in Eq. (1.1).



With the goal to effectively utilize the limited uranium resources and harness energy from abundant thorium reserves, India has envisioned a three stage nuclear program [24-28]. In the first stage, the natural uranium makes the use of thermal neutrons to produce electricity and plutonium in pressurized heavy water reactors (PHWR). The depleted uranium and plutonium from the spent nuclear fuel of PHWR are recovered by reprocessing and used to fuel sodium cooled fast breeder reactors (FBR) in the second stage. The FBR produce electricity from the fuel (depleted uranium and plutonium) present in the core and the thorium ( ${}^{232}\text{Th}$ ) based blanket material is converted to uranium ( ${}^{233}\text{U}$ ) by neutron capture followed by  $\beta$ -decay. The uranium-233 produced in the second stage is separated from thorium-232 by reprocessing and the recovered uranium-233 is employed as the fuel in the third stage. The third stage nuclear reactors use thorium blanket and operates in thermal spectrum of neutron. The thorium breeder reactors can produce electricity as well as breed uranium-233 from thorium-232 and hence third stage can be sustained for a long time. Through this indigenous approach the limited uranium reserves and abundant thorium reserves can be coupled to fulfil our long term energy needs.

### 1.5 Nuclear fuel cycle

Two types of nuclear fuel cycles namely, open fuel cycle and closed fuel cycle are adopted worldwide for the processing of nuclear materials [29]. In the open fuel cycle, initially, the uranium is mined from the ore, enriched, fabricated and irradiated in thermal reactors. Finally the spent nuclear fuel (SNF) is discharged into the repository without reprocessing after interim storage. In the closed fuel cycle, SNF is reprocessed to separate uranium and the plutonium from fission products. The recovered uranium and plutonium are

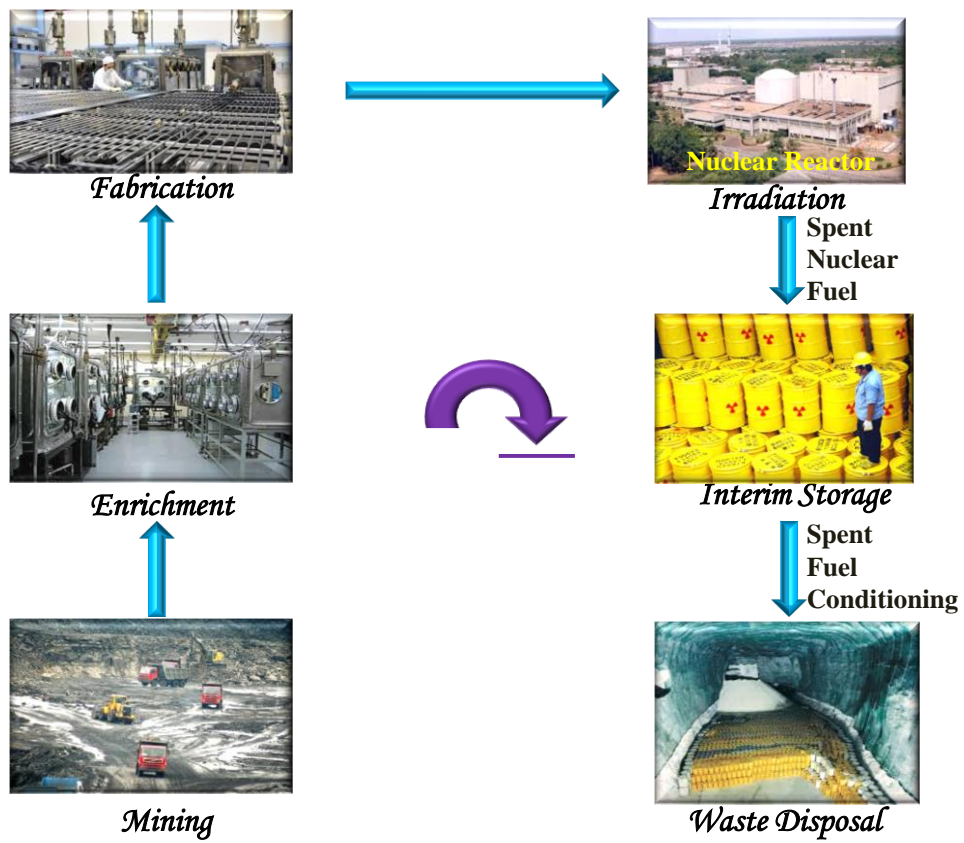


Fig. 1.1: Schematic representation of open fuel cycle.

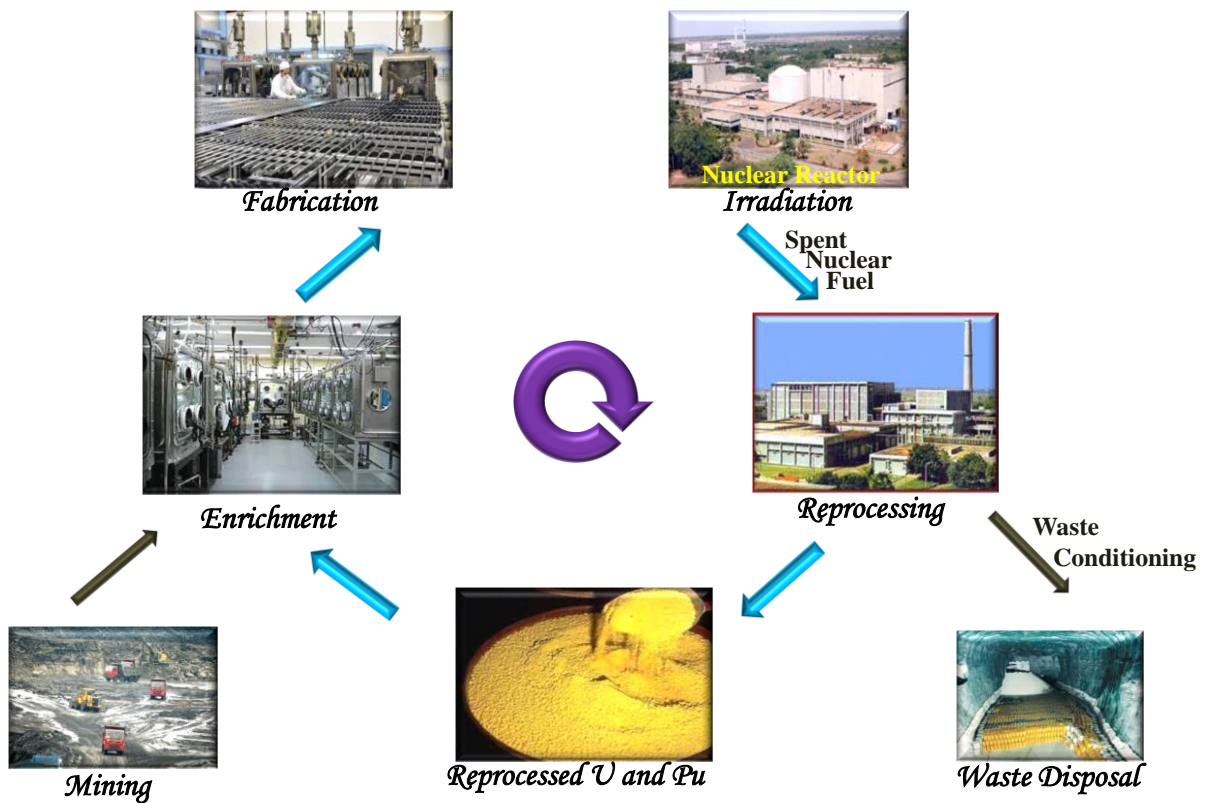


Fig. 1.2: Schematic representation of closed fuel cycle.

fabricated and reused in either thermal reactor or fast reactor. Reprocessing reduces the demand for the mining and milling of fresh uranium ores. Reprocessing of spent nuclear fuel enables the conversion of fission products and other waste materials into a suitable matrix for interim storage or disposal. It also helps to recover useful isotopes such as  $^{137}\text{Cs}$ ,  $^{90}\text{Sr}$ ,  $^{147}\text{Pm}$  etc. The open and closed fuel cycles are schematically represented in Figs. 1.1 and 1.2, respectively.

## 1.6 Properties of elements of interest to nuclear industry

The source, application, physical and chemical properties of various elements encountered during the processing of nuclear materials are discussed in this section.

### 1.6.1 Lanthanides

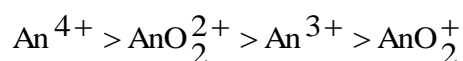
The series of inner transition elements from lanthanum (La) to lutetium (Lu) with atomic number 57 to 71 is referred as lanthanides (Ln). Even though lanthanum has the ground state electronic configuration without f electrons ( $[\text{Xe}] 4f^0 5d^1 6s^2$ ) it is considered a lanthanide due to the proximity of its chemical properties with f-block elements rather than d-block elements. Lighter lanthanides such as lanthanum, cerium, praseodymium, neodymium and promethium contribute significant portion of fission products [30] and therefore understanding of lanthanide chemistry is of paramount importance to separate them from actinides during reprocessing and waste treatment. Lanthanides find applications in superconducting magnets, permanent magnets, rechargeable batteries, MRI agents, NMR shift reagents, medicine and hydrogen storage [31-34].

Monazite and bastnasite are important ores of lighter lanthanides and xenotime is the principal ore of heavier lanthanides [35]. Analogous chemistry of lanthanides makes them complex to separate from their ores. The general valence electronic configuration of lanthanides is  $4f^{0-14} 5d^{0-1} 6s^2$ . Most of the lanthanides lose three electrons from 4f and 6s orbitals to form compounds with +3 oxidation state. Several lanthanides (cerium,

praseodymium, neodymium, terbium and dysprosium) form +4 oxidation state and some of the lanthanides (neodymium, samarium, europium, dysprosium, thulium and ytterbium) exhibit +2 oxidation state. As we move across the period of 4f elements in the periodic table the radius of trivalent lanthanides decreases from  $\text{La}^{3+}$  to  $\text{Lu}^{3+}$  and this property of lanthanides is termed as lanthanide contraction. The effective increase in the nuclear charge from  $\text{La}^{3+}$  to  $\text{Lu}^{3+}$  coupled with poor shielding of f-orbital electrons results in efficient attraction of valence electron towards the nucleus of the atom and hence the lanthanide contraction is observed.

### 1.6.2 Actinides

The actinide series is composed of elements from actinium (Ac) to lawrencium (Lr) with atomic number 89 to 103 in the periodic table. Among the actinides (An), uranium and thorium are the elements that are naturally abundant. All the other members of actinides are produced artificially in nuclear reactors or accelerators. However, actinium and protactinium are available in traces in the uranium ore. Unlike lanthanides, variable oxidation states from +3 to +8 are observed in early members of actinide series. The large size and effective shielding of 5f electrons from the nucleus lead to the decrease in the difference in the energy gap between 5f, 6d and 7s orbitals which results in variable oxidation states of actinides as compared to lanthanides. Therefore, the lighter actinides especially plutonium exhibit various oxidation states from +3 to +8 [36]. However, the shielding of 5f electrons is less effective from americium. The effective nuclear charge experienced by 5f electrons increases such that actinide contraction is more pronounced and therefore the oxidation state does not augment beyond +3. The effective charge on the actinide ions is reduced by forming actinyl ions. The effective charge on actinide cation decreases in the following order as shown below.



The properties of some of the actinides are explained in detail as follows.

### 1.6.2.1 Thorium

The word thorium was derived from the name ‘Thor’, the war god of Scandinavian mythology. Most of the thorium available in the earth is obtained from monazite ore. It has six isotopes with mass numbers 227, 228, 230, 231, 232 and 234. The half life of  $^{232}\text{Th}$  is 14 billion years which is higher as compared to its other isotopes and accounts for nearly all natural thorium. Thorium predominantly exists in +4 oxidation state and rarely exists in +3 and +2 oxidation states [37]. Earlier, thorium was used in gas mantles and welding electrodes. Thorium is used in the form of thoria to produce heat resistant ceramics which are used to make high temperature laboratory crucibles. Some of the properties of thorium are listed in Table 1.1.

**Table 1.1: Properties of thorium**

Atomic number	90
Electronic configuration	[Rn] $6d^2 7s^2$
Density	$11.7 \text{ gmL}^{-1}$
Atomic weight	$232.04 \text{ gmol}^{-1}$
Atomic radius	$1.80 \text{ \AA}$
Ionic radius ( $\text{Th}^{4+}$ )	$1.02 \text{ \AA}$
Melting point	2023 K
Boiling point	5063 K
Thermal neutron capture cross-section	Th-232 (7.35 barns)
Young's modulus	79 GPa

The abundance of thorium reserves in the earth crust is three to four times higher than uranium and therefore opportunities to use thorium based fuels for nuclear reactors are being explored [38-42]. In fact the three stage nuclear program was developed by India to utilize the limited uranium resources effectively and harness power from thorium. The introduction of thorium based fuels in the nuclear reactors has several advantages [43]. The thermal

neutron capture cross-section of Th-232 (7.4 barns) is higher than U-238 (2.7 barns) [44,45]. The production of long-lived minor actinides is less in thorium fuel cycle as compared to other fuel cycles. Unlike U-238 to Pu-239 conversion which can be efficiently attained using fast neutrons, Th-232 to U-233 conversion can be accomplished using fast, epithermal and thermal neutrons. Generally, thorium is used in the form of its oxide ( $\text{ThO}_2$ ) in nuclear reactors as it has high thermal conductivity, low thermal expansion co-efficient and resists oxidation unlike  $\text{UO}_2$ .

### 1.6.2.2 Uranium

The element uranium was named after the planet ‘Uranus’, which was newly discovered when the element was identified. In ancient times it had widespread use as a colouring agent in ceramic glasses. Uranium is considered as a strategic element for nuclear industry in terms of production of electricity. Natural uranium has three isotopes  $^{238}\text{U}$ ,  $^{235}\text{U}$  and  $^{234}\text{U}$  with a relative abundance of 99.275, 0.7200 and 0.0055, respectively [46]. Uraninite or pitchblende is the principal ore of uranium. The uranium is also available in carnotite, coffinite and monazite. Some of the properties of uranium are listed in Table 1.2.

**Table 1.2: Properties of Uranium**

Atomic number	92
Electronic configuration	$[\text{Rn}] 5f^3 6d^1 7s^2$
Density	$19.1 \text{ gmL}^{-1}$
Atomic weight	$238.03 \text{ gmol}^{-1}$
Atomic radius	$1.75 \text{ \AA}$
Melting point	1406 K
Boiling point	4404 K
Thermal neutron capture cross-section	U-233 (588 barns) U-235 (694 barns) U-238 (2.73 barns)
Young’s modulus	208 GPa

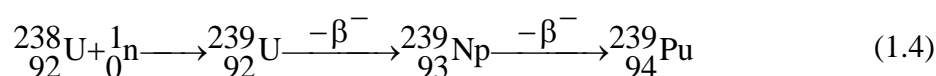
Aqueous solutions of uranium can exist in +3, +4, +5 and +6 oxidation states. Uranium exists as uranyl cation ( $\text{UO}_2^{2+}$ ) in aqueous solutions and is the most stable oxidation state [47]. Uranium rarely exists in +5 oxidation state ( $\text{UO}_2^+$ ) and it easily undergoes disproportionation.

### 1.6.2.3 Plutonium

The element plutonium was named after the planet 'Pluto'. Plutonium remains to be the first synthetic element to be produced in large scale [48]. Plutonium is a strategic element as it can be used to make nuclear weapons as well as produce electricity in a nuclear reactor. Infinitesimal quantity of plutonium is naturally available as  $^{239}\text{Pu}$  along with uranium ore [49]. Plutonium ( $^{238}\text{Pu}$ ) was first produced by bombarding  $^{238}\text{U}$  with deuterons followed by a  $\beta$ -decay as shown in Eqs. (1.2) and (1.3)



Around fifteen isotopes of plutonium are available with mass number 232 to 246 and all the isotopes are radioactive. Plutonium is produced from uranium in a nuclear reactor by neutron capture followed by two  $\beta$ -decays as shown in Eq. (1.4).



The plutonium formed in the nuclear reactor is recovered by dissolving the nuclear fuel in nitric acid followed by solvent extraction using tri-*n*-butyl phosphate (TBP). Uranium and plutonium are extracted together into the organic phase followed by the partitioning of plutonium and its purification by ion exchange method.

The aqueous chemistry of plutonium is complex as it exists in variable oxidation states from +3 to +8 depending upon various conditions. The complexity is such that under certain conditions a solution of plutonium simultaneously exhibits appreciable amount of four

different oxidation states [50,51]. Tetravalent plutonium polymerizes and disproportionates into tri, penta and hexavalent plutonium in solutions of acidity less than 0.5 M. The disproportionation and hydrolysis reactions of  $\text{Pu}^{4+}$  are shown in Eqs. (1.5) and (1.6), respectively [50]. Under certain conditions solutions containing  $\text{Pu}^{4+}$  form colloids [52]. Some of the physical and chemical properties of plutonium are listed in Table 1.3.

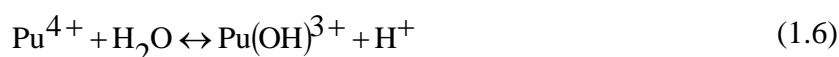
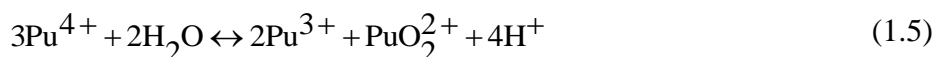


**Table 1.3: Properties of plutonium**

Atomic number	94
Electronic configuration	[Rn] $5f^6 7s^2$
Density	$19.7 \text{ gmL}^{-1}$
Atomic weight	$239 \text{ gmol}^{-1}$
Atomic radius	$1.59 \text{ \AA}$
Melting point	912 K
Boiling point	3505 K
Thermal neutron capture cross-section	Pu-238 (468 barns) Pu-239 (1025 barns) Pu-240 (350 barns) Pu-241 (1336 barns)
Young's modulus	96 GPa

### 1.6.3 Zirconium

The name zirconium comes from the Persian word 'Zargun' which means gold-like metal [53]. It is a lustrous, grayish-white and corrosion-resistant transition metal in the periodic table. Zirconium is wide spread in nature and constitutes about 0.028% of the earth's crust. Most important ores of zirconium are zircon and baddeleyite. It is also present in minerals containing titanium, niobium, tantalum and rare earth elements. Zirconium occurs

naturally in the form of five isotopes with mass numbers of 90, 91, 92, 94 and 96, and the natural abundance of its isotope with mass number 90 is maximum (51.46%). Some of the data on the properties of zirconium are shown in Table 1.4 [54].

Zirconium is used in refractories, foundry moulds, glaze opacifiers, glass industry, textile industry, oil industry, abrasives, ceramics, capacitors, piezoelectrics, pyroelectrics, solid electrolytes, water-proofing, photography, medicine and cosmetics. Around 90% of total zirconium metal produced is used in nuclear industry. Zirconium has been used in various forms for reactor applications. The low neutron capture cross-section and high corrosion resistant behaviour of zirconium metal have made it as an ideal material to prepare clad for thermal reactor fuel pins in the form of Zircaloy. Also, 10 wt % of zirconium metal is used in metal alloy fuels in order to increase the mechanical strength and solidus temperature of fuels.

**Table 1.4: Properties of zirconium**

Atomic number	40
Electronic configuration	[Kr] 4d <sup>2</sup> 5s <sup>2</sup>
Density	6.52 gmL <sup>-1</sup>
Atomic weight	91.22 gmol <sup>-1</sup>
Atomic radius	1.45 Å
Ionic radius (Zr <sup>4+</sup> )	0.74 Å
Melting point	2125 K
Boiling point	3853 K
Thermal neutron capture cross-section	Zr-91 (1.52 barns)
Young's modulus	88 GPa

Aqueous solutions of zirconium exhibit +4 oxidation state only. High charge and small size of Zr<sup>4+</sup> cation makes it amenable to undergo hydrolysis and polymerization. The free Zr<sup>4+</sup> ion in aqueous phase is stable only in highly acidic solutions and at low Zr

concentrations [55]. In nitric acid solutions with concentration of 3 M and above, zirconium predominantly exists as  $Zr^{4+}$  [56]. When the concentration of  $HNO_3$  is 1 M or less, the concentration of  $[ZrOH]^{3+}$  species is higher and further reduction in  $HNO_3$  concentration leads to the formation of species like  $[Zr(OH)_2]^{2+}$  and  $[Zr(OH)_3]^+$ . Concentrated solutions of  $Zr^{4+}$  are prone to undergo hydrolysis and polymerization. It has been observed that in perchloric acid medium,  $Zr^{4+}$  exists in monomer form when  $Zr^{4+}$  concentration is less than  $10^{-4}$  M and forms polymeric species like  $[Zr_3(OH)_4]^{8+}$  and  $[Zr_4(OH)_8]^{8+}$  for concentrations above 0.02 M [54].

#### 1.6.4 Hafnium

The element hafnium was named after ‘Hafnia’ which is the Latin name of Copenhagen, the place where the element was discovered. The ores of zirconium are always associated with 1-5 % of hafnium. Hafnium has six naturally occurring isotopes with mass numbers 174, 176, 177, 178, 179 and 180. It is used in filaments, electrodes, super alloys and as a polymerization catalyst. The neutron capture cross-section of hafnium is high and hence it can be used in the control rod materials to absorb neutrons.

**Table 1.5: Properties of hafnium**

Atomic number	72
Electronic configuration	$[Xe] 4f^{14} 5d^2 6s^2$
Density	$13.31 \text{ gmL}^{-1}$
Atomic weight	$178.4 \text{ gmol}^{-1}$
Atomic radius	$1.44 \text{ \AA}$
Ionic radius ( $Hf^{4+}$ )	$0.75 \text{ \AA}$
Melting point	2495 K
Boiling point	5673 K
Thermal neutron capture cross-section	Hf-174 (500 barns) Hf-177 (375 barns)
Young's Modulus	78 GPa

The chemical properties of hafnium are very much close to that of zirconium. The reason for the similarity is due to their comparable ionic radii. Generally, along a group in the periodic table, an increase in atomic radius is observed from 3d transition elements to 4d transition elements. However, in most of the cases such an increase in atomic radius is not observed between 4d transition elements and 5d transition elements as the increase in atomic radius is counteracted by lanthanide contraction [35]. Due to this reason zirconium and hafnium have similar ionic radii. Some of the properties of hafnium are shown in Table 1.5.

### **1.6.5 Estimation of metal ions and free acidity**

Determination of concentrations of metal ions and free acidity in solutions at various stages of experiments is necessary to understand the course of experiments. Estimation of a particular metal ion in pure form is relatively straightforward as compared to its estimation in the presence of other metal ions. The complexities associated with the analytical methods escalate with the number of foreign metal ions co-existing with the metal ion to be estimated. The quantitative estimation of the metal ion becomes complicated when the foreign metal ions possess similar chemical properties as the native metal ion especially in the case of lanthanides and actinides. Masking agents, buffer solutions, analysis medium etc., are carefully chosen to selectively suppress the influence of foreign metal ions to avoid their interference during the estimation of a particular metal ion [57,58].

Several methods such as complexometric titration, redox titration, spectrophotometry, gravimetry, potentiometry, amperometry, coulometry, radiometry, atomic emission spectroscopy, atomic absorption spectroscopy, chromatography and liquid scintillation counting are followed for the estimation of metal ions [57-66]. Each analytical method is unique and has its own merits and demerits. Generally, results obtained by electrometric methods have high precision and accuracy as compared to other techniques. Therefore, actinides such as plutonium and uranium can be estimated by such electrometric techniques.

However, it is difficult to employ potentiometric techniques for the estimation of metal ions such as Th(IV) and Zr(IV) due to the non-existence of stable multiple oxidation states in aqueous solutions. Complexometric titration is a simple and rapid analytical method to estimate such metal ions in milligram scale. Data obtained by spectrophotometric method have relatively higher uncertainty as compared to electrometric method; however, the former is preferred due to its simplicity in analysis. In general, the method adopted for the estimation of a metal ion is chosen based on several parameters such as medium, pH, foreign metal ions present in the solution, oxidation state of the metal ion to be estimated and its concentration [57].

Generally, the free acidity of a solution is estimated by acid-base titration. The alkali and the alkaline earth metal ions present in the solution do not hydrolyze at the end point of titration and hence the free acidity of solutions with these metal ions can be determined directly by acid-base titration. However, most of the other metal ions such as lanthanides and actinides interfere in the estimation of the free acidity [67-69]. These metal ions hydrolyze at higher pH particularly, near the end point of titration and give positively biased results. The results of the estimated free acidity could be erroneous if the metal ions present in the solution are weakly complexed or uncomplexed. Therefore, it is necessary to complex such metal ions prior to free acidity determination. The accurate determination of free acidity depends on the proper selection of complexing agents and their quantities required to completely complex the interfering metal ions. Various complexing agents such as oxalates, sulphates, citrates, fluorides etc, have been employed to complex metal ions [67-73]. Among them oxalate is the commonly used complexing agent to mask the metal ions owing to its higher stability constant for various metal ions due to chelation. Moreover, oxalate forms water soluble complexes with most of the hydrolyzable metal ions and hence the estimation

procedure is simple. Also, the metal-oxalate complexes are incinerable which makes it easy for the recovery of the metal ions [67].

## 1.7 Solvent extraction

### 1.7.1 Fundamental aspects of solvent extraction

When a solvent containing a solute is contacted with another immiscible solvent, the solute preferentially distributes between them. The technique based on the above principle used to separate the pure solute is known as liquid-liquid extraction or solvent extraction. The extent of distribution of a solute (A) between two immiscible liquids can be obtained from its distribution ratio ( $D_A$ ). It is defined as the ratio of analytical concentration of solute A in organic and aqueous phases at equilibrium which is expressed in Eq. (1.7) where, org and aq represent organic and aqueous phases, respectively.

$$D_A = \frac{[A]_{\text{org}}}{[A]_{\text{aq}}} \quad (1.7)$$

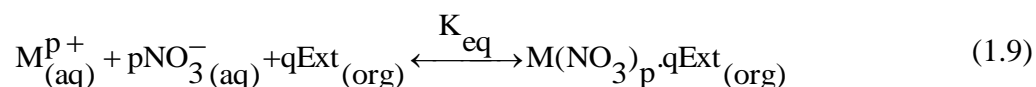
Solute particles in the solution interact with solvent molecules in four different ways through ion - dipole, dipole - dipole, dipole - induced dipole and induced dipole - induced dipole interactions [74]. The extraction of solute also depends upon temperature, hydrogen ion concentration, nature and concentration of the solvent, solute, complexing agent and salting agent in a solvent extraction system [74]. Aforementioned disparities lead to preferential extraction of one solute over the other in a particular solvent extraction system. Successful separation and purification of a solute is achieved by optimizing these parameters.

When aqueous solution contains more than one solute, then selective extraction of one of the solute particles comes into picture, where the term separation factor is required to quantify the preferential extraction of one solute over the other. In a system of two solutes (solute A and solute B) present in an aqueous solution, the extent of selective extraction of

solute A over solute B by the organic phase can be obtained from separation factor ( $\beta_{A/B}$ ) as shown in Eq. (1.8), where  $D_B$  represents the distribution ratio of solute B.

$$\beta_{A/B} = \frac{D_A}{D_B} \quad (1.8)$$

In general, the extraction of a metal nitrate by a solvating extractant can be expressed as shown in Eq. (1.9) [75].



The species present in aqueous and organic phases are represented as (aq) and (org), respectively.  $M^{p+}$  and Ext denote metal ion and free extractant, respectively. The equilibrium constant ( $K_{eq}$ ) shown in Eq. (1.10) can be derived from Eq. (1.9),

$$K_{eq} = \frac{[M(NO_3)_p \cdot qExt]_{(org)}}{[M^{p+}]_{(aq)} [NO_3^-]_{(aq)}^p [Ext]_{(org)}^q} \quad (1.10)$$

where, the terms in the square bracket indicate the activities of various species. For simplicity, activity coefficients for various species can be assumed to be unity, and hence the terms represent the concentration. The ratio  $[M(NO_3)_p \cdot qExt]_{(org)} / [M^{p+}]_{(aq)}$  is nothing but  $D_M$  (distribution ratio of metal ion) and hence the above Eq. (1.10) can be expressed as Eq. (1.11).

$$D_M = K_{eq} [NO_3^-]_{(aq)}^p [Ext]_{(org)}^q \quad (1.11)$$

Therefore,  $D_M$  can be correlated to nitrate ion concentration, free extractant concentration (concentration of uncomplexed extractant at equilibrium) and equilibrium constant as given by Eq. (1.11).

### 1.7.2 Advantages of solvent extraction

The solvent extraction technique has several advantages over other separation techniques as listed below [76,77].

- i) Solvent extraction can be used for the removal of substances in small as well as large concentrations.
- ii) Distillation of compounds with high boiling points requires more energy and in such cases solvent extraction proves to be economical.
- iii) Recovery of heat sensitive materials can be done at low cost by solvent extraction instead of employing vacuum distillation.
- iv) Separation of compounds with boiling points close to each other can be executed through solvent extraction, provided their separation factor is high.
- v) Mixtures which can form azeotropes can easily be separated by solvent extraction.
- vi) Continuous operation is feasible and the solvent extraction setups can be handled by remote operation especially, in a radioactive environment.
- vii) Solvent extraction setups involve no major corrosion problem and the solvent extraction process is well established on the industrial scale.

### **1.7.3 Characteristics of an ideal solvent**

The selection of the solvent plays a key role in the development of a solvent extraction process. Solvent extraction technique can be employed for the recovery and purification of metals present in aqueous solutions when the solvent fulfils some of the characteristics mentioned as follows [78].

- i) It must be stable, non-volatile, non-flammable, non-toxic, inexpensive, recoverable and available in pure form.
- ii) It should be highly selective for the extraction of element of interest and must strip back the loaded metal easily.
- iii) Less soluble in aqueous phase and highly soluble in diluents.
- iv) Faster extraction and stripping kinetics.

v) The density difference between the organic and aqueous phases must be higher, viscosity should be lower and the interfacial surface tension of the system should be optimum (5-25 dyne/cm) [79].

vi) The solvent should not undergo any thermal, chemical and radiation degradation.

#### **1.7.4 Requirement of diluents in solvent extraction**

A solvent must fulfil aforementioned criteria to be employed for a separation process. However, practically no reagent satisfies all the required conditions and in order to achieve the desirable properties, usually the reagent which extracts the metal ions (extractant) is mixed with another organic liquid called diluent [80]. Therefore, binary solutions of an extractant and a diluent are commonly encountered in solvent extraction processes. The addition of a diluent to an extractant reduces its density and viscosity. This facilitates efficient mass transfer and enables good phase separation between organic and aqueous phases. Generally, hydrocarbons in liquid state with high flash points and low volatility are chosen as diluents to avoid diluent loss and fire hazards. The use of diluents also reduces the extracting power of the extractant which increases the selectivity for the extraction of a particular metal ion and thereby improves the decontamination factor.

#### **1.7.5 Classification of extractants**

During solvent extraction, the hydrophilic metal ion present in the aqueous phase is converted into hydrophobic species at the organic-aqueous interphase and transferred into the organic phase. The extraction of a metal ion involves the substitution of water molecules present in the hydrated metal ion with extractant molecules and neutralization of the charge on the metal ion followed by the transfer of metal-extractant complex into the organic phase. The extractants are classified into acidic, basic, neutral and chelating extractants based on the nature of complex formation between the extractant and the metal ion [81].

Alkyl phosphorous acids and monocarboxylic acids are classic examples for acidic or cationic extractants. They extract metal ions by means of cation exchange mechanism. Therefore, the extraction of metal ion takes place at lower acidity and the stripping of the metal ion is accomplished at higher acidity. The basic extractants or anionic extractants extract metal ions by ion-pair formation. Tri-*n*-octyl amine and tri-octyl methyl ammonium chloride commonly referred as alamine 336 and aliquat 336, respectively belong to the category of basic extractants. Alkyl triesters of phosphoric, phosphonic and phosphinic acids, and alkyl sulphoxides are examples of neutral extractants. TBP is a common example of neutral organophosphorous extractant that is extensively utilized in various solvent extraction processes carried out in nuclear industry. Metal ions are extracted by neutral extractants through solvation mechanism, where the neutral inorganic species are solvated with the neutral extractant by the formation of addition complex which are more soluble in the organic phase. Hydroxyoximes and diketones belong to chelating extractants which complex metal ions by the formation of ring structures [82]. Thenoyl trifluoroacetone (TTA) and 5,8-diethyl-7-hydroxy-6-dodecanone oxime (LIX 63) are examples of chelating extractants.

### **1.7.6 Solvent extraction in various nuclear processes**

Solvent extraction is an important technique used in the nuclear industry for the separation and purification of various elements [74,83,84]. It is employed for the extraction of uranium and thorium from their ores. Solvent extraction is the key step in the reprocessing of spent nuclear fuel for the recovery of uranium and plutonium from the fission products. Separation of zirconium and hafnium which is considered to be challenging due to their similar chemical behaviour is executed successfully by solvent extraction technique. TBP, octyl(phenyl)-*N,N*-diisobutyl carbamoyl methyl phosphine oxide (CMPO), di-2-ethyl hexyl phosphoric acid (D2EHPA), 2-ethylhexyl 2-ethylhexyl phosphonic acid (PC88A), aliquat 336, alamine 336, TTA, tri-*n*-octyl phosphine oxide (TOPO) etc., are some of the extractants

employed for the processing of nuclear materials by solvent extraction. Chemical structures of some of the extractants commonly used in the extraction of nuclear materials are shown in Fig. 1.3.

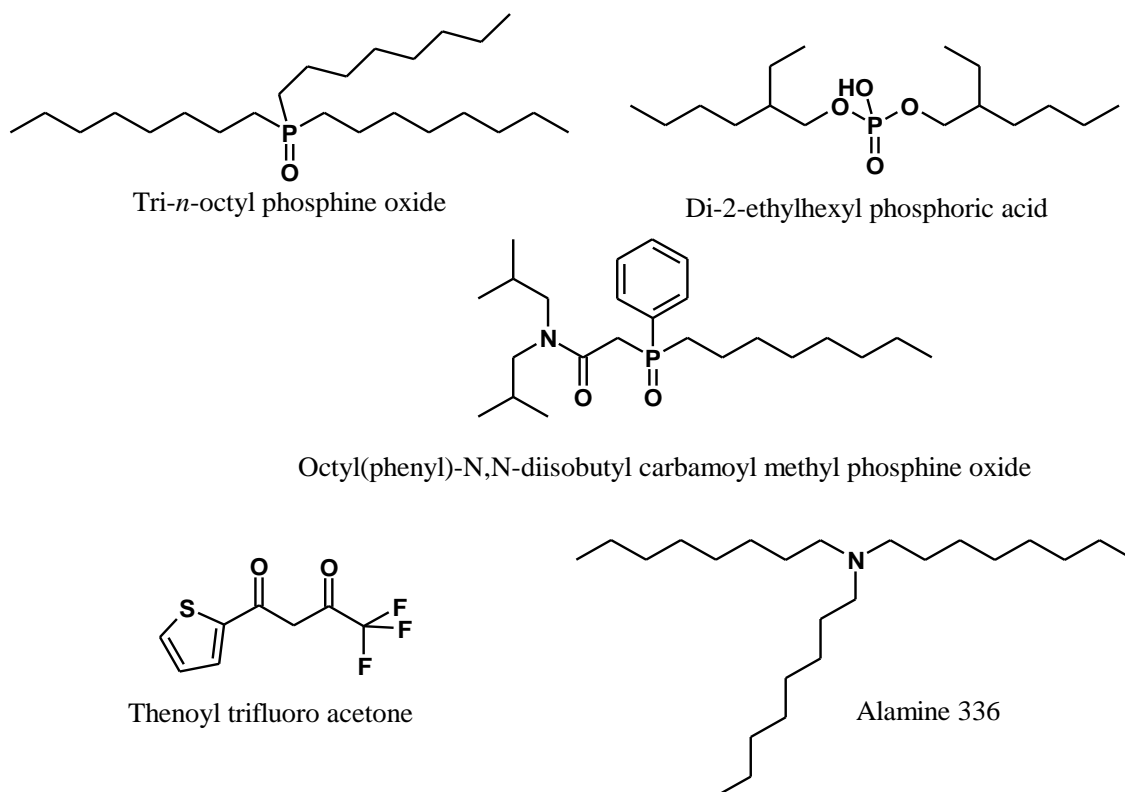


**Fig. 1.3:** Chemical structure of some of the extractants commonly used for the solvent extraction of nuclear materials.

### 1.8 Tri-*n*-butyl phosphate - A unique extractant of nuclear industry

Tri-*n*-butyl phosphate is a neutral organophosphorous extractant exploited to a maximum extent for the processing of nuclear materials. It is successfully utilized for several decades as an extractant owing to its advantages as mentioned below.

- i) It is non-toxic, inexpensive and easy to synthesize.
- ii) Due to its non-volatile nature with low vapour pressure, it can be handled without fire hazards.
- iii) Good extraction and stripping behaviour in nitric acid media.
- iv) It does not require any salting out agent other than nitric acid.

- v) It has good fission product decontamination factor.
- vi) It is quite stable in nitric acid media under reprocessing conditions.
- vii) The selectivity and extracting power of TBP can be adjusted by altering the TBP concentration.

## 1.9 Applications of tri-*n*-butyl phosphate

TBP is used for several processes such as processing of uranium and thorium ores, separation of uranium and plutonium from fission products in the spent nuclear fuels, U/Th, Zr/Hf and Nb/Ta separations. The details of various solvent extraction processes which are performed with TBP are listed as follows.

### 1.9.1 Uranium ore processing

The uranium ore is concentrated by removing sand particles followed by leaching. The leaching agent, acidity, extractant and its concentration, extraction and stripping conditions are chosen based on the chemical nature of the uranium ore. Nitric acid, sulphuric acid and sodium carbonate are generally used as leachant to remove uranium from its ore. Bis(2-ethylhexyl)phosphoric acid (HDEHP)-TOPO, trialkyl amine and TBP are commonly used as extractants to recover uranium from leach solution. High-grade pitchblende ores are leached with nitric acid solution followed by the solvent extraction of uranium with TBP [74]. Subsequently, the refining of crude uranium is performed with TBP in nitric acid medium. The pure uranyl nitrate obtained by solvent extraction is decomposed thermally to  $\text{UO}_3$ , reduced to  $\text{UO}_2$  and then converted to uranium tetrafluoride ( $\text{UF}_4$ ).  $\text{UF}_4$  is reduced with magnesium metal to obtain pure uranium metal.

### 1.9.2 PUREX process

The uranium and plutonium present in the spent nuclear fuel is universally recovered by PUREX process [76,85-88]. Earlier, diethyl ether, trigly, methyl isobutyl ketone (MIBK) and butex were used for the reprocessing of spent nuclear fuel. Although diethyl ether ( $\text{C}_2\text{H}_5$ -

O-C<sub>2</sub>H<sub>5</sub>) is capable of producing nuclear grade uranium it was least preferred due to the requirement of high concentration of salting agents and fire hazards. Trigly (Cl-C<sub>2</sub>H<sub>4</sub>-O-C<sub>2</sub>H<sub>4</sub>-O-C<sub>2</sub>H<sub>4</sub>-Cl) was used to recover only plutonium leaving behind uranium along with fission products and the chlorine released due to radiolysis of trigly caused corrosion of stainless steel. MIBK (CH<sub>3</sub>-CO-*i*C<sub>4</sub>H<sub>9</sub>) is highly soluble in water, has low flash point and requires Al(NO<sub>3</sub>)<sub>3</sub> as salting out agent as MIBK is unstable in concentrated nitric acid solutions. Butex (C<sub>4</sub>H<sub>9</sub>-O-C<sub>2</sub>H<sub>4</sub>-O-C<sub>2</sub>H<sub>4</sub>-O-C<sub>4</sub>H<sub>9</sub>) is highly viscous, requires salting out agents like NH<sub>4</sub>NO<sub>3</sub> and shows poor ruthenium decontamination. All these extractants were replaced with TBP owing to its superiority in various aspects as mentioned in section 1.8. The flow sheet for PUREX process is shown in Fig. 1.4.

The steps involved in PUREX process are briefly explained as follows.

- i) The irradiated fuel assemblies are dismantled, chopped and dissolved in boiling concentrated nitric acid in a stainless steel vessel.
- ii) The off-gases are treated, and the dissolved fuel solution is filtered and clarified.
- iii) The oxidation state of metal ions and acidity of the solution are adjusted to accomplish maximum decontamination factor.
- iv) The concentration of the solution is adjusted to prepare a feed suitable for the solvent extraction of metal ions by TBP.
- v) The extraction of U(VI) and Pu(IV) is performed with 30% TBP diluted in inert hydrocarbon diluent (1.1 M) from feed solution in 4 M HNO<sub>3</sub> medium and scrubbed with 3-4 M HNO<sub>3</sub> to remove undesirable metal ions from the loaded organic phase.
- vi) The valency of Pu(IV) is adjusted to Pu(III) to bring it to the aqueous phase for the separation of plutonium from uranium.
- vii) After the partitioning of plutonium from uranium, the uranium in the loaded organic phase is stripped using water or 0.01 M HNO<sub>3</sub>.

viii) The decontamination factor of  $10^6$  to  $10^8$  can be achieved by PUREX process.

ix) The high level waste (HLW) after U(VI) and Pu(IV) extraction is processed for storage or disposal.

x) The lean organic solution after the stripping of metal ions is washed with dilute sodium carbonate solution to remove the residual metal ions and degraded solvent, and the washed solvent is recycled.

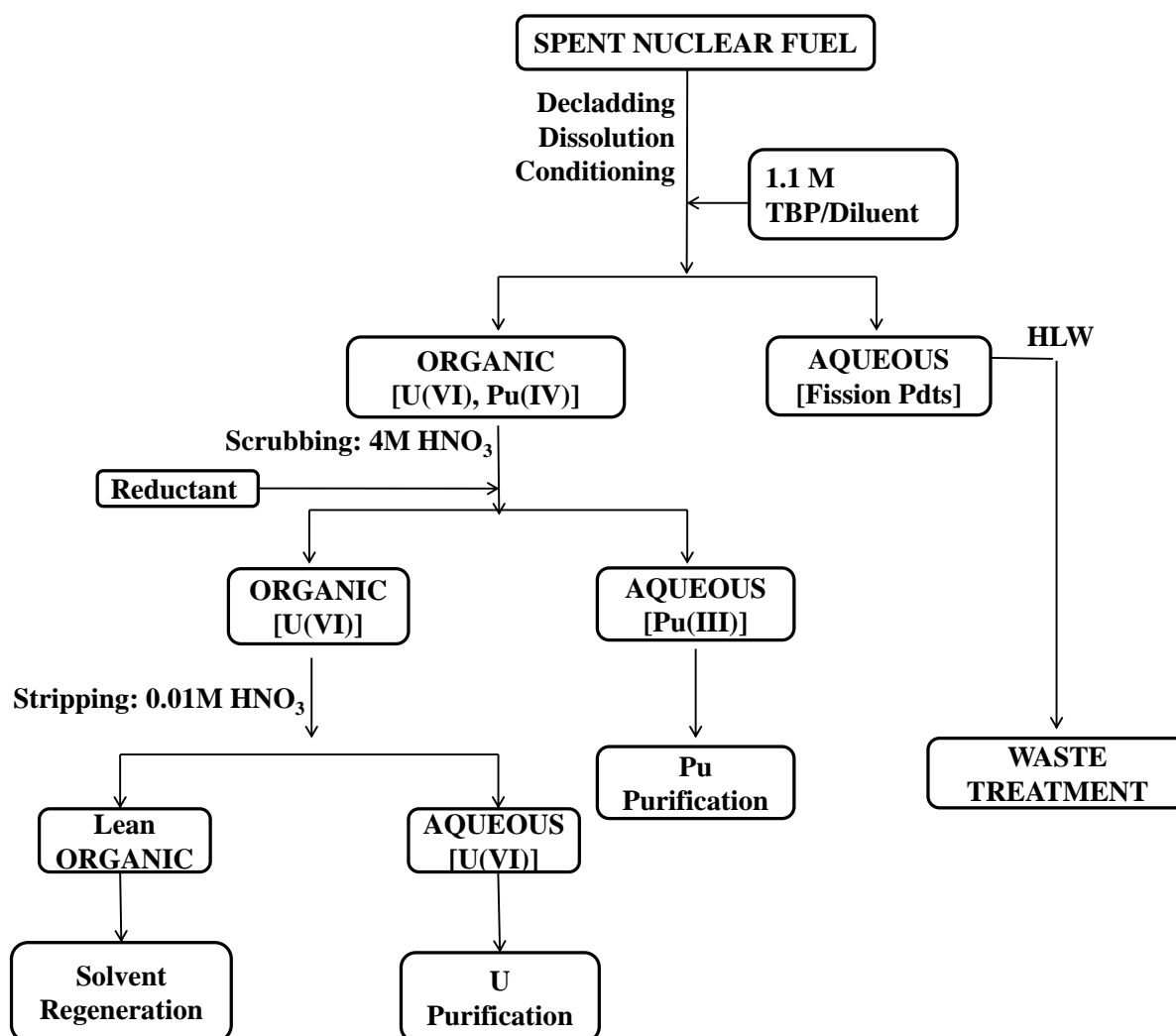


*Fig. 1.4: Flow sheet for the PUREX process.*

### 1.9.3 THOREX process

The separation of uranium and thorium from fission products is carried out by thorium-uranium extraction process commonly referred as THOREX process [89,90]. This process is used to separate  $^{233}\text{U}$  from irradiated  $^{232}\text{Th}$  targets and for the processing of spent U-Th nuclear fuel from high temperature gas cooled reactors. Unlike PUREX process, in THOREX process, the reduction of thorium is not feasible as thorium exists only in its stable +4 oxidation state in aqueous solutions. Furthermore, a higher organic to aqueous volume ratio is required for THOREX process in contrast to PUREX process as TBP forms third phase and the extractability of thorium by TBP is lesser than uranium and plutonium.

Thorium metal, thoria and urania-thoria fuels are dissolved in  $\text{HNO}_3$ -HF mixture. As a general practice, reprocessing plants use stainless steel vessels for the dissolution of spent fuels. To prevent the corrosion of stainless steel by HF,  $\text{Al}^{3+}$  has to be used. Generally, 13 M  $\text{HNO}_3$  - 0.05 M HF - 0.1 M  $\text{Al}(\text{NO}_3)_3$  mixture (commonly referred to as 'THOREX Reagent') is used for the dissolution of thorium based fuels. After the dissolution of fuel, the undissolved materials and the suspended solids are removed and the solution is clarified. Subsequently, the THOREX process is performed with either acid feed or acid-deficient feed. The acid deficient feed converts most of the troublesome fission products such as praseodymium, zirconium, niobium and ruthenium in the feed to hydrolyzed form which are least extractable by 30 % TBP in *n*-dodecane (*n*-DD). However, the fission products that are prone to hydrolysis precipitate in the acid deficient feed and the  $\text{Al}(\text{NO}_3)_3$  which is used as a salting out agent pose problem during waste management. These problems can be circumvented by a two-stage acid THOREX process where  $\text{HNO}_3$  acts as self salting agent instead of  $\text{Al}(\text{NO}_3)_3$  and the precipitation is prevented by using acid feed. In the first cycle, thorium and uranium are co-decontaminated from fission products and in the second cycle thorium and uranium are partitioned from the loaded organic phase. Initially thorium is

stripped from the loaded organic phase followed by uranium. The stripped solutions are further processed to enhance the purity of the elements.

#### **1.9.4 Monazite ore processing**

Monazite ore is the principal ore for thorium and rare earth elements as well as secondary ore for uranium. Typical concentrations of various components in the Indian monazite ore is shown in Table 1.6 [91]. The monazite ore, which exists in phosphate form, is subjected to sulfuric acid leaching or sodium hydroxide leaching methods depending on the chemical nature. Generally, the sodium hydroxide leaching method is preferred over sulfuric acid leaching method as the byproduct sodium phosphate can be recovered and used as fertilizers [92]. The hydroxide residue is then dissolved in acid solution and the metal ions are separated by solvent extraction. Amine extraction (Amex) process has been adopted for the recovery of uranium and thorium from rare earths solutions in sulfuric media [84]. In this process, initially thorium is extracted from the monazite leach solution by using a primary amine and later uranium can be extracted using a secondary amine. However, amines have low metal loading capacity, high crud formation tendency and there are also possibilities of amine entrainment in the aqueous phase. Some of the process plants utilize PC88A for the extraction of Th(IV) from monazite leach solution. TBP is utilized in several process plants for monazite ore processing. Thorium, uranium, cerium and cerium-free rare earth elements are recovered from monazite feed solution in 8 M HNO<sub>3</sub> by solvent extraction with TBP [93,94]. Solutions of TBP in a diluent are being used for the separation of uranium and thorium from rare earths in the processing of monazite ore [95,96]. Literature reports are also available on the separation and purification of individual lanthanides from monazite feed solutions by solvent extraction using TBP [97].

**Table 1.6: Concentration of various components present in the Indian monazite ore.**

Compounds	Ln <sub>2</sub> O <sub>3</sub>	ThO <sub>2</sub>	U <sub>3</sub> O <sub>8</sub>	P <sub>2</sub> O <sub>5</sub>	MgO	CaO	PbO	Al <sub>2</sub> O <sub>3</sub>	Fe <sub>2</sub> O <sub>3</sub>
Amount (%)	59	9	0.35	27	0.1	0.5	0.18	0.1	0.2

### 1.9.5 Zirconium-Hafnium separation

It is well known that the chemistry of zirconium is analogous to that of hafnium and consequently zirconium and hafnium always co-exist in nature. However, reactor grade materials demand hafnium free zirconium as the thermal neutron capture cross-section of hafnium is 600 times higher than that of zirconium. Zirconium metal used for nuclear applications is processed with stringent low level of hafnium content (Hf < 100 ppm). This necessitates the removal of hafnium from zirconium that is used in nuclear reactors. Globally, two methods are followed to separate zirconium from hafnium namely, MIBK - thiocyanate method and TBP - HNO<sub>3</sub> method [98,99]. Another method called hexone - thiocyanate process is employed for the separation of hafnium from zirconium.

TBP - HNO<sub>3</sub> method is followed in India for the production of reactor grade zirconium. The zircon is treated with molten sodium hydroxide to convert silica into water soluble sodium silicate and zirconium into insoluble zirconium hydroxide. Removal of silica from the ore is the crucial step as the unreacted silica forms gelatinous mass during the preparation of feed solution for solvent extraction. Subsequent to complete removal of silica the precipitate is dissolved in nitric acid and diluted to prepare the feed solution suitable for the solvent extraction of zirconium. Zirconium is extracted from the feed solution using 60% TBP in a diluent leaving behind hafnium and other impurities in the aqueous phase which is further treated for the recovery of hafnium. In general, a nitric acid concentration of 4-5 M is chosen as the feed solution acidity for Zr(IV)/Hf(IV) separation due to higher separation factor of Zr(IV) from Hf(IV) ( $\beta_{Zr(IV)/Hf(IV)}$ ) in this range of nitric acid concentration. The

zirconium loaded organic phase is scrubbed with nitric acid to achieve the desired decontamination factor from hafnium and stripped with dilute nitric acid. However, this process has also been modified with 33% TBP/*n*-DD and is being employed in zirconium sponge production plants in India.

### **1.9.6 Other applications**

TBP is also used for the extraction of several metal ions such as scandium, titanium, vanadium, chromium, molybdenum, tungsten, manganese, cobalt, iron, copper, silver, gold, iridium, osmium, palladium, rhodium, rhenium, ruthenium, yttrium, aluminium, gallium, indium, thallium, tin, lead, germanium, silicon, arsenic, antimony, bismuth, selenium, tellurium etc [97]. Similar to zirconium and hafnium, niobium and tantalum also have comparable ionic radii due to the consequence of lanthanide contraction and TBP aids in achieving successful separation of these elements. TBP is used in the production of synthetic resins, hydraulic fluids, adhesives and flame retardants. It is also used as an anti-foaming agent in detergent solutions.

### **1.10 Limitations of tri-*n*-butyl phosphate**

Even though TBP has several advantages, it possesses some limitations and are elaborated in following sections.

#### **1.10.1 Red oil formation**

Red oil formation takes place due to the solubility of TBP in water which is approximately 0.4 g/L at room temperature [100]. Though this value seems to be small there is a concern when the aqueous metal nitrate products are concentrated in an evaporator. During the evaporation of aqueous waste solution the dissolved TBP reacts with nitric acid and residual uranium, plutonium and thorium nitrates at higher temperature to form dense dark brown liquid commonly known as red oil. Decomposition of red oil can lead to explosive thermal run away reactions. Many accidents have been reported worldwide mostly

during the evaporation of aqueous solution in an evaporator due to red oil formation [101,102]. Moreover, the thermal and chemical degradation of TBP dissolved in aqueous solutions leads to the formation of phosphate residue which increases the volume of the waste and affects waste management activities.

### 1.10.2 Degradation

TBP undergoes chemical, thermal and radiation degradation [103-106]. The chemical and thermal degradation products of TBP are mostly dibutyl phosphate (DBP), monobutyl phosphate (MBP), phosphoric acid and butyl alcohol. In addition to above mentioned degradation products, the radiation degradation products of TBP include ketones, aldehydes, alkanes, alkenes, nitro compounds etc [105]. Among the various degradation products mentioned above DBP and MBP interfere seriously in the process of solvent extraction. Presence of these degradation products in the aqueous phase increases the distribution ratio of metal ions such as U(VI), Th(IV) and Pu(IV) at lower acidities and thereby the stripping of the extracted metal ions becomes complicated. In the presence of Zr(IV), dibutyl phosphate forms a white insoluble crud of Zr-DBP and settles at the organic-aqueous interface which interrupts the phase separation and increases the phase disengagement time. The degradation products also have high affinity towards fission products such as ruthenium and technetium that leads to poor decontamination factor. The physico-chemical properties of a solvent are severely influenced even at low concentration of degradation products [107]. In a nutshell, it can be mentioned that the degradation of the solvent reduces the fission product decontamination, increases the retention of actinides by the organic phase, alters the hydrodynamics of solvent extraction processes and delays the separation of mixed organic-aqueous phases.

### 1.10.3 Third phase formation

Third phase formation is a typical phenomenon in solvent extraction processes where the loading of metal ion or mineral acid beyond a threshold concentration, known as limiting organic concentration (LOC) splits the homogenous extractant-diluent solution into third phase (TP) and diluent-rich phase (DP). Figure 1.5 schematically shows the organic phase during third phase formation by TBP/alkane in the extraction of metal ion in nitric acid media above and below/at LOC. The picture of organic and aqueous phases after phase splitting during the extraction of Th(IV) by 1.1 M TBP/*n*-DD from Th(NO<sub>3</sub>)<sub>4</sub> solution in 1 M HNO<sub>3</sub> is shown in Fig. 1.6. The third phase or extractant-rich phase is a dense viscous organic phase rich in solutes and extractant, and deficient in diluent. The diluent-rich phase or the light organic phase is less dense than third phase with little solutes and extractant, and immense diluent.

The organic phase splitting behaviour of TBP with tetravalent metal ions such as Pu(IV), Th(IV), Zr(IV) etc., severely affects the solvent extraction processes [108-111]. The mixing of organic and aqueous phases as well as mass transfer between these phases become difficult due to the formation of a highly viscous third phase. Solvent extraction equipments are employed in PUREX plants for continuous large scale solvent extraction processes. Third phase formation can lead to flooding in solvent extraction equipments like pulsed columns, centrifugal extractors and mixer-settlers which are designed to handle only two phases. An accidental assembling of fissile materials like plutonium above critical mass in a small volume of third phase poses criticality threat in reprocessing plants. Since the plutonium content in PHWR fuel is less, the concentration of plutonium in the loaded organic phase is also less and the third phase formation is not a serious issue in the reprocessing of spent PHWR fuels. However, it is of prime concern in fast reactor fuel reprocessing due to high plutonium content of almost 200g/kg of irradiated fuel [112].

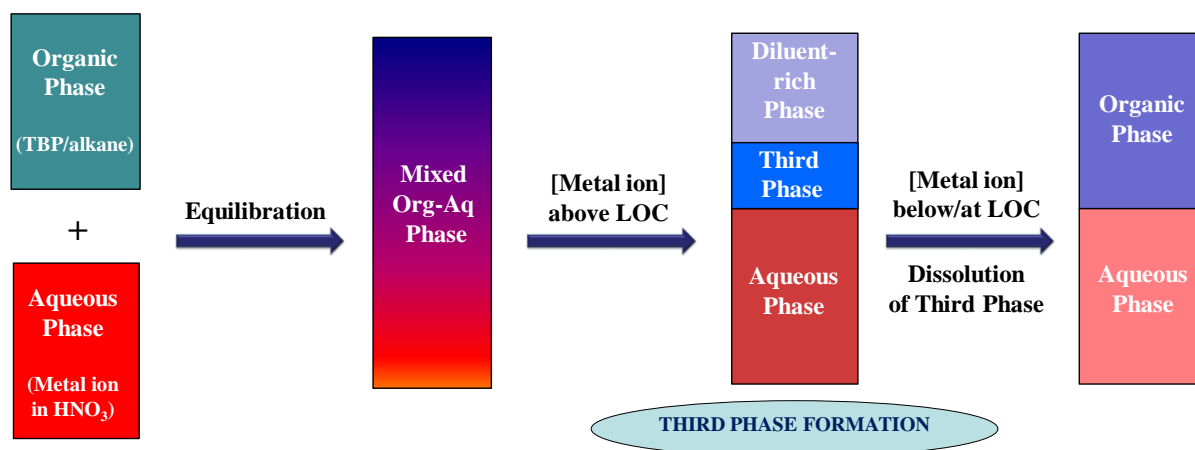


*Fig. 1.5: Schematic representation of third phase formation phenomenon.*

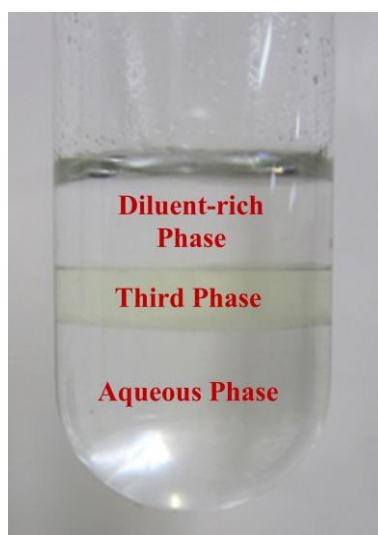


*Fig. 1.6: Third phase formation in 1.1 M TBP/n-DD - Th(NO<sub>3</sub>)<sub>4</sub>/1 M HNO<sub>3</sub> system.*

Modifications can be incorporated in solvent extraction flow sheets and conditions to avoid third phase formation, but this could lead to new technical issues. Generally, third phase formation can be prevented by using dilute feed solutions. Since the significant heavy metal loading of the organic phase cannot be attained with dilute feed solutions, the availability of free extractant enhances the extraction of undesirable metal ions and reduces the decontamination factor. The need to process large volume of solutions with diluted feed

solutions results in low process throughput. Another option to avert third phase is to deploy long chain alcohols or other polar compounds as modifiers [113] which reduce metal extraction and change physico-chemical properties of the solvent. It can also be avoided by formulating solvent with aromatic diluents [114] which are however susceptible for nitration and have low flash points. Third phase formation can also be avoided by maintaining the solvent extraction system at higher temperature around 60°C. However, maintaining huge volume of solution at higher temperature is commercially not viable, especially in a radioactive environment and favours the degradation of TBP.

### **1.11 Insights into third phase formation phenomenon**

Third phase formation is an undesirable phenomenon during solvent extraction which remains less understood. A good understanding of organic phase splitting behaviour is crucial in order to avoid third phase formation. Several parameters such as nature of diluent, acid, modifier, metal ion, extractant and their concentrations, and temperature influence third phase formation. Earlier, third phase formation studies were focussed mainly on the determination of third phase formation limits under various conditions as these data are required for process flow sheet development. A large number of publications are available in the literature on the determination of LOC and critical aqueous concentration (CAC) as a function of various parameters for different solvent extraction systems [111,115,116].

Review articles reported in the literature with respect to third phase formation give some insight into this behaviour [110,111]. Several attempts have been made to investigate the third phase formation phenomenon at the molecular level based on the principles of colloidal chemistry [117-119]. Techniques such as small angle x-ray scattering (SAXS), small angle neutron scattering (SANS), dynamic light scattering (DLS), vapour pressure osmometry (VPO), nuclear magnetic resonance (NMR) spectroscopy, infrared (IR) spectroscopy and mass spectrometry have been used to probe the third phase formation

tendency in various extractants such as TBP, CMPO, di-isoamylmethyl phosphonate, trialkyl phosphine oxide, N,N-dihexyl octanamide (DHOA) and malonamides [120-141].

Osseo-Asare highlighted the similarities in the properties of extractant molecules with surfactant molecules [117-119]. Due to the surface active properties of extractants, under certain conditions the extractant molecules and the extracted solutes in the organic phase reorganize into small reverse micelles with low free energy of micellization. Lefrancois et al. [120] and Erlinger et al. [126] have made an attempt to predict third phase formation by using Flory-Huggins theory of polymer solution and standard liquid theory, respectively. To understand the synergetic extraction properties of multi component extractants, Ellis et al. [127] probed the macroscopic phase behaviours of two extractants, TBP and di-*n*-butyl phosphoric acid in *n*-dodecane, using SAXS. This study reveals that the aggregate morphologies of the mixed extractant systems are not simple linear combinations of the individual species and the use of multi component extractant can yield a synergistic extraction.

Ferraro et al. studied the IR spectra of nitric acid loaded 0.73 M TBP/*n*-octane and found the predominant existence of hemisolvate complex of TBP with nitric acid (TBP·2HNO<sub>3</sub>) at high nitric acid loading in the organic phase [131]. IR and NMR spectroscopic studies provide evidence for the formation of molecule-ion complexes (hydronium ion) during the aggregation of species in the organic phase for the extraction of mineral acids by TBP in *n*-heptane [131,135]. Mass spectrometric study on the organic solutions obtained after the extraction of Th(NO<sub>3</sub>)<sub>4</sub> by 1.1 M TBP/*n*-dodecane in nitric acid media substantiates the aggregation of species in the third phase [136].

The effect of alkyl chain length and diluent chain length on the third phase formation tendency of malonamides in the extraction of nitric acid was investigated using SAXS, SANS and VPO by Berthon et al. [137]. Their studies revealed that decrease in alkyl chain length of

malonamides and increase in diluent chain length favours third phase formation. Similar results were also observed by Suresh et al. in the case of trialkyl phosphates [115,116]. Studies carried out by Borkowski et al. showed that the third phase is formed when the attractive force between reverse micelles overcomes the average thermal energy of the molecules present in the organic phase [139]. The scattering studies based on Baxter's sticky hard-sphere model [142] confirmed the extensive aggregation of species present in the organic phase into reverse micelles before organic phase splitting [121,126]. Interpretation of SANS results based on Baxter's model correlated the higher third phase formation tendency of TBP with the higher charge to size ratio of metal ions extracted by TBP [124]. Studies carried out by Dejugnat et al. on the extraction of monoacids by malonamides unveiled that the formation of third phase is driven by the hydration enthalpy of monoacids [128].

### **1.11.1 Interpretation of third phase formation - Particle growth model**

The results obtained from scattering based experiments on third phase formation phenomenon were originally elucidated by using particle growth model. According to this model the solute-extractant complexes extracted into the organic phase of TBP aggregate into reverse micelles due to the limited solubility of these complexes in diluent. A trialkyl phosphate molecule can be viewed as a surfactant molecule with P=O group as the polar head group and alkyl chains as the non-polar tail groups [122]. In general, trialkyl phosphate molecules stabilize polar molecules in a non-polar medium by forming reverse micelles in which polar molecules present at the core are surrounded by the P=O group of trialkyl phosphate molecules and non-polar alkyl groups of the extractant interact with the non-polar medium. It is well established in extractant-diluent system that even below LOC there is an organization of metal-solvates into smaller reverse micelles in organic phase to stabilize the polar species in non-polar medium [122]. An increase in the extraction of the solutes into the organic phase enhances the concentration of solute-extractant complexes and assists

micellization of the extracted species in the organic phase. This favours the incorporation of polar species into the core of the reverse micelles and promotes the coalescence of smaller reverse micelles into larger reverse micelles. The formation of such larger reverse micelles leads to the third phase formation.

This model used scattering data to compute the aggregation number of reverse micelles formed in the organic phases during third phase formation. The aggregation numbers calculated based on this model are too high to be expected for a solvent extraction system with trialkyl phosphates. The interfacial tension of solute loaded organic solutions of TBP was measured to confirm the non-existence of such large reverse micelles. The study revealed that TBP exhibits only moderate surfactant properties and large reverse micelles with high aggregation numbers cannot be expected [122]. The discrepancy in the aggregation number computed by this model arises due to the assumption that each particle behaves ideally without any interaction with neighbouring particles, which becomes invalid at high concentrations. In reality, interactions among particles cannot be ignored and therefore scattering data must be interpreted based on a new model which takes into consideration of all possible interactions.

### 1.11.2 Interpretation of third phase formation - Interparticle interaction model

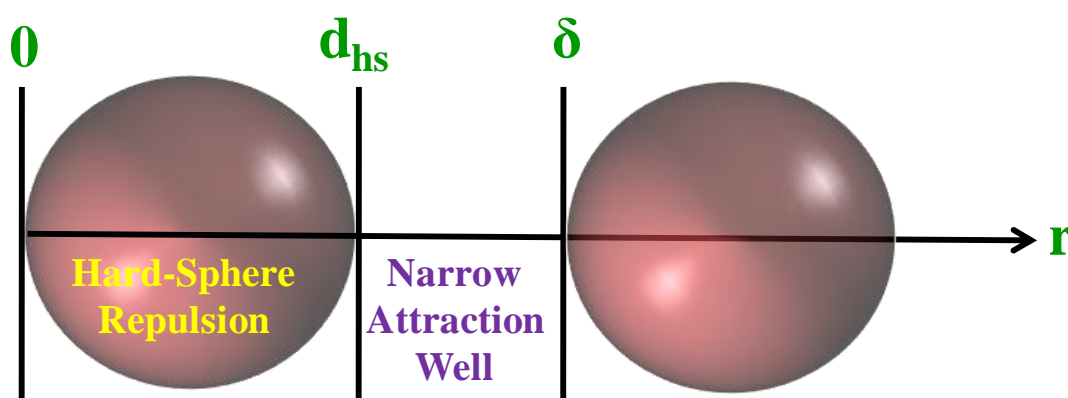


*Fig. 1.7: Schematic representation of interaction between reverse micelles using interparticle interaction model [122].*

The Baxter's sticky hard-sphere model forms the basis for the interparticle interaction model. The significance of this model lies in its ability to quantify short-range interactions between the aggregates using parameters such as potential energy of attraction and stickiness parameter [122]. According to the above model, a reverse micelle is considered as a hard sphere separated from another reverse micelle with a distance 'r'. The hard sphere diameter ( $d_{hs}$ ) is the distance from the origin below which the reverse micelle becomes incompressible. Schematic representation of interaction of particles explained based on Baxter's sticky hard-sphere model is shown in Fig. 1.7 [122]. The potential energy of attraction ( $U(r)$ ) between the hard spheres can be obtained from Eqs. (1.12) – (1.14).

$$U(r) = \infty \quad \text{for} \quad r < d_{hs} \quad (1.12)$$

$$U(r) = \lim_{\delta \rightarrow d_{hs}} \ln \left[ 12\tau \left( \frac{\delta - d_{hs}}{d_{hs}} \right) \right] \quad \text{for} \quad d_{hs} < r < \delta \quad (1.13)$$

$$U(r) = 0 \quad \text{for} \quad r > \delta \quad (1.14)$$

The above equations signify that two hard spheres attract each other when the distance between them is larger than  $d_{hs}$  and smaller than  $\delta$ . The interparticle attraction potential energy for small distance between hard spheres [ $(\delta - d_{hs})/d_{hs} \leq 0.1$ ] can be obtained from Eq. (1.13), where the stickiness parameter ( $\tau^{-1}$ ) gives the magnitude of adhesion between the hard spheres.

The aggregation number calculated by interparticle interaction model for TBP based solvents is around 3 to 4 which is expected when TBP based solvents undergo aggregation. As this model gives a more quantitative picture of the interaction between reverse micelles in the organic phase, this model is preferred to study the effects of various parameters on third phase formation using scattering based techniques. Schematic representations of reverse

micelles modelled using interparticle interaction model and particle growth model are shown in Fig. 1.8 [122].

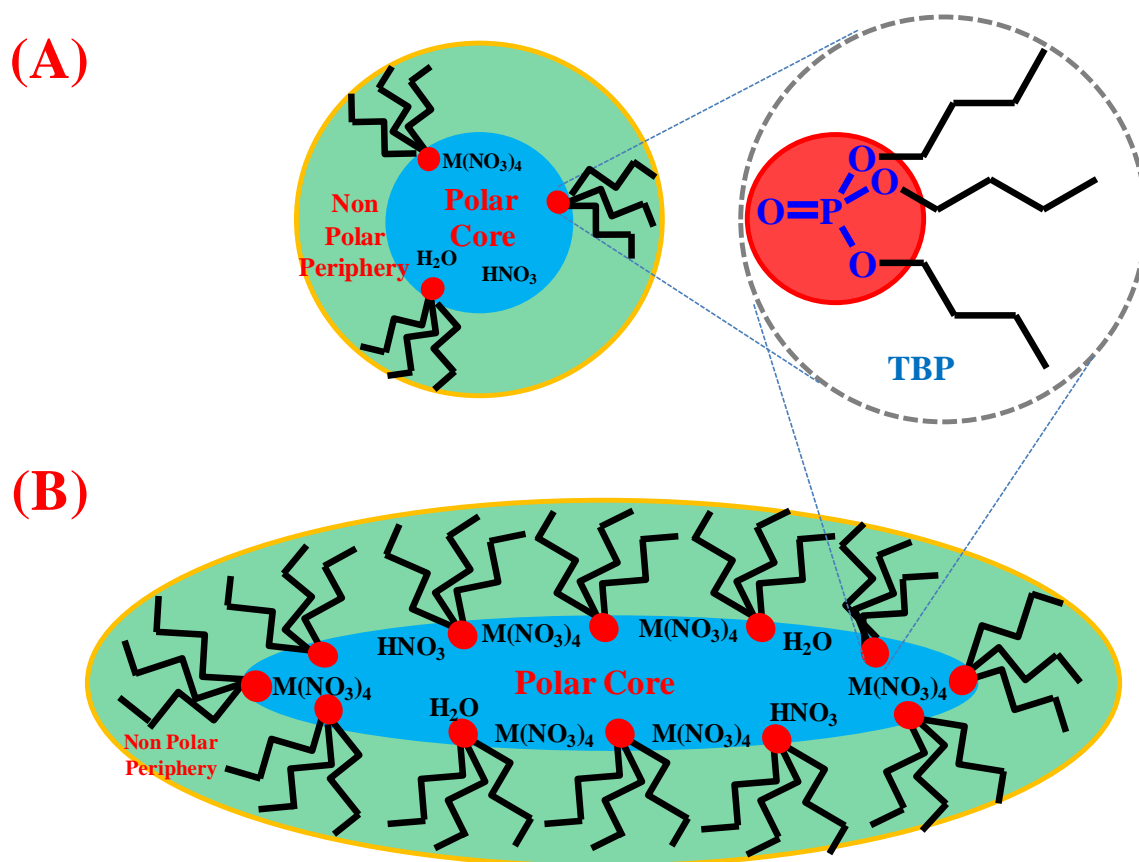


*Fig. 1.8: Schematic representation of reverse micelles formed during third phase formation interpreted by (A) Interparticle interaction model (B) Particle growth model [122].*

### 1.12 Alternate extractants for tri-*n*-butyl phosphate

The practical difficulties associated with the application of TBP for solvent extraction processes necessitate exploring an alternate extractant to TBP. Several extractants have been investigated by many researchers for the extraction of actinides. Pioneering work by Siddall on the extraction of uranium, plutonium and neptunium by symmetrical trialkyl phosphates revealed identical extraction behaviour among these extractants [143]. He specified that the extraction of Th(IV) is suppressed by bulky alkyl substituents of the symmetrical trialkyl phosphates due to steric hindrance. Siddall also reported that the effects of change in alkyl substituents of symmetrical trialkyl phosphates and phosphonates on the extraction of U(VI)

and Th(IV) are comparable [144]. Investigations on the extraction of uranium and plutonium by unsymmetrical trialkyl phosphates, phosphonates, phosphinates and phosphine oxides showed that the extraction of actinides is enhanced with increase in basicity of the phosphoryl group [145]. Studies carried out by Burger showed a decrease in the extraction of actinides by neutral organophosphorous extractant with electronegative alkyl substituents [146]. Healy et al. investigated the rate of extraction of uranium by neutral organophosphorous extractants and proposed a mechanism for the extraction [147,148]. The extraction and third phase formation tendency of tricyclohexyl phosphate with U(VI) and Th(IV) in nitric acid media was investigated by Rao et al. [149].

Besides organophosphorous extractants, several amide based extractants were also examined for the extraction of actinides [150]. Amides have low aqueous solubility, innocuous radiolysis degradation products, and are easy to synthesize and purify [151]. In contrast to organophosphorous extractants, amides are incinerable into gaseous products [152]. However, amides are viscous and have high tendency to form third phase during the extraction of actinides [153,154]. Some of the lower members of amide family of extractants form third phase even with nitric acid solutions.

The P=O group of TBP molecule is responsible for the metal ion extraction and hence to retain the favourable extractive properties of TBP it is worthwhile to explore alternate extractant in the same phosphate family of extractants. In this context, Suresh et al. investigated the extraction and third phase formation behaviour of various symmetrical trialkyl phosphates with respect to metal ions such as U(VI), Th(IV) and Pu(IV) as a function of diluent chain length, temperature, equilibrium aqueous phase metal ion and nitric acid concentrations, etc [115,116,155]. The results indicated that an increase in the chain length and branching of the alkyl substituents near the co-ordination site of a symmetrical trialkyl phosphate decrease the third phase formation tendency of the extractant [156]. The mutual



avoided in the case of *TiAP* based solvent systems. The chemical structure of *TiAP* and TBP are shown in Fig. 1.9.

#### 1.14 Literature survey on tri-*iso*-amyl phosphate

In contrast to TBP on which there is a large volume of literature, only limited literature data are available on *TiAP*. The extraction of U(VI) and Pu(IV) by 1.1 M solutions of *TiAP* and TBP in *n*-DD as a function of equilibrium aqueous phase nitric acid concentration reported by Suresh et al. showed a marginal increase in the distribution ratio of U(VI) and Pu(IV) for *TiAP* as compared to TBP [115]. Data on the LOC and CAC values for the extraction of Th(IV) by *TiAP* based solvents with respect to extractant concentration, temperature, nature of diluent and equilibrium aqueous phase acidity were also reported by Suresh et al. [116]. Extraction of scandium by *TiAP* from nitric acid, hydrochloric acid and perchloric acid media was evaluated by Kostikova et al. [159,160]. Studies performed by Prasanna et al. showed that the extraction of nitric acid by *TiAP* and TBP are comparable under identical conditions [161]. The studies carried out by Hasan et al. on the effect of solvent degradation due to acid hydrolysis, radiation effect, decontamination factor and phase separation showed that *TiAP* is a better extractant as compared to TBP [162].

Sahoo et al. determined the enthalpy of extraction of U(VI) by 0.55 M and 1.1 M solutions of *TiAP* in *n*-DD as a function of equilibrium aqueous phase nitric acid concentration ( $[\text{HNO}_3]_{\text{aq,eq}}$ ) by second law method [163]. The calorimetric studies carried out on the thermal decomposition of *TiAP* - nitric acid systems indicated that in terms of thermal degradation the performance of *TiAP* is either similar to TBP or sometimes better [164]. Thermodynamic parameters such as enthalpy, entropy and free energy changes during the extraction of U(VI), Th(IV) and Pu(IV) by 1.1 M *TiAP/n*-DD were reported by various authors [165,166]. Srinivasan et al. reported that the enthalpy change for the extraction of americium by 0.55 M *TiAP/n*-DD is exothermic and lower than that of 0.55 M

TBP/*n*-DD [167]. Das et al. reported that in contrast to TBP, the red oil formed by TiAP showed no sign of exothermic event while heating from 30°C to 200°C and concluded that TiAP is safer than TBP [168].

Balamurugan et al. measured the dispersion number, which is the measure of settling and coalescing property of a solvent, for 36% TiAP in *n*-DD and 100% TiAP [169]. Physical properties such as density, viscosity and interfacial tension of binary solutions of TiAP in *n*-DD were measured as a function of mole fraction of TiAP and gamma absorbed dose by Singh et al. [170]. Data on the vapor pressure of TiAP over a wide range of temperature have been reported by Muthukumar et al. [171]. Studies carried out by Sreenivasulu et al. showed that the distribution ratios of  $Zr^{4+}$ ,  $RuNO^{3+}$ ,  $TcO_4^-$ ,  $La^{3+}$ ,  $Ce^{3+}$ ,  $Nd^{3+}$  and  $Am^{3+}$  for their extraction by 1.1 M TiAP/*n*-alkane are lower or comparable with that of 1.1 M TBP/*n*-alkane [172]. The extraction of various elements from simulated HLW in 3 M  $HNO_3$  by 0.4 M TiAP/*n*-DD revealed that the fission products extraction by TiAP is negligible [173]. Nikiforov et al. reported the application of TiAP based solvents for the reprocessing of high burn up short cooled fast reactor fuels [174]. The feasibility of using TiAP as an alternate extractant to TBP for fast reactor fuel reprocessing was demonstrated by loading uranium under high solvent loading conditions as well as by separating U(VI) and Pu(IV) from Am(III) and trivalent lanthanides using ejector mixer-settler [175,176].

### 1.15 Scope of the present work

The literature survey on TiAP showed that most of the reported work focussed on the utilization of TiAP for fast reactor fuel reprocessing. A few preliminary studies were mentioned on the utilization of TiAP for thorium extraction owing to its lesser third phase formation tendency. Literature reports on the feasibility of using TiAP for the separation of zirconium and hafnium are few and scarce. The extraction studies on TiAP were carried out either with pure metal ion solutions mostly at high concentrations or with mixture of metal

ions in trace quantities. Some of the experiments were performed with low TiAP concentrations [173]. The actual extractant concentrations used in the process plants for the extraction of metal ions are usually high and the organic phase is often loaded with metal ions under high solvent loading conditions. In order to evaluate the viability of using TiAP for solvent extraction processes, the extraction of metal ions have to be studied under such process conditions. The work reported in this thesis investigates the extraction and third phase formation tendency of metal ions with TiAP and TBP based solvents under such conditions. The present work mainly focus on the feasibility of using TiAP for monazite ore processing and zirconium-hafnium separation under the process conditions generally followed in plants.

In general, the extraction of actinides by neutral organophosphorous extractants such as TiAP and TBP is performed at higher aqueous phase acidity and the stripping is executed at lower aqueous phase acidity. Therefore, adjustment of free acidity in solutions of actinides is essential to formulate the solvent extraction processes. When an organic phase loaded with metal ions and  $\text{HNO}_3$  is subjected to stripping operation, both get stripped and the concentration of the acid present in the organic phase decides the stripping efficiency. Therefore, precise determination of organic phase acidity is essential. Hence, a method adopted for free acidity determination in the present study by using a mixture of potassium oxalate and sodium fluoride for complexing U(VI) has been validated by comparing the data generated in the present study with literature data available for TBP under identical conditions. Also, the interference of U(VI), Th(IV) and Nd(III) in the presence of each other during their analyses by titrations has been authenticated in the concentration range used in the present study to account for the reliability of the analytical methods.

The batch extraction of U(VI) by 1.1 M TiAP/*n*-DD from uranyl nitrate solutions in nitric acid media has been investigated as a function of metal loading and equilibrium

aqueous phase acidity which is required for optimizing process flow sheets for the extraction of uranium in reprocessing plants. The scrubbing and stripping nature of U(VI) loaded organic phase (near theoretical metal loading) for *TiAP* and TBP has also been compared. The stripping behaviour of *TiAP* and TBP loaded with U(VI) and HNO<sub>3</sub> has been studied as a function of time to understand the effects of nitric acid induced degradation on stripping.

In order to compare the third phase formation behaviour of *TiAP* and TBP, the effect of parameters such as diluent chain length, equilibrium aqueous phase acidity and Th(IV) concentrations on the organic phase splitting behaviour of *TiAP* and TBP especially in three phase region have been investigated. Extraction isotherms for the extraction of Th(IV) and HNO<sub>3</sub> have been generated with respect to equilibrium aqueous phase Th(IV) concentration ( $[\text{Th(IV)}]_{\text{aq,eq}}$ ). Besides, difference in density between the third phase and the diluent-rich phase as well as the diluent-rich phase and the pure diluent, ratio of volume of the diluent-rich phase to that of the third phase have also been determined over a wide range of  $[\text{Th(IV)}]_{\text{aq,eq}}$  in the triphasic region.

Novel methods have been developed for the determination of TBP concentration after organic phase splitting based on the linear relationships of some of the properties of the solvent with TBP concentration in the solvent. An attempt has been made to theoretically predict the concentration of extractant present in the diluent-rich phase and third phase from the Th(IV) concentrations in the corresponding organic phases and the results have been verified by experiments.

The third phase formation tendency of organic solutions (*TiAP* and TBP in *n*-DD) used for the extraction of U(VI) and Th(IV) from monazite feed solution in nitric acid media has been investigated. Separation of U(VI) and Th(IV) from Nd(III) in nitric acid media with solutions of *TiAP* in *n*-DD has been studied by batch extraction in cross-current mode to

evaluate the feasibility of employing TiAP as an alternate extractant to TBP for monazite ore processing.

Distribution ratios for the extraction of Zr(IV) and Hf(IV) as well as third phase formation limits for the extraction of Zr(IV) by solutions of TiAP and TBP *n*-DD have been measured as a function of  $[\text{HNO}_3]_{\text{aq,eq}}$ . The organic phase splitting nature of 1.1 M solutions of TiAP and TBP in *n*-DD and *n*-tetradecane in the extraction of  $\text{Zr}(\text{NO}_3)_4$  from nitric acid media has been investigated as a function of equilibrium aqueous phase Zr(IV) concentration ( $[\text{Zr}(\text{IV})]_{\text{aq,eq}}$ ). The amount of the constituents (e.g.  $\text{Zr}(\text{NO}_3)_4$ ,  $\text{HNO}_3$ , water and extractant) of the organic phase in biphasic and triphasic regions at different  $[\text{Zr}(\text{IV})]_{\text{aq,eq}}$  was determined and correlated with the third phase formation tendency of TiAP and TBP. The third phase formation behaviour of TiAP and TBP based solvents have also been evaluated with concentrated and dilute feed solutions with the ratio of Zr(IV) to Hf(IV) identical to the feed solutions used in the Zr(IV)-Hf(IV) separation plants. The aggregation behaviour of 1.1 M solutions of TiAP and TBP in  $\text{C}_{12}\text{D}_{26}$  diluent has also been compared by using SANS technique.



# Chapter 2



**“By seeking and blundering we learn”**

*-Johann Wolfgang Von Goethe*

## EXPERIMENTAL

---

This chapter describes the experimental procedures employed in the present work, and about the chemicals, reagents, materials and instruments used for carrying out the experiments. Preparation of feed solutions, indicator solutions, buffer solutions, stock solutions, standard solutions and organic solutions are elaborated. The analytical methods used in the present study are also discussed in detail.

### 2.1 Chemicals

#### Acids

Nitric acid, hydrofluoric acid, perchloric acid, phosphoric acid, sulphamic acid, sulphosalicylic acid and sulphuric acid (all acids are of AR grade) obtained from M/s. Merck, India were used for the experiments. Hydrochloric acid (GR grade) procured from M/s. Fischer Chemicals, India was used as received. Acetic acid and formic acid (both AR grade) supplied by M/s. Ranbaxy Fine Chemicals, India was used as such without any purification.

#### Ammonium hydroxide ( $\text{NH}_4\text{OH}$ )

$\text{NH}_4\text{OH}$  (AR grade) procured from M/s. Merck, India was used as received.

#### Ammonium molybdate

Ammonium molybdate (AR grade) obtained from M/s. Fischer Inorganics and Aromatics, India was used.

***iso*-Amyl alcohol**

*iso*-Amyl alcohol (98% Pure) received from M/s. Lancaster, England was used as such for the synthesis of TiAP.

**Arsenazo-I**

Arsenazo-I indicator (AR grade) procured from M/s. Merck, India was used as received.

**Barium diphenylamine sulphonate**

Barium diphenylamine sulphonate (AR grade) supplied by M/s. Merck, India was used as the indicator in Davies-Gray method.

**Borax**

Borax (AR grade) obtained from M/s. Sarabhai Chemicals, India was used as such without purification.

**Deuterated *n*-Dodecane (*n*-C<sub>12</sub>D<sub>26</sub>)**

*n*-C<sub>12</sub>D<sub>26</sub> (98 atom% D) procured from M/s. Armar Chemicals, Switzerland was used as such for SANS experiments.

**Diethylene triamine pentaacetic acid (DTPA)**

DTPA (AR grade) obtained from M/s. Lancaster synthesis Ltd., England was used for the analysis of thorium.

**Disodium hydrogen phosphate**

Disodium hydrogen phosphate (AR grade) was received from M/s. Sarabhai Chemicals, India and used as received.

**Disodium salt of ethylene diamine tetraacetic acid (EDTA)**

EDTA (AR grade) purchased from M/s. Ranbaxy Fine Chemicals, India was used for the complexometric titration of metal ions.

### **Ethanol**

Ethanol (AR grade) procured from M/s. Shymlakhs International, UK was used as such without any purification.

### **Ferrous ammonium sulphate**

Ferrous ammonium sulphate (AR grade) received from M/s. Merck, India was used as such without purification.

### **Hafnium oxide**

Hafnium oxide (with ~0.04% of zirconium) purchased from M/s Beijing Cerametek Materials Co. Ltd., China was used for the extraction studies.

### ***n*-Heptane**

*n*-Heptane obtained from M/s. Ranbaxy Fine Chemicals, India was used as reaction medium for the synthesis of TiAP.

### **Hexamethylenetetramine (HMTA)**

HMTA (AR grade) supplied by M/s. Riedel-de Haen, Switzerland was used as received.

### **Hydrocarbon diluents**

Various linear chain alkane diluents such as *n*-decane, *n*-dodecane, *n*-tetradecane, *n*-hexadecane, and *n*-octadecane, each with 99% purity procured from M/s. Lancaster Synthesis Ltd. (England), M/s. Alfa Aesar Ltd. (UK) and M/s. Fluka Chemicals (Switzerland) were used for the preparation of organic solutions.

### **Karl Fischer solution**

Pyridine-free Karl Fischer solution obtained from M/s. Merck Specialities Pvt. Ltd., India was used for the estimation of water.

### **Lead nitrate**

Lead nitrate (AR grade) procured from M/s. Ranbaxy Fine Chemicals, India was used in the complexometric titration of Nd(III).

### **Neodymium oxide**

Neodymium oxide (~99% Pure) obtained from Indian Rare Earths Ltd. (IREL), India, was used as such to prepare neodymium nitrate solution by dissolving it in appropriate quantity of concentrated nitric acid.

### **Phenolphthalein**

Phenolphthalein (AR grade), supplied by M/s. Merck Specialities Pvt. Ltd., India was used as received.

### **Phosphorous oxychloride (POCl<sub>3</sub>)**

POCl<sub>3</sub> (98% Pure) received from M/s. Merck, India was used for the synthesis of TiAP.

### **Potassium dichromate**

Potassium dichromate (AR grade) supplied by M/s. Ranbaxy Fine Chemicals, India was used as received.

### **Potassium dihydrogen phosphate**

Potassium dihydrogen phosphate (AR grade) was purchased from M/s. Sarabhai Chemicals, India and used for the preparation of buffer solution.

### **Potassium hydrogen phthalate (KHP)**

KHP (AR grade) was procured from M/s. Glaxo Laboratories, India and used as received.

### **Potassium oxalate**

Potassium oxalate (AR grade) obtained from M/s. Loba Chemie, India was used for the determination of free acidity of solutions containing hydrolyzable metal ions.

### **Pyridine**

Pyridine (AR grade) procured from M/s. Ranbaxy Fine Chemicals, India was used.

### **Silver nitrate**

Silver nitrate (AR grade) received from M/s. Merck, India was used for the detection of chloride in the distilled water.

### **Sodium acetate**

Sodium acetate (AR grade) obtained from M/s. Merck, India was used for the preparation of buffer solution.

### **Sodium carbonate**

Sodium carbonate (AR grade) supplied by M/s. Ranbaxy Fine Chemicals, India was used as such without any purification.

### **Sodium fluoride**

Sodium fluoride (AR grade) obtained from M/s. Merck, India was used as received.

### **Sodium hydroxide (NaOH)**

NaOH pellets (AR grade) purchased from M/s. Ranbaxy Fine Chemicals, India was used for acid-base titration and washing organic solutions.

### **Sodium nitrate**

Sodium nitrate (AR grade) procured from M/s. S D Fine-Chem Ltd., India was used as received.

### **Thorium nitrate**

Thorium nitrate (Nuclear grade) procured from IREL, India was used as such without any purification.

**Trans-1,2-diaminocyclo-hexane-N,N,N',N'-tetraacetic acid (CyDTA)**

CyDTA (98% Pure) purchased from M/s. Acros Chemicals, USA was used for the preparation of complexing solution for U(VI) estimation by spectrophotometry.

**Tri-*iso*-amyl phosphate**

Details about the synthesis, purification and characterization of TiAP are provided elsewhere [116].

**Tri-*n*-butyl phosphate (TBP)**

TBP provided by M/s. Fluka Chemicals, Switzerland was used for the extraction studies.

**Triethanolamine (TEA)**

TEA (AR grade) received from M/s. Merck, India was used for the preparation of buffer solution.

**Uranyl nitrate**

Uranyl nitrate (Nuclear grade) supplied by Nuclear Fuel Complex (NFC), India and BDH Chemicals Ltd., England were used as received.

**Vanadyl sulphate**

Vanadyl sulphate (AR grade) was procured from M/s. BDH Chemicals Ltd., England.

**Xylenol Orange**

Xylenol orange indicator (AR grade) provided by M/s. TCI Chemicals, Japan was used as received.

**Zinc**

Zinc metal (AR grade) procured from M/s. Glaxo Laboratories India Ltd., was used to prepare standard zinc nitrate solution.

**Zirconium**

Zirconium sponge (Nuclear grade with < 150 ppm of hafnium) obtained from NFC, India was used to prepare zirconium nitrate solution.

**1-(2-pyridylazo)-2-naphthol (PAN)**

PAN (AR grade) procured from M/s. Aldrich, USA was used for the complexometric titration of Hf(IV).

**2-(5-Bromo-2-pyridylazo)-5-(diethylamino) phenol (Br-PADAP)**

Br-PADAP (AR grade) obtained from M/s. Merck, India was used for the spectrophotometric determination of U(VI).

**2,6-Pyridinedicarboxylic acid (PDCA)**

PDCA (98% Pure) procured from M/s. Lancaster, England was used as titrant for the complexometric determination of U(VI).

**2.2 Instruments****Electronic single pan balance**

A calibrated electronic balance (AUW220D SHIMADZU make) with a sensitivity of  $\pm 0.01$  mg was used for weighing various chemicals (both solids and liquids).

**Karl Fischer titrator**

The concentration of water in organic phase samples was estimated by Karl Fischer titration by using Metrohm KF-831 Karl Fischer titrator. Double distilled water was used to calibrate the instrument. The values obtained for the water analysis were within the error range of  $\pm 5\%$ .

### pH meter

A Cyberscan pH meter procured from M/s. Eutech Instruments, Singapore calibrated using standard pH buffers of 4.01, 6.86 and 9.18 was used for the measurement of pH of various solutions.

### Refractometer

Refractive index of organic solutions was measured at 303 K by using an ATAGO RX5000 refractometer connected to a water bath capable of controlling temperature change of  $\pm 0.1$  K. The refractometer was calibrated with double distilled water at 303 K.

### Small Angle Neutron Scattering Measurement

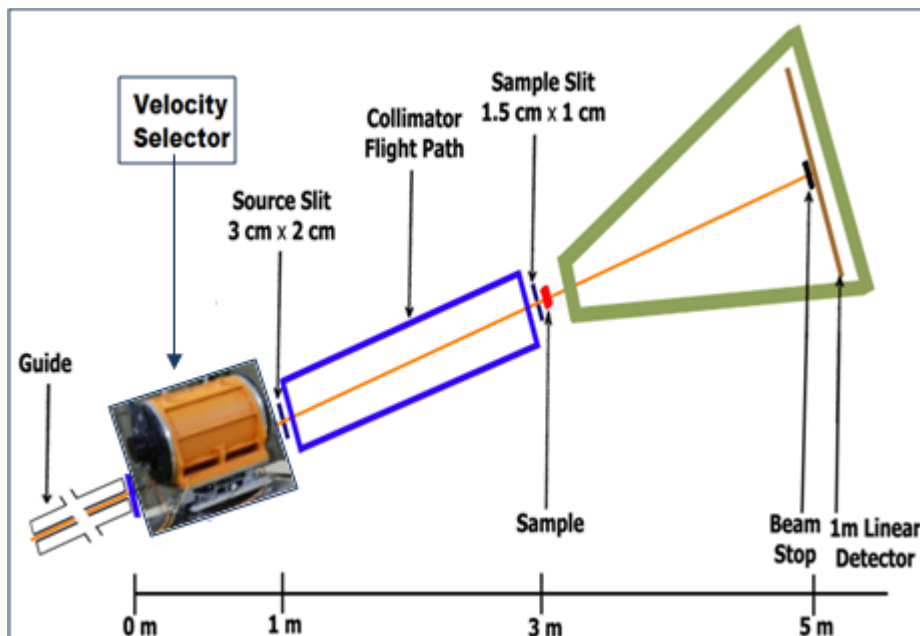


*Fig. 2.1: Schematic representation of SANS diffractometer.*

SANS experiments were carried out using the SANS diffractometer (Schematically shown in Fig. 2.1) installed at Dhruva reactor complex, Bhabha Atomic Research Centre

(BARC), Trombay, India. More details of the facility housing SANS diffractometer are provided elsewhere [177]. A mean neutron wavelength of 5.2 Å with a resolution of ~15% was used for the experiments. The samples were scanned in the scattering vector (Q) range from 0.017 to 0.35 Å<sup>-1</sup>. A quartz cell with a thickness of 2 mm was used for holding the sample during the measurements. The scattered neutrons were measured by using a one-dimensional <sup>3</sup>He gas detector.

### **UV-VIS-NIR spectrophotometer**

A SHIMADZU model UV-3600 spectrophotometer (shown in Fig. 2.2) with wavelength range of 200-800 nm and a cuvette with a path length of 1 cm were used for the measurement of absorbance of various metal complexes.



*Fig. 2.2: UV-Visible-NIR spectrophotometer (SHIMADZU UV-3600 model).*

### **Viscometer**

An Ostwald viscometer was used for the determination of viscosity of the organic solutions.

### **Water baths for solvent extraction experiments**

A JULABO make (F25-EC) water bath with refrigerated and heating circulator capable of controlling temperature change of  $\pm 0.01$  K was used for the experiments. Water bath procured from Poly Science, USA (Model-9100) with a temperature controlling accuracy of  $\pm 0.1$  K was

also used for the experiments. The pictures of water baths used for the experiments are shown in Fig. 2.3.

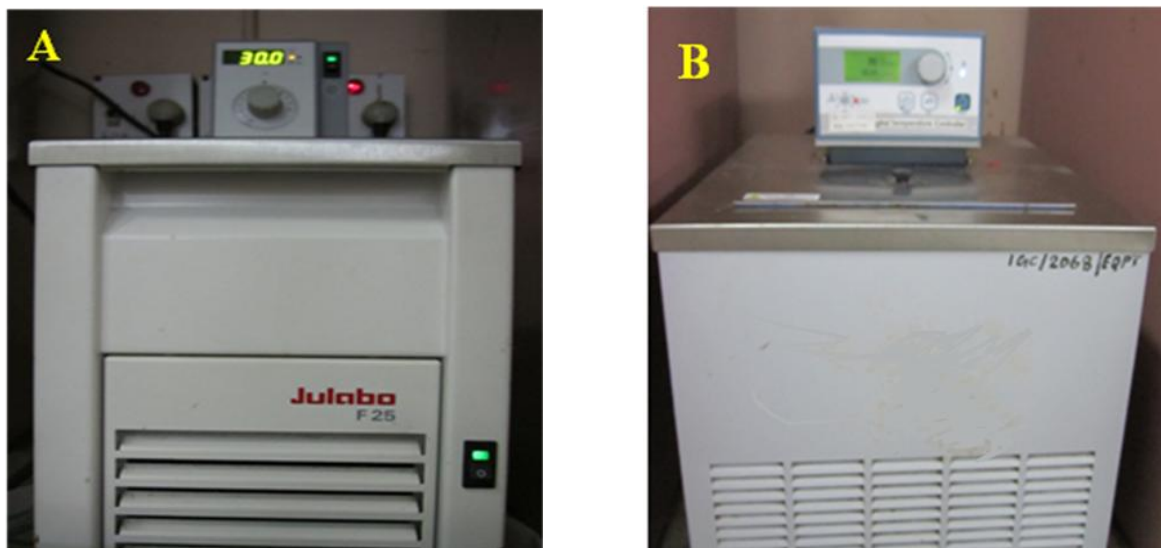


*Fig. 2.3: Water baths used for the experiments – (A) Julabo (F25-EC) (B) Polyscience (9100).*

## 2.3 Preparation of solutions

### 2.3.1 Standard solutions

#### Lead nitrate solution

Lead nitrate solution (0.05 M) was prepared by dissolving 0.8280 g of AR grade lead nitrate in distilled water in a 50 mL volumetric flask and made up to the mark.

#### Thorium nitrate solution

Nuclear grade  $\text{ThO}_2$  was dried in a furnace at 1073 K for four hours and cooled in a desiccator. About 10 g of  $\text{ThO}_2$  was dissolved in conc.  $\text{HNO}_3$  containing 0.001 M hydrofluoric acid (HF) by gently heating under IR lamp to obtain thorium nitrate solution in nitric acid media. This solution was evaporated to dryness and re-dissolved in 0.01 M  $\text{HNO}_3$ . A standard solution

of thorium nitrate was prepared by transferring the above solution to a dried, pre-weighed 100 mL volumetric flask followed by making up the solution with 0.01 M  $\text{HNO}_3$ . The flask was again weighed with the solution to calculate the concentration of the solution on weight basis.

### **Uranyl nitrate solution**

Nuclear grade  $\text{UO}_2$  powder was heated at 1133 K for four hours with a constant supply of air and cooled in a desiccator to obtain  $\text{U}_3\text{O}_8$ . About 10 g of  $\text{U}_3\text{O}_8$  was dissolved in conc.  $\text{HNO}_3$  by gently heating under IR lamp. The uranyl nitrate solution in nitric acid media obtained was evaporated to dryness and re-dissolved in 0.01 M  $\text{HNO}_3$ . This solution was quantitatively transferred to a dried, pre-weighed 100 mL volumetric flask and made up with 0.01 M  $\text{HNO}_3$ . The concentration of this standard uranyl nitrate solution was calculated by weight basis.

### **Zinc nitrate solution**

AR grade zinc metal (0.1664 g) was completely dissolved using 3 mL of 3 M  $\text{HNO}_3$  and made up with distilled water in a 500 mL volumetric flask to prepare 0.005 M standard zinc nitrate solution.

## **2.3.2 Indicator solutions**

### **Arsenazo-I solution**

Arsenazo-I indicator solution was prepared by dissolving 0.2 g of arsenazo-I in 100 mL of distilled water.

### **Br-PADAP solution**

A 0.05% Br-PADAP solution was prepared by dissolving 0.025 g of Br-PADAP in 50 mL of ethanol.

### **PAN solution**

PAN indicator solution was made by dissolving 0.1 g of PAN in 10 mL of ethanol.

### **Phenolphthalein solution**

About 0.5 g of phenolphthalein was dissolved in 100 mL of 1:1 mixture of distilled water and ethanol to prepare phenolphthalein indicator solution.

### **Xylenol orange solution**

This solution was prepared by dissolving 0.2 g of xylenol orange in 100 mL of distilled water.

## **2.3.3 Complexing solutions**

### **CyDTA complexing solution**

CyDTA complexing solution was prepared by dissolving 5 g of CyDTA, 1 g of sodium fluoride and 13 g of sulphosalicylic acid in 40 mL of distilled water. The pH of this solution was adjusted to 7.8 with NaOH pellets and diluted to 100 mL.

### **Neutral saturated potassium oxalate solution**

Potassium oxalate was dissolved in distilled water to saturation and adjusted to pH 7 by using dilute NaOH or dilute HNO<sub>3</sub> solutions. About 5 mL of this solution was used to complex metal ions prior to acid-base titration for the estimation of free acidity.

### **Potassium oxalate solution**

A 10% Potassium oxalate solution was prepared by dissolving 10 g of potassium oxalate in 100 mL of distilled water.

### **Sodium fluoride solution**

Sodium fluoride solution (1 M) was prepared by dissolving 4.2 g of sodium fluoride in 100 mL of distilled water.

### 2.3.4 Buffer solutions

#### Acetic acid – Sodium acetate buffer

About 90 mL of 0.2 M acetic acid solution and 10 mL of 0.2 M sodium acetate solution were mixed and adjusted to pH 3.7 using small volume of acetic acid or sodium acetate solution. This freshly prepared buffer solution (10 mL) was used to maintain a pH of 3.7 during the estimation of U(VI) with PDCA.

#### Borax buffer

A solution of 0.05 M borax ( $\text{Na}_2\text{B}_4\text{O}_7 \cdot 10\text{H}_2\text{O}$ ) was prepared by dissolving required quantity of borax in distilled water which showed a pH of 9.18 at 298 K.

#### KHP buffer

Required amount of KHP dried at 383 K was dissolved in distilled water to prepare 0.05 M KHP buffer solution of pH 4.01 at 298 K.

#### Potassium dihydrogen phosphate – Disodium hydrogen phosphate buffer

Potassium dihydrogen phosphate (0.0680 g) and disodium hydrogen phosphate (0.0891 g) were added in a 50 mL volumetric flask and made up to the mark with distilled water to prepare a buffer solution with pH 6.86 at 298 K.

#### TEA buffer

About 14 g of TEA was dissolved in 80 mL of distilled water, adjusted to pH 7.8 with conc.  $\text{HClO}_4$  and allowed to stand overnight. The pH of this solution was then re-adjusted to 7.8 with perchloric acid and diluted to 100 mL to prepare TEA buffer solution.

### 2.3.5 Stock solutions

#### Acid Mixture

Ammonium molybdate (0.4 g) was completely dissolved in 30 mL of distilled water and 60 mL of conc.  $\text{HNO}_3$  was added. This solution was mixed for 5 minutes to allow the heat produced to dissipate and 10 mL of saturated sulphamic acid was added to the solution to prepare the acid mixture which was used for the estimation of U(VI) by Davies-Gray method.

#### DTPA solution

DTPA solution (0.03 M) was prepared by dissolving 5.9 g of DTPA and 3 g of NaOH in 500 mL of distilled water. This solution was standardized with standard thorium nitrate solution using xylenol orange as the indicator. A similar procedure was also adopted for the preparation and standardization of 0.01 M DTPA solution.

#### Hafnium nitrate solution in nitric acid media

Concentrated HF was added to  $\text{HfO}_2$  in a Teflon beaker and heated to dissolve the  $\text{HfO}_2$  completely. The clear solution obtained was evaporated to form a residue and it was re-dissolved in concentrated  $\text{HNO}_3$ . The procedure was repeated several times to prepare fluoride-free  $\text{Hf}(\text{NO}_3)_4$  solution in desired nitric acid concentration.

#### $\text{H}_2\text{SO}_4$ solution

The volume of  $\text{H}_2\text{SO}_4$  required to prepare 1 M of its solution was added dropwise in a volumetric flask with distilled water and shaken. The heat generated was dissipated by cooling the sides of the flask in a water bath. After the removal of the liberated heat, the solution was made up to the mark and standardized by acid-base titration with NaOH solution by using phenolphthalein as the indicator. Dilute  $\text{H}_2\text{SO}_4$  solution (0.2 N) was also prepared and standardized by the aforementioned procedure.

**NaOH solution**

NaOH solution was prepared by dissolving required quantity of NaOH pellets in distilled water in a volumetric flask. This solution was standardized by acid-base titration with KHP using phenolphthalein indicator.

**NH<sub>4</sub>OH solution**

NH<sub>4</sub>OH solution (5 M) was prepared by mixing required volume of commercially available NH<sub>4</sub>OH solution with distilled water in a volumetric flask and made up to the mark. The same procedure was also followed for the preparation of 0.1 M NH<sub>4</sub>OH solution from 5 M NH<sub>4</sub>OH solution.

**Nitric acid solutions**

Nitric acid stock solution (10 M) was prepared from the commercially available nitric acid solution and standardized by acid-base titration with NaOH solution by using phenolphthalein as the indicator. This standardized nitric acid stock solution was used for the preparation of various concentrations of nitric acid solutions.

**Perchloric acid solution (0.3 M)**

The volume of perchloric acid required to prepare 0.3 M of its solution was taken in a volumetric flask and made up with distilled water.

**PDCA solution**

About 2.5 g of PDCA and 1.2 g of NaOH were dissolved in 500 mL of distilled water to prepare 0.03 M PDCA solution. This solution was standardized by using standard uranyl nitrate solution with arsenazo-I as the indicator. Similarly, 0.01 M PDCA solution was prepared by dissolving 0.83 g of PDCA and 0.4 g of NaOH in 500 mL of distilled water, and standardized using dilute standard uranyl nitrate solution.

**Phosphoric acid treated with potassium dichromate solution**

About 2.5 g of 0.05 N potassium dichromate solution was mixed with 500 mL of phosphoric acid to prepare phosphoric acid treated with potassium dichromate.

**Thorium nitrate solution in nitric acid media**

A nearly saturated solution of thorium nitrate in 1 M HNO<sub>3</sub> was prepared in a volumetric flask by mixing saturated thorium nitrate solution in distilled water with the required quantity of 10 M HNO<sub>3</sub> solution. The aforementioned procedure was also used for the preparation of nearly saturated solution of thorium nitrate in 5 M HNO<sub>3</sub>.

**Trialkyl phosphate (TalP) solutions in *n*-alkane**

Solutions of TalP (TiAP and TBP) in various diluents were prepared by taking required weight of the extractant in volumetric flasks, followed by mixing it with respective diluents near the mark and allowing to stand for a day to adjust for any volume change and later made up to the mark. These solutions were washed with 5 M NaOH solution followed by water wash to remove impurities from the extractant solution before carrying out the experiments.

**Uranyl nitrate solution in nitric acid media**

The procedure mentioned for the preparation of stock solution of thorium nitrate in nitric acid media was also adopted for the preparation of nearly saturated solution of uranyl nitrate in nitric acid media (0.1 M, 0.5 M, 2 M, 4 M and 6 M) using saturated uranyl nitrate solution. The free acidity of the solution was estimated by acid-base titration using mixed oxalate-fluoride solution as the complexing agent.

**Zirconium nitrate solution in nitric acid media**

A few grams of zirconium metal were washed with conc. HCl to remove the dust particles and taken in a round bottomed flask. The required amount of concentrated HCl was

added to immerse the metal completely in the acid and heated under reflux at 353 K. During heating, zirconium metal and HCl in the flask were mixed thoroughly using a Teflon coated magnetic stirring bar and a magnetic stirrer. Around 3 - 5 drops of dilute HF were also added to initiate the dissolution. Refluxing was continued for about 12 hours. The solution of zirconium chloride was concentrated by the evaporation of HCl. Dropwise addition of 5 M  $\text{NH}_4\text{OH}$  solution into the concentrated solution of zirconium chloride with stirring and heating yielded hydrated zirconia as precipitate. The precipitate was washed thoroughly with 0.1 M  $\text{NH}_4\text{OH}$  solution until free from chloride ions and then washed with double distilled water to remove excess  $\text{NH}_4\text{OH}$ . The washed precipitate was then dissolved in minimum amount of concentrated  $\text{HNO}_3$  under heating. The solution was then evaporated and concentrated by the addition of water or  $\text{HNO}_3$  with heating to get the desired concentration of  $\text{Zr}(\text{NO}_3)_4$  in nitric acid media [122].

### **2.3.6 Feed solutions**

#### **U(VI)-Th(IV)-Nd(III) feed solution**

Uranyl nitrate, thorium nitrate and neodymium nitrate (as representative of rare earths (RE)) solutions in nitric acid media that represent the amount of U(VI), Th(IV), and RE(III) present in Indian monazite feed solution [91] were mixed to prepare U(VI)-Th(IV)-Nd(III) feed solution. For this, 18.7 mL of uranyl nitrate solution ( $[\text{U(VI)}] = 30 \text{ g/L}$ ), 33.2 mL of thorium nitrate solution ( $[\text{Th(IV)}] = 530 \text{ g/L}$ ) and 40.3 mL of neodymium nitrate solution ( $[\text{Nd(III)}] = 500 \text{ g/L}$ ) were mixed in a beaker. This solution was then evaporated to dryness and dissolved in minimum quantity of nitric acid required to prepare nearly saturated feed solution of U(VI)-Th(IV)-Nd(III) in nitric acid media.

### Zr(IV)-Hf(IV) feed solution

Concentrated feed solution of Zr(IV)-Hf(IV) with the ratio of concentration of Zr(IV) to Hf(IV) commonly used as feed for Zr(IV)/Hf(IV) separation was prepared from Zr(IV) and Hf(IV) solutions in nitric acid media. About 7.7 mL of Zr(IV) solution ( $[\text{Zr(IV)}] = 87 \text{ g/L}$  in 4 M  $\text{HNO}_3$ ) was mixed with 1.4 mL of Hf(IV) solution ( $[\text{Hf(IV)}] = 14 \text{ g/L}$  in 4 M  $\text{HNO}_3$ ) in a beaker to prepare Zr(IV)-Hf(IV) feed solution in 4 M  $\text{HNO}_3$ .

## 2.4 Experimental procedure

### 2.4.1 Extraction of U(VI) as a function of $[\text{U(VI)}]_{\text{aq,eq}}$



*Fig. 2.4: Double walled vessel used for solvent extraction experiments.*

Concentrated uranyl nitrate solution in 0.1 M  $\text{HNO}_3$  and 1.1 M TiAP/*n*-DD pre-equilibrated with 0.1 M nitric acid (each phase 2 mL) were mixed in an equilibration tube by using a magnetic stirrer for 15 minutes. The temperature of the system was maintained at 303 K

by keeping the equilibration tube in a double walled vessel (shown in Fig. 2.4) through which water from a constant temperature water bath was circulated. After equilibration the phases were allowed to stand for a while for settling. Required volumes of organic and aqueous solutions were taken out from equilibration tube for the analysis of U(VI) and HNO<sub>3</sub>. In order to dilute the concentration of U(VI) in aqueous phase and maintain 1:1 organic to aqueous volume ratio, appropriate volumes of 0.1 M HNO<sub>3</sub> and organic solution pre-equilibrated with 0.1 M HNO<sub>3</sub> were added. The organic and the aqueous solutions were again equilibrated and analysis was done as mentioned above for various equilibrium aqueous phase U(VI) concentrations. The experiment was repeated with uranyl nitrate solutions in various concentrations of nitric acid (0.5 M, 2 M, 4 M and 6 M).

#### 2.4.2 Extraction and stripping of U(VI) in cross-current mode

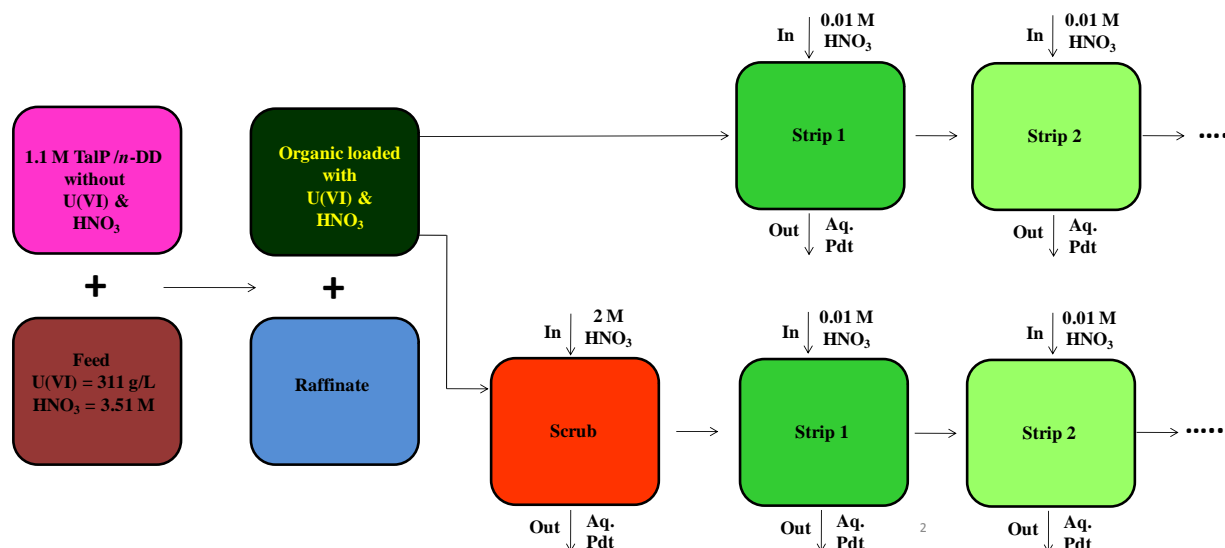


**Fig. 2.5. Schematic representation of extraction, scrubbing and stripping of U(VI) with 1.1 M TalP/n-DD.**

About 2 mL of an aqueous solution containing 311 g/L of U(VI) in 3.51 M HNO<sub>3</sub> was equilibrated with an organic solution (1.1 M TalP in *n*-DD) for 1 hour at 303 K in a thermo-

stated vessel. After the isolation of loaded organic phase from the equilibration tube, it was divided into two fractions. One portion was subjected to stripping (five times) consecutively with 0.01 M HNO<sub>3</sub>. The other portion was scrubbed once with 2 M HNO<sub>3</sub> and subsequently subjected to stripping in consecutive stages. Scrubbing and stripping of organic solutions were carried out in cross-current mode where the same loaded organic solution was fed into subsequent stages and fresh aqueous solutions were used in all the stages. The equilibration was done with an organic to aqueous volume ratio of 1:1 for about 1 hour at 303 K. Schematic representation of the experiment performed is shown in Fig. 2.5.

#### **2.4.3 Stripping of U(VI) as a function of time**

Equal volumes (30 mL) of organic (1.1 M TalP/*n*-DD) and aqueous (~ 3 g/L of U(VI) in 4 M HNO<sub>3</sub>) solutions were equilibrated by using a magnetic stirrer for 1 hour at 303 K. After the phase separation, loaded organic phases were isolated from aqueous solutions and stored as stock solutions for stripping. Organic solutions (2mL) were withdrawn from the stock solutions at regular intervals (14 - 28 days) and stripped three times with 0.01 M HNO<sub>3</sub> at 303 K for an hour and then the organic phase was analyzed for U(VI) by spectrophotometry to know the fraction of U(VI) retained in the organic phase.

#### **2.4.4 Extraction of Th(IV) as a function of [Th(IV)]<sub>aq,eq</sub> in biphasic and triphasic regions under near-zero free acid condition**

Equal volumes (2 mL) of 1.1 M TalP in *n*-alkane solution and Th(NO<sub>3</sub>)<sub>4</sub> solution with near-zero free acidity were equilibrated in a round bottomed equilibration tube by using a magnetic stirrer for about 30 minutes at 303 K and allowed to settle by gravity. Well-separated organic and aqueous phase samples were analyzed for the concentration of Th(IV). The extraction of Th(IV) was carried out as a function of [Th(IV)]<sub>aq,eq</sub> by the frequent addition of

thorium nitrate salt and organic solution to the same equilibration tube followed by organic-aqueous equilibration. The organic and the aqueous phases were again analyzed for Th(IV) after the separation of phases at equilibrium and the procedure was repeated in the biphasic region until the TP was formed.

Third phase formation can be visually detected either through the presence of three distinctly separated phases or as the appearance of turbidity. Initially, water was added dropwise to reduce the concentration of the metal ion close to LOC. It was followed by the dropwise addition of the corresponding barren organic solution until the TP was dissolved. Concentrations of Th(IV) in organic and aqueous phases at the point of dissolution of the TP that correspond to LOC and CAC, respectively, were determined.

In some of the experiments, the TP was not dissolved and the distribution of Th(IV) in the triphasic region was investigated as a function of  $[\text{Th(IV)}]_{\text{aq,eq}}$  at 303 K. Initially, organic and aqueous phases were equilibrated for 30 minutes at 303 K to ensure proper distribution of Th(IV) among the phases and settled with the aid of gravity. The phases were separated and their volumes were indirectly calculated from their weights and densities. The amount of Th(IV) in the isolated phases was estimated. All the experiments in the triphasic region at each  $[\text{Th(IV)}]_{\text{aq,eq}}$  were carried out with fresh organic and aqueous solutions.

#### **2.4.5 Extraction of Th(IV) as a function of $[\text{Th(IV)}]_{\text{aq,eq}}$ in biphasic and triphasic regions in nitric acid media**

A known volume of 1.1 M TalP/*n*-alkane (pre-equilibrated with 1 M HNO<sub>3</sub>) was equilibrated with the same volume of Th(NO<sub>3</sub>)<sub>4</sub> solution in 1 M HNO<sub>3</sub> in a round bottomed equilibration tube by using a magnetic stirrer for about 30 minutes at 303 K and the phases were settled with the aid of gravity. Both organic and aqueous phase samples were analyzed for the

concentrations of Th(IV) and HNO<sub>3</sub>. After the analysis, thorium nitrate solution in 1 M HNO<sub>3</sub> and organic solution (pre-equilibrated with 1 M HNO<sub>3</sub>) were added to the same equilibration tube followed by the equilibration of both the phases and the analysis of solutes (Th(IV) and HNO<sub>3</sub>). This procedure was repeated throughout the biphasic region as a function of [Th(IV)]<sub>aq,eq</sub> at 303 K.

When the TP was observed, the point of dissolution of the TP was attained by adding either 1 M HNO<sub>3</sub> solution or organic solution pre-equilibrated with 1 M HNO<sub>3</sub> to the equilibration tube. Concentrations of Th(IV) and HNO<sub>3</sub> in organic and aqueous phases at the point of dissolution of the TP were determined.

The experiments in the triphasic regions were carried out by equilibrating equal volumes of 1.1 M TalP/*n*-alkane (pre-equilibrated with 1 M HNO<sub>3</sub>) and Th(NO<sub>3</sub>)<sub>4</sub> solution in 1 M HNO<sub>3</sub> at 303 K for about 30 minutes. The distribution of Th(IV) and HNO<sub>3</sub> between the TP and the DP above third phase formation limit was investigated with respect to [Th(IV)]<sub>aq,eq</sub> with constant HNO<sub>3</sub> concentration (1 M). The phases were settled, separated and their volumes were determined from their weights and densities. The concentrations of solutes were also estimated in all the phases.

The aforementioned procedure was repeated for third phase formation experiments with Th(NO<sub>3</sub>)<sub>4</sub> solution in 5 M HNO<sub>3</sub> as the aqueous phase and 1.1 M TalP/*n*-alkane (pre-equilibrated with 5 M HNO<sub>3</sub>) as the organic phase.

#### **2.4.6 Determination of LOC and CAC for the extraction of Th(IV) as a function of extractant concentration under near-zero free acid condition**

About 2 mL of TalP/*n*-alkane solution of a particular concentration was equilibrated with 2 mL of Th(NO<sub>3</sub>)<sub>4</sub> solution with near-zero free acidity in an equilibration tube for 15 minutes at

303 K. When the TP was formed, it was visually monitored and dissolved by the dropwise addition of water or barren organic solution with intermittent stirring. The Th(IV) concentration in organic and aqueous phase samples was determined. The same procedure was repeated for the determination of LOC and CAC for TalP/*n*-alkane solutions with various concentrations.

#### **2.4.7 Determination of LOC and CAC for the extraction of Th(IV) from Th(IV)-Nd(III) feed solution**

The third phase formation experiments were conducted with organic solutions of 1.47 M TalP/*n*-DD (pre-equilibrated with 4 M HNO<sub>3</sub>) and aqueous solution containing Th(IV) and Nd(III) in 4 M HNO<sub>3</sub> at 303 K. The methods described in section 2.4.5 were followed for the formation and dissolution of the TP and also for the determination of LOC and CAC.

#### **2.4.8 Determination of LOC and CAC for the extraction of Zr(IV) as a function of [HNO<sub>3</sub>]<sub>aq,eq</sub>**

The experimental procedure mentioned in section 2.4.5 was adopted for the determination of LOC and CAC in the extraction of Zr(IV) metal ion using TalP/*n*-DD (1.1 M and 2.2 M) as organic solution and Zr(NO<sub>3</sub>)<sub>4</sub> solution in nitric acid media as aqueous solution at 303 K. At the point of dissolution of the TP, the concentration of nitric acid in the aqueous phase and LOC and CAC values for Zr(IV) metal ion were determined. LOC and CAC were determined as a function of [HNO<sub>3</sub>]<sub>aq,eq</sub> at 303 K.

#### **2.4.9 Third phase formation experiments for the extraction of Zr(IV) in nitric acid media**

The procedure mentioned in section 2.4.5 was also followed for this experiment using 1.1 M solutions of TalP in *n*-alkane (pre-equilibrated with 4 M HNO<sub>3</sub>) and Zr(NO<sub>3</sub>)<sub>4</sub> solution in 4 M HNO<sub>3</sub> at room temperature (~298 K).

#### 2.4.10 Extraction of metal ion/s from U(VI)-Th(IV)-Nd(III) feed solution in nitric acid media

The extraction experiments were carried out by equilibrating equal volumes of U(VI)-Th(IV)-Nd(III) aqueous feed solution and organic solution of TalP in *n*-DD (with and without pre-equilibration with HNO<sub>3</sub>) in a reagent bottle by using a magnetic stirrer. The equilibration was continued for 30 minutes at 303 K and the solutions were allowed to stand for phase separation. After the isolation of phases, volume was measured (for calculating mass balance of metal ions) and samples were analyzed for the concentration of metal ions and nitric acid. The extraction was carried out in cross-current mode where the same aqueous solution was fed into subsequent extraction stages and fresh organic solutions were used in all the extraction stages. The same procedure was used for scrubbing and stripping experiments except that the organic phase was laden with metal ions and the aqueous phase was without metal ions. The percentage of extraction of metal ions ( $E_M$ ) for all the extraction experiments was calculated from Eq. (2.1), where,  $A_i$  and  $A_f$  represent the initial and final concentrations of metal ion in the aqueous phase during extraction, respectively.

$$E_M = \frac{A_i - A_f}{A_i} \times 100 \quad (2.1)$$

The percentage of stripping of metal ions ( $S_M$ ) was obtained from Eq. (2.2), where the terms  $O_i$  and  $O_f$  denote metal ion concentrations in organic phases before and after the stripping, respectively.

$$S_M = \frac{O_i - O_f}{O_i} \times 100 \quad (2.2)$$

#### 2.4.11 Measurement of distribution ratios of Zr(IV) and Hf(IV)

Around 2 mL of 0.0006 M (0.055 g/L) Zr(IV) in a particular nitric acid solution and 2 mL of 1.1 M TalP/*n*-DD (pre-equilibrated thrice with the corresponding nitric acid solution) were equilibrated for 30 minutes at 303 K. The organic and the aqueous phases were allowed to settle and samples were withdrawn to estimate the concentration of Zr(IV) and HNO<sub>3</sub>. The procedure was repeated with 0.0006 M Zr(IV) solutions in various nitric acid concentrations to measure the distribution ratio of Zr(IV) as a function of nitric acid concentration. The above-mentioned method was also adopted for the determination of distribution ratio of Hf(IV) as a function of nitric acid concentration.

#### 2.4.12 Estimation of extractant by nitric acid equilibration method

Around 2 mL of the organic solution (TalP/*n*-alkane) was taken in an equilibration tube and, the same volume of HNO<sub>3</sub> (8 M) was added and equilibrated at 303 K for about 15 minutes. The phases were allowed to settle by gravity. After the phase separation, the aqueous phase was removed and the nitric acid loaded organic phase was further equilibrated twice with fresh 8 M HNO<sub>3</sub> solution. The phases were settled by gravity and the organic phase was analyzed to estimate the HNO<sub>3</sub> by acid-base titration. A calibration graph was generated by plotting the amount of HNO<sub>3</sub> extracted by TalP/*n*-alkane solutions of known concentrations when saturated with 8 M HNO<sub>3</sub> as a function of TalP/*n*-alkane concentration. This calibration graph and the estimated HNO<sub>3</sub> values for TalP/*n*-alkane solutions of unknown concentrations were used to determine the TalP concentrations.

#### 2.4.13 Preparation of samples for SANS experiments

The organic phase samples loaded with Zr(IV) and HNO<sub>3</sub> collected from the biphasic and triphasic regions of 1.1 M TBP/C<sub>12</sub>D<sub>26</sub> – Zr(NO<sub>3</sub>)<sub>4</sub>/HNO<sub>3</sub> and 1.1 M TiAP/C<sub>12</sub>D<sub>26</sub> –

Zr(NO<sub>3</sub>)<sub>4</sub>/HNO<sub>3</sub> systems were generated by equilibrating equal volumes of organic phase with Zr(NO<sub>3</sub>)<sub>4</sub> solution in 4 M HNO<sub>3</sub> by using a magnetic stirrer at room temperature (~298 K) for about 30 minutes. The phases were allowed to settle by gravity and separated. The isolated organic phases were used for SANS experiments.

## **2.5 Analytical methods**

### **2.5.1 Determination of density and volume**

An analytical balance of  $\pm 0.1$  mg sensitivity and a class A glass micropipette of 500  $\mu$ L capacity were used to measure the densities of organic and aqueous solutions. The density of a solution was calculated from weights of the micropipette before and after the loading of the solution, and volume of the micropipette. Volumes of organic and aqueous solutions were obtained indirectly from their weights and densities.

### **2.5.2 Determination of concentration of Hf(IV)**

#### **2.5.2.1 Complexometry**

Estimation of Hf(IV) in concentrated solutions ( $[\text{Hf(IV)}] > 1$  g/L) was done by complexometric titration. Initially, pink colour was developed when a few drops of PAN indicator was mixed with an aliquot of Hf(IV). Subsequently, an excess of standardized EDTA solution (0.005 M) was added to the Hf(IV) solution till the colour changed to yellow. The excess EDTA was back titrated with zinc nitrate solution (0.005 M) at pH 6 and the end point was detected with the colour change from yellow to pink [178].

#### **2.5.2.2 Spectrophotometry**

The concentrations of Hf(IV) in dilute solutions ( $< 1$  g/L) was estimated by spectrophotometry using xylenol orange as the chromogenic agent at  $535 \pm 1$  nm in 0.3 M HClO<sub>4</sub> medium [178].

### 2.5.3 Determination of concentration of Nd(III)

The amount of Nd(III) present in samples was determined by the addition of excess DTPA solution at pH 2.5 - 3.0 and back-titration of uncomplexed DTPA with standardized lead nitrate solution (0.05 M) to a red-violet colour end point at pH 5.0 - 5.5 adjusted using solid HMTA [179]. In the case of solutions containing Th(IV) and Nd(III), titration of Nd(III) was carried out with the same solution after performing Th(IV) titration with DTPA solution.

### 2.5.4 Determination of concentration of nitric acid

Nitric acid in organic and aqueous samples was estimated by acid-base titration with standardized NaOH solution (0.1 M) by using phenolphthalein as the indicator with the appearance of pink colour as the end point. Concentrations of nitric acid in organic and aqueous samples in the presence of metal ion/s were determined after complexing metal ion/s with neutral saturated potassium oxalate solution by acid-base titration with standardized NaOH solution using phenolphthalein as the indicator.

Nitric acid in organic and aqueous samples containing U(VI) and nitric acid was estimated by using a method involving the use of dual complexing agents. In this method, 25 ml of 10% potassium oxalate solution was taken in a beaker, pH was adjusted to 7 and required volume of aliquot of the U(VI) sample solution was added. Sodium fluoride solution (1 M) was added to the solution to maintain a U(VI):F<sup>-</sup> mole ratio of 1:5. The nitric acid in the solution was titrated against standardized NaOH solution to pH 7. Concentrations of nitric acid in both organic and aqueous samples were obtained from titre value and concentration of NaOH solution [180].

### **2.5.5 Determination of concentration of Th(IV)**

The concentration of Th(IV) in organic and aqueous samples was determined by complexometric titration in the pH range 2.5 - 3.0 using DTPA solution as the titrant and xylenol orange as the indicator with the colour change from pink to yellow [179]. Concentrated and dilute solutions of  $\text{Th}(\text{NO}_3)_4$  were analyzed with 0.03 M and 0.01 M DTPA solutions, respectively.

### **2.5.6 Determination of concentration of U(VI)**

#### **2.5.6.1 Complexometry**

U(VI) content in its concentrated solutions was determined by complexometric titration by using PDCA as titrant and arsenazo-I as the indicator at pH 3.6 with the colour change from blue to red [64].

#### **2.5.6.2 Davies-Gray method**

The concentration of U(VI) in organic and aqueous phase samples ( $> 1$  g/L) was determined by Davies-Gray method [63].

#### **2.5.6.3 Spectrophotometry**

The concentration of U(VI) in organic and aqueous phase samples ( $< 1$  g/L) was determined by spectrophotometry using Br-PADAP as the chromogenic agent at  $577 \pm 1$  nm in ethanol medium [181].

### **2.5.7 Determination of Zr(IV)**

#### **2.5.7.1 Complexometry**

The concentration of Zr(IV) in organic and aqueous samples in macro level was estimated by the addition of excess EDTA solution followed by the back titration of excess EDTA with standard  $\text{Th}(\text{NO}_3)_4$  solution using xylenol orange as the indicator. Initially, the

sample was mixed with 0.01 M HNO<sub>3</sub> solution and a few drops of xylenol orange indicator. Subsequently, a known volume of 0.1 M standardized EDTA solution was added to change the colour of the solution from pink to yellow. The excess EDTA was back titrated with 0.01 M Th(NO<sub>3</sub>)<sub>4</sub> solution up to a sharp colour change from yellow to pink. The pH of the solution was maintained between 2.5 to 3.0 by adding 6 drops of formic acid and 3 drops of pyridine during back-titration [122].

### 2.5.7.2 Spectrophotometry

The concentration of Zr(IV) in samples (< 1 g/L) was determined by spectrophotometry using xylenol orange as the chromogenic agent at 535±1 nm in 0.2 N H<sub>2</sub>SO<sub>4</sub> medium [182].

In the present study, all the calibration graphs used for the spectrophotometric determination of metal ions were validated by cross-checking the molar extinction co-efficient values derived from the calibration graphs with the literature values. In all the cases, the values were comparable.

### 2.5.8 Determination of concentration of water

The concentration of water in various organic phase samples was determined by Karl Fischer titration [183]. A known amount of the sample was titrated with Karl Fischer reagent to estimate the amount of water. The Karl Fischer reagent composed of sulphur dioxide and iodine with imidazole or primary amine (PA) as buffering agent and methanol as solvent. The water present in the sample reacts with iodine in 1:1 mole ratio and the unreacted iodine is estimated by non-aqueous titration. The reaction of water with Karl Fischer reagent is shown in Eq. (2.3).



All complexometric and acid-base titrations were carried out on weight basis and aliquot volumes were chosen in such a way that weight of titrant consumed was around 1 g to yield a precision of  $\pm 1\%$ .

### 2.5.9 Determination of viscosity

The viscosity was determined by using Ostwald viscometer by the comparative method, where water was used as the reference liquid whose density ( $\rho_w$ ) and viscosity ( $\eta_w$ ) were known for a particular temperature. The viscometer was kept in a double walled glass container through which water from a constant temperature water bath was circulated to maintain a temperature of  $303 \pm 0.1$  K. Initially, the viscometer was filled with a known volume ( $\sim 15$  mL) of the sample and the time taken for the sample to cross the marked region of the viscometer ( $t_s$ ) was determined. Subsequently, the procedure was repeated with the same volume of water to obtain the time taken for water to cross the marked region ( $t_w$ ). The viscosity of the sample solution ( $\eta_s$ ) was calculated from the following expression where,  $\rho_s$  represents the density of the sample.

$$\eta_s = \frac{\eta_w \rho_s t_s}{\rho_w t_w} \quad (2.4)$$

### 2.5.10 SANS - Data analysis

In SANS, the differential scattering cross-section per unit volume ( $d\Sigma/d\Omega$ ) was measured as a function of scattering vector ( $Q$ ), where  $Q$  is expressed as shown in Eq. (2.5)

$$Q = \frac{4\pi \sin \theta}{\lambda} \quad (2.5)$$

Here,  $\theta$  is the half-scattering angle and  $\lambda$  is the mean wavelength of the incident neutrons used.

Theoretically, the  $d\Sigma/d\Omega$  from a collection of particles is given by the product of particle form factor ( $P(Q)$ ) and structure factor ( $S(Q)$ ). The  $d\Sigma/d\Omega$  can be expressed by Eq. (2.6).

$$\frac{d\Sigma}{d\Omega}(\mathbf{Q}) = N_p V_p^2 (\rho_p - \rho_s)^2 P(\mathbf{Q}) S(\mathbf{Q}) \quad (2.6)$$

where,  $N_p$  is the number of scattering particles per unit volume,  $V_p$  is the particle volume,  $\rho_p$  and  $\rho_s$  are the scattering length densities of the extractant and the diluent, respectively.  $P(\mathbf{Q})$  depends on the individual particle and therefore provides information about the particle size and shape. On the other hand,  $S(\mathbf{Q})$  is decided by the correlation of particles and hence interaction of particles can be determined through this term. For a system with low concentration or in a non-interacting system  $S(\mathbf{Q})$  is  $\sim 1$  and the Eq. (2.6) can be simplified to Eq. (2.7).

$$\frac{d\Sigma}{d\Omega}(\mathbf{Q}) = N_p V_p^2 (\rho_p - \rho_s)^2 P(\mathbf{Q}) \quad (2.7)$$

The form factor  $P(\mathbf{Q})$  for spherical particle of radius  $R$  can be expressed as shown in Eq. (2.8).

$$P(\mathbf{Q}) = \left[ \frac{3[\sin(\mathbf{Q}R) - (\mathbf{Q}R)\cos(\mathbf{Q}R)]}{(\mathbf{Q}R)^3} \right]^2 \quad (2.8)$$

For the particles that undergo attraction, the value of  $S(\mathbf{Q})$  can be calculated based on the attractive interaction between the particles using Baxter's sticky hard-sphere model [142]. The stickiness parameter ( $\tau^{-1}$ ), diameter of micelle ( $\sigma$ ), width of the square-well potential ( $\Delta$ ), depth of the square-well potential ( $U_0$ ) and temperature ( $T$ ) can be co-related to each other as shown in Eq. (2.9). Further details on the quantification of these parameters are provided elsewhere [134,140].

$$\tau = \frac{\sigma + \Delta}{12\Delta} \exp\left(\frac{U_0}{k_B T}\right) \quad (2.9)$$



# Chapter 3



**“If we knew what we were doing it wouldn't be research”**

*-Albert Einstein*

### **3.1 Introduction**

The extraction and stripping behaviour of TiAP with metal ions such as U(VI), Th(IV) and trivalent lanthanides must be comparable or superior to the behaviour of TBP based solvents in order to employ TiAP based solvents for monazite ore processing. Third phase formation limits for the extraction of Th(IV) by TBP based solvents are low even at lower aqueous phase nitric acid concentrations [116]. Consequently, comparison of extraction profiles of TiAP and TBP with respect to Th(IV) metal ion under high solvent loading conditions becomes impractical due to third phase formation tendency of TBP. In this scenario, the extraction and stripping behaviour of both the solvents with U(VI) alone has been compared under high solvent loading conditions as TBP does not form the TP with U(VI) under process conditions. Besides, U(VI) is a constituent of monazite ore as well as spent nuclear fuel and it is therefore relevant to perform solvent extraction studies of U(VI) with TiAP based solvents.

Estimation of nitric acid in the aqueous feed solutions is crucial in order to control the extraction of actinides by organophosphorous extractants such as TiAP and TBP. Likewise, the determination of nitric acid concentration in the metal loaded organic phase is also important as the stripping process involves the co-stripping of acid and metal ions. This increases the aqueous phase acidity during stripping and a reduction in stripping efficiency of metal ions is expected. Hence, accurate and precise determination of nitric acid concentration in both organic as well as aqueous phases is required for optimising the solvent extraction processes.

In the literature, different values have been reported for the nitric acid loading in the organic phase in the extraction of actinides by the same extractant-diluent system. Plaue et al. have reported a higher  $\text{HNO}_3$  loading in the organic phase at the LOC for the extraction of Pu(IV) by 30% TBP/Hydrogenated polypropylene tetramer at 295 K as compared to data provided by the KfK – 2536 report [184,185]. Earlier, the concentrations of  $\text{HNO}_3$  in organic phases loaded with U(VI) and  $\text{HNO}_3$  were measured in our laboratory by acid-base titration using potassium oxalate as complexing agent for 1.1 M TiAP/Heavy Normal Paraffins (HNP) -  $\text{UO}_2(\text{NO}_3)_2/\text{HNO}_3$  system and the values were higher than the literature data. [175,176,186]. Therefore, the reliability of nitric acid analysis in the presence of U(VI) had to be validated before carrying out the extraction experiments.

Extraction behaviour of several actinides and fission products under various process conditions have been well established for TBP based solvent systems [75,187]. However, such data on TiAP are scarce in literature. Prior to the deployment of TiAP in a processing plant, batch extraction data for the extraction of U(VI) and fission products are required under various conditions for the development of suitable process flow sheets. In this context, extraction profiles of U(VI) and  $\text{HNO}_3$  for various concentrations of nitric acid as a function of U(VI) loading have been generated for 1.1 M TiAP/*n*-DD.

Apart from the extraction characteristics, knowledge about the stripping behaviour of the solvent is also essential for flow sheet development. In this connection, stripping behaviour of TiAP and TBP loaded with U(VI) has been compared with and without scrubbing. The presence of nitric acid in the organic phase can enhance the degradation of an extractant. In order to compare the effects of degradation induced by  $\text{HNO}_3$  on the stripping behaviour, studies have also been carried out on the stripping of U(VI) from 1.1 M TiAP/*n*-DD and 1.1 M TBP/*n*-DD loaded with U(VI) and  $\text{HNO}_3$  as a function of time.

### 3.2 Validation of the analytical method for free acidity determination

#### 3.2.1 Comparison of literature data on U(VI) and HNO<sub>3</sub> extraction with the present study

Consistency of analysed values for the free acidity has been verified with literature data by investigating the extraction of U(VI) by 1.1 M TBP/*n*-DD from UO<sub>2</sub>(NO<sub>3</sub>)<sub>2</sub> solution in 4 M HNO<sub>3</sub>. The experimental values are compared with the literature values as shown in Table 3.1. It is observed in Table 3.1 that the concentration of U(VI) in organic and aqueous phases as well as the concentration of HNO<sub>3</sub> in the aqueous phase are comparable with literature values, whereas there is a considerable difference in HNO<sub>3</sub> loading of the organic phase between the experimental and literature values.

**Table 3.1: Comparison of experimental data for the extraction of U(VI) and HNO<sub>3</sub> by 1.1 M TBP/*n*-DD from U(VI) solutions in nitric acid media with literature data (KfK – 2536).**

Study	[U(VI)] <sub>aq</sub> (mol/L)	[U(VI)] <sub>org</sub> (mol/L)	[HNO <sub>3</sub> ] <sub>aq</sub> (mol/L)	[HNO <sub>3</sub> ] <sub>org</sub> (mol/L)	[TBP] <sub>Free</sub> (mol/L)
<b>KfK Report [185]</b>	0.810	0.420	4.18	0.150	0.110
<b>Present Study</b>	0.873	0.477	4.27 <sup>a</sup>	0.611 <sup>a</sup>	-0.465
<b>KfK Report [185]</b>	1.000	0.440	2.19	0.050	0.170
<b>Present Study</b>	1.04	0.488	2.28 <sup>b</sup>	0.044 <sup>b</sup>	0.080

Complexing agents - Potassium oxalate<sup>a</sup> / Potassium oxalate and sodium fluoride<sup>b</sup>

Generally, TBP forms monosolvate and disolvate complexes with nitric acid and uranyl nitrate, respectively [161,188]. Therefore, the amount of TBP not complexed with uranyl nitrate and nitric acid ([TBP]<sub>Free</sub>) can be calculated by subtracting the amount of TBP complexed with uranyl nitrate and nitric acid from total amount of TBP present in the organic phase by using Eq. (3.1).

$$[\text{TBP}]_{\text{Free}} = 1.1 - (2[\text{U(VI)}]_{\text{org}} + [\text{HNO}_3]_{\text{org}}) \quad (3.1)$$

Table 3.1 shows the  $[TBP]_{Free}$  values calculated from the data from present study and literature data using the above equation. Table 3.1 indicates that the  $[TBP]_{Free}$  computed from literature data are positive and it is negative for the present study where the concentration of  $HNO_3$  is determined by acid-base titration with potassium oxalate as complexing agent. The  $[TBP]_{Free}$  values indirectly confirm the inconsistency in the estimation of  $HNO_3$  by using potassium oxalate as complexing agent.

### **3.2.2 Comparison of estimation of free acidity with oxalate and oxalate-fluoride mixture as complexing agents**

It is reported in the literature that potassium oxalate can be used for the complexation of U(VI) during free acid determination, particularly for the samples with lower U(VI): $HNO_3$  ratio. However for systems with higher U(VI): $HNO_3$  ratio, the uranyl oxalate complex undergoes hydrolysis near the end point due to its lesser stability at higher pH and gives biased results [67,180]. Mayankutty et al. had mentioned that the uranyl ion forms a stable complex with oxalate and fluoride ( $M_3[UO_2(C_2O_4)F_3 \cdot H_2O]$ ) which does not undergo hydrolysis near the end point [180].

Hence by using oxalate and fluoride mixture as a dual complexing agent, free acid analysis was carried out and the results are displayed in Table 3.1. Comparison of literature values with values obtained in the present study for the extraction of U(VI) and  $HNO_3$  by 1.1 M TBP/*n*-DD from  $UO_2(NO_3)_2$  solution with 2 M  $HNO_3$  shows that the concentrations of U(VI) and  $HNO_3$  in both organic as well as aqueous phases are in good agreement with each other. Table 3.1 also shows that the  $[TBP]_{Free}$  values computed from the data obtained for aforementioned solvent systems are positive. This confirms the reliability in the estimation of  $HNO_3$  by using oxalate - fluoride mixture as complexing agents.

### 3.2.3 Validation of HNO<sub>3</sub> estimation using oxalate-fluoride as dual complexing agent

The uniformity of HNO<sub>3</sub> concentrations determined by using potassium oxalate and sodium fluoride mixture as complexing agent for samples with a wide range of U(VI):HNO<sub>3</sub> mole ratios has been studied by mixing saturated UO<sub>2</sub>(NO<sub>3</sub>)<sub>2</sub> solution with nitric acid solutions of different concentrations as indicated in Table 3.2. The results shown in Table 3.2 illustrate that the volume of NaOH solution consumed during the analysis is equivalent to the amount of HNO<sub>3</sub> present in the solution, irrespective of the U(VI):HNO<sub>3</sub> mole ratio in the sample.

**Table 3.2: Determination of HNO<sub>3</sub> concentration in samples with various U(VI):HNO<sub>3</sub> mole ratios by using potassium oxalate - sodium fluoride mixture as complexing agent.**

Sample	A	B	C
U(VI) : HNO <sub>3</sub>	1:1	10:1	100:1
U(VI) <sub>sample</sub> (m.mol)	0.0675	0.2700	0.2700
HNO <sub>3</sub> <sub>sample</sub> (m.mol)	0.0505	0.0289	0.0049
NaOH <sub>consumed</sub> (m.mol)	0.0513	0.0269	0.0045
A: 25 µL ~2.7 mol/L (satd.) U(VI) + 25 µL 2.00 mol/L HNO <sub>3</sub> B: 100 µL ~2.7 mol/L (satd.) U(VI) + 250 µL 0.11 mol/L HNO <sub>3</sub> C: 100 µL ~2.7 mol/L (satd.) U(VI) + 250 µL 0.0092 mol/L HNO <sub>3</sub>			

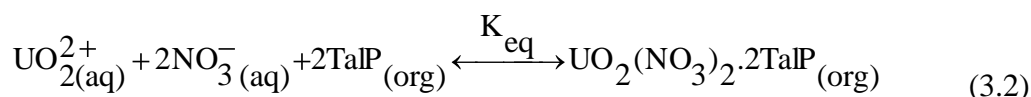
Results obtained from the experiments carried out to further confirm the reliability of this analytical method for 1.1 M TBP/*n*-DD - U(VI)/HNO<sub>3</sub> systems are shown in Table 3.3. Data given in Table 3.3 illustrate that there is a good mass balance in the concentrations of HNO<sub>3</sub> and U(VI) before and after their extraction. Hence this method was chosen for nitric acid determination in both organic and aqueous phases in the present study.

**Table 3.3: Mass balance data for the extraction of U(VI) and HNO<sub>3</sub> by 1.1 M TBP/*n*-DD from U(VI) solutions in 0.2 M & 2 M HNO<sub>3</sub>.**

Solute	0.2 M HNO <sub>3</sub> System		2 M HNO <sub>3</sub> System	
	Before Extraction	After Extraction	Before Extraction	After Extraction
U(VI) <sub>aq</sub> (mg)	932	696	923	698
U(VI) <sub>org</sub> (mg)	-	238	-	239
U(VI) <sub>aq+org</sub> (mg)	932	934	923	937
HNO <sub>3</sub> <sub>aq</sub> (m.mol)	0.375	0.372	4.17	4.28
HNO <sub>3</sub> <sub>org</sub> (m.mol)	-	0.009	-	0.053
HNO <sub>3</sub> <sub>aq+org</sub> (m.mol)	0.375	0.381	4.17	4.33

### 3.3 Extraction of U(VI) by 1.1 M TiAP/*n*-DD as a function of metal loading and aqueous phase acidity

Distribution ratios for the extraction of U(VI) ( $D_{U(VI)}$ ) by 1.1 M TiAP/*n*-DD from UO<sub>2</sub>(NO<sub>3</sub>)<sub>2</sub> solutions at various concentrations of HNO<sub>3</sub> (0.1 M, 0.5 M, 2 M, 4 M and 6 M) have been determined as a function of [U(VI)]<sub>aq,eq</sub>. Suresh et al. investigated the variation of  $D_{U(VI)}$  as a function of [U(VI)]<sub>aq,eq</sub> for UO<sub>2</sub>(NO<sub>3</sub>)<sub>2</sub> solutions in 1 M and 5 M HNO<sub>3</sub> at 303 K [155]. The variation of  $D_{U(VI)}$  with respect to [U(VI)]<sub>aq,eq</sub> (0 to 0.5 mol/L) for various concentrations of HNO<sub>3</sub> for U(VI) extraction by 1.1 M TiAP/*n*-DD is shown in Fig. 3.1. Trialkyl phosphates are expected to form disolvate complexes with UO<sub>2</sub>(NO<sub>3</sub>)<sub>2</sub> [189] as represented by Eq. (3.2), where (aq) and (org) represent species present in the aqueous and organic phases, respectively.



The equilibrium constant ( $K_{eq}$ ) can be correlated to the concentration and the activity co-efficient of various species as shown in Eq. (3.3), where terms in square brackets represent concentrations and  $\gamma$  terms stand for corresponding activity co-efficients.

$$K_{eq} = \frac{[\text{UO}_2(\text{NO}_3)_2 \cdot 2\text{TaIP}]_{(\text{org})}}{[\text{UO}_2^{2+}]_{(\text{aq})} [\text{NO}_3^-]_{(\text{aq})}^2 [\text{TaIP}]_{(\text{org})}^2} \times \frac{\gamma_{\text{UO}_2(\text{NO}_3)_2 \cdot 2\text{TaIP}_{(\text{org})}}}{\gamma_{\text{UO}_2^{2+}} \gamma_{\text{NO}_3^-}^2 \gamma_{\text{TaIP}_{(\text{org})}}^2} \quad (3.3)$$

The rearrangement of Eq (3.3) by taking the activity co-efficient terms to the LHS of Eq. (3.3) gives Eq. (3.4),

$$K_{eq} \times \frac{\gamma_{\text{UO}_2^{2+}} \gamma_{\text{NO}_3^-}^2 \gamma_{\text{TaIP}_{(\text{org})}}^2}{\gamma_{\text{UO}_2(\text{NO}_3)_2 \cdot 2\text{TaIP}_{(\text{org})}}} = \frac{[\text{UO}_2(\text{NO}_3)_2 \cdot 2\text{TaIP}]_{(\text{org})}}{[\text{UO}_2^{2+}]_{(\text{aq})} [\text{NO}_3^-]_{(\text{aq})}^2 [\text{TaIP}]_{(\text{org})}^2} \quad (3.4)$$

The activity co-efficients can be assumed as constants for a particular solvent extraction system and therefore, the product of activity co-efficients and  $K_{eq}$  can be equated to another constant ( $K$ ) as shown in Eq. (3.5).

$$K = K_{eq} \times \frac{\gamma_{\text{UO}_2^{2+}} \gamma_{\text{NO}_3^-}^2 \gamma_{\text{TaIP}_{(\text{org})}}^2}{\gamma_{\text{UO}_2(\text{NO}_3)_2 \cdot 2\text{TaIP}_{(\text{org})}}} \quad (3.5)$$

$$\text{Accordingly, } K = \frac{[\text{UO}_2(\text{NO}_3)_2 \cdot 2\text{TaIP}]_{(\text{org})}}{[\text{UO}_2^{2+}]_{(\text{aq})} [\text{NO}_3^-]_{(\text{aq})}^2 [\text{TaIP}]_{(\text{org})}^2} \quad (3.6)$$

The ratio  $[\text{UO}_2(\text{NO}_3)_2 \cdot 2\text{TaIP}]_{(\text{org})} / [\text{UO}_2^{2+}]_{(\text{aq})}$  represents  $D_{\text{U(VI)}}$  and hence the above Eq. (3.6) can be expressed as Eq. (3.7).

$$D_{\text{U(VI)}} = K [\text{NO}_3^-]_{(\text{aq})}^2 [\text{TaIP}]_{(\text{org})}^2 \quad (3.7)$$

Therefore,  $D_{\text{U(VI)}}$  can be correlated to the nitrate ion concentration and the free extractant concentration as given by Eq. (3.7).

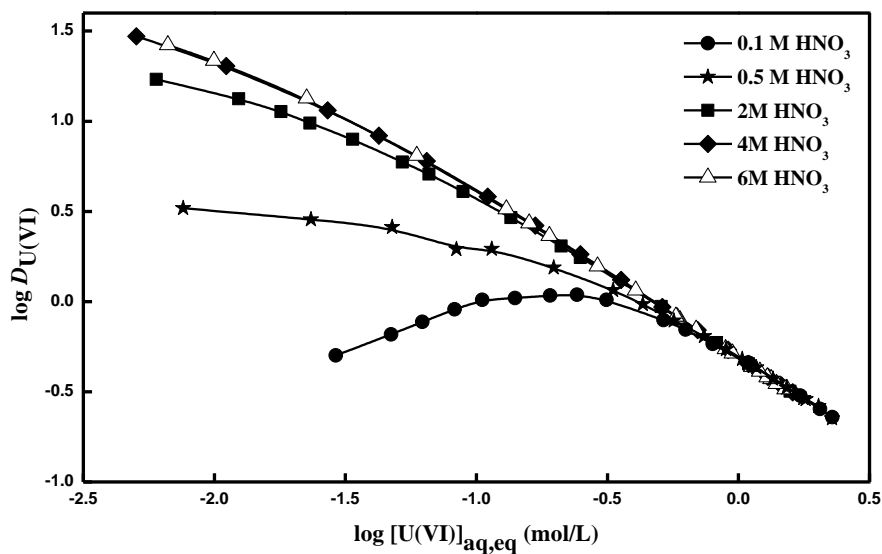


**Fig. 3.1:** Variation of  $D_{U(VI)}$  as a function of  $[U(VI)]_{aq,eq}$  for its extraction by 1.1 M TiAP/n-DD from U(VI) solutions in nitric acid media at 303 K.

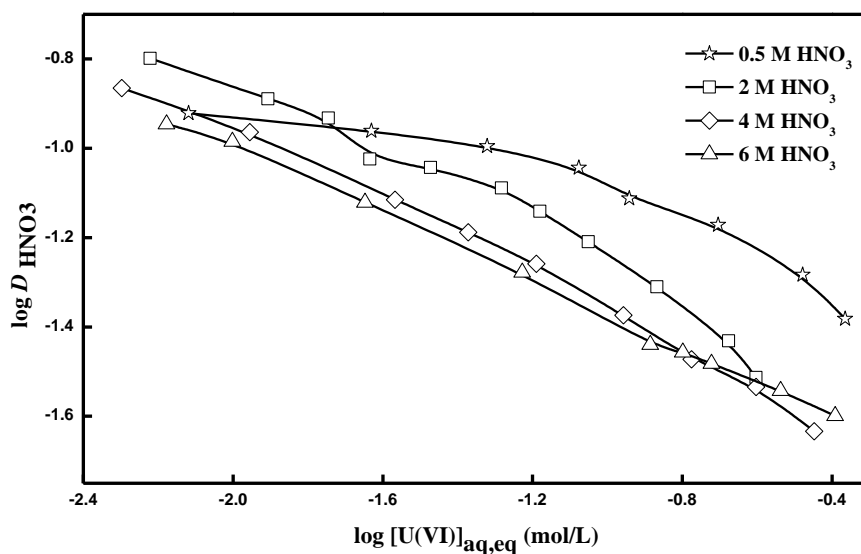
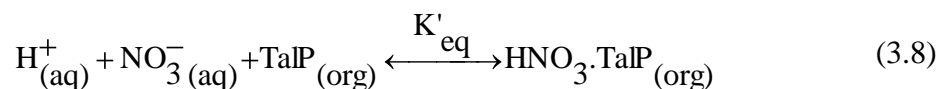


**Fig. 3.2:** Variation of  $D_{HNO_3}$  with  $[U(VI)]_{aq,eq}$  for the extraction of U(VI) by 1.1 M TiAP/n-DD from U(VI) solutions in nitric acid media at 303 K.

Equation (3.7) implies that an increase in the nitrate ion concentration in the aqueous phase and an increase in the free extractant concentration in the organic phase lead to increase in  $D_{U(VI)}$ . Figure 3.1 indicates that for a dilute solution,  $D_{U(VI)}$  increases with

increasing  $[\text{HNO}_3]_{\text{aq,eq}}$  due to the enhanced nitrate ion concentration. Also, the  $D_{\text{U(VI)}}$  decreases with increasing  $[\text{U(VI)}]_{\text{aq,eq}}$  which can be attributed to the reduced free extractant concentration at high metal loading. Figure 3.1 depicts that  $D_{\text{U(VI)}}$  for 0.1 M  $\text{HNO}_3$  system is by far lower for all equilibrium aqueous phase U(VI) concentrations.

During the extraction of actinides from nitric acid media,  $\text{HNO}_3$  also gets extracted by extractant molecules as represented by Eq. (3.8).



Therefore, distribution ratios for  $\text{HNO}_3$  ( $D_{\text{HNO}_3}$ ), nitrate ion concentration, free extractant concentration and the proportionality constant ( $K'$ ) can be correlated as shown in Eq. (3.9).

$$D_{\text{HNO}_3} = K' [\text{NO}_3^-]_{(\text{aq})} [\text{TaIP}]_{(\text{org})} \quad (3.9)$$

Trends in the variation of  $D_{\text{HNO}_3}$  as a function of  $[\text{U(VI)}]_{\text{aq,eq}}$  (0 to 0.5 mol/L) for various concentrations of  $\text{HNO}_3$  are shown in Fig. 3.2. It was already discussed that with increasing concentration of  $\text{HNO}_3$  in the aqueous phase there is an increase in  $D_{\text{U(VI)}}$ . This leads to an increase in U(VI) concentration in the organic phase and as a result there is a corresponding reduction in the free extractant concentration which is responsible for a decrease in  $D_{\text{HNO}_3}$  with increase in  $[\text{HNO}_3]_{\text{aq,eq}}$  as well as  $[\text{U(VI)}]_{\text{aq,eq}}$ .

Data for  $D_{\text{U(VI)}}$  and  $D_{\text{HNO}_3}$  as a function of  $[\text{U(VI)}]_{\text{aq,eq}}$  for various concentrations of nitric acid are shown in Tables 3.4 - 3.6. It can be seen from Table 3.4 that  $D_{\text{U(VI)}}$  for U(VI) extraction from its solution in 0.1 M  $\text{HNO}_3$  by 1.1 M  $\text{TiAP}/n\text{-DD}$  initially increases with increase in  $[\text{U(VI)}]_{\text{aq,eq}}$  and then decreases after passing through a maximum value. The initial rise in  $D_{\text{U(VI)}}$  can be attributed to the increase in nitrate ion concentration and further decrease in  $D_{\text{U(VI)}}$  is due to reduction in free extractant concentration with loading. However, Tables 3.4 - 3.6 show that  $D_{\text{U(VI)}}$  decreases with increase in  $[\text{U(VI)}]_{\text{aq,eq}}$  for U(VI) extraction from its

solution in 0.5 M, 2 M, 4 M and 6 M HNO<sub>3</sub>. The  $D_{\text{HNO}_3}$  marginally drops with the increase in  $[\text{U(VI)}]_{\text{aq,eq}}$  due to the decrease in free extractant concentration. For extraction from UO<sub>2</sub>(NO<sub>3</sub>)<sub>2</sub> solutions in 6 M HNO<sub>3</sub> as shown in Table 3.6,  $D_{\text{HNO}_3}$  remains almost independent of the  $[\text{U(VI)}]_{\text{aq,eq}}$ .

**Table 3.4: Data on extraction of U(VI) and HNO<sub>3</sub> by 1.1 M TiAP/*n*-DD from U(VI) solutions in 0.1 M and 0.5 M nitric acid at 303 K.**

0.1 M HNO <sub>3</sub> System			0.5 M HNO <sub>3</sub> System			
$[\text{U(VI)}]_{\text{aq}}$ (mol/L)	$D_{\text{U(VI)}}$	$[\text{HNO}_3]_{\text{aq}}$ (mol/L)	$[\text{U(VI)}]_{\text{aq}}$ (mol/L)	$D_{\text{U(VI)}}$	$[\text{HNO}_3]_{\text{aq}}$ (mol/L)	$D_{\text{HNO}_3}$
0.047	0.657	0.106	0	-	0.485	0.142
0.062	0.772	0.109	0.008	3.30	0.505	0.120
0.082	0.906	0.110	0.567	0.786	0.505	0.038
0.105	1.02	0.112	0.740	0.642	0.503	0.031
0.242	1.09	0.110	0.896	0.543	0.514	0.028
0.629	0.701	0.095	1.03	0.480	0.510	0.023
0.799	0.583	0.094	1.17	0.431	0.505	0.024
1.09	0.458	0.100	1.35	0.374	0.504	0.025
1.12	0.442	0.098	1.53	0.333	0.490	0.023
1.72	0.301	0.098	1.77	0.291	0.517	0.016
2.05	0.254	0.107	1.80	0.287	0.517	0.017
2.28	0.228	0.102	2.28	0.225	0.525	0.016

For a better clarity, variations of concentration of U(VI) and HNO<sub>3</sub> in organic phase for their extraction by 1.1 M TiAP/*n*-DD from UO<sub>2</sub>(NO<sub>3</sub>)<sub>2</sub> solution in various concentrations of nitric acid as a function of  $[\text{U(VI)}]_{\text{aq,eq}}$  are shown in Figs. 3.3 and 3.4. It can be seen in Figs. 3.3 and 3.4 that in general, the concentration of U(VI) in the organic phase increases with increase in  $[\text{U(VI)}]_{\text{aq,eq}}$  whereas, the concentration of HNO<sub>3</sub> decreases. This indicates that when a relatively high U(VI) concentration is extracted into the organic phase, an

equivalent amount of  $\text{HNO}_3$  is stripped into the aqueous phase. However, it is observed in Fig. 3.4(B) that at higher  $[\text{U(VI)}]_{\text{aq,eq}}$  there is a marginal increase in the concentration of  $\text{HNO}_3$  with increase in  $[\text{U(VI)}]_{\text{aq,eq}}$ .

**Table 3.5: Data on extraction of U(VI) and  $\text{HNO}_3$  by 1.1 M TiAP/n-DD from U(VI) solutions in 2 M and 4 M nitric acid at 303 K.**

2 M $\text{HNO}_3$ System				4 M $\text{HNO}_3$ System			
$[\text{U(VI)}]_{\text{aq}}$ (mol/L)	$D_{\text{U(VI)}}$	$[\text{HNO}_3]_{\text{aq}}$ (mol/L)	$D_{\text{HNO}_3}$	$[\text{U(VI)}]_{\text{aq}}$ (mol/L)	$D_{\text{U(VI)}}$	$[\text{HNO}_3]_{\text{aq}}$ (mol/L)	$D_{\text{HNO}_3}$
0	-	2.00	0.217	0	-	4.00	0.207
0.006	17.1	2.02	0.159	0.005	29.5	3.96	0.136
0.012	13.3	2.04	0.129	0.513	0.932	4.05	0.021
0.066	5.10	2.09	0.072	0.699	0.694	4.08	0.018
0.508	0.940	2.12	0.021	0.914	0.540	4.11	0.019
0.542	0.876	2.02	0.027	1.09	0.452	4.10	0.016
0.826	0.591	2.04	0.015	1.30	0.384	4.07	0.015
1.09	0.451	2.22	0.014	1.46	0.344	4.09	0.017
1.57	0.318	2.05	0.016	1.61	0.314	4.06	0.015

**Table 3.6: Data on extraction of U(VI) and  $\text{HNO}_3$  by 1.1 M TiAP/n-DD from U(VI) solution in 6 M nitric acid at 303 K.**

$[\text{U(VI)}]_{\text{aq}}$ (mol/L)	$D_{\text{U(VI)}}$	$[\text{HNO}_3]_{\text{aq}}$ (mol/L)	$D_{\text{HNO}_3}$	$[\text{U(VI)}]_{\text{aq}}$ (mol/L)	$D_{\text{U(VI)}}$	$[\text{HNO}_3]_{\text{aq}}$ (mol/L)	$D_{\text{HNO}_3}$
0	-	6.10	0.164	0.950	0.516	6.04	0.022
0.007	26.5	5.96	0.113	1.13	0.437	6.03	0.022
0.010	21.7	5.99	0.104	1.21	0.410	6.01	0.022
0.059	6.45	6.04	0.053	1.29	0.380	6.15	0.023
0.577	0.828	5.92	0.022	1.33	0.372	6.00	0.023
0.585	0.819	6.05	0.022	1.40	0.350	6.04	0.024
0.598	0.790	6.25	0.021	1.51	0.326	5.92	0.022
0.892	0.545	6.25	0.024	1.53	0.328	6.06	0.024

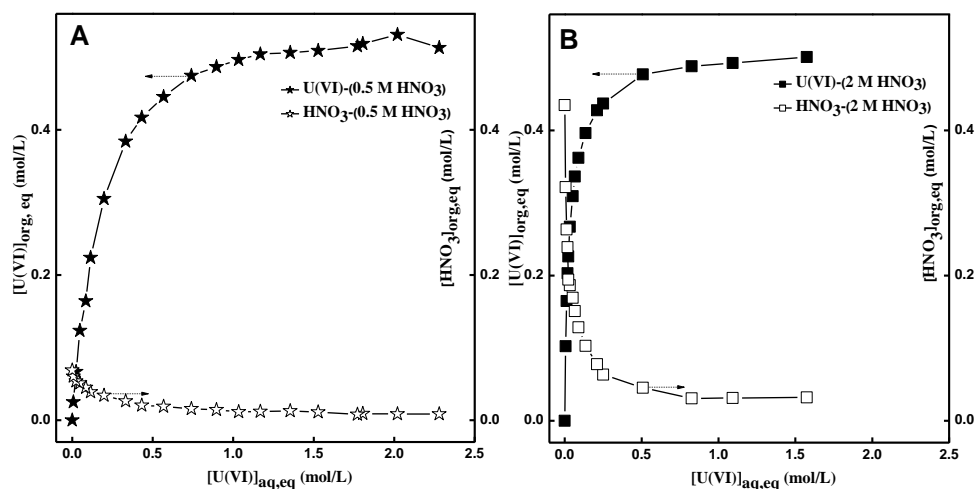


**Fig. 3.3:** Variation of U(VI) and HNO<sub>3</sub> concentrations in the organic phase with [U(VI)]<sub>aq,eq</sub> for their extraction by 1.1 M TiAP/n-DD from U(VI) solutions in nitric acid media at 303 K. (A) 0.5 M HNO<sub>3</sub> system (B) 2 M HNO<sub>3</sub> system.

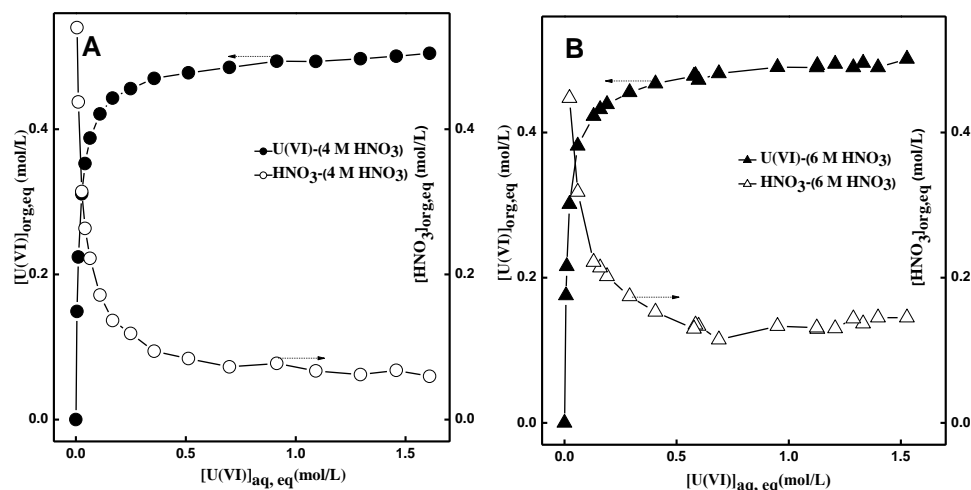


**Fig. 3.4:** Variation of U(VI) and HNO<sub>3</sub> concentrations in the organic phase with [U(VI)]<sub>aq,eq</sub> for their extraction by 1.1 M TiAP/n-DD from U(VI) solutions in nitric acid media at 303 K. (A) 4 M HNO<sub>3</sub> system (B) 6 M HNO<sub>3</sub> system.

It is well known that U(VI) and HNO<sub>3</sub> form disolvate and monosolvate complexes with TalPs, respectively [161,162,173,188]. If free extractant is not available in the nitric acid loaded organic phase, further loading of metal nitrate takes place with the replacement of already extracted nitric acid. Under such conditions, for the formation of one mole of U(VI)-TalP complex, two moles of HNO<sub>3</sub>-TalP complex undergo dissociation in the organic phase and the liberated HNO<sub>3</sub> molecules are transferred to the aqueous phase [141]. This leads to a

steep increase in the difference in concentration of U(VI) and HNO<sub>3</sub> in the organic phase at lower [U(VI)]<sub>aq,eq</sub>. When the metal loading in organic phase reaches saturation, extraction of U(VI) as well as stripping of HNO<sub>3</sub> do not occur and hence there is no drastic change in the difference in concentration between U(VI) and HNO<sub>3</sub> at higher [U(VI)]<sub>aq,eq</sub>.

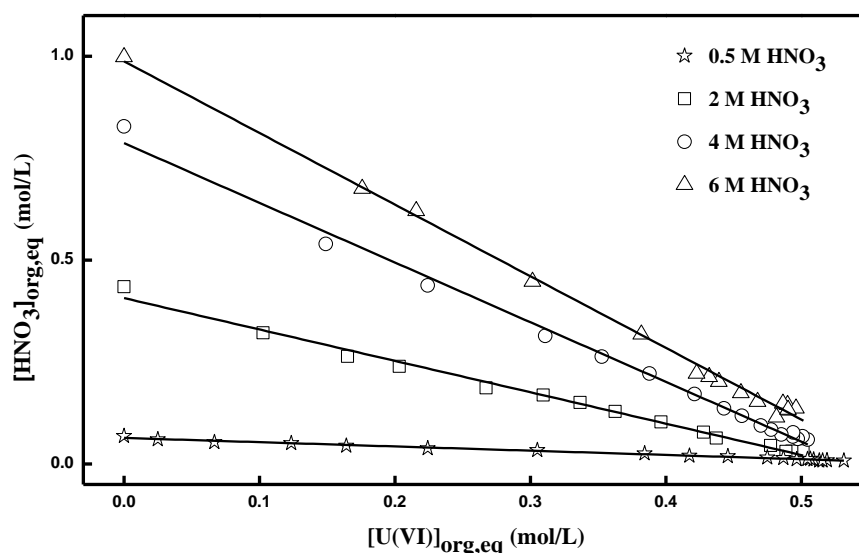


**Fig. 3.5:** Variation of the HNO<sub>3</sub> concentration in the organic phase as a function of [U(VI)]<sub>org,eq</sub> for the extraction by 1.1 M TiAP/n-DD from U(VI) solutions in nitric acid media at 303 K.

Trend in the loading of HNO<sub>3</sub> in the organic phase with respect to [U(VI)]<sub>org,eq</sub> shown in Fig. 3.5 depicts a reduction in HNO<sub>3</sub> loading of the organic phase with an increase in U(VI) loading. A linear relationship between [HNO<sub>3</sub>]<sub>org,eq</sub> and [U(VI)]<sub>org,eq</sub> can be observed in Fig. 3.5 for the extraction from all nitric acid solutions. Therefore, an extraction flow sheet has to be designed in such a way that the organic loading of U(VI) is near saturation so that HNO<sub>3</sub> loading is minimum in the organic phase and the nitric acid induced degradation of organic phase components can be minimized. As the free extractant concentration becomes negligible when the U(VI) loading in the organic phase is close to saturation, the extraction of other metal ions into the organic phase is reduced. This improves the decontamination factor

of U(VI) and therefore, it is essential to design solvent extraction flow sheets such that the U(VI) extraction by the organic phase is as high as practically feasible.

It is worthwhile to compare the extraction behaviour of both TiAP and TBP based solvents with U(VI) in nitric acid media under similar conditions. In this regard,  $D_{U(VI)}$  for 1.1 M TBP/Odourless Kerosene (OK) -  $UO_2(NO_3)_2/HNO_3$  system at 298 K reported in the literature has been compared with that of 1.1 M TiAP/*n*-DD -  $UO_2(NO_3)_2/HNO_3$  system at 303 K in Table 3.7. Data shown in Table 3.7 indicate that  $D_{U(VI)}$  values for TiAP are only marginally higher than that of TBP and therefore, in general, it can be concluded that the extraction behaviour of both the solvents are comparable.

**Table 3.7: Comparison of  $D_{U(VI)}$  for 1.1 M TiAP/*n*-DD -  $UO_2(NO_3)_2/HNO_3$  and 1.1 M TBP/OK -  $UO_2(NO_3)_2/HNO_3$  systems under similar extraction conditions.**

1.1 M TiAP/ <i>n</i> -DD			1.1 M TBP/OK [185]		
[HNO <sub>3</sub> ] <sub>aq</sub>	[U(VI)] <sub>aq</sub>	$D_{U(VI)}$	[HNO <sub>3</sub> ] <sub>aq</sub>	[U(VI)] <sub>aq</sub>	$D_{U(VI)}$
0.112	0.105	1.02	0.100	0.105	0.890
0.492	0.023	2.85	0.488	0.023	2.78
2.02	0.006	17.1	1.85	0.007	13.4
4.02	0.011	20.2	4.00	0.016	15.2

### 3.4 Extraction, scrubbing and stripping of U(VI) in cross-current mode - 1.1 M TalP/*n*-DD - U(VI)/HNO<sub>3</sub> systems

With the aim to compare the stripping behaviour of TiAP and TBP, both the solvents were saturated with U(VI) upto the theoretical loading and stripped under identical conditions. Generally, in reprocessing plants, the loaded organic phase is scrubbed to remove the undesirable metal ions co-extracted by the organic phase. In order to simulate the actual scrubbing conditions prior to stripping of U(VI) the organic phase was scrubbed with nitric acid. Data on the extraction and stripping of U(VI) by both TiAP as well as TBP without and

with scrubbing of organic phases are shown in Table 3.8 and 3.9, respectively. The pictures of organic and aqueous phases after each stage of extraction and stripping of U(VI) by 1.1 M TiAP/*n*-DD and 1.1 M TBP/*n*-DD are shown in Fig. 3.6.

**Table 3.8: Data on extraction and stripping of U(VI) with 1.1 M TiAP/*n*-DD and 1.1 M TBP/*n*-DD at 303 K.**

Steps	TiAP				TBP			
	[HNO <sub>3</sub> ] (mol/L)		[U(VI)] (g/L)		[HNO <sub>3</sub> ] (mol/L)		[U(VI)] (g/L)	
	org	Aq	org	Aq	org	aq	org	aq
<b>Extraction</b>	0.057	3.60	113	204	0.052	3.53	115	193
<b>Strip-1</b>	0.003	0.063	57.3	54.8	0.004	0.075	54.1	55.7
<b>Strip-2</b>	< 0.001	0.013	26.0	32.3	< 0.001	0.018	22.7	31.3
<b>Strip-3</b>	< 0.001	0.011	8.26	18.0	< 0.001	0.014	7.15	16.6
<b>Strip-4</b>	< 0.001	0.011	1.13	7.38	< 0.001	0.012	0.755	6.04
<b>Strip-5</b>	< 0.001	0.010	0.174	1.12	< 0.001	0.011	0.156	0.758

**Table 3.9: Data on extraction, scrubbing and stripping of U(VI) with 1.1 M TiAP/*n*-DD and 1.1 M TBP/*n*-DD at 303 K.**

Steps	TiAP				TBP			
	[HNO <sub>3</sub> ] (mol/L)		[U(VI)] (g/L)		[HNO <sub>3</sub> ] (mol/L)		[U(VI)] (g/L)	
	org	Aq	Org	Aq	org	aq	org	aq
<b>Extraction</b>	0.057	3.60	113	204	0.052	3.53	115	193
<b>Scrub (Sc)</b>	0.094	1.90	86.8	26.3	0.109	1.91	86.5	28.4
<b>Sc-Strip-1</b>	0.008	0.106	45.3	41.0	0.007	0.113	42.1	40.1
<b>Sc-Strip-2</b>	< 0.001	0.015	19.1	26.9	< 0.001	0.020	16.6	26.0
<b>Sc-Strip-3</b>	< 0.001	0.012	5.31	14.3	< 0.001	0.013	4.19	13.0
<b>Sc-Strip-4</b>	< 0.001	0.010	0.436	4.55	< 0.001	0.011	0.285	3.70
<b>Sc-Strip-5</b>	< 0.001	0.010	0.145	0.681	< 0.001	0.012	0.050	0.560

Table 3.8 and 3.9 illustrate that the stripping of U(VI) into the aqueous phase is efficient in both the cases where stripping is done with and without scrubbing. It is observed

that co-extracted  $\text{HNO}_3$  is completely stripped back to aqueous phase in two stripping stages in the case of TiAP as well as TBP. Table 3.8 and 3.9 depict that the number of stages required for the complete stripping of U(VI) is 4 to 5 for both TiAP and TBP. Table 3.8 and 3.9 also show that mass balance of U(VI) before and after extraction, scrubbing and stripping stages are in good agreement.

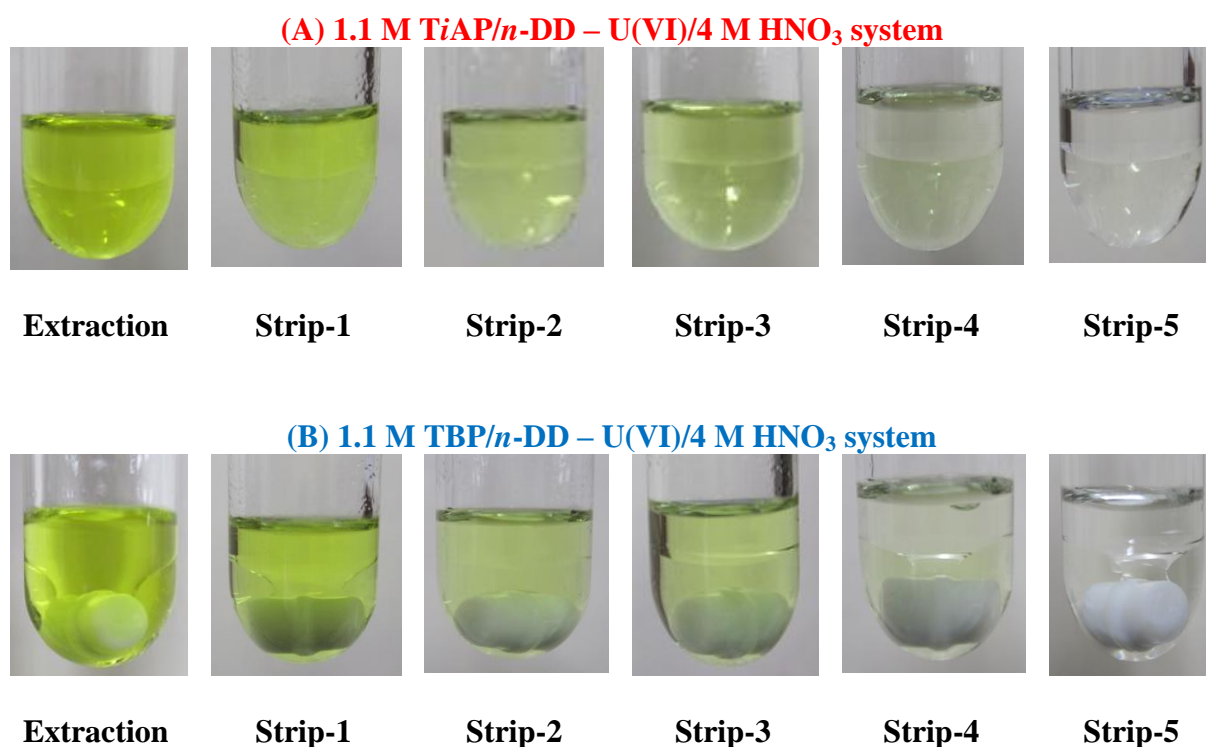


**Fig. 3.6: Extraction and stripping of U(VI) by 1.1 M TalP/n-DD from U(VI) solutions in 4 M  $\text{HNO}_3$  at 303 K. (A) TiAP system (B) TBP system.**

### 3.5 Stripping behaviour of U(VI) as a function of time

The effects of nitric acid induced degradation on the stripping behaviour of U(VI) with TiAP and TBP based solvents have been investigated as a function of time. Data on the concentration of U(VI) remaining in the organic phase after stripping from nitric acid loaded organic phase as a function of time are shown in Fig. 3.7. Results shown in Fig. 3.7 indicate

that the concentration of U(VI) retained in the organic phase increases with time and the concentration of U(VI) remaining in the organic phase is comparable for both TiAP and TBP based solvents.

It is known that the extracted nitric acid induces hydrolysis of trialkyl phosphates to dialkyl phosphates, monoalkyl phosphates and phosphoric acid [106]. These degradation products of trialkyl phosphates have high affinity for U(VI) and hence the stripping of U(VI) from TalP phase containing degradation products becomes intricate. Increasing the time of contact of organic phase with  $\text{HNO}_3$  favours the degradation of trialkyl phosphates and leads to an increase in the concentration of residual U(VI) remaining in the organic phase after stripping. The data shown in Fig. 3.7 also highlight the similarity in the extraction chemistry of TiAP and TBP in the presence of their degradation products.

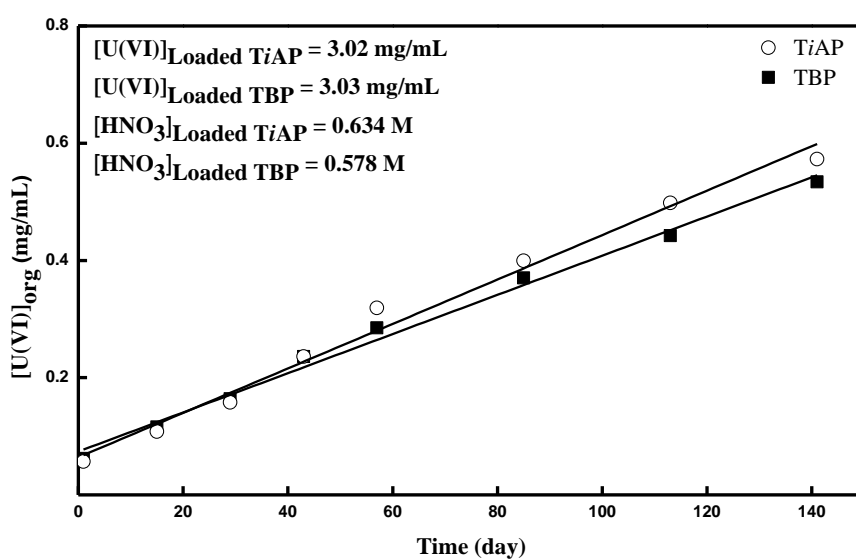


**Fig. 3.7:** Variation of the U(VI) concentration retained in the organic phase (1.1 M TalP/n-DD) after the stripping of U(VI) from loaded organic phase as a function of time at 303K.

### 3.6 Conclusions

The method utilized for the determination of free acidity in U(VI) solutions for high U(VI) to HNO<sub>3</sub> ratios using a potassium oxalate - sodium fluoride mixture as a complexing agent is authenticated. The extraction of U(VI) and HNO<sub>3</sub> into 1.1 M TiAP/*n*-DD from nitric acid media is investigated as a function of equilibrium aqueous phase acidity and U(VI) concentration. The comparable extraction, scrubbing and stripping behaviour of TiAP and TBP based solvents with U(VI) are confirmed in the present study. The deterioration of organic phase loaded with nitric acid and metal ion increases with time for both TiAP and TBP. The data obtained in this study can be used to design new flow sheets with TiAP based solvents for the extraction of U(VI) from spent nuclear fuel solutions in nitric media.



# Chapter 4



**“Research serves to make building stones out of stumbling blocks”**

*-Arthur D. Little*

# THIRD PHASE FORMATION BEHAVIOUR OF TiAP AND TBP IN THE EXTRACTION OF Th(NO<sub>3</sub>)<sub>4</sub>

# 4

---

---

## 4.1 Introduction

The addition of a non-polar diluent to a polar extractant improves the hydrodynamics of solvent extraction systems. However, the use of such a binary liquid mixture (eg. TBP in hydrocarbon) as the solvent is primarily responsible for third phase formation in the extraction of tetravalent metal ions like Th(IV), Zr(IV), Pu(IV) etc., under certain conditions [111,116]. Apart from diluent chain length several parameters such as metal ion and nitric acid concentrations also influence third phase formation. Organic phase splitting results in an uneven distribution of the extracted metal ions and nitric acid between the TP and the DP.

Knowledge about the concentrations of solutes in organic phases before and after the phase splitting is essential to understand the phase splitting behaviour of solvent extraction system and design the flow sheet. Therefore, the phase splitting tendency of TiAP and TBP based solvents has been studied as a function of various parameters with respect to Th(IV) metal ion. The variations of concentrations of solutes (Th(IV) and HNO<sub>3</sub>) and densities of organic phases as well as the ratio of the volume of DP to that of TP ( $V_{DP}/V_{TP}$ ) have been investigated as a function of diluent chain length,  $[Th(IV)]_{aq,eq}$  and  $[HNO_3]_{aq,eq}$  for both TiAP and TBP based solvent systems at 303 K. The experiments have been carried out at 303 K as extraction processes in most of the processing plants in India are performed at ambient temperature which is close to 303 K.

## 4.2 Distribution of Th(IV) and HNO<sub>3</sub> in organic phases

### 4.2.1 Effects of parameters on the distribution ratio of Th(IV) in biphasic region

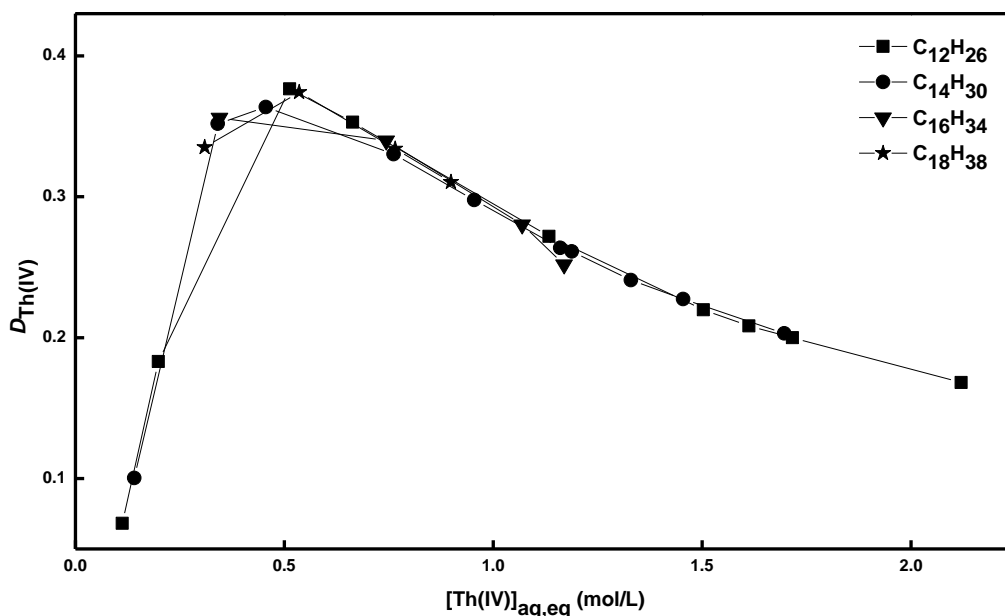


**Fig. 4.1:** Distribution ratio of Th(IV) for its extraction by 1.1 M TiAP/*n*-alkane from Th(NO<sub>3</sub>)<sub>4</sub> solution with near-zero free acidity at 303 K.

Variation of distribution ratio of Th(IV) ( $D_{\text{Th(IV)}}$ ) for its extraction from Th(NO<sub>3</sub>)<sub>4</sub> solution with near-zero free acidity by 1.1 M solutions of TiAP in *n*-DD, *n*-tetradecane (*n*-TD), *n*-hexadecane and *n*-octadecane as a function of [Th(IV)]<sub>aq,eq</sub> at 303 K is shown in Fig. 4.1. In general, the  $D_{\text{Th(IV)}}$  increases with increase in [Th(IV)]<sub>aq,eq</sub> and after passing through a maximum value it decreases. This is a typical trend observed in the extraction of a metal ion by a neutral extractant. Srinivasan et al. measured the  $D_{\text{Th(IV)}}$  as a function of Th(IV) loading in the organic phase to determine the metal-solvate stoichiometry of trialkyl phosphate (TalP) - Th(NO<sub>3</sub>)<sub>4</sub> systems [188]. Their studies revealed the formation of a trisolvate complex of TalP with Th(NO<sub>3</sub>)<sub>4</sub>. The  $D_{\text{Th(IV)}}$  can be correlated to nitrate ion concentration, free extractant concentration and equilibrium constant as shown in Eq. (4.1). It can be deduced from Eq. (4.1) that initial increase in the  $D_{\text{Th(IV)}}$  is due to the increase in self-salting with increase in nitrate ion

concentration. However, the free extractant concentration in the organic phase decreases with increase in metal loading and after passing through a maximum value, the effect of decrease in the free extractant concentration due to loading dominates and the  $D_{\text{Th(IV)}}$  decreases. It can also be seen in Fig. 4.1 that the  $D_{\text{Th(IV)}}$  values for various 1.1 M TiAP/*n*-alkane systems are comparable at a particular  $[\text{Th(IV)}]_{\text{aq,eq}}$  and hence diluent does not influence the extraction significantly. This corroborates our previous observations [155].

$$D_{\text{Th(IV)}} = K_{\text{eq}} [\text{NO}_3^-]_{\text{(aq)}}^4 [\text{TaIP}]_{\text{(org)}}^3 \quad (4.1)$$

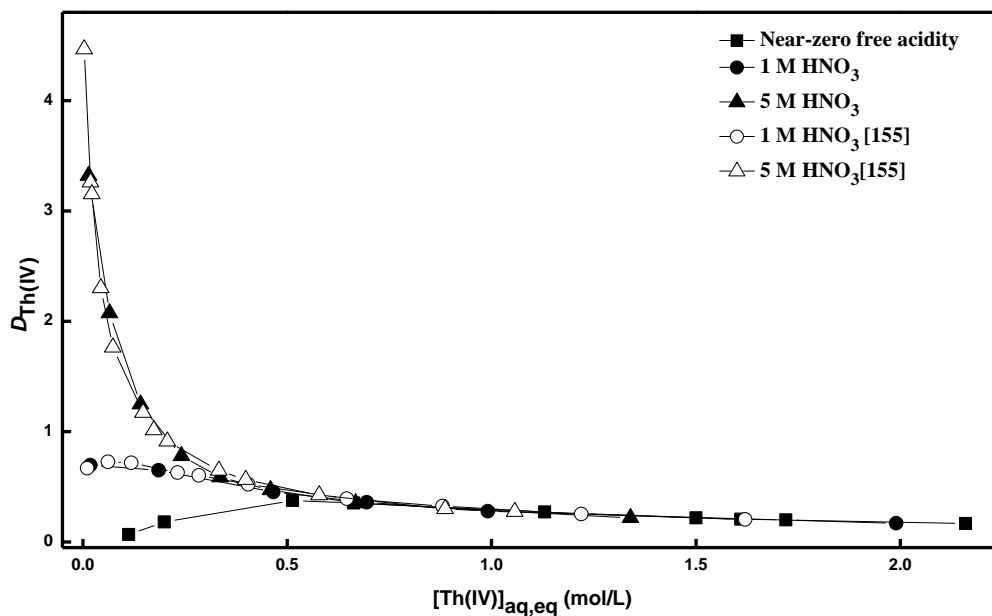


**Fig. 4.2:** Variation of the  $D_{\text{Th(IV)}}$  for Th(IV) extraction by 1.1 M TiAP/*n*-DD from  $\text{Th}(\text{NO}_3)_4$  solutions with near-zero free acidity, 1 M and 5 M nitric acid as a function of  $[\text{Th(IV)}]_{\text{aq,eq}}$  at 303 K.

Variation of the  $D_{\text{Th(IV)}}$  for the extraction of Th(IV) by 1.1 M TiAP/*n*-DD as a function of  $[\text{HNO}_3]_{\text{aq,eq}}$  and  $[\text{Th(IV)}]_{\text{aq,eq}}$  at 303 K is shown in Fig. 4.2. The  $D_{\text{Th(IV)}}$  values reported by Suresh et al. under similar conditions are also shown in Fig. 4.2 [155]. It can be seen from Fig. 4.2 that

the  $D_{\text{Th(IV)}}$  values reported in the present study agree very well with the  $D_{\text{Th(IV)}}$  values reported by Suresh et al. Figure 4.2 also depicts that at lower  $[\text{Th(IV)}]_{\text{aq,eq}}$ , the  $D_{\text{Th(IV)}}$  increases with increase in  $[\text{HNO}_3]_{\text{aq,eq}}$  due to increment in nitrate ion concentration. However, at higher  $[\text{Th(IV)}]_{\text{aq,eq}}$ , the  $D_{\text{Th(IV)}}$  decreases with increase in  $[\text{HNO}_3]_{\text{aq,eq}}$  due to the competition for free extractant between  $\text{HNO}_3$  and  $\text{Th(IV)}$ . Data on the  $D_{\text{Th(IV)}}$  for the extraction of  $\text{Th(IV)}$  from its solution in nitric acid media by 1.1 M solutions of  $\text{TiAP}$  and  $\text{TBP}$  in  $n\text{-DD}$  at 303 K are shown in Fig. 4.3. Data reported by Mallick et al. [190] was used to generate the plot of the  $D_{\text{Th(IV)}}$  vs  $[\text{Th(IV)}]_{\text{aq,eq}}$  for 1.1 M  $\text{TBP}/n\text{-DD}$  -  $\text{Th}(\text{NO}_3)_4/\text{near-zero}$  free acidity system shown in Fig. 4.3. Figure 4.3 indicates that the  $D_{\text{Th(IV)}}$  for 1.1 M  $\text{TiAP}/n\text{-DD}$  and 1.1 M  $\text{TBP}/n\text{-DD}$  are comparable under  $[\text{Th(IV)}]_{\text{aq,eq}}$  and  $[\text{HNO}_3]_{\text{aq,eq}}$  ranges investigated in the present study. These results reveal the comparable extraction behaviour of  $\text{TiAP}$  and  $\text{TBP}$  based solvents with respect to  $\text{Th(IV)}$  metal ion. Sze et al. developed a model to predict distribution ratios of  $\text{Th(IV)}$  under various conditions and validated the predicted values by experiments [191]. Although, this paper reports the data on  $D_{\text{Th(IV)}}$  as a function of various parameters, they cannot be compared with the present data as those experiments were performed with a solution of 30%  $\text{TBP}$  in a mixture of 10% diethylbenzene and 60% isopar at 298 K.

#### 4.2.2 Effects of parameters on third phase formation in the extraction of $\text{Th(IV)}$

The trends in the concentration of  $\text{Th(IV)}$  for its extraction by 1.1 M solutions of  $\text{TiAP}$  in  $n\text{-DD}$ ,  $n\text{-TD}$ ,  $n\text{-hexadecane}$  and  $n\text{-octadecane}$  as diluents from  $\text{Th}(\text{NO}_3)_4$  solution with near-zero free acidity at 303 K with respect to  $[\text{Th(IV)}]_{\text{aq,eq}}$  are shown in Fig. 4.4. Data shown in Fig. 4.2 are used to generate the extraction isotherms of  $\text{TiAP}/n\text{-alkane}$  in biphasic region and displayed in Fig. 4.4 along with data in triphasic region. It can be seen from Fig. 4.4 that at a certain point, the organic phase splits into TP and DP and this is observed as a divergence in the curve. The

point at which the curve diverges corresponds to CAC and LOC. Overlapping of extraction isotherms in biphasic region for systems comprising of 1.1 M TiAP in various diluents shows the independency of Th(IV) extraction with diluent chain length. Figure 4.4 depicts that the difference in Th(IV) concentration between the TP and the DP increases with increase in  $[\text{Th(IV)}]_{\text{aq,eq}}$  and chain length of the diluent which indicates the increase in degree of phase splitting. Literature data on the extraction of Th(IV) by 1.1 M TBP/*n*-DD from  $\text{Th}(\text{NO}_3)_4$  solution with near-zero free acidity at 303 K are also shown in Fig. 4.4 [190]. The results indicate that the phase splitting range of Th(IV) for TBP/*n*-DD system is much higher than TiAP/*n*-DD system.

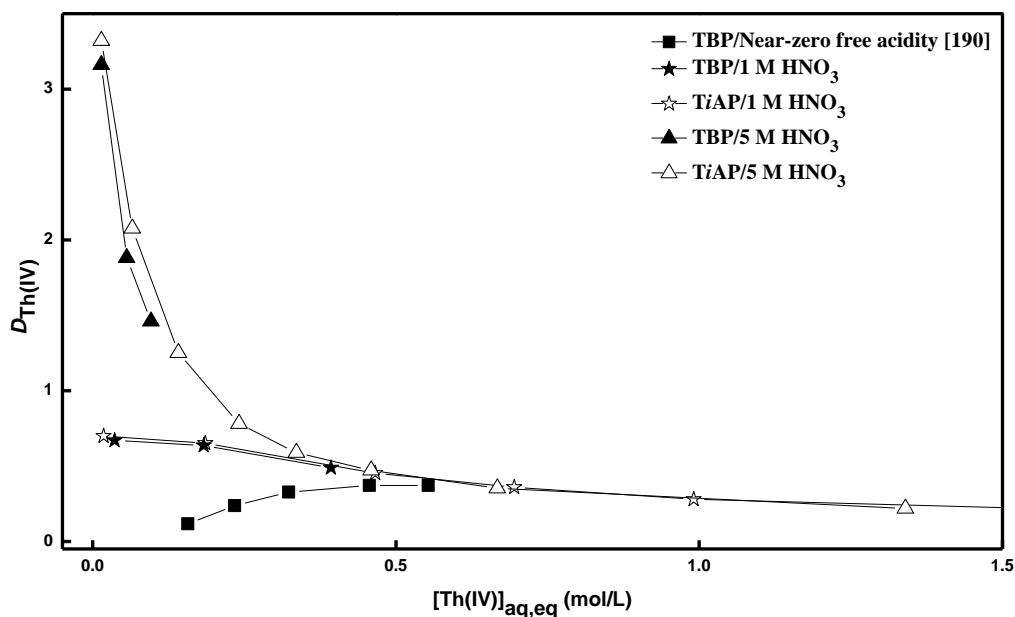


**Fig. 4.3:** Variation of the  $D_{\text{Th(IV)}}$  for Th(IV) extraction by 1.1 M TalP/*n*-DD from  $\text{Th}(\text{NO}_3)_4$  solutions with near-zero free acidity, 1 M and 5 M nitric acid as a function of  $[\text{Th(IV)}]_{\text{aq,eq}}$  at 303 K.

With the assumption that there is no organic phase splitting, the TP and the DP together can be visualized as a single homogeneous phase which can be termed as the virtual organic

phase. The concentration of Th(IV) in that virtual un-split organic phase ( $[\text{Th(IV)}]_{\text{Vir Org}}$ ) can be computed by using Eq. (4.2) where, the terms  $[\text{Th(IV)}]_{\text{TP}}$  and  $[\text{Th(IV)}]_{\text{DP}}$  represent the concentrations of Th(IV) in the third phase and the diluent-rich phase, respectively.  $V_{\text{TP}}$  and  $V_{\text{DP}}$  denote the volumes of the corresponding organic phases. Th(IV) concentrations in the virtual un-split organic phase for various systems are shown in Fig.4.4 with hollow symbols.

$$[\text{Th(IV)}]_{\text{Vir Org}} = \frac{([\text{Th(IV)}]_{\text{TP}} \times V_{\text{TP}}) + ([\text{Th(IV)}]_{\text{DP}} \times V_{\text{DP}})}{V_{\text{TP}} + V_{\text{DP}}} \quad (4.2)$$

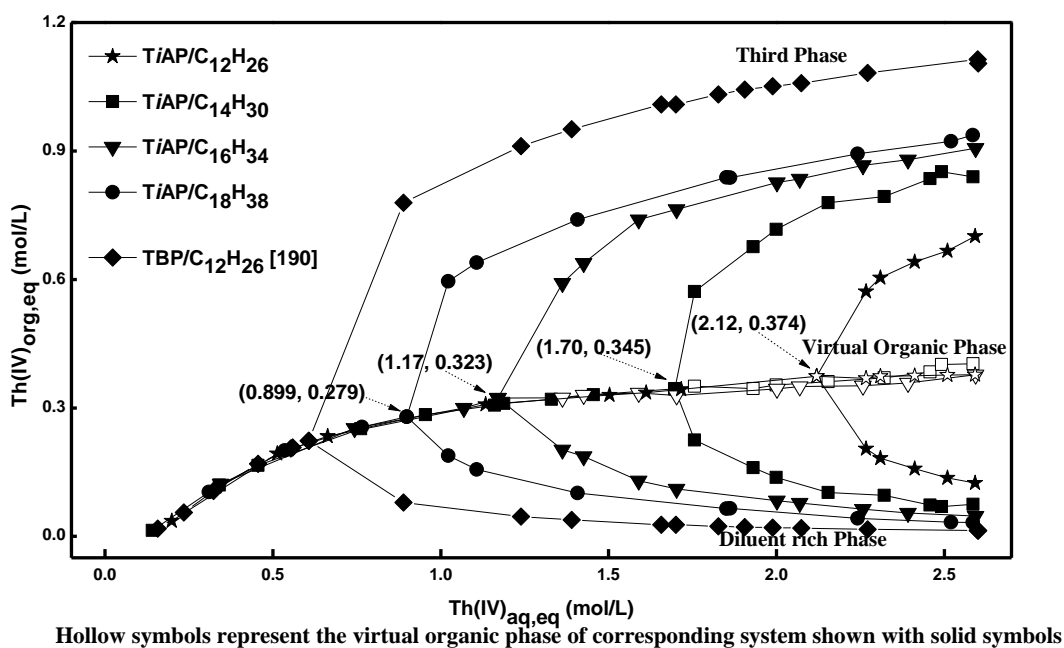


**Fig. 4.4:** Extraction isotherms for the extraction of Th(IV) by 1.1 M TalP/n-alkane from  $\text{Th}(\text{NO}_3)_4$  solution with near-zero free acidity as a function of  $[\text{Th(IV)}]_{\text{aq,eq}}$  at 303 K.

A similar investigation with organic phases in triphasic region was done by Borkowski for 20% TBP/n-octane -  $\text{Th}(\text{NO}_3)_4/\text{HNO}_3$  system [192]. Figure 4.4 illustrates that in the virtual un-split organic phase, there is a marginal increasing trend in the extraction of Th(IV) by

1.1 M TiAP/*n*-alkane as a function of  $[\text{Th(IV)}]_{\text{aq,eq}}$ . Also the plots merge with each other for different TiAP/*n*-alkane systems and they are just an extrapolation of real biphasic region. This clearly indicates that even though there is increase in degree of phase splitting behaviour due to increase in diluent chain length and  $[\text{Th(IV)}]_{\text{aq,eq}}$ , the percentage extraction of Th(IV) by TiAP based solvents with various diluents is comparable.

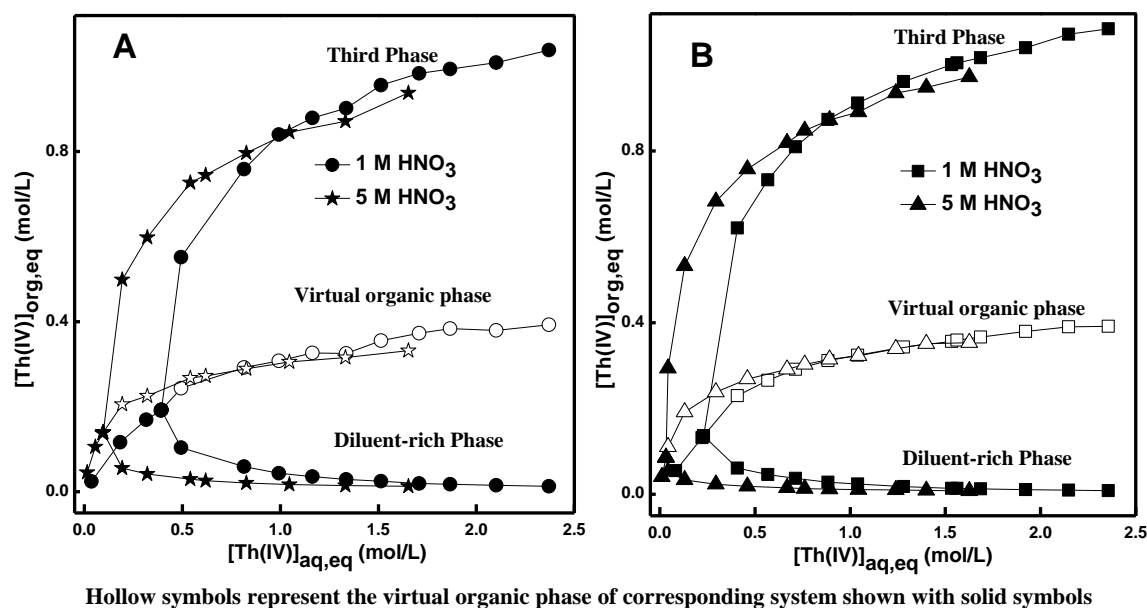


**Fig. 4.5:** Extraction isotherms for the extraction of Th(IV) by 1.1 M TBP/*n*-alkane from  $\text{Th}(\text{NO}_3)_4$  solutions with 1 M and 5 M nitric acid as a function of  $[\text{Th(IV)}]_{\text{aq,eq}}$  at 303 K; (A) *n*-dodecane system (B) *n*-tetradecane system.

Trends in the variations of extraction isotherms for the extraction of Th(IV) by 1.1 M solutions of TBP in *n*-DD and *n*-TD from  $\text{Th}(\text{NO}_3)_4$  solutions with 1 M and 5 M HNO<sub>3</sub> as a function of  $[\text{Th(IV)}]_{\text{aq,eq}}$  at 303 K are shown in Fig. 4.5. Data displayed in Fig. 4.3 are used to generate the extraction isotherm plots of corresponding TBP/*n*-alkane systems in biphasic region and are shown in Fig. 4.5. In the triphasic region, at a particular  $[\text{Th(IV)}]_{\text{aq,eq}}$  the phase splitting range for Th(IV) increases with increase in chain length of the diluent which is similar to the

trend observed with respect to *TiAP* based solvents for the extraction of Th(IV) from Th(NO<sub>3</sub>)<sub>4</sub> solution with near-zero free acidity.

Mallick et al. observed a higher third phase formation tendency of TBP for longer diluents in 1.1 M TBP/*n*-alkane - Th(NO<sub>3</sub>)<sub>4</sub>/near-zero free acid systems at 303 K [190]. Berthon et al. reported an increase in third phase formation behaviour of malonamides with an increase in the chain length of *n*-alkane diluents [137]. In the present study, a similar trend is observed in the case of *TiAP* also. As compared to longer diluents, shorter diluents can easily penetrate and swell the apolar region of reverse micelles that are formed by the reorganization of species in the organic phase. This reduces the energy of attraction between the polar cores of the reverse micelles and consequently, the phase splitting tendency of *TalPs* increase with increase in diluent chain length.

In the triphasic region, at lower [Th(IV)]<sub>aq,eq</sub>, the concentration of Th(IV) in the TP is higher in the case of 5 M HNO<sub>3</sub> as compared to 1 M HNO<sub>3</sub> due to the presence of higher nitrate ion concentration in the aqueous Th(NO<sub>3</sub>)<sub>4</sub> solution with 5 M HNO<sub>3</sub> than Th(NO<sub>3</sub>)<sub>4</sub> solution with 1 M HNO<sub>3</sub>. However, in the extraction of Th(IV) from concentrated solutions the concentration of Th(IV) in the TP for Th(NO<sub>3</sub>)<sub>4</sub> solution with 5 M HNO<sub>3</sub> is lesser than that of Th(NO<sub>3</sub>)<sub>4</sub> solution with 1 M HNO<sub>3</sub>. This decrease in Th(IV) concentration in the TP is attributed to the decrease in the free extractant concentration. Figure 4.5 shows that at higher [Th(IV)]<sub>aq,eq</sub> extraction isotherms for the DP become identical and independent of diluents, [Th(IV)]<sub>aq,eq</sub> and [HNO<sub>3</sub>]<sub>aq,eq</sub>. This is due to the ingress of more extractant-metal complex to the TP leaving behind only the diluent in the DP with increase in the aforementioned factors.

The trends in the Th(IV) concentration in the virtual un-split organic phase for 1.1 M TBP/*n*-alkane systems are shown in Fig. 4.5 with hollow symbols. Figure 4.5 indicates that the

extraction isotherms for Th(IV) in the virtual organic phase are a mere extension of real biphasic region and they are comparable to each other for all 1.1 M TBP/*n*-alkane - Th(NO<sub>3</sub>)<sub>4</sub>/HNO<sub>3</sub> systems which again confirms the independency of Th(IV) extraction on diluent chain length. In reality, it is possible to achieve the theoretical metal loading in the organic phase by decreasing the chain length of the diluent, increasing the temperature of the extraction system etc., to avoid third phase formation. Under such situations, the extraction isotherm of the virtual un-split organic phase represents that of the modified biphasic region.

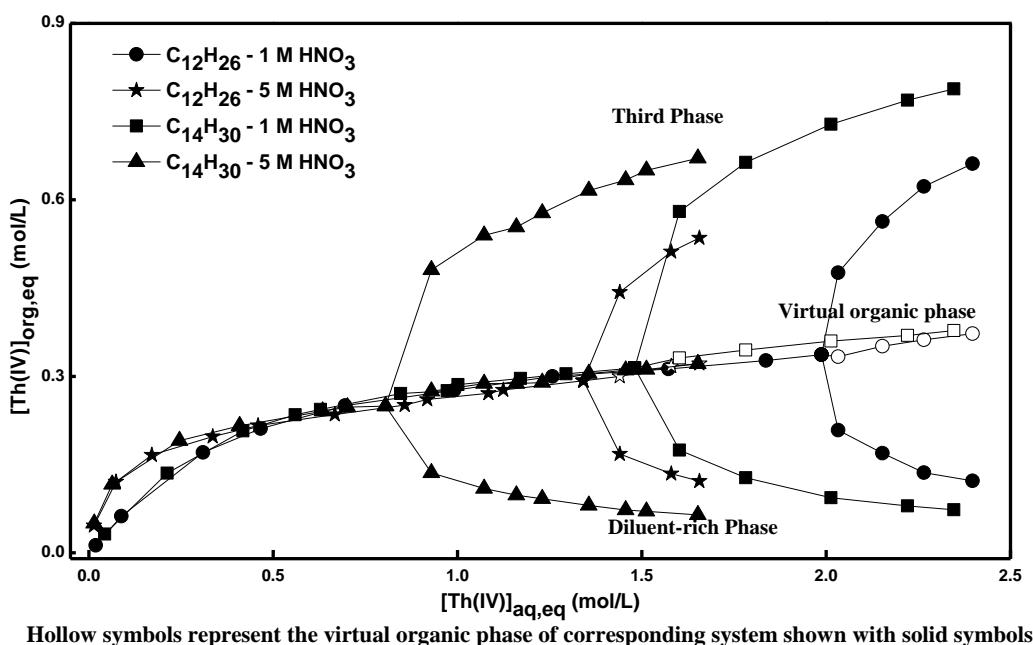


**Fig. 4.6:** Extraction isotherms for the extraction of Th(IV) by 1.1 M TiAP/*n*-alkane from Th(NO<sub>3</sub>)<sub>4</sub> solutions with 1 M and 5 M nitric acid as a function of [Th(IV)]<sub>aq,eq</sub> at 303 K.

Figure 4.6 shows the extraction isotherms for the extraction of Th(IV) by 1.1 M solutions of TiAP in *n*-DD and *n*-TD from Th(NO<sub>3</sub>)<sub>4</sub> solutions with 1 M and 5 M HNO<sub>3</sub>. Comparison of data given in Figs. 4.5 and 4.6 signify that in the biphasic region, extraction of Th(IV) by 1.1 M TBP/*n*-alkane - Th(NO<sub>3</sub>)<sub>4</sub>/HNO<sub>3</sub> systems is comparable with 1.1 M TiAP/*n*-alkane - Th(NO<sub>3</sub>)<sub>4</sub>/HNO<sub>3</sub> systems. Figure 4.6 depicts that in the triphasic region, with increase in

$[\text{Th(IV)}]_{\text{aq,eq}}$  the difference in Th(IV) concentration between the TP and the DP also increases. Unlike TBP systems, the triphasic regions of 1.1 M *TiAP/n-DD* -  $\text{Th(NO}_3)_4$ /1 M  $\text{HNO}_3$  system (1.99 mol/L - 2.40 mol/L) and 1.1 M *TiAP/n-DD* -  $\text{Th(NO}_3)_4$ /5 M  $\text{HNO}_3$  system (1.34 mol/L - 1.66 mol/L) do not overlap; and the triphasic regions of 1.1 M *TiAP/n-TD* -  $\text{Th(NO}_3)_4$ /1 M  $\text{HNO}_3$  system (1.48 mol/L - 2.35 mol/L) and 1.1 M *TiAP/n-TD* -  $\text{Th(NO}_3)_4$ /5 M  $\text{HNO}_3$  system (0.805 mol/L - 1.65 mol/L) overlap only in a small range of  $[\text{Th(IV)}]_{\text{aq,eq}}$ . Nevertheless, Fig. 4.6 illustrates that the difference in Th(IV) concentration between the TP and the DP is higher for *n-TD* as compared to *n-DD*. As in the case of TBP/*n*-alkane systems, extraction of Th(IV) by the virtual un-split organic phase in *TiAP/n*-alkane systems also shows a marginal increasing trend with increase in  $[\text{HNO}_3]_{\text{aq,eq}}$ . Comparison of data provided in Figs. 4.5 and 4.6 depicts that the phase splitting tendency with respect to difference in Th(IV) concentration between the TP and the DP is lower for 1.1 M *TiAP/n*-alkane -  $\text{Th(NO}_3)_4$ / $\text{HNO}_3$  systems than 1.1 M TBP/*n*-alkane -  $\text{Th(NO}_3)_4$ / $\text{HNO}_3$  systems.

#### 4.2.3 Effects of parameters on the extraction of $\text{HNO}_3$

Figure 4.7 shows the extraction isotherms for the extraction of  $\text{HNO}_3$  by 1.1 M solutions of TBP in *n-DD* and *n-TD* from  $\text{Th(NO}_3)_4$  solutions with 1 M and 5 M  $\text{HNO}_3$  as a function of  $[\text{Th(IV)}]_{\text{aq,eq}}$ . In the biphasic region, extraction of  $\text{HNO}_3$  by the organic phase decreases with increase in  $[\text{Th(IV)}]_{\text{aq,eq}}$ . For all TBP/*n*-alkane systems, in the triphasic region, at a particular  $[\text{Th(IV)}]_{\text{aq,eq}}$ , the extraction of  $\text{HNO}_3$  from  $\text{Th(NO}_3)_4$  solution with 5 M  $\text{HNO}_3$  is higher than from  $\text{Th(NO}_3)_4$  solution with 1 M  $\text{HNO}_3$  owing to the presence of more nitrate ions. Figure 4.7 (B) depicts a steep increase in the concentration of  $\text{HNO}_3$  in the TP at lower  $[\text{Th(IV)}]_{\text{aq,eq}}$  in the triphasic region of 1.1 M TBP/*n-TD* -  $\text{Th(NO}_3)_4$ / $\text{HNO}_3$  system. Subsequently, it decreases and again increases marginally with increase in  $[\text{Th(IV)}]_{\text{aq,eq}}$ . Though the reason for this trend is not

clear, it may be a result of the volume contraction of TBP based solvents and the relative interaction between the extracted species in the organic phase. Initially, when the TP is formed the attractive interaction between the aggregates of  $\text{HNO}_3$ -TBP and  $\text{Th}(\text{NO}_3)_4$ -TBP complexes overcome the average thermal energy of the system and hence most of these complexes gets concentrated in a small volume of the TP. In the triphasic region, at lower  $[\text{Th}(\text{IV})]_{\text{aq,eq}}$ , the  $\text{HNO}_3$  concentration reaches a maximum value due to the accumulation of  $\text{HNO}_3$  into a compact TP. Further increase in  $[\text{Th}(\text{IV})]_{\text{aq,eq}}$  leads to a drastic increase in volume of the TP and concentration of  $\text{HNO}_3$  in the TP decreases. Beyond a particular  $[\text{Th}(\text{IV})]_{\text{aq,eq}}$ , the concentration of  $\text{HNO}_3$  increases marginally as the increase in the volume of the TP is not significant. More details about the volume of TP are provided in subsequent discussions.

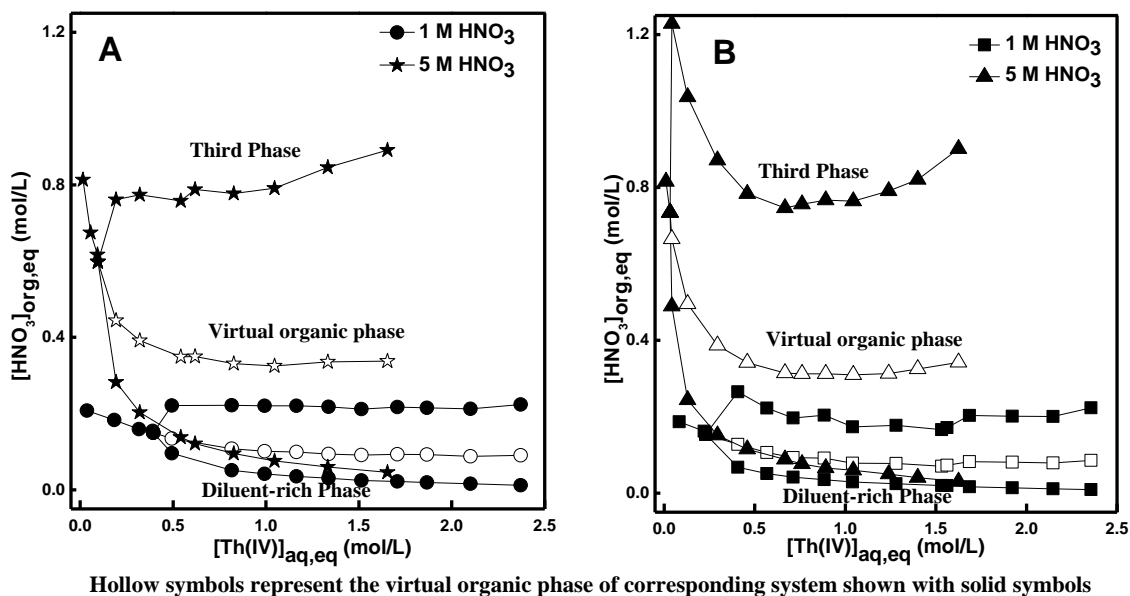


**Fig. 4.7:** Extraction isotherms for the extraction of  $\text{HNO}_3$  by 1.1 M TBP/n-alkane from  $\text{Th}(\text{NO}_3)_4$  solutions with 1 M and 5 M nitric acid as a function of  $[\text{Th}(\text{IV})]_{\text{aq,eq}}$  at 303 K; (A) n-dodecane system (B) n-tetradecane system.

Such a behaviour with respect to the extraction of  $\text{HNO}_3$  is not observed in the case of 1.1 M TBP/*n*-DD for its extraction from  $\text{Th}(\text{NO}_3)_4$  solutions with 1 M and 5 M  $\text{HNO}_3$ , where there is a gradual increase in  $\text{HNO}_3$  concentration in the TP with increase in  $[\text{Th}(\text{IV})]_{\text{aq,eq}}$ . This indicates the strong interaction among the extracted species in the TP of TBP for *n*-TD system as compared to *n*-DD system. In triphasic region, for all TBP/*n*-alkane -  $\text{Th}(\text{NO}_3)_4/\text{HNO}_3$  systems as in the case of extraction of Th(IV), concentration of  $\text{HNO}_3$  in the DP also decreases with increase in  $[\text{Th}(\text{IV})]_{\text{aq,eq}}$  and merge together at higher  $[\text{Th}(\text{IV})]_{\text{aq,eq}}$ . Figures 4.7 and 4.8 depict that the extraction of  $\text{HNO}_3$  by the virtual organic phases marginally decreases with increase in  $[\text{Th}(\text{IV})]_{\text{aq,eq}}$ .

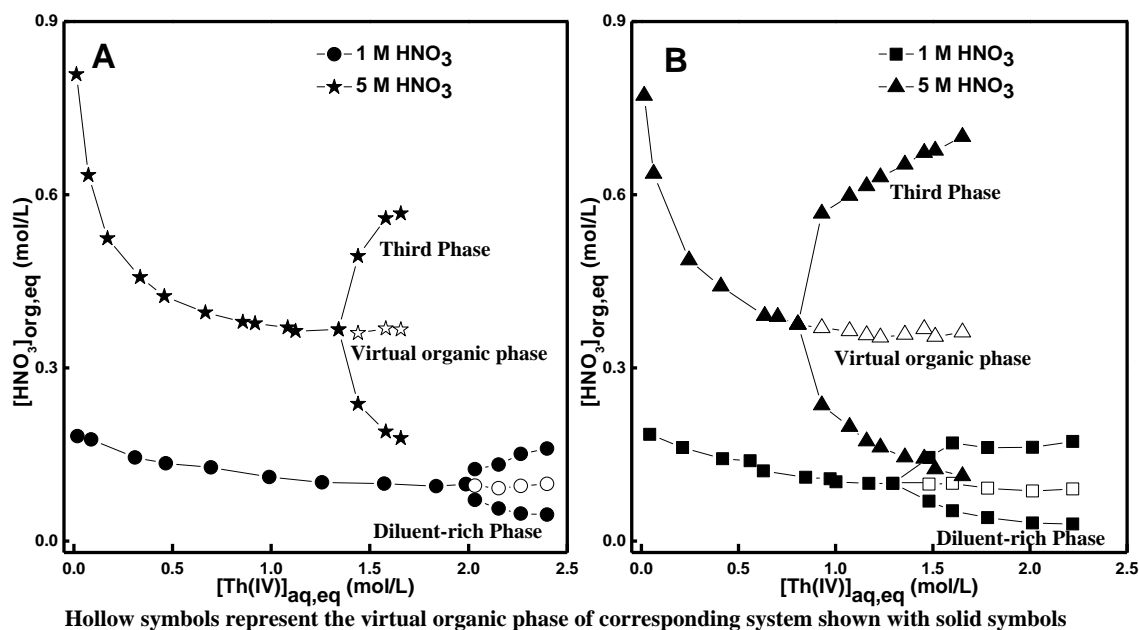


**Fig. 4.8:** Extraction isotherms for the extraction of  $\text{HNO}_3$  by 1.1 M TiAP/*n*-alkane from  $\text{Th}(\text{NO}_3)_4$  solutions with 1 M and 5 M nitric acid as a function of  $[\text{Th}(\text{IV})]_{\text{aq,eq}}$  at 303 K; (A) *n*-dodecane system (B) *n*-tetradecane system.

Figure 4.8 shows extraction isotherms for the extraction of  $\text{HNO}_3$  by TiAP based solvents from  $\text{Th}(\text{NO}_3)_4$  solutions in nitric acid media. Figures 4.7 and 4.8 illustrate that the extraction

isotherms of  $\text{HNO}_3$  for TBP and TiAP based solvents resemble each other in the biphasic regions. Data also reveal that in the triphasic region unlike TBP systems splitting pattern of Th(IV) and  $\text{HNO}_3$  are similar for TiAP/*n*-DD and TiAP/*n*-TD systems. With increase in  $[\text{Th(IV)}]_{\text{aq,eq}}$ , the concentrations of both Th(IV) and  $\text{HNO}_3$  in the TP increase, whereas their concentrations decrease in the DP. These differences in distribution of solutes between the TP and the DP for TiAP and TBP systems only reveal the difference in the interaction among the organic phase species between TiAP and TBP systems. The results confirm that the phase splitting of  $\text{HNO}_3$  as a function of diluent chain length,  $[\text{HNO}_3]_{\text{org,eq}}$  and  $[\text{Th(IV)}]_{\text{aq,eq}}$  are higher for TBP based solvents as compared to TiAP based solvents.

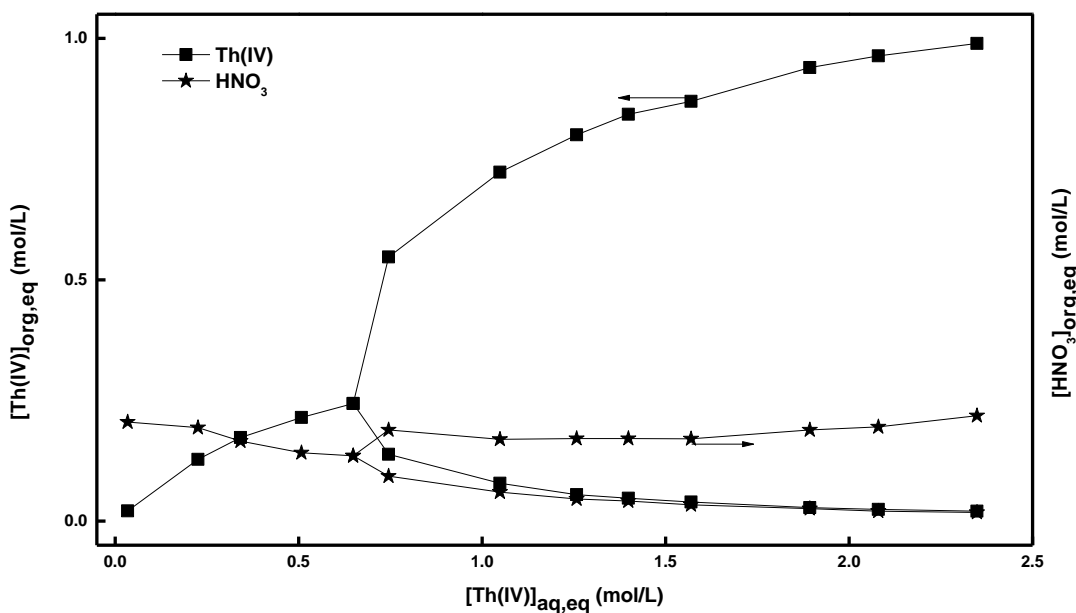


**Fig. 4.9:** Extraction isotherms for the extraction of Th(IV) and  $\text{HNO}_3$  by 1.1 M TBP/*n*-decane from  $\text{Th}(\text{NO}_3)_4$  solution in 1 M  $\text{HNO}_3$  at 303 K.

Trends in the extraction of Th(IV) and  $\text{HNO}_3$  by 1.1 M TBP/*n*-decane from  $\text{Th}(\text{NO}_3)_4$  solution in 1 M  $\text{HNO}_3$  are compared in Fig. 4.9. The extraction isotherms of Th(IV) and  $\text{HNO}_3$  in

biphasic region for 1.1 M TBP/*n*-decane - Th(NO<sub>3</sub>)<sub>4</sub>/HNO<sub>3</sub> system show that when more Th(IV) is loaded in the organic phase a proportional amount of HNO<sub>3</sub> is stripped into the aqueous phase with increase in [Th(IV)]<sub>aq,eq</sub>. The extraction patterns of Th(IV) and HNO<sub>3</sub> in the triphasic region shown in Fig. 4.9 are similar to the trends observed for TBP systems with other diluents displayed in Figs. 4.5 and 4.7, respectively. Similar study carried out with 1.1 M TBP/*n*-hexadecane - Th(NO<sub>3</sub>)<sub>4</sub>/HNO<sub>3</sub> system also exhibits same trend and the results are shown in Fig. 4.10.

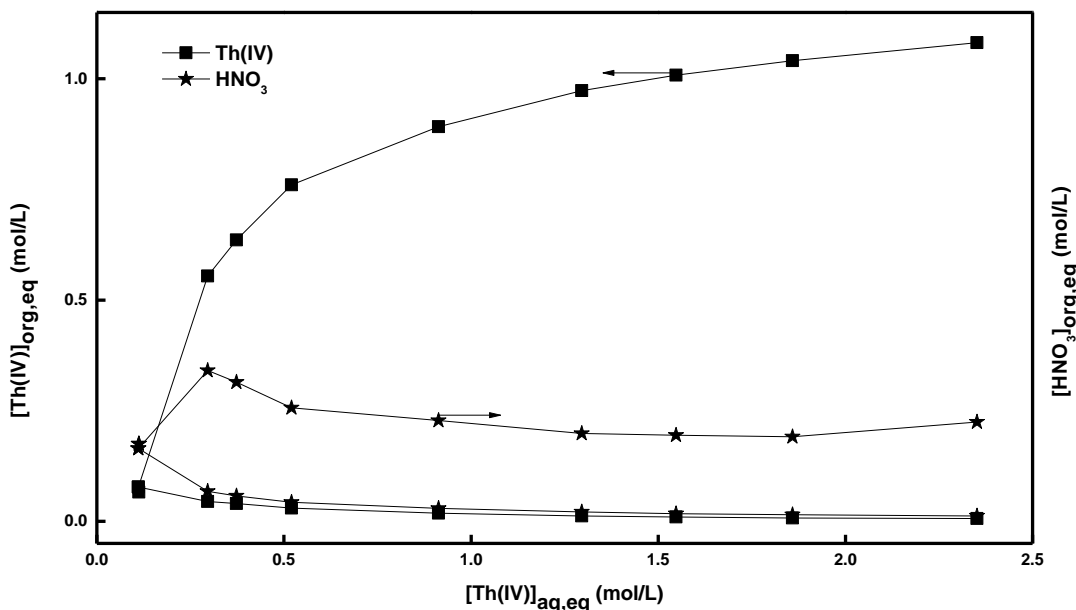


**Fig. 4.10:** Extraction isotherms for the extraction of Th(IV) and HNO<sub>3</sub> by 1.1 M TBP/*n*-hexadecane from Th(NO<sub>3</sub>)<sub>4</sub> solution in 1 M HNO<sub>3</sub> at 303 K.

#### 4.2.4 Effects of parameters on the ratio of concentration of Th(IV) in TP to DP

Variation of ratio of Th(IV) concentration between the TP and the DP generated from data shown in Fig. 4.4 is depicted in Fig. 4.11. An increase in the ratio of Th(IV) concentration with increase in the diluent chain length is observed for TalP/*n*-alkane - Th(NO<sub>3</sub>)<sub>4</sub>/HNO<sub>3</sub> systems. The results also highlight that this ratio linearly increases with increase in [Th(IV)]<sub>aq,eq</sub>

for both the solvents. However, this ratio is around ten times higher for TBP/*n*-DD system as compared to TiAP/*n*-DD.

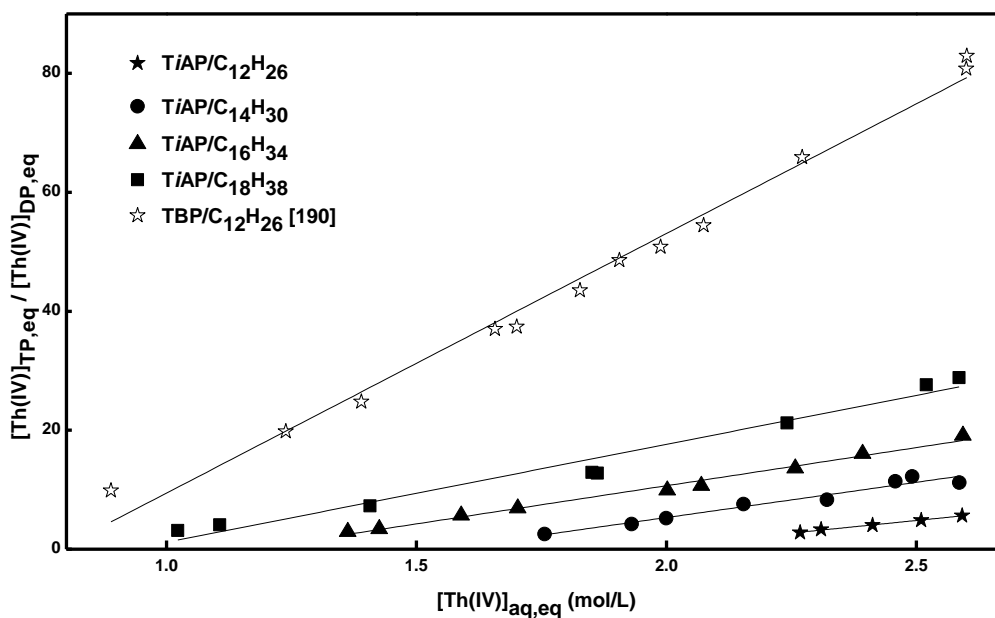


Fig. 4.11: Variation of ratio of Th(IV) in TP to that of DP with  $[Th(IV)]_{aq,eq}$  for the extraction of Th(IV) by 1.1 M TalP/*n*-alkane from  $Th(NO_3)_4$  solution with near-zero free acidity at 303 K.

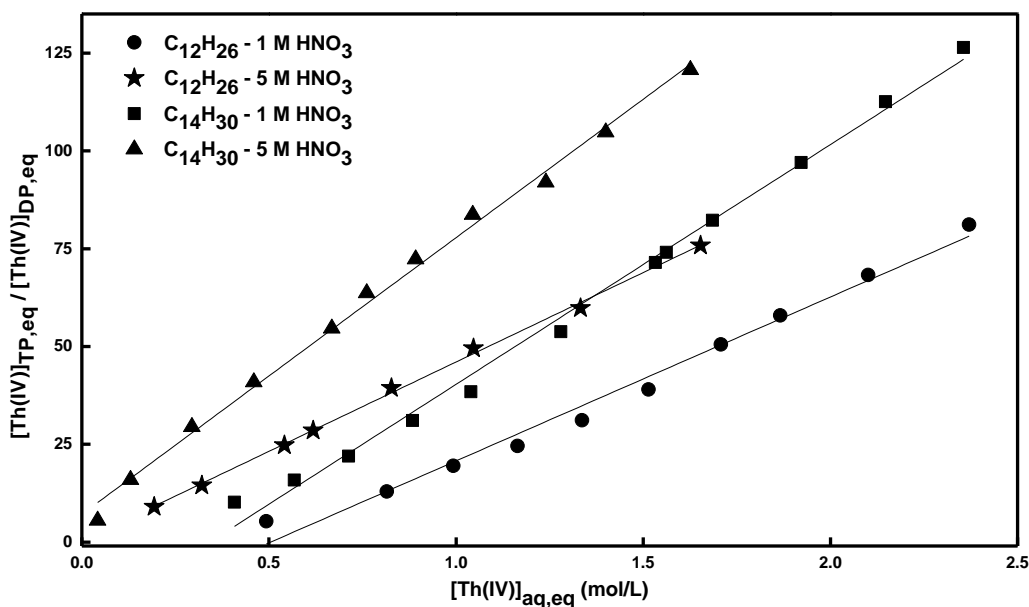
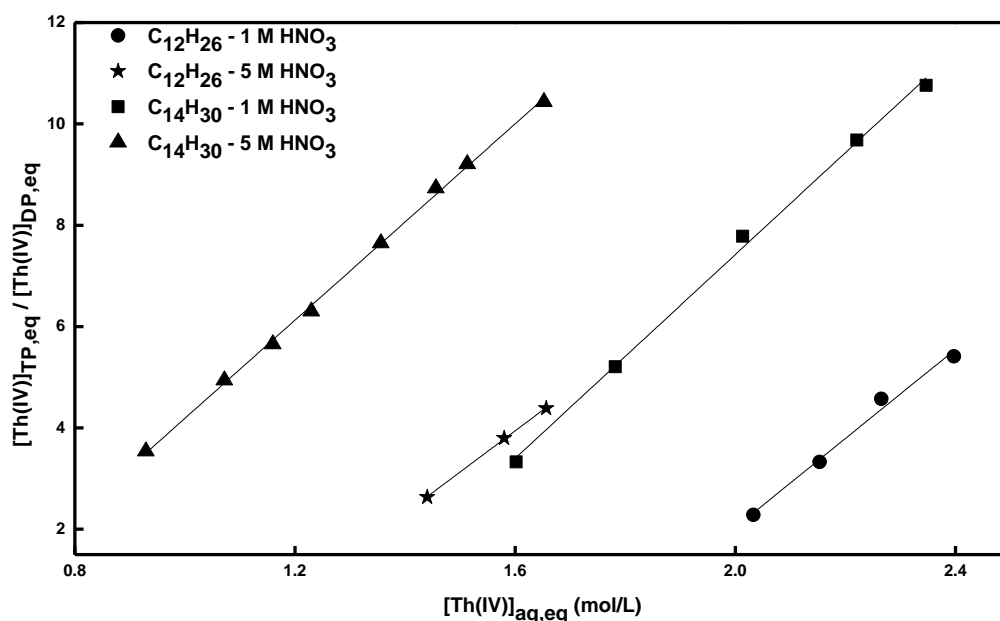


Fig. 4.12: Variation of ratio of Th(IV) concentration between the TP and the DP in the extraction of Th(IV) by 1.1 M TBP/*n*-alkane from  $Th(NO_3)_4$  solutions with 1 M and 5 M nitric acid as a function of  $[Th(IV)]_{aq,eq}$  at 303 K.

Data obtained from Figs. 4.5 and 4.6 have been used to generate the trends in the variation of ratio of Th(IV) concentration between the TP and the DP as shown in Figs. 4.12 and 4.13, respectively. When Figs. 4.12 and 4.13 are compared it is observed that the increase in Th(IV) concentration ratio with respect to  $[\text{Th(IV)}]_{\text{aq,eq}}$  is higher for TBP system as compared to TiAP system under similar extraction conditions. This clearly indicates the incompatibility of TBP-Th( $\text{NO}_3$ )<sub>4</sub> species with DP as compared to TiAP-Th( $\text{NO}_3$ )<sub>4</sub> species. Figure 4.13 depicts that the variation of this ratio is comparable with increase in  $[\text{HNO}_3]_{\text{aq,eq}}$  and slightly increases with increase in the diluent chain length which indicates the least influence of these parameters on the phase splitting tendency of TiAP.



**Fig. 4.13:** Variation of ratio of Th(IV) concentration between the TP and the DP in the extraction of Th(IV) by 1.1 M TiAP/*n*-alkane from Th( $\text{NO}_3$ )<sub>4</sub> solutions with 1 M and 5 M nitric acid as a function of  $[\text{Th(IV)}]_{\text{aq,eq}}$  at 303 K.

#### 4.2.5 Effects of parameters on the ratio of concentration of HNO<sub>3</sub> in TP to DP

Trends in the variation of ratio of HNO<sub>3</sub> concentration between the TP and the DP derived from data shown in Figs. 4.7 and 4.8 are depicted in Figs. 4.14 and 4.15, respectively. In general, the ratio of HNO<sub>3</sub> concentration between the TP and the DP is higher for system with *n*-TD as diluent in the organic phase and 5 M HNO<sub>3</sub> in the aqueous phase as compared to systems consisting of *n*-DD and 1 M HNO<sub>3</sub>. The ratio of HNO<sub>3</sub> concentration between the TP and the DP increases with increase in the chain length of the diluent for both the solvents. Surprisingly, ratio of HNO<sub>3</sub> concentration increase in linear and non-linear manner for TiAP and TBP solvent systems, respectively, with increase in [Th(IV)]<sub>aq,eq</sub>. The reason for this difference in trends is not clear and it needs further investigation. For TBP systems, even though the increase in this ratio is not very steep at lower equilibrium aqueous phase, there is a drastic increase in this ratio at higher Th(IV) concentration.

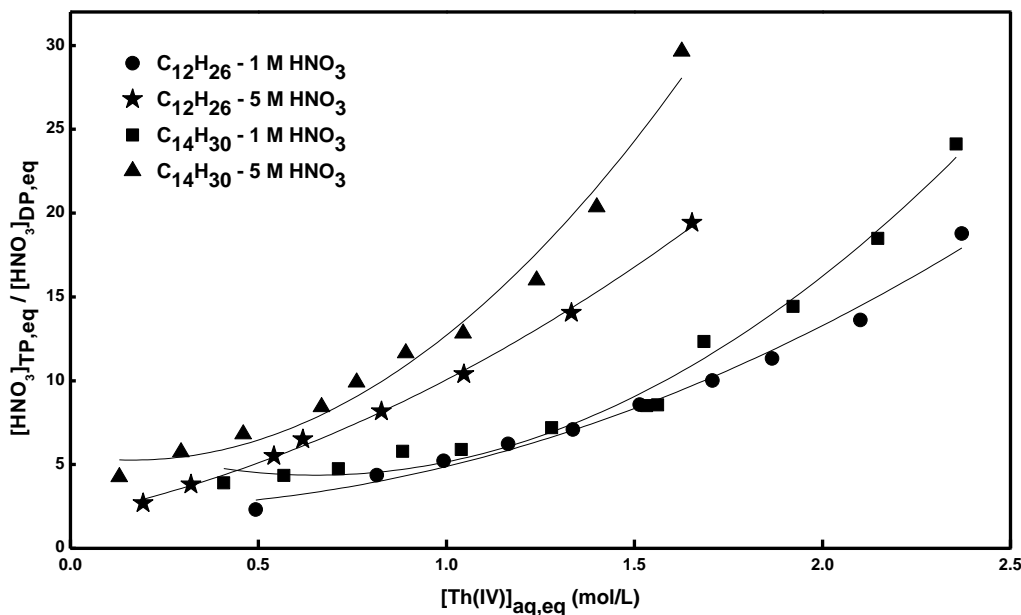


**Fig. 4.14:** Variation of ratio of concentration of HNO<sub>3</sub> between TP and DP in the extraction of Th(IV) by 1.1 M TBP/*n*-alkane from Th(NO<sub>3</sub>)<sub>4</sub> solutions with 1 M and 5 M nitric acid as a function of [Th(IV)]<sub>aq,eq</sub> at 303 K.

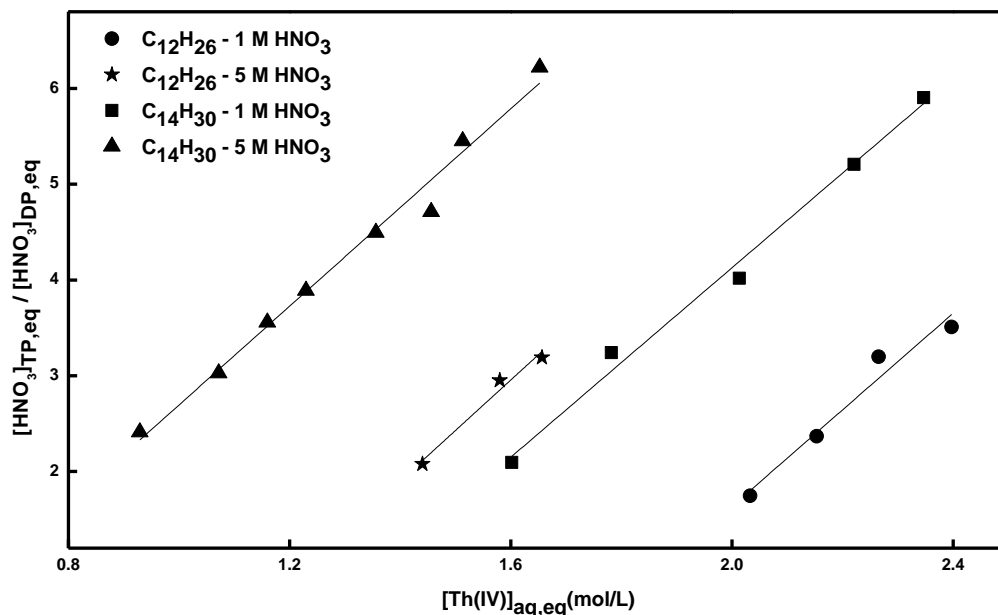


**Fig. 4.15:** Variation of ratio of concentration of HNO<sub>3</sub> between TP and DP in the extraction of Th(IV) by 1.1 M TiAP/*n*-alkane from Th(NO<sub>3</sub>)<sub>4</sub> solutions with 1 M and 5 M nitric acid as a function of [Th(IV)]<sub>aq,eq</sub> at 303 K.

#### 4.2.6 Effects of parameters on the concentration of solutes at CAC and SAC

Data on the concentration of Th(IV) and HNO<sub>3</sub> in organic and aqueous phases at the lower and upper limits of third phase formation (point of dissolution of the TP and with saturated Th(NO<sub>3</sub>)<sub>4</sub> solution, respectively) are summarized in Table 4.1. It is observed in Table 4.1 that for the extraction of Th(IV) by 1.1 M TalPs/*n*-alkane from Th(NO<sub>3</sub>)<sub>4</sub> solutions in nitric acid media, LOC and CAC values are higher for systems with shorter diluent chain length and lesser aqueous phase nitric acid concentration. However, the effects of diluent chain length and [Th(IV)]<sub>aq,eq</sub> on HNO<sub>3</sub> loading in the organic phase at the point of dissolution of the TP are opposite to the effects of the above parameters on Th(IV) loading. In general, the concentration of Th(IV) and HNO<sub>3</sub> in the TP which is in equilibrium with saturated aqueous solution is higher and solute concentration in the DP is lesser for *n*-TD systems as compared to *n*-DD systems. When the [HNO<sub>3</sub>]<sub>aq,eq</sub> increases from 1 M to 5 M, the concentration of Th(IV) in the TP as well as the DP decreases,

whereas  $\text{HNO}_3$  concentrations in both the organic phases (TP & DP) increase. The concentrations of Th(IV) and  $\text{HNO}_3$  in the TP and the DP at SAC are also listed in Table 4.1.

**Table 4.1: Data on concentration of Th(IV) and  $\text{HNO}_3$  in organic phases at CAC and SAC for the extraction of Th(IV) by 1.1 M TalP/*n*-alkane from  $\text{Th}(\text{NO}_3)_4$  solutions with 1 M and 5 M nitric acid as a function of  $[\text{Th}(\text{IV})]_{\text{aq,eq}}$  at 303 K.**

Extractant System	[Th(IV)] (mol/L)		[Th(IV)] <sub>SAC</sub> (mol/L)		[HNO <sub>3</sub> ] <sub>CAC</sub> (mol/L)	[HNO <sub>3</sub> ] <sub>SAC</sub> (mol/L)	
	LOC	CAC	TP	DP	Org	TP	DP
TBP/C <sub>12</sub> H <sub>26</sub> -1 M HNO <sub>3</sub>	0.192	0.393	1.04	0.013	0.150	0.223	0.012
TBP/C <sub>12</sub> H <sub>26</sub> -5 M HNO <sub>3</sub>	0.140	0.096	0.938	0.012	0.598	0.891	0.046
TBP/C <sub>14</sub> H <sub>30</sub> -1 M HNO <sub>3</sub>	0.136	0.230	1.08	0.009	0.154	0.223	0.009
TBP/C <sub>14</sub> H <sub>30</sub> -5 M HNO <sub>3</sub>	0.086	0.033	0.973	0.008	0.734	0.901	0.030
TiAP/C <sub>12</sub> H <sub>26</sub> -1 M HNO <sub>3</sub>	0.337	1.99	0.661	0.122	0.098	0.160	0.046
TiAP/C <sub>12</sub> H <sub>26</sub> -5 M HNO <sub>3</sub>	0.292	1.34	0.535	0.122	0.366	0.567	0.178
TiAP/C <sub>14</sub> H <sub>30</sub> -1 M HNO <sub>3</sub>	0.314	1.48	0.789	0.073	0.100	0.172	0.029
TiAP/C <sub>14</sub> H <sub>30</sub> -5 M HNO <sub>3</sub>	0.249	0.805	0.671	0.064	0.375	0.700	0.113

### 4.3 Variation of density of organic phases

Variations of density of organic phases in biphasic and triphasic regions in the extraction of Th(IV) by 1.1 M TiAP/*n*-alkane from  $\text{Th}(\text{NO}_3)_4$  solution with near-zero free acidity are depicted in Fig. 4.16. Literature data on the density of organic phases for 1.1 M TBP/*n*-DD system under similar extraction conditions are also shown in Fig. 4.16 [190]. The biphasic region shows an increase in the density of organic phase with increase in  $[\text{Th}(\text{IV})]_{\text{aq,eq}}$ . Figure 4.16 also depicts that the density difference between the heavy and light organic phases increases with increase in the chain length of the diluent and  $[\text{Th}(\text{IV})]_{\text{aq,eq}}$ . A comparison of density plots shown in Fig. 4.16 with extraction isotherms of Th(IV) in Fig. 4.4 clearly indicates the correlation of

Th(IV) concentration with density. This confirms that when  $[\text{Th(IV)}]_{\text{aq,eq}}$  increases, more Th(IV) gets extracted into organic phase without significant volume change and hence density increases. The pattern in the variation of density of TiAP/*n*-DD and TBP/*n*-DD are comparable however, the density range between the TP and the DP is much higher for TBP system as compared to TiAP system.

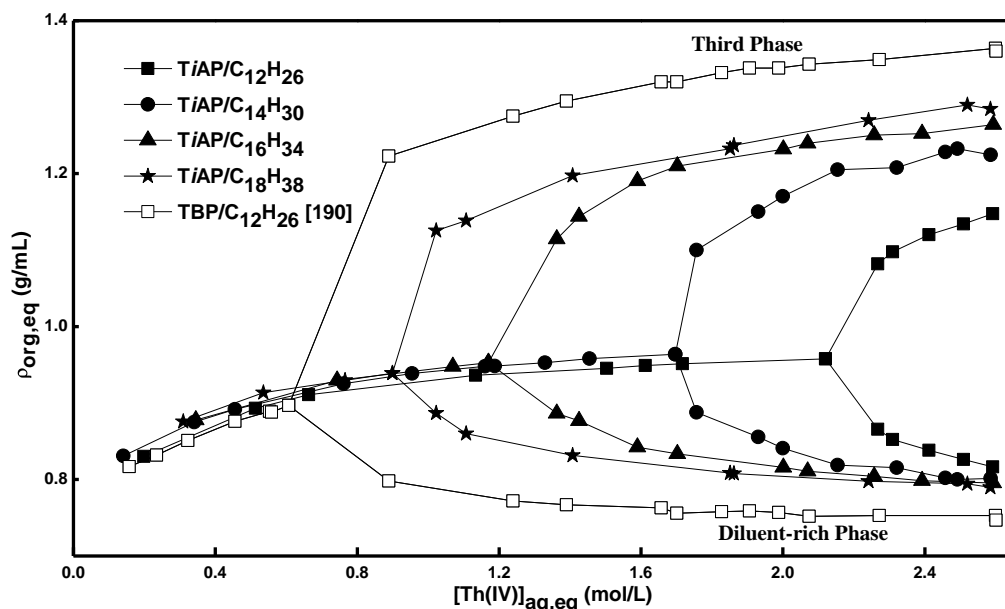


**Fig. 4.16:** Density of organic phases in the extraction of Th(IV) by 1.1 M TiAP/*n*-alkane from  $\text{Th}(\text{NO}_3)_4$  solution with near-zero free acidity as a function of  $[\text{Th(IV)}]_{\text{aq,eq}}$  at 303 K.

Trends in the variation of density of Th(IV) and  $\text{HNO}_3$  loaded organic phases for their extraction by 1.1 M TBP/*n*-alkane and 1.1 M TiAP/*n*-alkane from  $\text{Th}(\text{NO}_3)_4$  solutions in nitric acid media are shown in Figs. 4.17 and 4.18, respectively. The difference in density between the TP and the DP is higher for TBP system than TiAP system. In general, the mixing of liquid phases becomes inefficient with increase in the difference in density between the phases. Therefore, complications due to the third phase formation in solvent extraction processes with the above solvent systems are severe in the case of TBP as compared to TiAP. Comparison of

Th(IV) extraction isotherm plots in Figs. 4.5 and 4.6 with density plots in Figs. 4.17 and 4.18, respectively, shows that in the triphasic region both Th(IV) extraction and density follow a similar phase splitting pattern.

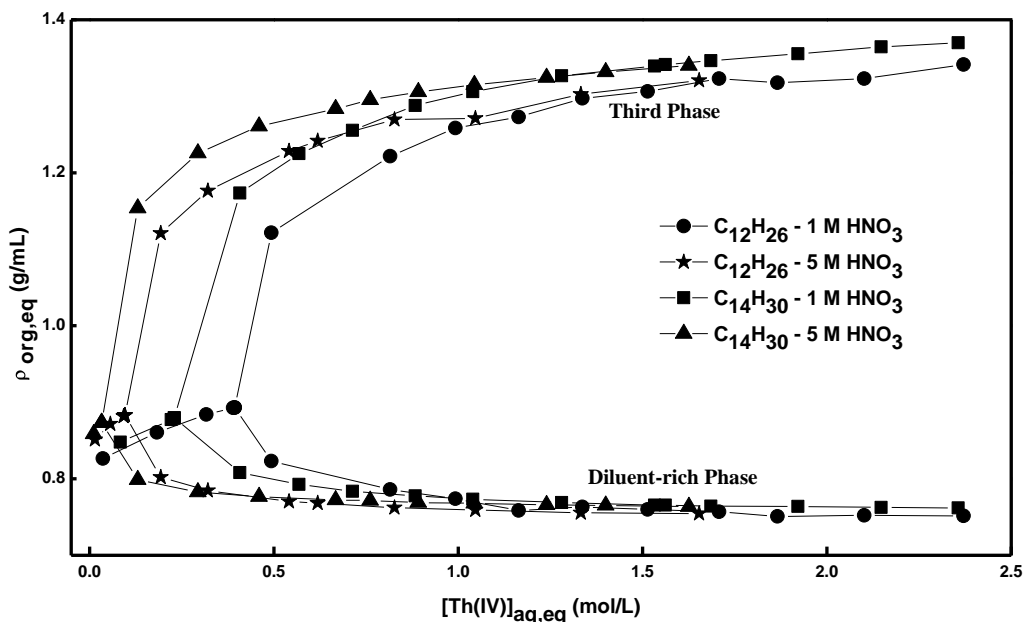


**Fig. 4.17:** Density of organic phases in the extraction of Th(IV) by 1.1 M TBP/n-alkane from  $Th(NO_3)_4$  solutions with 1 M and 5 M nitric acid as a function of  $[Th(IV)]_{aq,eq}$  at 303 K.

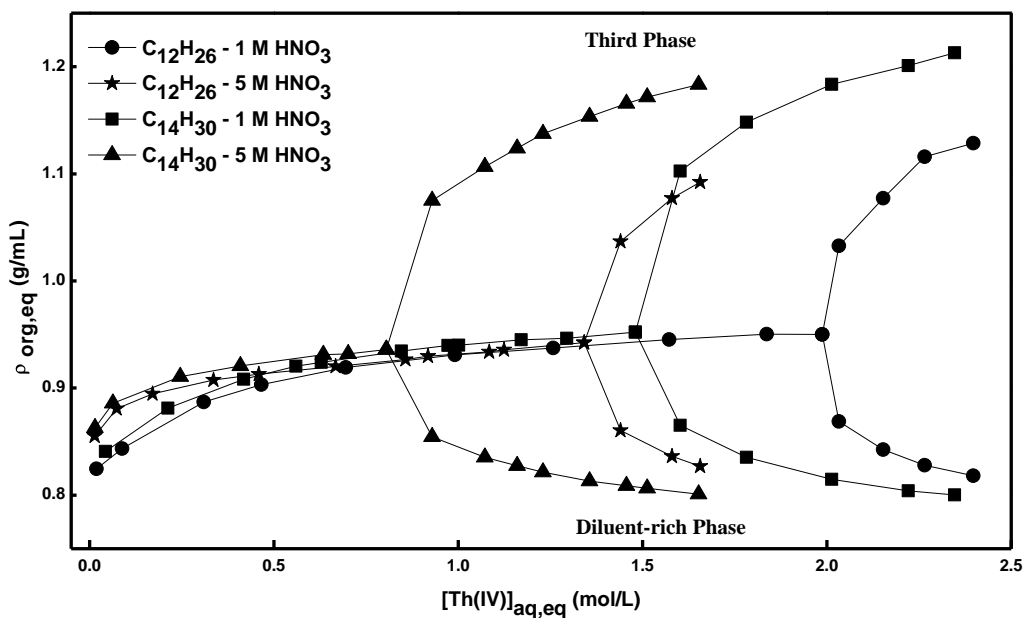


**Fig. 4.18:** Density of organic phases in the extraction of Th(IV) by 1.1 M TiAP/n-alkane from  $Th(NO_3)_4$  solutions with 1 M and 5 M nitric acid as a function of  $[Th(IV)]_{aq,eq}$  at 303 K.

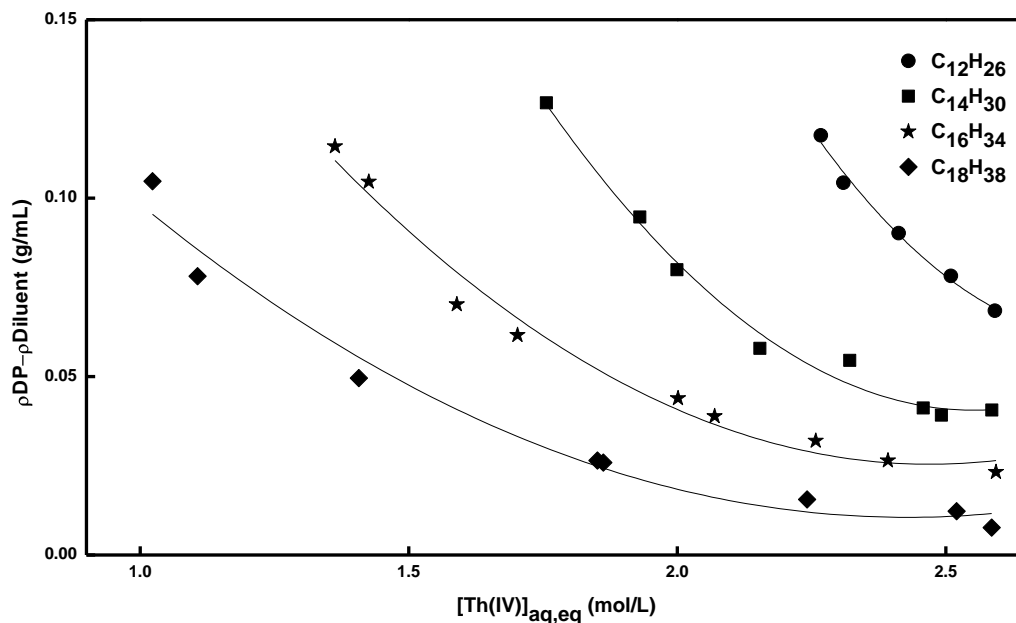


**Fig. 4.19:** Difference in density between DP and the corresponding diluent in the extraction of Th(IV) by 1.1 M TiAP/*n*-alkane from Th(NO<sub>3</sub>)<sub>4</sub> solution with near-zero free acidity as a function of [Th(IV)]<sub>aq,eq</sub> at 303 K.

It is clear from Figs. 4.4 – 4.15 that the compatibility of extractant-metal and extractant-nitric acid complexes with diluent decreases with increase in phase splitting nature of the extractant. Therefore, closeness of properties such as density, viscosity, refractive index of the pure diluent with the DP can be correlated to the extent of phase splitting behaviour of an extractant. In this context, the difference in density between the DP and the corresponding pure diluent was calculated to ascertain the extent of phase splitting nature of a particular solvent system. Data on the difference in density between DP and the corresponding diluent in the extraction of Th(IV) by TiAP/*n*-alkane are shown in Fig. 4.19. The difference in density approaches zero with increase in [Th(IV)]<sub>aq,eq</sub> and chain length of the diluent.

Variations of difference in density between the DP and the corresponding diluent for the extraction of Th(IV) in nitric acid media by 1.1 M solutions of TiAP and TBP in *n*-DD and *n*-TD are shown in Fig. 4.20. It is observed in Fig. 4.20 that the difference in density between the DP

and the diluent tends to zero with increase in  $[\text{HNO}_3]_{\text{aq,eq}}$ . An increase in  $\text{HNO}_3$  concentration in the aqueous phase favours the formation of extractant-solute complexes that have less solubility in the diluent and therefore, they get concentrated in the TP. Therefore, the extractant concentration in the DP decreases with increase in  $\text{HNO}_3$  concentration and the density of the DP becomes very close to the density of pure diluent.

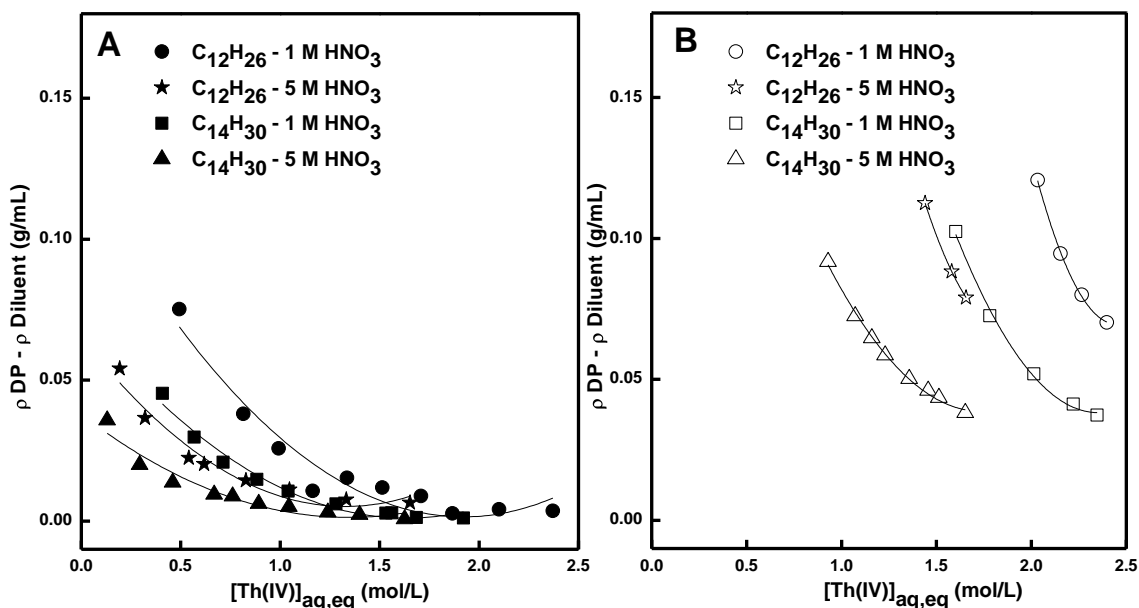


**Fig. 4.20:** Difference in density between the DP and the corresponding diluent in the extraction of  $\text{Th(IV)}$  by 1.1 M TalP/*n*-alkane from  $\text{Th(NO}_3)_4$  solutions with 1 M and 5 M nitric acid as a function of  $[\text{Th(IV)}]_{\text{aq,eq}}$  at 303 K; (A) TBP systems (B) TiAP systems.

Density difference between the DP and the diluent for a TBP/*n*-alkane system tends to become negligible at much lower  $[\text{Th(IV)}]_{\text{aq,eq}}$  than that of the corresponding TiAP/*n*-alkane system. These observations clearly indicate that the reverse micelles constituted by TBP and  $\text{Th(NO}_3)_4$  interact so strongly to exist as a single phase (TP) with the rejection of a major fraction of diluent to a new phase (DP) as compared to TiAP system. The chain length and branching of the alkyl groups of extractant as well as the diluent structure and the solute concentration in the

aqueous phase can influence the reorganization of the species present in the organic phase during solvent extraction.

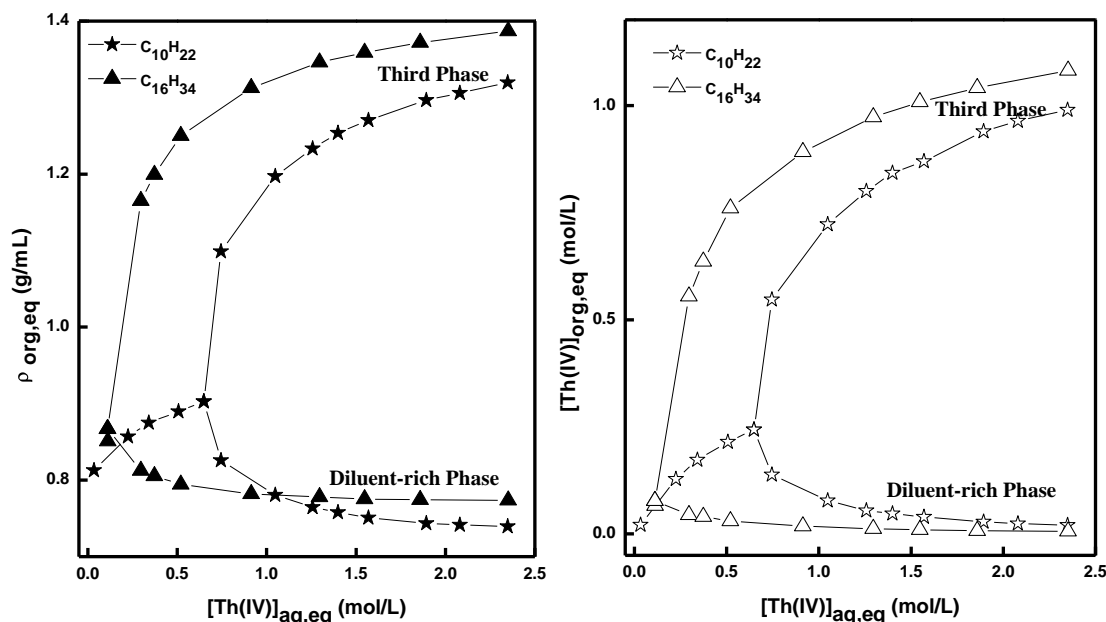


**Fig. 4.21:** Density and concentration of Th(IV) in the organic phases for 1.1 M TBP/*n*-decane -  $Th(NO_3)_4/1$  M  $HNO_3$  and 1.1 M TBP/*n*-hexadecane -  $Th(NO_3)_4/1$  M  $HNO_3$  systems as a function of  $[Th(IV)]_{aq,eq}$  at 303 K.

Figure 4.21 shows the variation of the concentration of Th(IV) and density of organic phases in the extraction of Th(IV) by 1.1 M solutions of *n*-decane and *n*-hexadecane from  $Th(NO_3)_4$  solution with 1 M  $HNO_3$  as a function of  $[Th(IV)]_{aq,eq}$  at 303 K. Figure 4.21 illustrates that the extraction isotherm of Th(IV) for the organic phase in the biphasic region and the TP in the triphasic region, resembles the density of their corresponding organic phases for both TBP/*n*-decane and TBP/*n*-hexadecane systems. However, the trends in the extraction isotherm of Th(IV) in the DP and the density of DP are different for TBP/*n*-decane and TBP/*n*-hexadecane systems particularly at higher  $[Th(IV)]_{aq,eq}$ . The reason for this observation can be obtained based on the difference in density between the DP and the pure diluent. The density of DP tends to approach

the density of the pure diluent with increase in  $[\text{Th(IV)}]_{\text{aq,eq}}$ . Therefore, at higher  $[\text{Th(IV)}]_{\text{aq,eq}}$  the density of the DP for TBP/*n*-decane and TBP/*n*-hexadecane systems becomes close to the density of their corresponding diluent. As the density of *n*-decane (0.730 g/mL) is lower than that of *n*-hexadecane (0.773 g/mL), an intersection is observed in the density plot of DP at higher  $[\text{Th(IV)}]_{\text{aq,eq}}$  which is not seen in the plot of Th(IV) extraction isotherm. This peculiar difference in profile between density and concentration of Th(IV) in the DP is clearly visible only in solvent extraction systems with diluents having large difference in carbon chain length, as in the case of *n*-decane and *n*-hexadecane.

#### 4.4 Variation of the ratio of the volume of DP to TP in triphasic region

The data on  $V_{\text{DP}}/V_{\text{TP}}$  ratio in the extraction of Th(IV) by 1.1 M TiAP/*n*-alkane from  $\text{Th(NO}_3)_4$  solution with near-zero free acidity are shown in Fig. 4.22. Trends shown in Fig. 4.22 illustrate that  $V_{\text{DP}}/V_{\text{TP}}$  ratio increases with increase in diluent chain length and decreases with increase in  $[\text{Th(IV)}]_{\text{aq,eq}}$ . The third phase is formed by supramolecular reorganization of extracted metal-complex, extractant and water molecules into spherical reverse micelles held together by strong attractions between their polar cores. As the sphere occupies minimum volume for a given mass, volume reduction can be expected for the formation of a spherical species and attraction between such species leads to the further contraction of the phase which is constituted by such species. Therefore,  $V_{\text{TP}}$  for systems with high third phase formation tendency is much smaller as compared to  $V_{\text{DP}}$  and this in turn increases  $V_{\text{DP}}/V_{\text{TP}}$  ratio. When  $[\text{Th(IV)}]_{\text{aq,eq}}$  increases, more Th(IV) gets extracted from aqueous phase to TP which increases the volume of TP and therefore leads to a decrease in  $V_{\text{DP}}/V_{\text{TP}}$  ratio. Borkowski has also observed a similar trend and reported a decrease in the volume of TP and an increase in the volume of DP to yield an overall increase in

the  $V_{DP}/V_{TP}$  ratio with the dilution of  $TBP \cdot 1.6HNO_3$  adduct with  $n$ -DD for  $TBP/n$ -DD system [192].

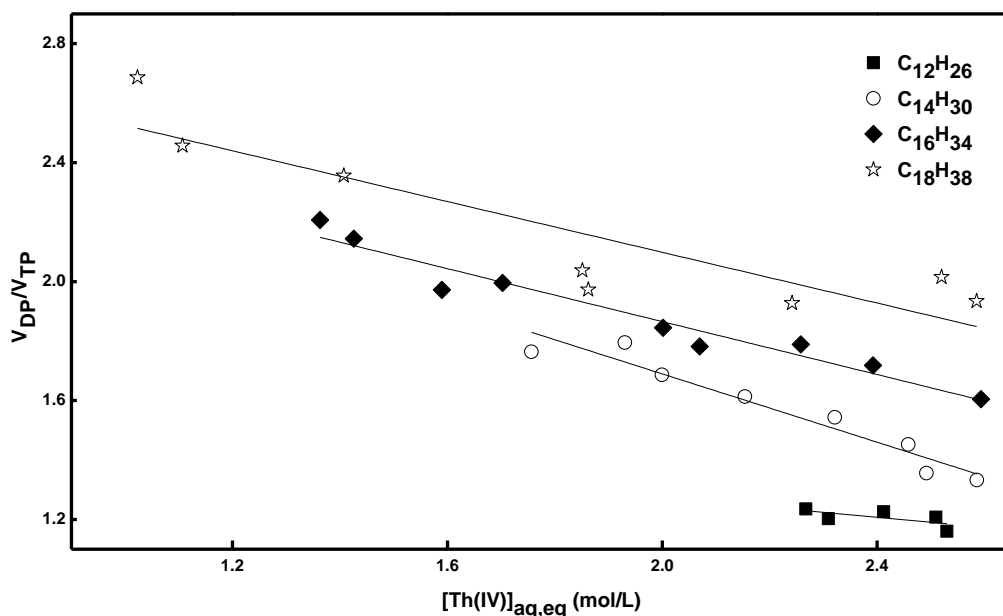


**Fig. 4.22:**  $V_{DP}/V_{TP}$  ratio in the extraction of  $Th(IV)$  by 1.1 M  $TiAP/n$ -alkane from  $Th(NO_3)_4$  solution with near-zero free acidity as a function of  $[Th(IV)]_{aq,eq}$  at 303 K.

The increase in  $V_{DP}/V_{TP}$  ratio with increase in chain length of the diluent for the same  $[Th(IV)]_{aq,eq}$  can be explained based on the penetration effect of the diluents [137]. Shorter diluent molecules can easily penetrate into the apolar region of the reverse micelle formed by a particular extractant than diluents with longer chain length and can effectively swell the apolar region where the alkyl groups of the extractant are located. The increase in the volume of apolar region of a reverse micelle increases the inter-micellar distance and hence there is an increase in  $V_{TP}$ . Also, due to the association of larger number of diluent molecules with TP,  $V_{DP}$  decreases and hence  $V_{DP}/V_{TP}$  ratio is lower for shorter diluents than longer diluents for the same  $[Th(IV)]_{aq,eq}$ .

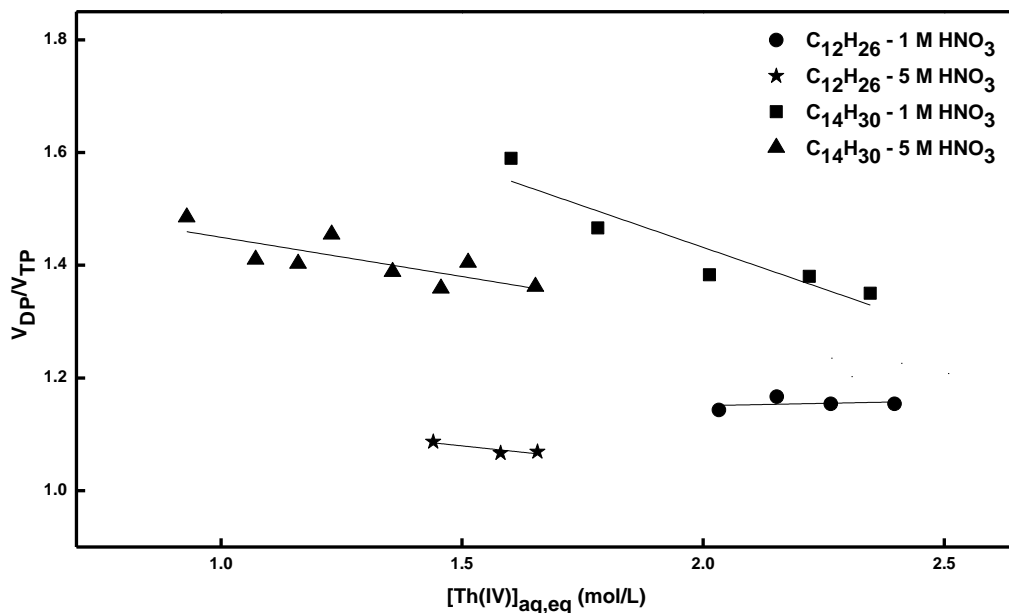


Fig. 4.23:  $V_{DP}/V_{TP}$  ratio in the extraction of Th(IV) by 1.1 M TiAP/n-alkane from  $Th(NO_3)_4$  solutions with near-zero free acidity, 1 M and 5 M nitric acid as a function of  $[Th(IV)]_{aq,eq}$  at 303 K.

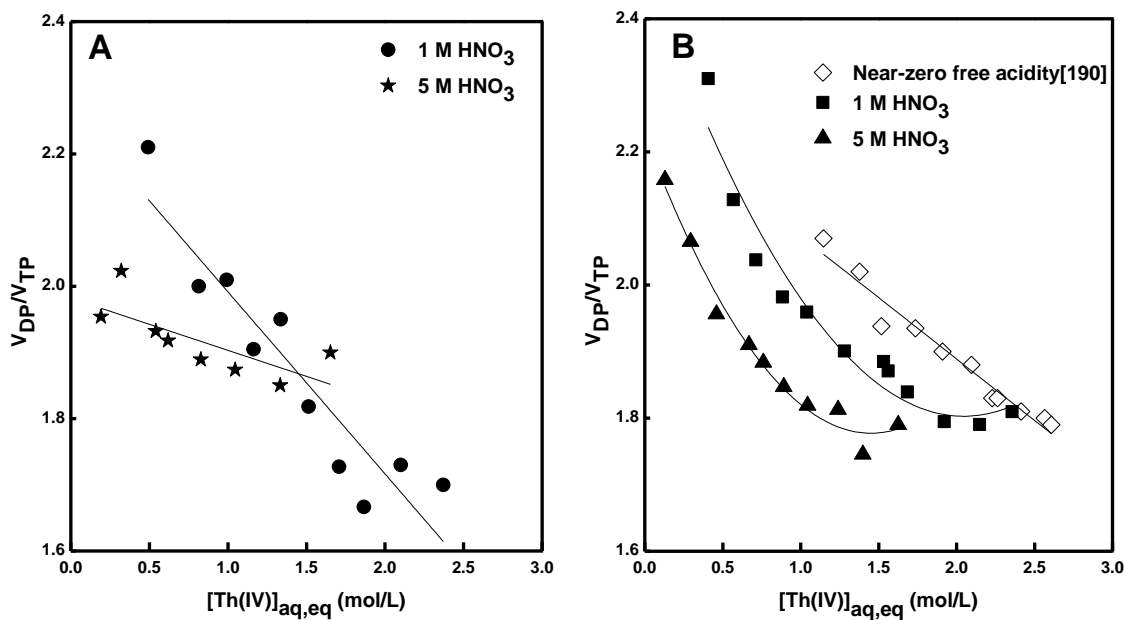


Fig. 4.24:  $V_{DP}/V_{TP}$  ratio in the extraction of Th(IV) by 1.1 M TBP/n-alkane from  $Th(NO_3)_4$  solutions with near-zero free acidity, 1 M and 5 M nitric acid as a function of  $[Th(IV)]_{aq,eq}$  at 303K; (A) n-dodecane systems (B) n-tetradecane systems.

Trends in the variation of  $V_{DP}/V_{TP}$  ratio in the extraction of Th(IV) from nitric acid media by 1.1 M TiAP/*n*-alkane and 1.1 M TBP/*n*-alkane are shown in Figs. 4.23 and 4.24, respectively. Literature data on the  $V_{DP}/V_{TP}$  ratio obtained with 1.1 M TBP/*n*-TD under near-zero free acid condition are also shown in Fig. 4.24. Figures 4.23 and 4.24 depict that for both TiAP/*n*-alkane and TBP/*n*-alkane systems at a particular  $[\text{Th(IV)}]_{\text{aq,eq}}$ ,  $V_{DP}/V_{TP}$  ratio decreases with increase in  $[\text{HNO}_3]_{\text{aq,eq}}$  which can be explained based on the reverse micelle concept. The extractant-metal and extractant- $\text{HNO}_3$  complexes which are incompatible with the binary solution of extractant in diluent will aggregate into supramolecular reverse micelles and separate out from diluent as a new phase (Third phase) where metal,  $\text{HNO}_3$ , water and polar group of the extractant are surrounded by non-polar groups of the extractant. When  $[\text{HNO}_3]_{\text{aq,eq}}$  increases from near-zero free acidity to 5 M  $\text{HNO}_3$  more extractant- $\text{HNO}_3$  complex forms and converts as reverse micelle which increases its volume and hence increase in volume of the TP leading to an overall decrease in the  $V_{DP}/V_{TP}$  ratio.

It can be seen in Fig. 4.24 for TBP/*n*-TD -  $\text{Th}(\text{NO}_3)_4/\text{HNO}_3$  systems that at lower  $[\text{Th(IV)}]_{\text{aq,eq}}$ ,  $V_{DP}/V_{TP}$  ratio decreases drastically and later on with increase in  $[\text{Th(IV)}]_{\text{aq,eq}}$  it decreases gradually. This is the reason for the trend observed for the concentration of  $\text{HNO}_3$  in the TP with increase in  $[\text{Th(IV)}]_{\text{aq,eq}}$  which is shown in Fig. 4.7. Figure 4.24 also shows that in TBP/*n*-DD system,  $V_{DP}/V_{TP}$  ratio decreases with increase in  $[\text{HNO}_3]_{\text{aq,eq}}$ , but in a small range of  $[\text{Th(IV)}]_{\text{aq,eq}}$ .  $V_{DP}/V_{TP}$  ratios for Th(IV) extraction from solutions with 1 M and 5 M  $\text{HNO}_3$  are comparable.

Variation of  $V_{DP}/V_{TP}$  ratios for TiAP and TBP solvent systems shown in Figs. 4.23 and 4.24, respectively, can be compared under similar conditions. In general, volume ratios of TBP system are higher than TiAP. These trends observed in various systems can be correlated to the

size of the apolar regions of the reverse micelles and their mutual interactions. Smaller apolar shell thickness in the case of TBP due to lower number of carbon atoms (4 C atoms) per alkyl chain as compared to TiAP which contains 5 carbon atoms per alkyl group as well as the associated difference in their inter-micellar interaction energies are the main reasons. Branching of alkyl groups in TiAP can probably cause an increase in the apolar shell thickness and a decrease in the inter-micellar interaction energy due to the possible expansion of the apolar region.

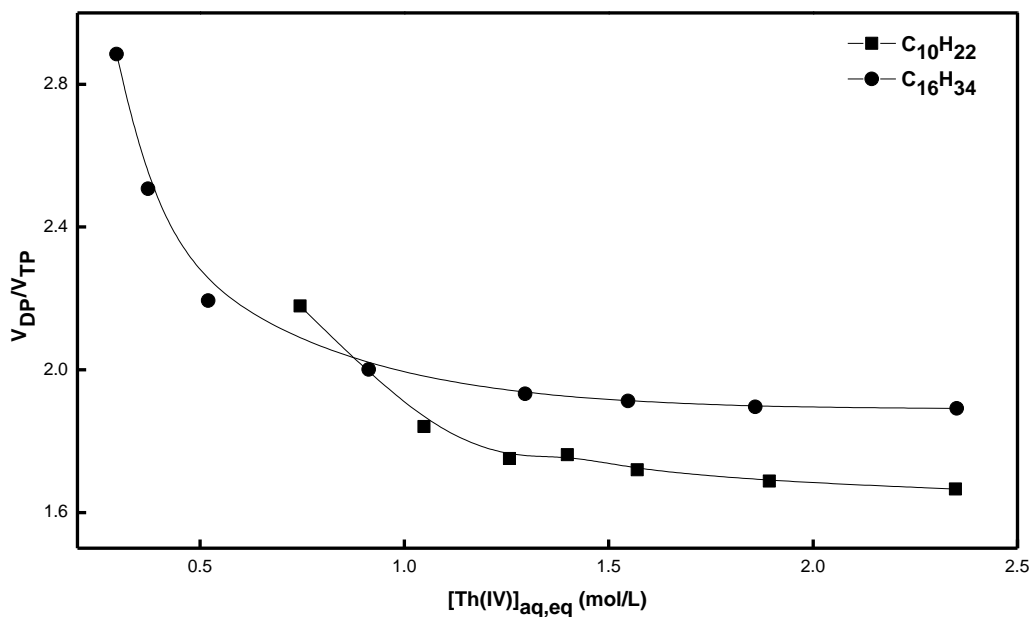


**Fig. 4.25:**  $V_{DP}/V_{TP}$  ratio for the extraction of Th(IV) by 1.1 M TBP/*n*-alkane from Th(NO<sub>3</sub>)<sub>4</sub> solution with 1 M HNO<sub>3</sub> at 303 K.

In order to clearly visualize the effect of volume ratio on diluent chain length, volume ratios were obtained for 1.1 M TBP in diluents with large difference in carbon numbers, say *n*-decane and *n*-hexadecane. Variation of the  $V_{DP}/V_{TP}$  ratio with respect to  $[\text{Th(IV)}]_{\text{aq,eq}}$  for 1.1 M TBP/*n*-decane – Th(NO<sub>3</sub>)<sub>4</sub>/1 M HNO<sub>3</sub> and 1.1 M TBP/*n*-hexadecane – Th(NO<sub>3</sub>)<sub>4</sub>/1 M HNO<sub>3</sub>

systems are shown in Fig. 4.25. The result observed in Fig. 4.25 corroborates the result shown in Fig. 4.24.

#### **4.5 Scope of third phase formation studies with TalP/*n*-alkane - Pu(IV)/HNO<sub>3</sub> systems in triphasic regions**

Earlier studies have shown that theoretical loading can be achieved in the organic phase without third phase formation in the extraction of Pu(IV) by 1.1 M TiAP/*n*-DD from nitric acid media at 303 K [193]. However, it may be possible to induce third phase formation in TiAP systems by altering the extraction conditions. For example, the TP can be induced by carrying out the experiment at lower temperature and also by employing diluents with longer chain length. This also demands the handling of highly concentrated plutonium solutions and under such situations one can expect difficulties associated with the visual detection of the TP due to the intense colour of plutonium loaded organic solutions. Therefore, considering the complexities involved in making measurements on plutonium systems, it is beneficial to cautiously extrapolate the results of the present study to TalP-Plutonium systems for the prediction of third phase formation in such systems.

#### **4.6 Conclusions**

This chapter has discussed the effects of  $[\text{Th(IV)}]_{\text{aq,eq}}$ ,  $[\text{HNO}_3]_{\text{aq,eq}}$  and diluent chain length on the extraction of Th(IV) and HNO<sub>3</sub> by TiAP and TBP based solvents from Th(NO<sub>3</sub>)<sub>4</sub> solutions with near-zero free acidity, as well as nitric acid media in biphasic as well as triphasic regions. The results confirm that diluent chain length does not influence the extraction of Th(IV) by TiAP as well as TBP. Solute concentrations of virtual organic phase follow the extraction pattern of solute in real biphasic region for all TalP/*n*-alkane - Th(NO<sub>3</sub>)<sub>4</sub>/HNO<sub>3</sub> systems. The difference in the density between the DP and the pure diluent becomes negligible with increase

in organic phase splitting behaviour of both the solvents. In biphasic regions, the extraction behaviour of both the solvents is comparable. Phase splitting pattern of *TiAP* and TBP in the extraction of  $\text{Th}(\text{NO}_3)_4$  as well as  $\text{HNO}_3$  with respect to  $[\text{HNO}_3]_{\text{aq,eq}}$  are different. The degree of phase splitting in the extraction of  $\text{Th}(\text{NO}_3)_4$  with respect to the difference in solute concentrations, and density between the TP and the DP as well as the  $V_{\text{DP}}/V_{\text{TP}}$  ratio for *TiAP* system is much lesser as compared to TBP. Overall results confirm that *TiAP* has lesser phase splitting tendency with respect to extraction of Th(IV) when compared to TBP. In real scenario, hydrodynamic problems due to the co-existence of two organic solutions with large difference in solute concentrations and density in a solvent extraction process are likely to be a concern for TBP systems as compared to *TiAP* systems. The effects of parameters such as  $[\text{Th}(\text{IV})]_{\text{aq,eq}}$  and diluent chain length on the extractant concentration in organic phases after phase splitting for *TiAP* and TBP based solvents are elaborated in Chapter 5.



# Chapter 5



**“What is research, but a blind date with knowledge”**

*-William Henry*

# NOVEL METHODS FOR THE ESTIMATION OF EXTRACTANT CONCENTRATION AFTER ORGANIC PHASE SPLITTING

---

# 5

## 5.1 Introduction

In any solvent extraction process, the concentration of the extractant in a solvent plays a crucial role in the separation of metal ion(s) from the impurities and it is chosen based on several parameters including the nature of the metal ion(s) to be separated. For example, 30 vol% TBP is used in PUREX process to separate U(VI) and Pu(IV) from fission products, 45 vol% TBP is utilized to separate U(VI) and Th(IV) from rare earths, 5 vol% TBP is employed for the separation of U(VI) from Th(IV), 60 vol% TBP is used to separate Zr(IV) from Hf(IV), etc [76,89,95,98]. Therefore, accurate estimation of the extractant in a freshly prepared solvent prior to its use is essential.

From the economic point of view, a solvent has to be recycled in a processing plant. However, radiation and chemical degradation of TBP lead to the formation of undesirable compounds that affect the process performance. Consequently, washing is required to remove the degradation products for the regeneration of the spent solvent. Therefore, the concentration of TBP in the regenerated solvent can be different from that of the original solvent and the composition of the regenerated solvent has to be adjusted to restore the specified concentration in order to achieve maximum efficiency in the solvent extraction process. Therefore, accurate and precise determination of the concentration of TBP in the regenerated solvent is also essential for the recycling of solvent.

Various analytical methods based on chromatography, spectrometry, titrimetry, potentiometry, electrophoresis etc., have been reported for the qualitative and quantitative determination of TBP in a solvent [194-201]. The results obtained by chromatographic techniques such as gas chromatography and liquid chromatography are accurate but the

techniques are relatively expensive and the samples need to be derivatized prior to analysis which consumes longer time. Comparatively, spectrometric techniques are relatively fast and easier but the analysis becomes complex with increase in the number of species in the sample. Titrimetric methods have been considered to be relatively simple, easy and precise. Nevertheless, all the analytical methods mentioned above have some advantages and limitations.

It is well known that the equilibration of TBP with 8 M  $\text{HNO}_3$  saturates the organic phase with  $\text{HNO}_3$  by forming 1:1 TBP- $\text{HNO}_3$  complex [201]. The nitric acid equilibration method makes use of the complexing ability of TBP with  $\text{HNO}_3$  where the nature of the diluent does not influence the extraction and therefore this method can be universally employed to estimate the concentration of TBP solutions in any non-polar diluent. The concentration of  $\text{HNO}_3$  in nitric acid loaded TBP solutions obtained by acid-base titration directly corresponds to the concentration of TBP. This is considered to be an important method for the determination of extractant concentration in TBP based solvents and is currently being employed in reprocessing plants.

Uneven distribution of TBP between the TP and the DP is expected during third phase formation. Therefore it is essential to estimate TBP in the corresponding organic phases after organic phase splitting to understand third phase formation tendency of TBP. Most of the classical techniques for TBP estimation require a large volume of sample for analysis. However, the volume of the TP generated by TBP based solvents near LOC is less and it is worthwhile to develop techniques that require only a small volume of sample. In this regard, new methods for the estimation of TBP in organic phases after the organic phase splitting have been developed by exploiting the linear relationships of the density and refractive index of the solvent with TBP concentration in the solvent. The LOC for third phase formation in the extraction of Th(IV) from solution with near-zero free acidity can also be employed for

this purpose. TBP concentrations estimated by the aforementioned methods have been authenticated by nitric acid equilibration method.

An effort has been made to theoretically predict the concentration of extractant in the TP and the DP in the extraction of Th(IV) from  $\text{Th}(\text{NO}_3)_4$  solutions with near-zero free acidity and nitric acid media. Based on a model that assumes the existence of trisolvate and monosolvate complexes of  $\text{Th}(\text{NO}_3)_4$  and  $\text{HNO}_3$  with TalP respectively, the extractant concentrations have been deduced. The extractant concentrations computed using the model have been verified with experimentally obtained values for various solvent extraction systems.

## 5.2 Estimation of TBP in the TP and the DP

Investigation on the measurements of various properties of TBP solutions such as density, refractive index, LOC, nitric acid loading etc., of TBP solutions as a function of its concentration revealed linear relationships between such properties and TBP concentration. Hence, the calibration plots between the aforementioned properties and the TBP concentration generated with various TBP solutions in *n*-alkane with known concentration have been used to estimate the TBP concentration in organic phases after phase splitting. Various properties of the unknown samples of the TP and the DP have been measured after the stripping of the extracted solutes ( $\text{Th}(\text{NO}_3)_4$  and  $\text{HNO}_3$ ) from the organic phase with distilled water.

### 5.2.1 By using density and refractive index

The estimation of commercial grade TBP in its solutions in kerosene which is in equilibrium with  $\text{UO}_2(\text{NO}_3)_2$  solutions in nitric acid media by measuring solution densities is reported in the literature [194]. In the present study, solutions of TBP in a particular *n*-alkane diluent after the stripping of loaded Th(IV) and  $\text{HNO}_3$  have been used for density measurement. Figure 5.1 shows the densities of dry and water-saturated solutions of TBP in

*n*-decane and *n*-hexadecane measured as a function of TBP concentration. The densities of water-saturated solutions of TBP in *n*-dodecane are also shown in Fig. 5.1. The values of dry densities determined for *n*-decane (0.726 g/mL), *n*-dodecane (0.750 g/mL), *n*-hexadecane (0.771 g/mL) and TBP (0.973 g/mL) in the present study are in good agreement with the literature values reported for *n*-decane (0.723 g/mL), *n*-dodecane (0.742 g/mL), *n*-hexadecane (0.766 g/mL) and TBP (0.968 g/mL), respectively [202-204].

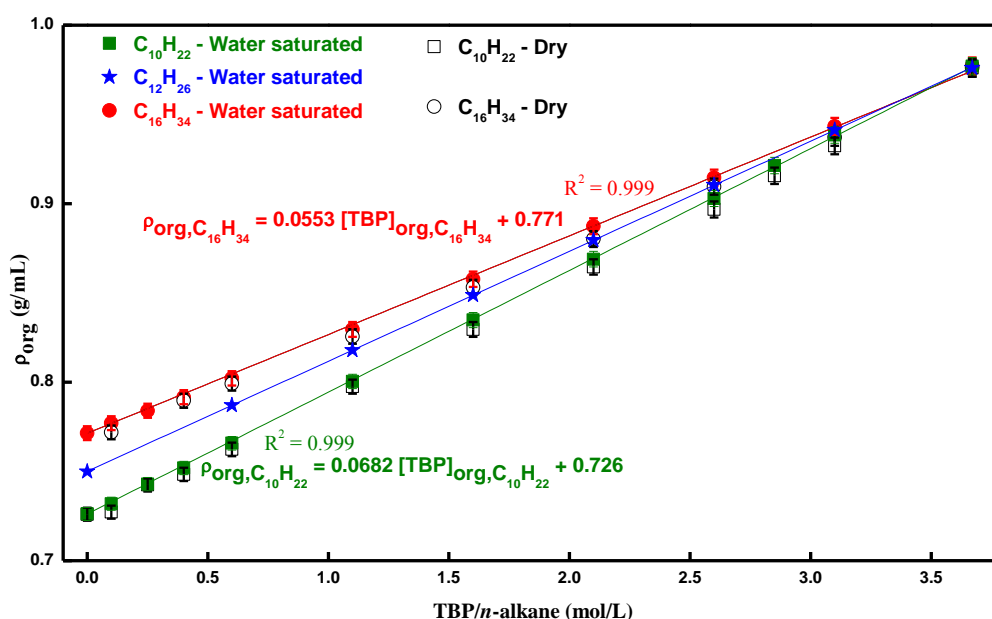


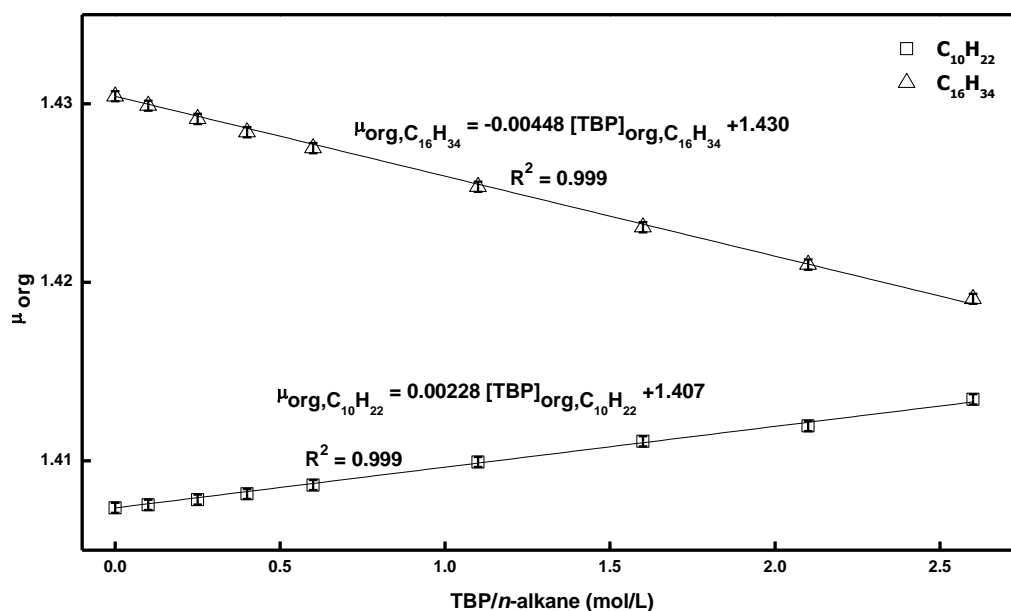
**Fig. 5.1:** Variation of density of solutions of TBP in *n*-alkane as a function of TBP concentration.

It can be seen from Fig. 5.1 that the density of water-saturated TBP/*n*-alkane is higher than the corresponding dry solutions. An increase in the TBP concentration in the organic phase increases the extraction of water and hence there is an increase in the mass per unit volume of the TBP solution. As a result, the density of water-saturated TBP/*n*-alkane is always higher than the density of dry TBP/*n*-alkane. The organic solutions are equilibrated with aqueous solutions in the extraction experiments and the appropriate calibration plots generated from the water-saturated TBP systems have been used for the TBP estimation.

Figure 5.1 illustrates that the trend in the variation of density with the TBP concentration is linear for the entire range from 0% TBP (pure diluent) to 100% TBP (undiluted TBP). The TBP concentrations have been calculated from the density of the organic solutions for TBP/*n*-decane and TBP/*n*-hexadecane systems by using Eqs. (5.1) and (5.2), respectively. These equations are shown along with the calibration plots in Fig. 5.1.

$$\rho_{\text{org}, \text{C}_{10}\text{H}_{22}} = 0.0682 [\text{TBP}]_{\text{org}, \text{C}_{10}\text{H}_{22}} + 0.726 \quad (5.1)$$

$$\rho_{\text{org}, \text{C}_{16}\text{H}_{34}} = 0.0553 [\text{TBP}]_{\text{org}, \text{C}_{16}\text{H}_{34}} + 0.771 \quad (5.2)$$



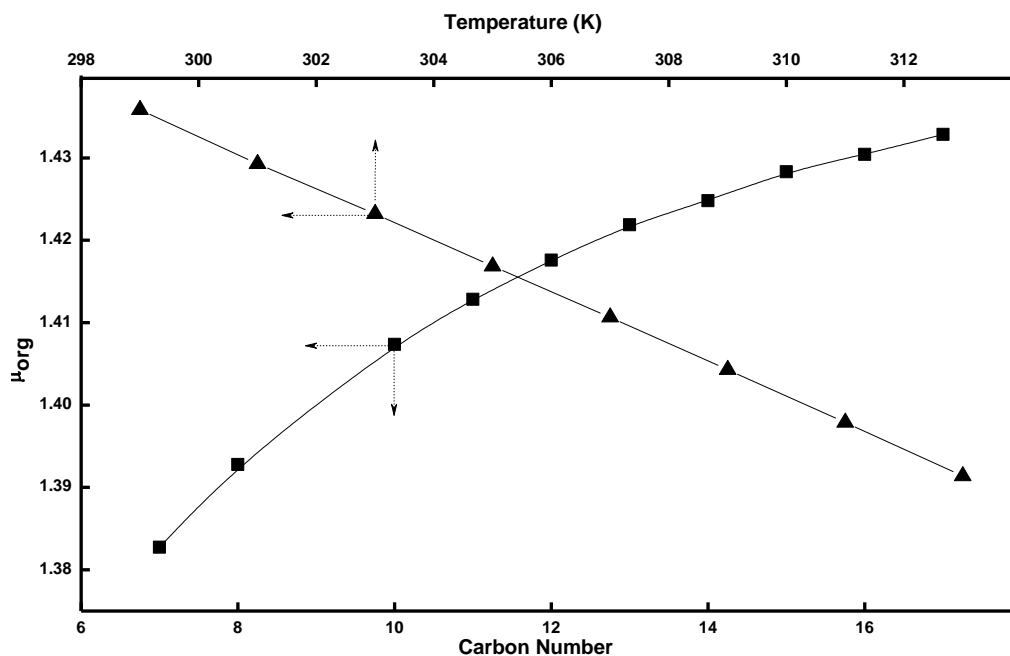
**Fig. 5.2: Variation of refractive index of water saturated solutions of TBP in *n*-alkane as a function of TBP concentration at 303 K.**

Figure 5.2 shows the trends in the refractive index of water-saturated standard solutions of TBP in *n*-decane and *n*-hexadecane as a function of TBP concentration at 303 K. The refractive index of *n*-decane (1.407) and *n*-hexadecane (1.430) determined in the present study are comparable with the reported values of *n*-decane (1.408) and *n*-hexadecane (1.433), respectively [203,205]. The refractive index of the water-saturated TBP (1.417) determined in the present study has been reported for the first time.

The relationship between refractive index of the standard solutions and TBP concentration is linear from 0 to 2.6 mol/L TBP concentration. Consequently, this range was used for the determination of unknown concentration of TBP in the TP and the DP. Equations (5.3) and (5.4) obtained from calibration plots shown in Fig. 5.2 have been used to estimate the unknown TBP concentrations for *n*-decane and *n*-hexadecane systems, respectively. Figure 5.2 shows that for *n*-decane system refractive index increases as the TBP concentration increases, whereas it decreases with TBP concentration for *n*-hexadecane system. As the refractive index of TBP is higher than *n*-decane and lesser than *n*-hexadecane, the trends in the variation of refractive index with TBP concentration for *n*-decane and *n*-hexadecane systems have positive and negative slopes, respectively.

$$\mu_{\text{org, C}_{10}\text{H}_{22}} = 0.0228 [\text{TBP}]_{\text{org, C}_{10}\text{H}_{22}} + 1.407 \quad (5.3)$$

$$\mu_{\text{org, C}_{16}\text{H}_{34}} = -0.0448 [\text{TBP}]_{\text{org, C}_{16}\text{H}_{34}} + 1.430 \quad (5.4)$$



**Fig. 5.3:** Variation of refractive index of *n*-alkane as a function of carbon chain length and refractive index of *n*-dodecane as a function of temperature.

Refractive index of a substance ( $\mu$ ) can be represented as the ratio of the speed of light in vacuum to the speed of light in the medium i.e. organic solution. Usually, speed of light

decreases as the density of the medium through which it passes increases. This has been illustrated by measuring the refractive index of various *n*-alkane and also by measuring the refractive index of *n*-dodecane as a function of temperature. It is well known that density of *n*-alkane increases with increase in the chain length and in general a liquid becomes denser with decrease in temperature. Therefore, it is not surprising to see in Fig. 5.3 that there is a steady increase in refractive index with increase in the carbon chain length of *n*-alkane and also the refractive index of *n*-dodecane decreases as the temperature increases.

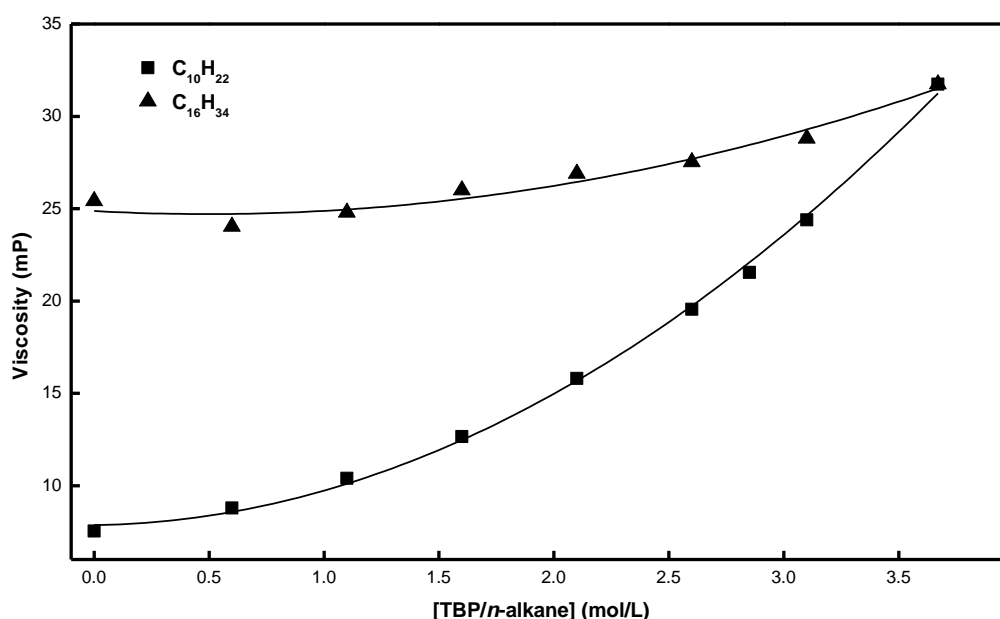


**Fig. 5.4:** Variation of viscosity of water saturated solutions of TBP in *n*-alkane as a function of TBP concentration at 303 K.

Apart from the determination of TBP concentration based on the measurements of the density and the refractive index of the organic solutions, the possibilities of using the viscosities of organic solutions to determine the TBP concentration have also been examined. The variations of the viscosity of water-saturated solutions of TBP in *n*-alkane as a function of TBP concentration are shown in Fig. 5.4. The values of viscosities determined for *n*-decane (7.55 mP) and *n*-hexadecane (25.4 mP) in the present study are marginally higher than the literature values reported for *n*-decane (7.86 mP) and *n*-hexadecane (27.8 mP),

respectively [206,207]. Also, the viscosity data of TBP reported in the present study (31.7 mP) is in good agreement with the viscosity of TBP reported in the literature (30.1 mP) [206]. Linear relationships between viscosity and TBP concentrations are not seen in Fig. 5.4. Though the data on viscosity can be fitted polynomially, the change in viscosity is small for a large variation in TBP concentration, especially in the case of TBP/*n*-decane system. This may lead to large uncertainties in the calculated values. Therefore, the method based on viscosity measurement has not been used for the estimation of TBP.

### 5.2.2 By using third phase formation limit (LOC)

The LOC in the extraction of a metal ion by an extractant can be considered as a unique parameter as it is a constant for a particular metal-extractant-diluent system under a given set of conditions like temperature, extractant concentration etc. Earlier, the tendency of TBP/kerosene to form stoichiometric complex with  $\text{HClO}_4$  ( $1.5 \text{ TBP} \cdot \text{HClO}_4$ ) followed by its separation from kerosene as a new phase has been exploited to estimate the TBP in kerosene from the amount of acid present in the TP [194]. In addition, the TBP/kerosene composition has also been quantified by measuring the volumes of the TP and the DP formed when the organic phase is equilibrated with  $\text{HClO}_4$  or  $\text{HCl}$  [194].

The LOC values for the extraction of Th(IV) by solutions of TBP in *n*-alkane with various concentrations from  $\text{Th}(\text{NO}_3)_4$  solution with near-zero free acidity have been measured to obtain a relationship between LOC and TBP concentration and the results are shown in Fig. 5.5. For both the diluent systems (*n*-decane and *n*-hexadecane), the trend is linear only between 0 mol/L to 2.1 mol/L of TBP and the data fitted in the above concentration range are shown in Fig. 5.5. There is a deviation in the slope of the trend due to a steep increase in LOC above 2.1 mol/L TBP concentration. Therefore, this method based on LOC measurement for TBP estimation can be employed only for the systems which exhibit third phase formation within the above range. Equations (5.5) and (5.6) have been obtained

from the linear plots in Fig. 5.5 to calculate unknown TBP concentration for TBP/*n*-decane and TBP/*n*-hexadecane systems, respectively. Some of the solute-free TP samples with high TBP concentration and the solute-free DP samples with low TBP concentration do not form the TP with  $\text{Th}(\text{NO}_3)_4$  solution with near-zero free acidity at 303 K. Hence those samples have not been analyzed for the concentration of TBP by LOC measurement method.

$$[\text{LOC}]_{\text{C}_{10}\text{H}_{22}} = 0.254 [\text{TBP}]_{\text{org}, \text{C}_{10}\text{H}_{22}} \quad (5.5)$$

$$[\text{LOC}]_{\text{C}_{16}\text{H}_{34}} = 0.135 [\text{TBP}]_{\text{org}, \text{C}_{16}\text{H}_{34}} \quad (5.6)$$

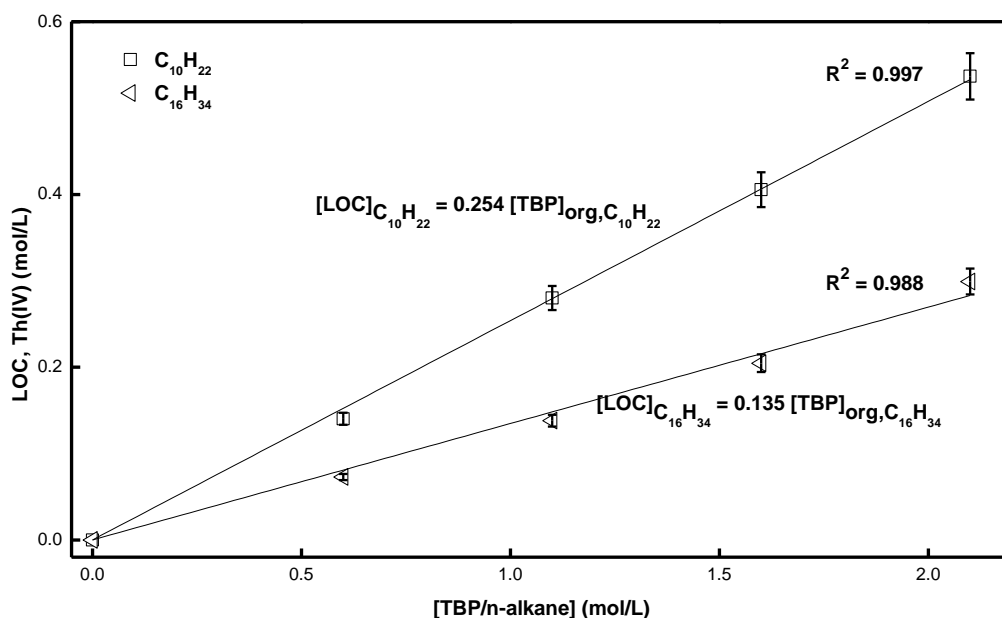


**Fig. 5.5:** Variation of LOC in the extraction of Th(IV) by TBP/*n*-alkane solutions from  $\text{Th}(\text{NO}_3)_4$  solution with near-zero free acidity at 303 K.

### 5.2.3 By using nitric acid loading in the extraction from 8 M $\text{HNO}_3$

The nitric acid equilibration method is universally employed in the process plants for the estimation of TBP content in solvents. However, this method as such may not be suitable for the estimation of TBP in *n*-alkane solutions with higher concentrations of TBP and requires some modification in the analytical procedure to estimate TBP in its highly concentrated solutions. For solutions with higher TBP concentrations,  $\text{HNO}_3$  extraction leads to significant increase in the volume which leads to a decrease in the measured concentration.

Comparison of the volume of one of the concentrated solutions of TBP/*n*-alkane before and after the HNO<sub>3</sub> extraction confirmed the increase in the organic phase volume after HNO<sub>3</sub> extraction. For instance, it has been observed that 2.01 mL of 3.1 M TBP/*n*-decane solution expanded to 2.23 mL after the extraction of nitric acid from 8 M HNO<sub>3</sub> solution. Therefore, the change in the solution volume after the extraction of HNO<sub>3</sub> has to be considered in the estimation of TBP by nitric acid equilibration method.

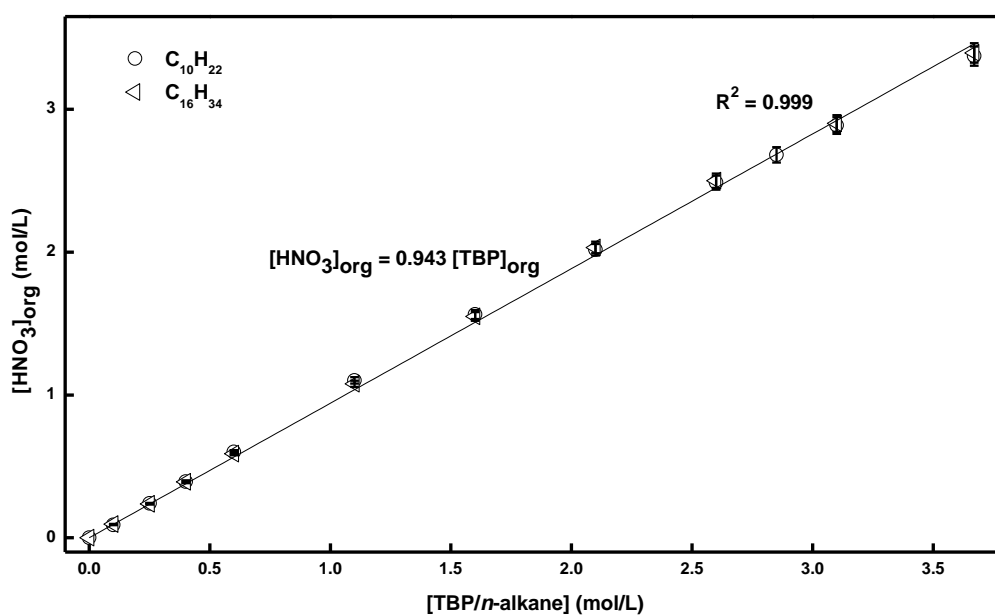


**Fig. 5.6:** Variation of HNO<sub>3</sub> loading in TBP/*n*-alkane solutions in the extraction from 8 M HNO<sub>3</sub> solution as a function of TBP concentration at 303 K.

In order to overcome this limitation, the existing procedure and mode of calculation of TBP concentration by nitric acid equilibration method was modified. For this, a series of TBP/*n*-alkane solutions with known concentrations have been prepared and used for nitric acid extraction from 8 M HNO<sub>3</sub>. The organic phase nitric acid concentrations estimated by acid-base titration have been plotted against concentration of TBP/*n*-alkane for both the diluents as shown in Fig. 5.6. This plot was used to calculate the TBP concentration, instead of directly using the concentration of HNO<sub>3</sub> extracted by the organic phase for TBP estimation. The variation of the organic phase nitric acid concentration with TBP concentration is linear throughout the whole range of TBP concentrations for both the

diluents. As the slopes of the linear fits for TBP solutions in *n*-decane and *n*-hexadecane are very close to each other (0.941 for *n*-decane and 0.945 for *n*-hexadecane), the common linear fit for the combined data as shown in Fig. 5.6 has been used for TBP estimation in both the diluents. The common linear fit can be represented by Eq. (5.7).

$$[\text{HNO}_3]_{\text{org}} = 0.943 [\text{TBP}]_{\text{org}} \quad (5.7)$$

#### 5.2.4 Comparison of the methods for TBP estimation

The concentrations of TBP in the TP and the DP estimated as a function of  $[\text{Th(IV)}]_{\text{aq,eq}}$  for the extraction of Th(IV) by 1.1 M solutions of TBP in *n*-decane and *n*-hexadecane from  $\text{Th}(\text{NO}_3)_4$  solution with 1 M  $\text{HNO}_3$  by the above methods and their average values are shown in Tables 5.1 to 5.4. The standard deviation of all the data points generated for the estimation of TBP by various methods is also shown in Tables 5.1 to 5.4. The error bars of the data points used for the generation of calibration plots are shown in Figs. 5.1, 5.2, 5.5 and 5.6 along with the linear fit. These figures show that the  $R^2$  values of all the calibration plots are close to unity which indicates the proximity of the fit used for the estimation of unknown TBP solutions. The error range of the TBP concentration values calculated for all the methods reveals that the TBP concentrations are precise and are close to values obtained by conventional nitric acid equilibration method. The overall agreement between the TBP concentrations estimated by various methods is good in most of the cases.

#### 5.2.5 Volume correction in the determination of TBP concentrations in organic phases

Washing of organic phases with distilled water removes  $\text{Th}(\text{NO}_3)_4$  as well as  $\text{HNO}_3$  and consequently, a reduction in the volume of the corresponding phases can be expected particularly, if the loading is high. Therefore, the average concentration of TBP in organic phases obtained by various methods does not represent the actual concentration unless the volume correction is incorporated. However, the volume measurement of various TP and DP samples before and after stripping of solutes indicated that only TP samples undergo

significant volume reduction after the stripping, whereas the volume change of DP samples is negligible. This indirectly shows that the volume correction depends upon the amount of solutes present in the organic phases.

**Table 5.1: Data on the concentration of TBP in the TP obtained by various experimental methods and model for 1.1 M TBP/n-decane - Th(NO<sub>3</sub>)<sub>4</sub>/1 M HNO<sub>3</sub> system.**

[Th(IV)] <sub>aq,eq</sub> (mol/L)	[TBP] (mol/L)					
	Density Method	Refractive Index Method	Acid Equilibration Method	Average C <sub>a</sub>	Average C <sub>b</sub>	Model
0.745	2.23±0.01	2.43±0.01	2.27±0.01	2.3±0.1	2.2	-
1.05	2.67±0.01	#	2.69±0.01	2.68±0.01	2.48	2.58
1.26	2.88±0.01	#	2.86±0.01	2.87±0.01	2.64	2.66
1.40	2.94±0.01	#	2.92±0.01	2.93±0.01	2.66	2.72
1.57	2.97±0.01	#	2.92±0.01	2.94±0.03	2.73	2.73
1.89	3.09±0.01	#	3.04±0.01	3.06±0.03	2.75	2.77
2.35	3.15±0.01	#	3.09±0.01	3.12±0.02	2.74	2.80

Data obtained by LOC method were out of linearity range;

C<sub>a</sub> = [TBP] after the stripping of solutes; C<sub>b</sub> = [TBP] before the stripping of solutes;

# Out of linearity range

A third phase sample of 1.1 M TBP/n-decane with a volume of 2.41 mL reduced to 2.18 mL after the solute stripping. Hence, volume correction has been applied for all TP samples by measuring the volume of samples before and after the stripping of the solutes. Hence, volume correction has been applied for all TP samples by measuring the volume of samples before and after the stripping of the solutes. Actual concentration of TBP in the TP samples were calculated by using Eq. (5.8), where C<sub>a</sub> and C<sub>b</sub> correspond to TBP concentrations after and before the stripping of solutes, respectively, and V<sub>a</sub> and V<sub>b</sub> represent the volume of the corresponding samples. The average concentrations of TBP obtained after

the volume correction for 1.1 M TBP/*n*-decane - Th(NO<sub>3</sub>)<sub>4</sub>/1 M HNO<sub>3</sub> and 1.1 M TBP/*n*-hexadecane - Th(NO<sub>3</sub>)<sub>4</sub>/1 M HNO<sub>3</sub> systems have been shown in Tables 5.1 to 5.4.

$$C_b = \frac{V_a C_a}{V_b} \quad (5.8)$$

**Table 5.2: Data on the concentration of TBP in the DP obtained by various experimental methods and model for 1.1 M TBP/*n*-decane - Th(NO<sub>3</sub>)<sub>4</sub>/1 M HNO<sub>3</sub> system.**

[Th(IV)] aq,eq (mol/L)	[TBP] (mol/L)					
	Density Method	Refractive Index Method	LOC Method	Acid Equilibration Method	Average	Model
0.745	0.610±0	0.570±0.001	0.596±0.003	0.674±0.003	0.61±0.04	-
1.05	0.306±0.003	0.259±0.001	0.326±0.002	0.351±0.002	0.31±0.04	0.29
1.26	0.195±0.002	0.162±0.001	*	0.230±0.001	0.20±0.03	0.21
1.40	0.154±0.006	0.136±0.001	*	0.188±0.002	0.16±0.03	0.18
1.57	0.126±0.008	0.105±0.001	*	0.154±0.002	0.13±0.02	0.15
1.89	0.10±0.01	0.0877±0.0001	*	0.107±0.001	0.10±0.01	0.11
2.35	0.064±0.004	0.0789±0.0001	*	0.0727±0.0001	0.072±0.007	0.080

\* No third phase formation by the solute-free samples

**Table 5.3: Data on the concentration of TBP in the TP obtained by various experimental methods and model for 1.1 M TBP/*n*-hexadecane - Th(NO<sub>3</sub>)<sub>4</sub>/1 M HNO<sub>3</sub> system.**

[Th(IV)] <sub>aq,eq</sub> (mol/L)	[TBP] (mol/L)				
	Density Method	Acid Equilibration Method	Average C <sub>a</sub>	Average C <sub>b</sub>	Model
0.296	3.08±0.01	3.04±0.01	3.06±0.02	2.84	-
0.373	3.12±0.01	3.08±0	3.10±0.02	2.91	-
0.520	3.27±0.01	3.22±0.01	3.25±0.03	2.96	-
0.913	3.39±0.01	3.32±0.01	3.36±0.05	2.99	3.13
1.55	3.48±0.01	3.39±0.02	3.43±0.06	2.86	3.12
1.86	3.51±0.01	3.45±0.01	3.48±0.04	2.92	3.11
2.35	3.51±0.01	3.46±0.01	3.49±0.03	3.05	3.12

Data obtained by LOC and refractive index methods were out of linearity range;  
C<sub>a</sub> = [TBP] after the stripping of solutes; C<sub>b</sub> = [TBP] before the stripping of solutes

**Table 5.4: Data on the concentration of TBP in the DP obtained by various experimental methods and model for 1.1 M TBP/*n*-hexadecane - Th(NO<sub>3</sub>)<sub>4</sub>/1 M HNO<sub>3</sub> system.**

[Th(IV)] aq,eq (mol/L)	[TBP] (mol/L)					
	Density Method	Refractive Index Method	LOC Method	Acid Equilibration Method	Average	Model
0.296	0.446±0.004	0.480±0.001	0.424±0.003	0.465±0.005	0.45±0.02	-
0.373	0.325±0	0.362±0.001	0.345±0.001	0.368±0.004	0.35±0.02	-
0.520	0.21±0.01	0.230±0.001	0.259±0.001	0.236±0.001	0.23±0.02	-
0.913	0.109±0	0.098±0.001	0.148±0.001	0.114±0.002	0.12±0.02	0.084
1.55	0.073±0.006	0.056±0.001	*	0.049±0.001	0.06±0.01	0.046
1.86	0.039±0.009	0.040±0.001	*	0.040±0.001	0.040±0.001	0.037
2.35	0.036±0.009	0.031±0.001	*	0.029±0.002	0.032±0.004	0.030

\* No third phase formation by the solute-free samples

A change in the volume of organic phase is expected after Th(IV) extraction and therefore, it is worthwhile to ensure the mass balance of TBP before and after third phase formation. In this connection, the amount of TBP present in the organic phase (biphasic region before Th(IV) extraction) as well as the TP and the DP (triphasic region after Th(IV) extraction) have been determined. The amount of TBP in the biphasic region (TBP<sub>Bi</sub>) and the triphasic region (TBP<sub>Ti</sub>) are calculated from the volume of corresponding phases and their TBP concentrations using Eqs. (5.9) and (5.10). The term V<sub>Org</sub> corresponds to the volume of TBP in the organic phase in the biphasic region. V<sub>TP</sub> and V<sub>DP</sub> represent the volume of TBP in the TP and the DP, respectively. C<sub>TP</sub> and C<sub>DP</sub> denote the volume of the corresponding phases in the triphasic region. The results on the mass balance of TBP for the extraction of Th(IV) in 1.1 M TBP/*n*-decane - Th(NO<sub>3</sub>)<sub>4</sub>/1 M HNO<sub>3</sub> and 1.1 M TBP/*n*-hexadecane - Th(NO<sub>3</sub>)<sub>4</sub>/1 M HNO<sub>3</sub> systems are shown in Table 5.5. The good mass balance of TBP before and after third phase formation validates the reliability of the measurements made in the present study.

$$\text{TBP}_{\text{Bi}} = 1.1 \times V_{\text{Org}} \quad (5.9)$$

$$\text{TBP}_{\text{Tri}} = (V_{\text{TP}} \times C_{\text{TP}}) + (V_{\text{DP}} \times C_{\text{DP}}) \quad (5.10)$$

**Table 5.5: Mass Balance of TBP before and after the extraction of Th(IV) by 1.1 M TBP/*n*-alkane from 1 M Th(IV) solution in 1 M HNO<sub>3</sub> at 303 K.**

System	Before Th(IV)		After Th(IV)				
	Extraction		Extraction				
	V <sub>Org</sub> (mL)	TBP <sub>Bi</sub> (m.mol)	V <sub>TP</sub> (mL)	V <sub>DP</sub> (mL)	C <sub>TP</sub> (M)	C <sub>DP</sub> (M)	TBP <sub>Tri</sub> (m.mol)
1.1 M TBP/ <i>n</i> -decane	10.06	11.07	3.63	6.69	2.48	0.31	11.07
1.1 M TBP/ <i>n</i> -hexadecane	10.10	11.11	3.49	6.98	2.99	0.12	11.27

In general, the volume of the TP formed during the phase splitting is less as compared to the volume of the DP. The reduction in the volume of the TP after the stripping of extracted solutes is also large and it can further lead to a situation where the amount of sample required for the estimation of constituents in the TP as well as the volume measurements is insufficient. In order to overcome these difficulties, a large volume (~ 10 mL) of the organic phase has been used for the third phase formation experiment to generate significant amount of the TP.

### 5.3 Estimation of extractant in the TP and the DP by model

It has been confirmed that the difference in density between the DP and its corresponding diluent approaches zero with increase in [Th(IV)]<sub>aq,eq</sub> for all TalP/*n*-alkane systems. During the extraction of Th(IV) by TalP/*n*-alkane solvents from saturated aqueous solution of Th(NO<sub>3</sub>)<sub>4</sub>, major fraction of extractant of the original organic phase resides in the TP with a small amount of extractant in the DP. Therefore, the DP can be considered as a dilute solution of Th(NO<sub>3</sub>)<sub>4</sub>-TalP metal solvate in the corresponding diluent, whereas reverse

micelles formed by the aggregation of trialkyl phosphate molecules,  $\text{Th}(\text{NO}_3)_4$  and  $\text{H}_2\text{O}$  are expected to be present in the TP.

Since  $\text{Th}(\text{NO}_3)_4$  forms trisolvate and  $\text{HNO}_3$  forms monosolvate complexes with TalP, the mole ratios of  $\text{Th}(\text{NO}_3)_4$  to TalP and  $\text{HNO}_3$  to TalP in the light organic phase can be 1:3 and 1:1, respectively. Therefore, for a given system, the number of moles of extractant in the DP can be calculated by adding three times the number of moles of Th(IV) and the number of moles of  $\text{HNO}_3$ . The number of moles of extractant present in the TP was calculated by subtracting the number of moles of extractant present in the DP from the number of moles of extractant of the original organic phase. The same theoretical approach can also be extended to systems below saturation.

The analytical techniques employed for the estimation of extractant involves the stripping of the extracted solutes from the organic phases prior to the estimation of extractant. The stripping of solutes from the organic phase as well as the estimation of extractant is cumbersome. The above model which is proposed to predict the extractant concentration requires only the knowledge about the concentration of solutes present in corresponding organic phases and hence is simpler.

### **5.3.1 Validation of the model to calculate extractant concentration in the TP and the DP**

The TBP concentrations calculated based on the aforementioned theoretical approach for 1.1 M TBP/*n*-alkane -  $\text{Th}(\text{NO}_3)_4$ /1 M  $\text{HNO}_3$  systems are compared with experimentally obtained values in Tables 5.1 to 5.4. It can be seen from Tables 5.1 to 5.4 that the model values and the experimental values after volume correction are in good agreement with each other at higher  $[\text{Th}(\text{IV})]_{\text{aq,eq}}$ . Hence these results confirm the reliability of the assumptions made for the determination of TBP concentration.

It is also confirmed that this theoretical method cannot be extrapolated to systems involving aqueous solutions with moderate or dilute  $\text{Th}(\text{NO}_3)_4$  concentrations as the

difference in model and experimental values increase with decrease in  $[\text{Th(IV)}]_{\text{aq,eq}}$ . It is assumed in the model that the TBP molecules in the DP are complexed with either  $\text{Th}(\text{NO}_3)_4$  or  $\text{HNO}_3$  and the concentration of free TBP is negligible. However, some amount of uncomplexed TBP is likely to be present in the DP and the concentration of uncomplexed TBP is higher at lower  $[\text{Th(IV)}]_{\text{aq,eq}}$  and is responsible for the deviation between the model and experimental values at lower  $[\text{Th(IV)}]_{\text{aq,eq}}$ .

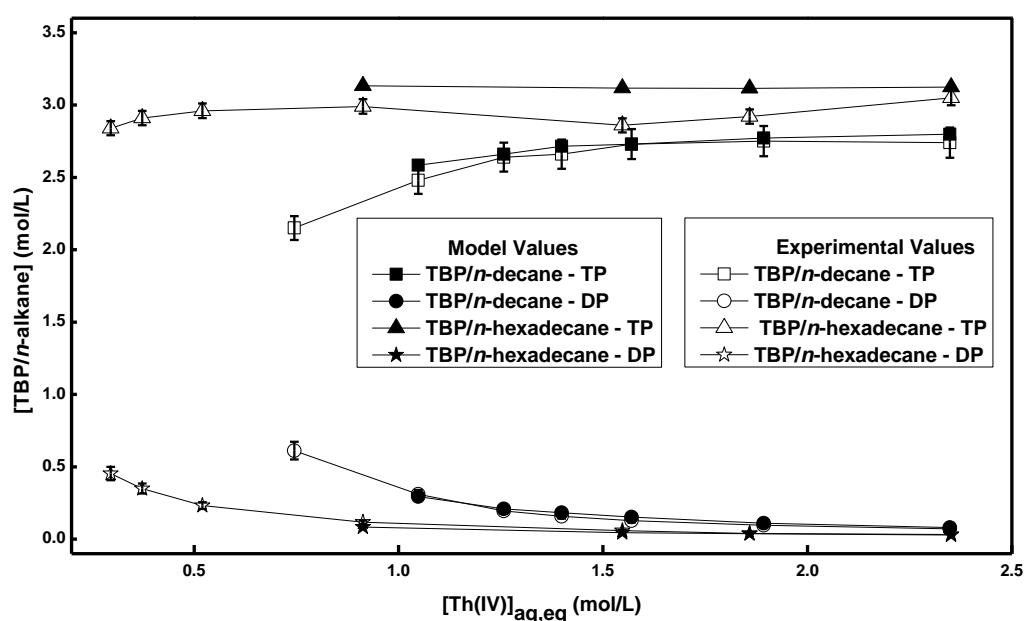


**Fig. 5.7:** Variation of concentration of TBP in the TP and the DP for the extraction of  $\text{Th(IV)}$  by 1.1 M TBP/ $n$ -alkane from  $\text{Th}(\text{NO}_3)_4$  solution with 1 M  $\text{HNO}_3$  as a function of  $[\text{Th(IV)}]_{\text{aq,eq}}$  at 303 K.

The trends in the concentration of TBP in the TP and the DP for the extraction of  $\text{Th(IV)}$  by 1.1 M TBP/ $n$ -alkane from  $\text{Th}(\text{NO}_3)_4$  solution in 1 M  $\text{HNO}_3$  as a function of  $[\text{Th(IV)}]_{\text{aq,eq}}$  at 303 K obtained by the experiment and the model as a function of  $[\text{Th(IV)}]_{\text{aq,eq}}$  are depicted in Fig. 5.7 for a better clarity. Figure 5.7 illustrates that initially the concentration of TBP in the TP increases with increase in  $[\text{Th(IV)}]_{\text{aq,eq}}$  and then remains almost constant. However, the TBP concentration in the DP decreases initially and tends to become negligible at higher  $[\text{Th(IV)}]_{\text{aq,eq}}$ . The difference in TBP concentration between the

TP and the DP during the phase splitting increases with increase in the diluent chain length. Comparison of Fig. 5.7 with the extraction isotherm plots of Th(IV) in triphasic region shown in Fig. 4.7 and 4.8 (Chapter 4) indicates the similarity in the trend in the variation of Th(IV) extraction and TBP concentration.

### **5.3.2 Estimation of extractant in the TP and the DP as a function of various parameters by the model**

Even though the model and the experimental values for TBP concentration are in good agreement with each other for TBP based solvents, this method can also be extended to *TiAP* solvent systems for the estimation of *TiAP* concentration in corresponding solvents due to the similar extraction behaviour of TBP and *TiAP*. Hence, this model has been used to determine the extractant concentration in the TP and the DP for the extraction of Th(IV) from its saturated solution in near-zero free acidity and nitric acid media for both *TiAP* and TBP based solvents.

The variation of the *TiAP* concentration in the TP and the DP with respect to diluent chain length for the extraction of Th(IV) from saturated Th(NO<sub>3</sub>)<sub>4</sub> solution with near-zero free acidity at 303 K is shown in Table 5.6. The *TiAP* concentrations increase in the TP and decrease in the DP with increase in the diluent chain length. The results indicate that during organic phase splitting extractant molecules prefer to remain in the TP due to the interaction between the reverse micelles, whereas the diluent molecules are accommodated in the DP.

The trend in the concentration of *TalP* in the extraction of Th(IV) from saturated Th(NO<sub>3</sub>)<sub>4</sub> solutions in 1 M and 5 M HNO<sub>3</sub> by 1.1 M solutions of *TiAP* and TBP in *n*-alkane at 303 K are shown in Table 5.7. The *TalP* concentration in the TP increase with diluent chain length for Th(IV) extraction from both 1 M and 5 M HNO<sub>3</sub>, however in the case of *TalP* concentration in the DP the effects are opposite. The data shown in Table 5.7 also

indicate that the difference in extractant concentration between the TP and the DP is higher for TBP systems as compared to TiAP systems.

**Table 5.6: The concentration of TiAP in the TP and the DP obtained by model for the extraction of Th(IV) by 1.1 M TiAP/n-alkane from saturated Th(NO<sub>3</sub>)<sub>4</sub> solution with near-zero free acidity at 303 K.**

Extractant System	TP (mol/L)	DP (mol/L)
C <sub>12</sub> H <sub>26</sub>	2.03	0.374
C <sub>14</sub> H <sub>30</sub>	2.27	0.225
C <sub>16</sub> H <sub>34</sub>	2.64	0.142
C <sub>18</sub> H <sub>38</sub>	3.04	0.097

**Table 5.7: The concentration of extractant in the TP and the DP obtained by model in the extraction of Th(IV) by 1.1 M TalP/n-alkane from saturated Th(NO<sub>3</sub>)<sub>4</sub> solutions with 1 M and 5 M HNO<sub>3</sub> at 303 K.**

Extractant System	1 M HNO <sub>3</sub>		5 M HNO <sub>3</sub>	
	TP (mol/L)	DP (mol/L)	TP (mol/L)	DP (mol/L)
TBP/C <sub>10</sub> H <sub>22</sub>	2.80	0.080	-	-
TBP/C <sub>12</sub> H <sub>26</sub>	2.89	0.050	3.03	0.083
TBP/C <sub>14</sub> H <sub>30</sub>	2.93	0.035	3.00	0.055
TBP/C <sub>16</sub> H <sub>34</sub>	3.12	0.030	-	-
TiAP/C <sub>12</sub> H <sub>26</sub>	1.87	0.424	1.69	0.544
TiAP/C <sub>14</sub> H <sub>30</sub>	2.20	0.249	2.18	0.306

#### 5.4 Applications of newly developed TBP estimation methods

The methods reported in the present study can be used for the estimation of TBP in freshly prepared as well as regenerated spent solvents of TBP. As these methods involve the measurement of physical properties of the solvent, the results are sensitive to variation in the concentration of TBP and therefore, small changes in the TBP concentration can be detected

easily. Unlike nitric acid equilibration method, the methods based on the measurement of density and refractive index developed in the present study do not require any equilibration or analysis of samples and these parameters can be measured directly with the washed TBP samples. Generally, the measurement of density and refractive index is performed using instruments that give instantaneous data and hence save time. Moreover, density and refractive index probes can be installed in process plants for online monitoring. Determination of density and refractive index does not require any reagents for analysis and hardly generates any waste.

The measurement of density of TBP solutions at various temperatures revealed that 2 K variation in temperature from 298 K to 308 K does not influence the density measurements significantly and hence this method can be employed without maintaining a constant temperature during the measurement. On the other hand, the refractive indices of solutions are sensitive to temperature variations and hence temperature should be kept constant while measuring the refractive indices. However, further studies have to be performed under various conditions to know the feasibility of using these methods for the estimation of extractants that are employed in process plants. In the present study, *n*-decane and *n*-hexadecane were chosen as representative diluents and these studies can also be performed with *n*-DD which is the commonly preferred diluent. However, studies have to be performed to validate the influence the diluents with mixture of alkanes such as HNP and OK on the estimation of TBP by using the methods mentioned in the present study.

## 5.5. Conclusions

The methods based on the measurement of density, refractive index, LOC etc., can be used for the accurate determination of TBP concentration in organic phases after the phase splitting. The present study confirmed that the extractant accumulates in the TP along with solutes ( $\text{Th}(\text{NO}_3)_4$  and  $\text{HNO}_3$ ) during phase splitting. Also, the diluent chain length influences

the distribution of extractant between the TP and the DP as in the case of extracted solutes. The tendency of TBP to preferentially occupy in the TP leaving behind the DP is higher as compared to TiAP. The theoretical method developed for the estimation of TBP in the TP and the DP has been authenticated with experimentally obtained values. The TBP concentrations deduced by the model are in proximity with the experiment values for Th(IV) extraction from concentrated  $\text{Th}(\text{NO}_3)_4$  solutions as compared to dilute solutions. The methods developed in the present study can also be used for the estimation of TBP in freshly prepared TBP solution as well as regenerated spent solvents to ensure the requirements of flow sheet conditions. These methods can be extended to the estimation of other extractants in their solutions in diluents such as TiAP/*n*-alkane solvents.



# Chapter 6



**“Research is to see what everybody else has seen, and to think what nobody else has thought”**

*-Albert Szent-Gyorgyi*

# SEPARATION OF U(VI) AND Th(IV) FROM Nd(III) BY CROSS-CURRENT SOLVENT EXTRACTION MODE USING TiAP

---

---

# 6

## 6.1 Introduction

India has a huge quantity of thorium (around 10% of world's reserves) in the form of monazite which is considered to be a rich source of thorium as well as lighter rare earth elements and also a secondary source of uranium [208,209]. Moreover, the abundance of thorium in Indian monazite found along the coastal regions is highest (~9%) as compared to other monazite ores available elsewhere in the world [210]. The processing of monazite ore is essential for the recovery of uranium and thorium in order to sustain the nuclear program for energy production.

Solutions of 5 vol% (0.183 M) and 40 vol% (1.47 M) TBP in an inert hydrocarbon diluent are being used for the separation of uranium and thorium, respectively, from rare earths in nitric acid media during the processing of monazite ore [89,93,95,96]. As the third phase formation tendency and aqueous solubility of TiAP are lesser as compared to TBP, the consequences of organic phase splitting and red oil formation can be avoided in the case of TiAP systems. Studies on the extraction of U(VI) and Th(IV) by TiAP as well as TBP based solvents under identical conditions discussed in Chapters 3 and 4 revealed the similar extraction behaviour of both the extractants. Also, the extraction chemistry of TiAP and TBP are similar with respect to lanthanides [172].

Although the circumstances favour the deployment of TiAP based solvents for monazite ore processing, detailed extraction studies have to be carried out to ascertain the feasibility of using it as an alternate extractant to TBP. In this context, the extraction, scrubbing and stripping behaviour of TiAP with respect to U(VI), Th(IV) and Nd(III) in nitric acid media has been investigated in cross-current mode. In the present study, Nd(III) has been

chosen as a representative element for all the rare earth elements likely to be present in monazite ore.

It is reported that the extraction of Th(IV) and its separation factor from lanthanides are maximum for the extraction from 8 M HNO<sub>3</sub> and hence the extraction experiments were also executed with feed solutions in 8 M HNO<sub>3</sub> apart from 4 M HNO<sub>3</sub> [211]. The third phase formation behaviour of TiAP and TBP are also compared and the data reported can be utilized for the development of flow sheets for the processing of monazite ore using TiAP based solvents. The interference of U(VI), Th(IV) and Nd(III) during their analyses has also been investigated in order to assess the reliability of the analytical procedures followed in the present study.

## 6.2 Validation of analytical methods

As the solutions used in the present study consisted of U(VI), Th(IV) and Nd(III) in nitric acid media, it is important to know their mutual interference during their analysis. Davies and Gray have examined the interference of various metal ions in the estimation of U(VI), however the interference of Th(IV) and Nd(III) are not reported [63]. Even though literature reports that Th(IV) and Nd(III) do not interfere with each other in complexometric titrations, information on the interference of U(VI) on their analyses are unavailable [179,212]. In this context, titrimetric methods employed for the estimation of U(VI), Th(IV) and Nd(III) in the presence of each other in nitric acid media have been validated to ascertain any bias.

In the studies pertaining to the investigation on the mutual interference of metal ions, the concentrations of these metal ions have been chosen in such a way that they represent the maximum concentrations expected in the sample solutions generated from the separation studies. Initially, the concentration of a particular metal ion in its solution in nitric acid without other metal ions was estimated. Later on the analysis of the same metal ion has been

performed after the addition of known amounts of other metal ions. The results of the analysis carried out in the presence and absence of interfering metal ions are shown in Table 6.1. It can be seen in Table 6.1 that the difference in the concentration determined with and without other metal ions is less than 1% in most of the cases. Therefore, it can be concluded that the mutual interference of metal ions in the estimation of U(VI), Th(IV) and Nd(III) is negligible within the concentration range used in the present study.

**Table 6.1: Interference of U(VI), Th(IV) and Nd(III) in nitric acid media during their estimation by titration.**

Amount of metal ion present in the sample (mg)			Concentration of native metal ion without foreign metal ion (g/L)	Amount of native metal ion determined in the presence of foreign metal ion (mg)
U(VI)	Th(IV)	Nd(III)		
0	1.27	9	[Th(IV)] = 5.07	Th(IV) = 1.28
12.5	1.27	0		Th(IV) = 1.28
0	8	0.46	[Nd(III)] = 18.5	Nd(III) = 0.46
0	26	0.46		Nd(III) = 0.46
3	0	0.46		Nd(III) = 0.46
6	0	0.46		Nd(III) = 0.46
2.61	26	0	[U(VI)] = 10.4	U(VI) = 2.58
2.61	0	12.5		U(VI) = 2.58
2.61	0	25		U(VI) = 2.60

### 6.3 Third phase formation behaviour of 0.183 M solutions of TiAP and TBP in *n*-DD

The knowledge about the third phase formation limits of a solvent extraction system is essential in order to restrict the metal loading in the organic phase to avoid organic phase splitting. Therefore, third phase formation tendency of 0.183 M solutions of TiAP and TBP in *n*-DD with a solution containing U(VI), Th(IV) and Nd(III) in 4 M HNO<sub>3</sub> has been studied. Nd(III) was chosen as the representative element for the rare earth elements and was used in the feed solutions in such a way that its concentration is in the range of the total concentration

of all rare earths elements likely to be present in the monazite ore. A concentrated solution containing U(VI), Th(IV) and Nd(III) (as the representative of total rare earths) near-saturation was employed as the feed to mimic the dissolver solution encountered during the processing of Indian monazite ore [91].

**Table 6.2: Mass Balance of Th(IV) before and after the extraction by 0.183 M TalP/*n*-DD from solution containing U(VI), Th(IV) and Nd(III) in 4 M HNO<sub>3</sub>.**

0.183 M TalP/ <i>n</i> - DD	Before Th(IV) Extraction				After Th(IV) Extraction		
	Volume- Org (mL)	Volume- Feed (mL)	[Th(IV)]- Feed (g/L)	Th(IV)- Feed (mg)	Th(IV)- Aq (mg)	Th(IV)- DP (mg)	Th(IV)- Total (mg)
TBP	1	1	226 <sup>a</sup>	226	214	2.3	216
	1	1	198 <sup>b</sup>	198	190	2.5	192
	1	1	184 <sup>b</sup>	184	172	2.8	175
	1	1	160 <sup>b</sup>	160	152	3.0	155
	1	1	130 <sup>b</sup>	130	125	4.1	129
	1	1	110 <sup>b</sup>	110	105	4.9	110
	1	1	91.5 <sup>b</sup>	91.5	87.3	4.3 <sup>c</sup>	91.6
TiAP	1	1	226 <sup>a</sup>	226	218	9.0 <sup>c</sup>	227

<sup>a</sup> Concentration of solutes in the feed solution used before dilution with 4 M HNO<sub>3</sub> ([Th(IV)] = 226 g/L; [Nd(III)] = 262 g/L; [U(VI)] = 7.17 g/L; [HNO<sub>3</sub>] = 4.02 M;

<sup>b</sup> Feed solution diluted with 4 M HNO<sub>3</sub>;

<sup>c</sup> As the third phase was not formed, the values represent organic phase Th(IV) concentration in the biphasic region

When the concentrated solution near-saturation ([Th(IV)] = 226 g/L; [Nd(III)] = 262 g/L; [U(VI)] = 7.17 g/L; [HNO<sub>3</sub>] = 4.02 M) was contacted with 0.183 M solutions of TiAP and TBP in *n*-DD pre-equilibrated with 4 M HNO<sub>3</sub> at 303 K with an organic to aqueous volume ratio of 1 it was observed that TiAP does not form TP, whereas TBP forms TP. As the concentration of TBP (0.183 M) in the organic phase is less, the volume of TP formed was too small and its visual detection was extremely difficult. Therefore, third phase formation was further confirmed by analyzing the concentration of Th(IV) in the upper layer

of the organic phase and the corresponding aqueous phase after extraction, followed by checking the mass balance of Th(IV). The results of the mass balance experiment carried out with 0.183 M solutions of TiAP and TBP at various feed concentrations are shown in Table 6.2. It can be seen from Table 6.2 that in the case of TiAP, there is a good mass balance before and after the extraction indicating the absence of any deposits at the organic-aqueous interface. However, in the case of TBP, at higher concentrations there is a mismatch in the mass balance before and after the extraction which in turn indicates the presence of a thin layer of TP at the interface.

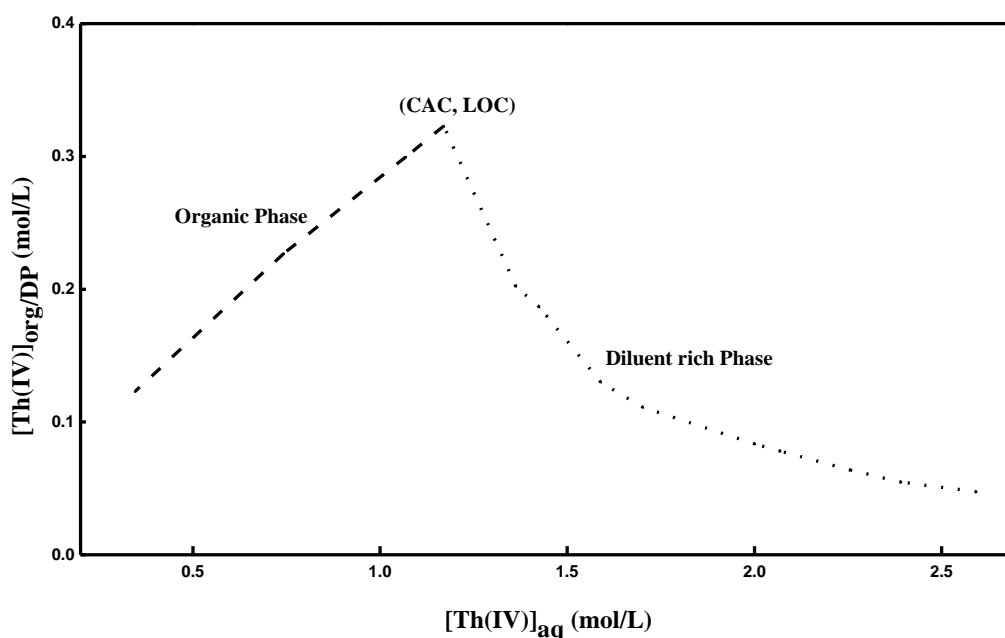


**Fig. 6.1:** Schematic representation of general trend in the concentration of Th(IV) in organic and diluent-rich phases in the extraction of Th(IV) by TalP/n-alkane as a function of aqueous phase Th(IV) concentration.

Figure 6.1 schematically represents the concentration of Th(IV) in organic phase (biphasic region) and diluent-rich phase (triphasic region) in the extraction of Th(IV) by TalP based solvents that was discussed in Chapter 4. Figure 6.1 depicts that the concentration of Th(IV) in the DP increases with decrease in aqueous phase Th(IV) concentration until CAC. However the Th(IV) concentration in the organic phase decreases with further decrease in aqueous phase Th(IV) concentration below CAC.

It can be seen from Table 6.2 that the organic phase Th(IV) concentration steadily increases (from 2.3 g/L to 4.9 g/L) with decrease in Th(IV) concentration in the feed solution (from 226 g/L to 110 g/L) which is a typical trend observed in the case of the diluent-rich phase. Moreover, a sudden drop in Th(IV) concentration in the organic phase (4.9 g/L to 4.3 g/L) with decrease in Th(IV) concentration in the feed solution (from 110 g/L to 91.5 g/L) indicates the transition of solvent extraction system from triphasic region to biphasic region. Also, when Th(IV) concentration in the feed is 110 g/L the difference in mass of Th(IV) before and after the extraction of metal ions is negligible which shows that TBP does not form TP when Th(IV) concentration in the feed is close to 110 g/L. This clearly illustrates that in the case of TBP, dilution of the concentrated feed solution to reduce the Th(IV) concentration from 226 g/L to 110 g/L is necessary for restricting the metal loading below third phase formation limits. Such a large dilution of the feed solution results in the reduction of throughput and increase in the operation time of the contactors employed in the process plants. In the case of *TiAP*, the near-saturation feed solution can be used directly without any dilution and therefore, throughput can be improved.

#### **6.4 Separation of U(VI) from Th(IV) and Nd(III) with 0.183 M *TaIP*/*n*-DD**

The extraction of U(VI) by TBP was carried out with a feed solution obtained after the dilution of the concentrated feed solution (near-saturation) below its third phase formation limit and in the case of *TiAP* the concentrated feed solution was used after adjusting the acidity to 4 M HNO<sub>3</sub>. The schematics of cross-current modes used for the extraction of U(VI) by 0.183 M solutions of *TiAP* and TBP in *n*-DD with an organic to aqueous volume ratio of 1 at 303 K are shown in Figs. 6.2 and 6.3, respectively. Both the figures depict that *TiAP* and TBP require 4 and 3 extraction stages, respectively, for 95% of U(VI) extraction. The results indicate that to attain a similar U(VI) extraction percentage *TiAP* requires an additional extraction stage than TBP. However, comparison of Fig. 6.2 with Fig. 6.3 shows that the

U(VI) concentration in the aqueous feed of first and second extraction stages of TBP and TiAP, respectively are similar. Therefore, the concentration of U(VI) extracted by both TiAP and TBP are comparable with each other under identical conditions which corroborates our result shown in Chapter 3 that the extraction behaviour of TiAP and TBP are comparable with respect to U(VI) metal ion. The concentration of Nd(III) in the organic phases after the extraction was found to be less than 0.5 g/L for both TiAP and TBP in all the extraction stages. The deviation in the mass balance of metal ions and HNO<sub>3</sub> for all the extraction stages is within 2%.

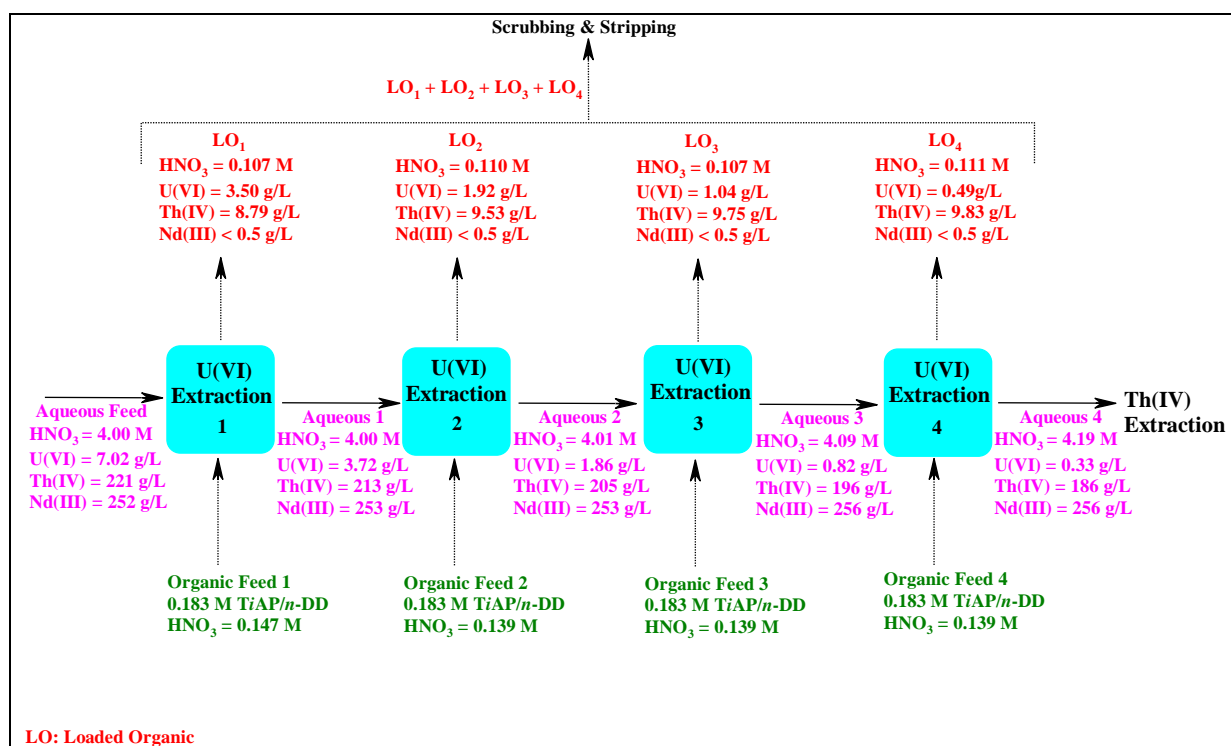


**Fig. 6.2:** Separation of U(VI) from Th(IV) and Nd(III) in 4 M HNO<sub>3</sub> by 0.183 M TiAP/n-DD in cross-current mode at 303 K.

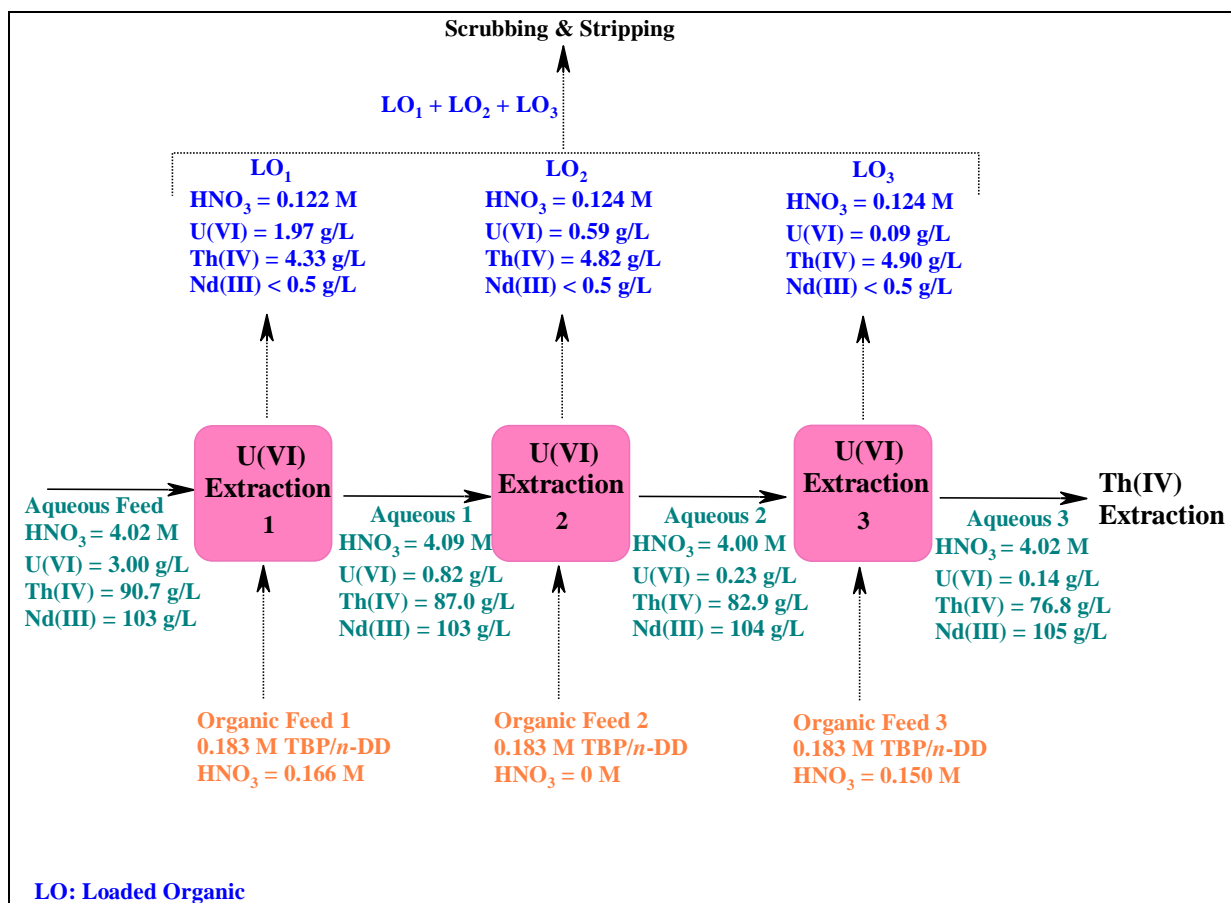


Fig. 6.3: Separation of U(VI) from Th(IV) and Nd(III) in 4 M  $HNO_3$  by 0.183 M TBP/n-DD in cross-current mode at 303 K.

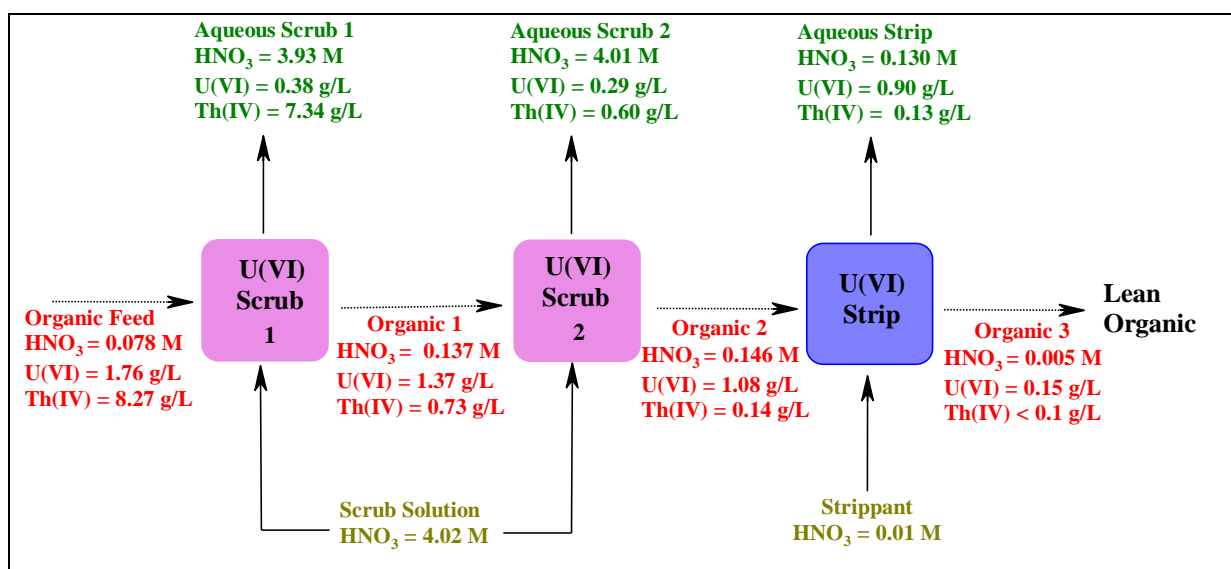
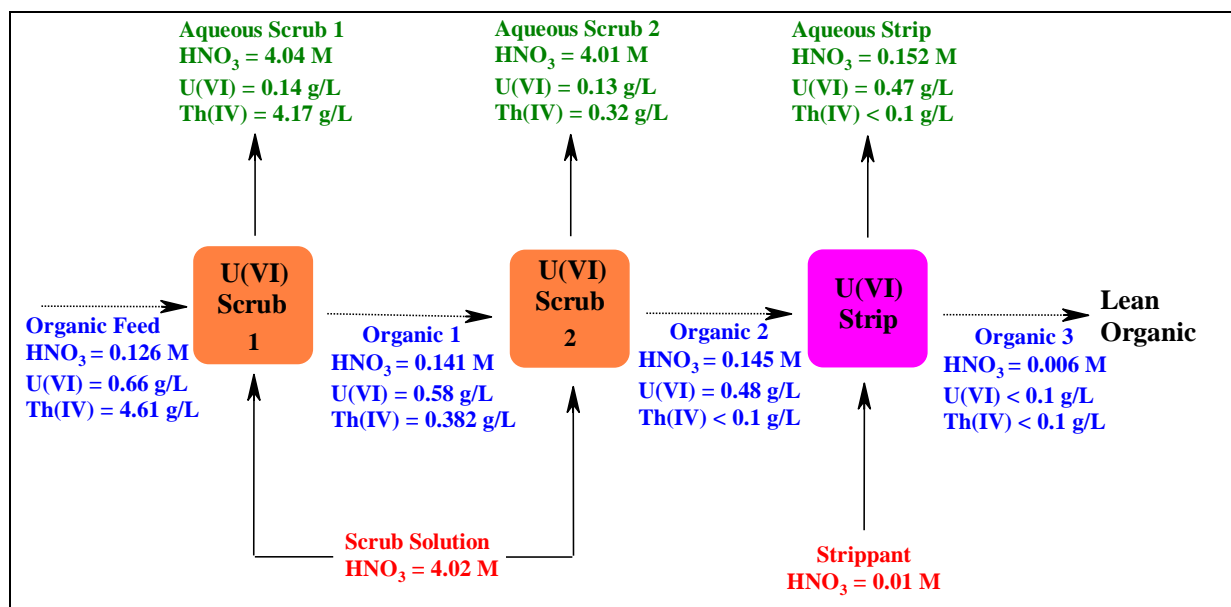


Fig. 6.4: Scrubbing and stripping of U(VI) from loaded 0.183 M TiAP/n-DD in cross-current mode at 303 K.

After the extraction the metal loaded 0.183 M TalP/*n*-DD was scrubbed twice with 4 M HNO<sub>3</sub> to remove the co-extracted Th(IV) from the organic phase and subsequently, stripping of U(VI) was carried out with 0.01 M HNO<sub>3</sub>. The concentration profile of metal loaded organic phases during their scrubbing and stripping for both TiAP and TBP systems are shown in Figs. 6.4 and 6.5, respectively. Stripping percentages of 86% and 79% were achieved by TiAP and TBP, respectively, in a single stage. The deviation in the mass balance of scrubbing and stripping experiments was below 2%.



**Fig. 6.5:** Scrubbing and stripping of U(VI) from loaded 0.183 M TBP/*n*-DD in cross-current mode at 303 K.

### 6.5 Third phase formation limits for the extraction of Th(IV) by 1.47 M TalP/*n*-DD

The aqueous feed solution obtained after the U(VI) extraction by 0.183 M TiAP/*n*-DD was equilibrated with 1.47 M TalP/*n*-DD to examine the third phase formation behaviour. It was observed that 1.47 M solutions of both TiAP and TBP in *n*-DD form TP at 303 K during Th(IV) extraction (The picture of third phase formed during the extraction are shown in Fig. 6.6). The concentration of Th(IV) and Nd(III) in organic and aqueous phases at the point of dissolution of the third phase for both the extractant systems are shown in Table 6.3. The

LOC and the CAC represent the metal ion concentrations in organic and aqueous phases, respectively, at the point of dissolution of the TP. Table 6.3 shows that the LOC and the CAC values for 1.47 M TiAP/*n*-DD are very much higher as compared to 1.47 M TBP/*n*-DD.

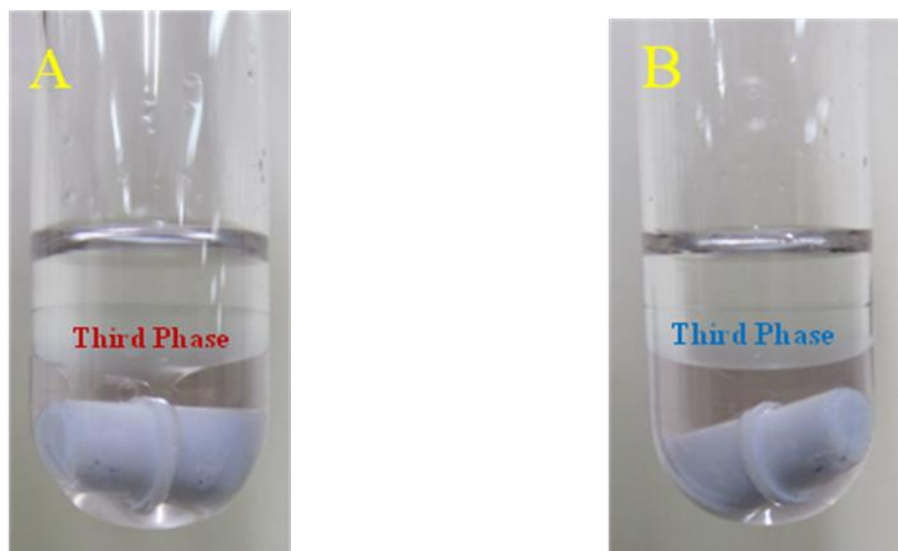


**Fig. 6.6:** Third phase formation in the extraction of Th(IV) from Th(IV)-Nd(III) feed solution in 4 M HNO<sub>3</sub> by 1.47 M TalP/*n*-DD (A) TBP system (B) TiAP system.

**Table 6.3:** Data on the concentration of metal ions in organic and aqueous phases at the point of dissolution of the third phase for their extraction from solution in 4 M HNO<sub>3</sub> by 1.47 M TalP/*n*-DD at 303 K.

TalP	[Th(IV)] (g/L)			[Nd(III)] (g/L)		
	[Th(IV)] <sub>org</sub>	[Th(IV)] <sub>aq</sub>	[Th(IV)] <sub>total</sub>	[Nd(III)] <sub>org</sub>	[Nd(III)] <sub>aq</sub>	[Nd(III)] <sub>total</sub>
TBP	44.5	12.7	57.2	< 0.5	75.0	75.0
TiAP	82.8	96.4	179.2	< 0.5	251.5	251.5

As the LOC and the CAC values of a solvent extraction system represent organic and aqueous metal ion concentration at equilibrium, the maximum concentration limit of feed solution that can be used for the extraction without third phase formation would be the sum of the LOC and the CAC with an organic to aqueous volume ratio of 1. Therefore, the maximum concentration of Th(IV) that can be used as the aqueous feed for Th(IV) extraction can be the sum of the concentrations of Th(IV) in organic and aqueous phases at the point of dissolution

of the TP. This value corresponds to around 179 g/L which is very close to the concentration of the Th(IV) present in the aqueous feed solution ( $[\text{Th(IV)}] = 186 \text{ g/L}$ ) obtained after U(VI) extraction by 0.183 M *TiAP/n-DD*. Therefore, slight dilution of feed solution is sufficient to avoid the splitting of organic phase during the extraction of Th(IV) by 1.47 M *TiAP/n-DD*. In contrast, Th(IV) concentration in the feed solution has to be diluted from 186 g/L to 57.2 g/L in the case of TBP which is enormous as compared to the dilution in the case of *TiAP*. These results indicate that concentrated feed solution cannot be used for Th(IV) extraction with 1.47 M TBP/*n-DD*. Subsequently, experiments were carried out with 1.47 M *TiAP/n-DD* after the slight dilution of the feed concentration with 4 M  $\text{HNO}_3$  to avoid third phase formation.

#### **6.6 Separation of Th(IV) from Nd(III) under high solvent loading conditions with 1.47 M *TiAP/n-DD***

The schematic representation of the separation of Th(IV) from Nd(III) in nitric acid media by 1.47 M *TiAP/n-DD* in cross-current mode with an organic to aqueous volume ratio of 1 at 303 K is shown in Fig. 6.7. It is observed in Fig. 6.7 that 169 g/L of Th(IV) in the aqueous feed has been reduced to less than 0.2 g/L in four extraction stages. Figure 6.7 also shows that in the first extraction stage when the concentration of Th(IV) in the loaded organic phase is 80.8 g/L, the concentration of Nd(III) is less than 0.5 g/L, and in the fourth extraction stage the concentrations of Th(IV) and Nd(III) in the loaded organic phase are 1.12 g/L and 8.49 g/L, respectively. This clearly reveals that when Th(IV) loading in the organic phase increases, it suppresses Nd(III) extraction. Consequently, the separation factor of Th(IV) with respect to rare earths can be improved as high solvent loading conditions can be achieved in the case of *TiAP*.

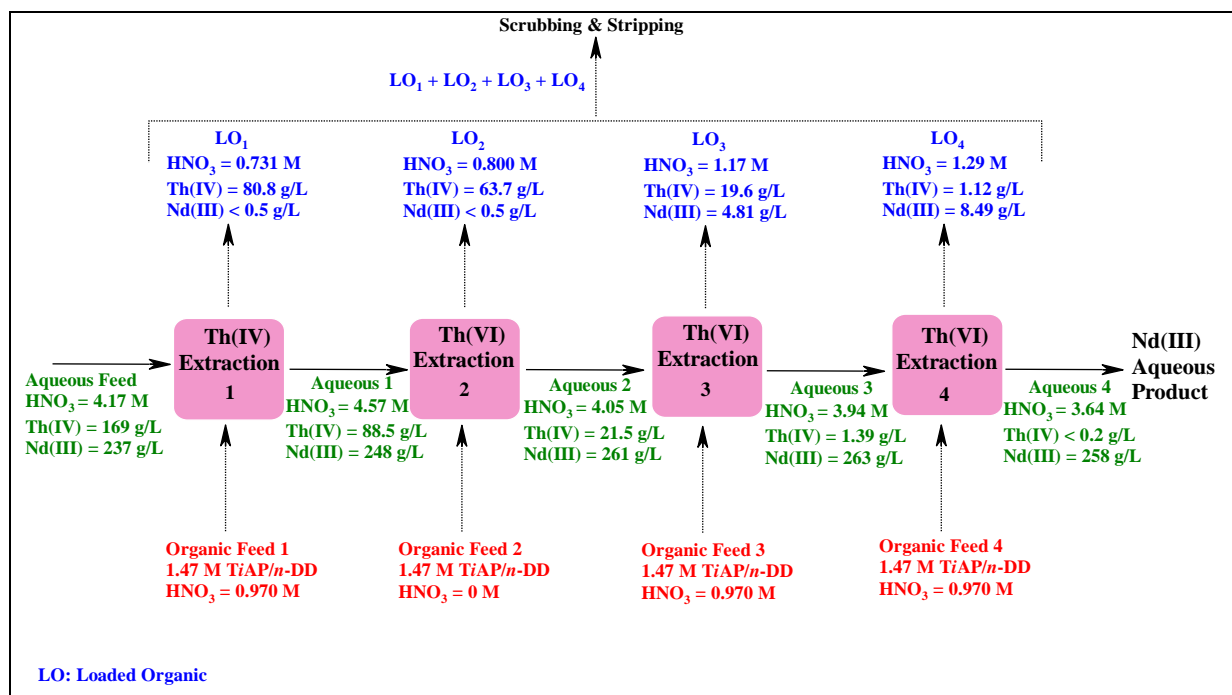


**Fig. 6.7:** Separation of Th(IV) from Nd(III) in 4 M HNO<sub>3</sub> by 1.47 M TiAP/n-DD in cross-current mode at 303 K.

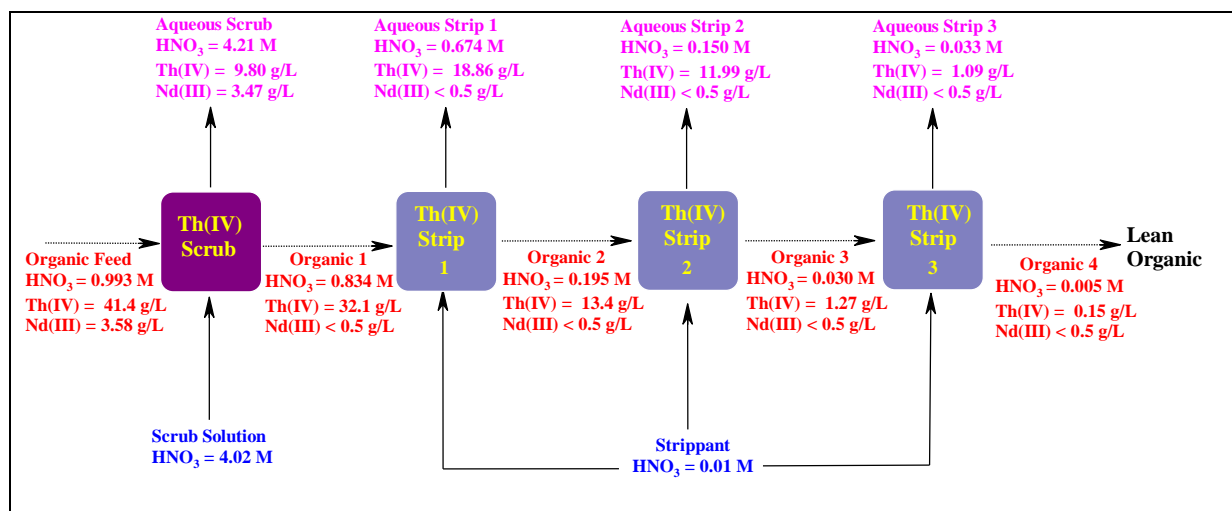


**Fig. 6.8:** Scrubbing and stripping of Th(IV) from loaded 1.47 M TiAP/n-DD in cross-current mode at 303 K.

It is also observed in Fig. 6.7 that there is a gradual increase in the concentration of Nd(III) in the aqueous feed during initial three extraction stages. This increase in Nd(III)

concentration can be illustrated based on the reduction in the volume of the aqueous solution after Th(IV) extraction. An aqueous feed solution of 15.9 mL used in the first extraction stage has become 15.2 mL after Th(IV) extraction which has led to an increase in Nd(III) concentration from 237 g/L to 248 g/L and such a decrease in the volume of aqueous solution was also observed in other extraction stages. However, the deviation in the mass balance of Th(IV), Nd(III) and HNO<sub>3</sub> before and after all the extraction stages is within 2%. The extraction percentage of Th(IV) by 1.47 M TiAP/*n*-DD was found to be 99.9%.

The schematic of the scrubbing and stripping of Th(IV) from loaded 1.47 M TiAP/*n*-DD is shown in Fig. 6.8. A small quantity of Nd(III) that is extracted into the organic phase was scrubbed completely in a single scrubbing stage with 4 M HNO<sub>3</sub>. Subsequently, Th(IV) free from Nd(III) was stripped from loaded organic phase in three stages with a stripping percentage of 99.5%. The difference in amount of metal ions and HNO<sub>3</sub> before and after scrubbing and stripping stages is below 2%.

### **6.7 Separation of Th(IV) from feed solution in 8 M HNO<sub>3</sub>**

The literature reports reveal that the separation factor for Th(IV) with respect to other metal ions and the extraction of Th(IV) by TBP are maximum at 8 M HNO<sub>3</sub> [211]. Earlier studies indicate that the extraction behaviour of TiAP and TBP are similar with respect to Th(IV) and lanthanides [155,172]. Therefore, higher separation factor and extraction efficiency of Th(IV) can be expected for its extraction from feed solution in 8 M HNO<sub>3</sub>. In order to confirm this, the separation of Th(IV) from Nd(III) was performed with feed solution in 8 M HNO<sub>3</sub>.

Initially a solution containing U(VI), Th(IV) and Nd(III) in 4 M HNO<sub>3</sub> was equilibrated with 0.183 M TiAP/*n*-DD for the separation of U(VI) from Th(IV) and Nd(III). The extraction of U(VI) was done from 4 M HNO<sub>3</sub> as the U(VI) separation factor with respect to other metal ions is maximum at this acidity. The loaded organic phase was

scrubbed with 4 M HNO<sub>3</sub> followed by stripping with 0.01 M HNO<sub>3</sub>. The flow sheet adopted for this run consists of 3, 2 and 1 stages for extraction, scrubbing and stripping, respectively, by cross-current mode and is similar to schemes shown in Figs. 6.2 and 6.4. The profiles for extraction, scrubbing and stripping are shown in Fig. 6.9. The percentage of U(VI) extraction works out to around 95%. The stripping percentage of U(VI) is around 89% and the difference in mass balance is less than 2%.

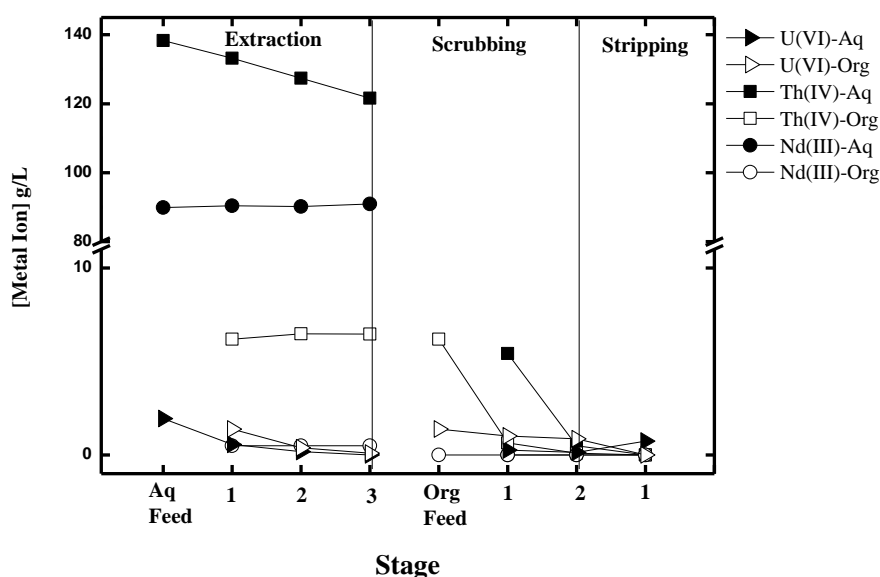


**Fig. 6.9:** Data on the concentration of U(VI), Th(IV) and Nd(III) in various stages of extraction, scrubbing and stripping for U(VI) separation from Th(IV) and Nd(III) by 0.183 M TiAP/*n*-DD in cross-current mode at 303 K.

The feed solution after U(VI) extraction was evaporated and adjusted with solutions of thorium nitrate, neodymium nitrate and nitric acid (12 M) to get a solution of desired metal ion concentrations close to 8 M HNO<sub>3</sub>. This solution was used as feed for Th(IV) extraction and the results of the Th(IV) extraction, scrubbing and stripping studies are shown in Fig. 6.10. The cross-current flow sheet for Th(IV) separation from Nd(III) consists of 4, 1 and 3 stages of extraction, scrubbing and stripping, respectively. The extraction of Th(IV) was achieved with 1.47 M TiAP/*n*-DD solution with an extraction percentage of 99.9% in four stages. It is observed that in the fourth Th(IV) extraction stage the amount of Nd(III)

extracted into the organic phase from feed solution is only 2.62 g/L which is much lesser as compared to 8.49 g/L observed in the case of separation from 4 M HNO<sub>3</sub> medium as shown in Fig. 6.7. This clearly demonstrates that the separation factor of Th(IV) can be improved if the feed acidity is maintained at 8 M HNO<sub>3</sub>. The scrubbing of organic phase was done with 8 M HNO<sub>3</sub> to remove the small amount of Nd(III) loaded in the organic phase. The stripping efficiency of Th(IV) was also found to be 99.3% which is similar to the one obtained with stripping of Th(IV) where its extraction was performed with feed solution in 4 M HNO<sub>3</sub>. The difference in mass balance of metal ions and HNO<sub>3</sub> in all the extraction, scrubbing and stripping stages was found to be less than 2%.

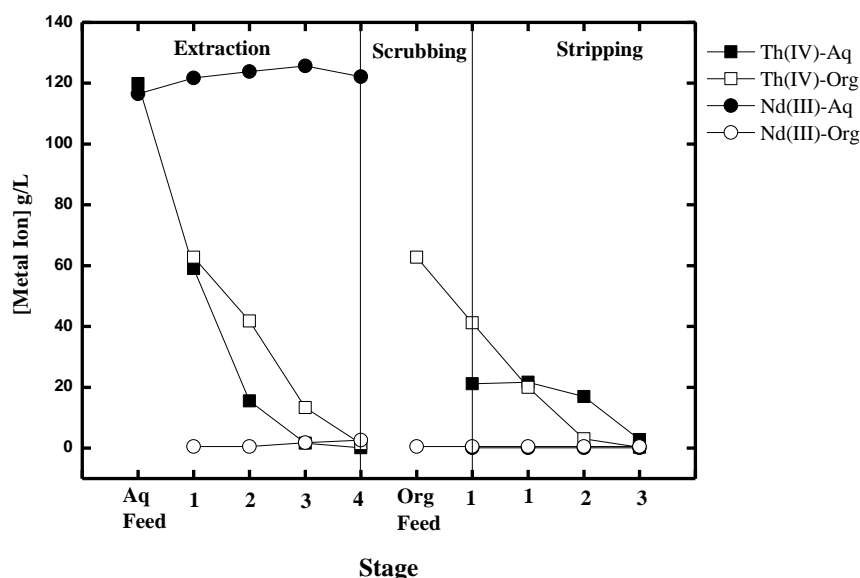


**Fig. 6.10:** Data on the concentration of Th(IV) and Nd(III) in various stages of extraction, scrubbing and stripping during the separation of Th(IV) from Nd(III) by 1.47 M TiAP/n-DD in cross-current mode at 303 K.

## 6.8 Conclusions

The consistency of analytical methods employed for the estimation of U(VI), Th(IV) and Nd(III) in the presence of each other has been authenticated within the concentration range used in the present study. The extraction, scrubbing and stripping behaviour of TBP and TiAP with respect to U(VI), Th(IV) and Nd(III) are similar. Unlike TBP, in the case of TiAP high solvent loading conditions can be achieved without organic phase splitting. The

separation factor for Th(IV) with respect to Nd(III) can be improved by using TiAP based solvents and it can also be enhanced by carrying out Th(IV) extraction from 8 M HNO<sub>3</sub> media. The present study provides an opportunity for the development of new process flow sheets for monazite ore processing using TiAP based solvents. Though the present study deals with the separation of U(VI) and Th(IV) from a single rare earth element Nd(III), it is expected to behave in a similar manner with a system consisting of a mixture of rare earth elements as in the case of monazite. Therefore, there is a scope for the development of alternate monazite ore processing flow sheets based on the present study.



# Chapter 7



**“Do research. Feed your talent. Research not only wins the war on cliché, it's the key to victory over fear and it's cousin, depression”**

*-Robert McKee*

# EXTRACTION AND THIRD PHASE FORMATION BEHAVIOUR OF *TiAP* AND TBP WITH Zr(IV) AND Hf(IV)

---

---

# 7

## 7.1 Introduction

Third phase formation in the extraction of Zr(IV) by TBP is a major drawback in TBP based Zr/Hf separation process. Therefore, *TiAP* can be an appropriate alternate to TBP for Zr/Hf separation since the third phase formation tendency of *TiAP* is lesser than TBP and their extraction behaviours are comparable with respect to these metal ions. Although the extraction and third phase formation behaviour of *TiAP* have been investigated with metal ions such as U(VI), Th(IV), Pu(IV) and Zr(IV) [115,116,172,173], studies with Hf(IV) are not reported. Consequently, the present study focuses on the comparison of the extraction and third phase formation tendency of *TiAP* and TBP with Zr(IV) and Hf(IV) in nitric acid media. Distribution ratios for the extraction of Zr(IV) and Hf(IV) by *TiAP* and TBP based solvents have been measured as a function of  $[\text{HNO}_3]_{\text{aq,eq}}$  to ascertain the analogous extraction behaviour of both the extractants. Also, the LOC and the CAC values for the extraction of Zr(IV) by both the solvents have been measured as a function of  $[\text{HNO}_3]_{\text{aq,eq}}$  to substantiate the lesser third phase tendency of *TiAP*.

SANS is a powerful technique used to probe colloidal particles. It can provide the information on both structure and interaction of the colloidal particles under native conditions. Moreover, the contrast between the particles (reverse micelles) and the solvent (solution of the extractant in the diluent) can be easily enhanced by deuterating either of them as the neutron scattering is very different for the isotopes of hydrogen (protium and deuterium). Therefore, SANS technique is considered to be an important technique to study the aggregation behaviour in solvent extraction systems. In fact, it has been mentioned in the literature that third phase formation in the extraction of tetravalent metal ions such as Th(IV)

and Zr(IV) is due to the aggregation of extracted species into reverse micelles [121,122]. Hence, third phase formation behaviour of 1.1 M solutions of *TiAP* and TBP in deuterated *n*-dodecane ( $C_{12}D_{26}$ ) has been investigated by using SANS technique for the extraction of Zr(IV) from  $Zr(NO_3)_4$  solutions in nitric acid media.

The concentrations of various components such as Zr(IV),  $HNO_3$ , water and extractant present in the organic phases have been determined to understand the phase splitting behaviour of *TiAP* and TBP based solvent systems as a function of  $[Zr(IV)]_{aq,eq}$  and diluent chain length. In view of the lesser third phase formation tendency of *TiAP*, the feasibility of using *TiAP* as an alternate extractant to TBP for the separation of Zr(IV) from Hf(IV) has been initiated in the present study. The third phase formation tendency of both *TiAP* and TBP based solvents have also been evaluated with the concentrated as well as dilute Zr(IV)-Hf(IV) feed solutions in nitric acid with the metal concentration ratio that is generally being used in process plants for the separation of Zr(IV) from Hf(IV).

## 7.2 Distribution ratios for the extraction of Zr(IV) and Hf(IV) as a function of nitric acid concentration

The variations of distribution ratios for the extraction of Zr(IV) and Hf(IV) ( $D_{Zr(IV)}$  and  $D_{Hf(IV)}$ , respectively) by 1.1 M solutions of *TiAP* and TBP in *n*-DD as a function of  $[HNO_3]_{aq,eq}$  at 303 K are shown in Fig. 7.1. It can be seen from Fig. 7.1 that the distribution ratios for the extraction of both the metal ions increase with an increase in  $[HNO_3]_{aq,eq}$ . The increase in  $D_{Zr(IV)}$  and  $D_{Hf(IV)}$  can be attributed to the increase in nitrate ion concentration with increase in nitric acid concentration. Literature reveals that trialkyl phosphates such as TBP extract Zr(IV) metal ion by forming disolvate complexes with  $Zr(NO_3)_4$  [187]. Therefore, the  $D_{Zr(IV)}$  is directly proportional to nitrate ion concentration and free extractant concentration as shown in Eq. (7.1), where  $K_{eq}$  is the equilibrium constant.

$$D_{\text{Zr(IV)}} = K_{\text{eq}} [\text{NO}_3^-]_{\text{(aq)}}^4 [\text{TaIP}]_{\text{(org)}}^2 \quad (7.1)$$

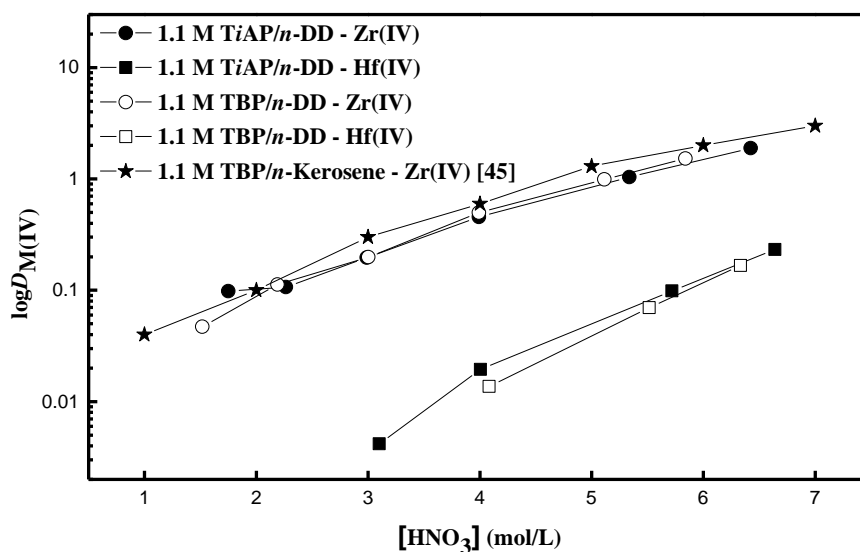


**Fig. 7.1:** Variation of distribution ratios for the extraction of Zr(IV) and Hf(IV) by 1.1 M TaIP/diluent as a function of  $[\text{HNO}_3]_{\text{aq,eq}}$  at 303 K.

It is also clear from Fig. 7.1 that  $D_{\text{Zr(IV)}}$  is always higher than  $D_{\text{Hf(IV)}}$  for both TiAP and TBP solvent systems for the entire  $[\text{HNO}_3]_{\text{aq,eq}}$  range investigated in this chapter. Also,  $D_{\text{Zr(IV)}}$  and  $D_{\text{Hf(IV)}}$  values of TiAP/n-DD are comparable with the corresponding values of TBP/n-DD system for all  $[\text{HNO}_3]_{\text{aq,eq}}$ . The  $D_{\text{Zr(IV)}}$  for the extraction of Zr(IV) from its solution in nitric acid media by 1.1 M TBP/Kerosene as a function of nitric acid concentration reported in the literature are also shown in Fig. 7.1, for comparison [56]. Figure 7.1 indicates that the  $D_{\text{Zr(IV)}}$  values for TBP solvent systems reported in the literature and the present study are comparable.

### 7.3 Third Phase formation limits for Zr(IV) as a function of extractant and nitric acid concentrations

As described earlier, the LOC and the CAC values correspond to the threshold concentration of metal ion in the organic and the aqueous phases, respectively, above which

the TP is formed. The LOC and the CAC values for the extraction of Zr(IV) from its solution in nitric acid media by solutions of TalP in *n*-DD as a function of  $[\text{HNO}_3]_{\text{aq,eq}}$  at 303 K are shown in Figs. 7.2 and 7.3, respectively. As expected, the LOC decreases linearly with  $[\text{HNO}_3]_{\text{aq,eq}}$  and it increases with increase in the extractant concentration. This can be explained on the basis of the limited solubility of TalP-Zr(NO<sub>3</sub>)<sub>4</sub> and TalP-HNO<sub>3</sub> complexes in the diluent (*n*-DD). An increase in the extractant concentration from 1.1 to 2.2 M decreases the amount of *n*-DD present in the binary solution of TalP/*n*-DD. As the concentration of *n*-DD decreases, the solubility of extracted complexes in the extractant-diluent solution increases and thereby LOC and CAC increase with increase in the extractant concentration. An increase in  $[\text{HNO}_3]_{\text{aq,eq}}$  favours the extraction of Zr(NO<sub>3</sub>)<sub>4</sub> into the organic phase by forming large amount of Zr(NO<sub>3</sub>)<sub>4</sub>.2TalP complex which has limited solubility in *n*-DD, thus resulting in a decrease in LOC and CAC.

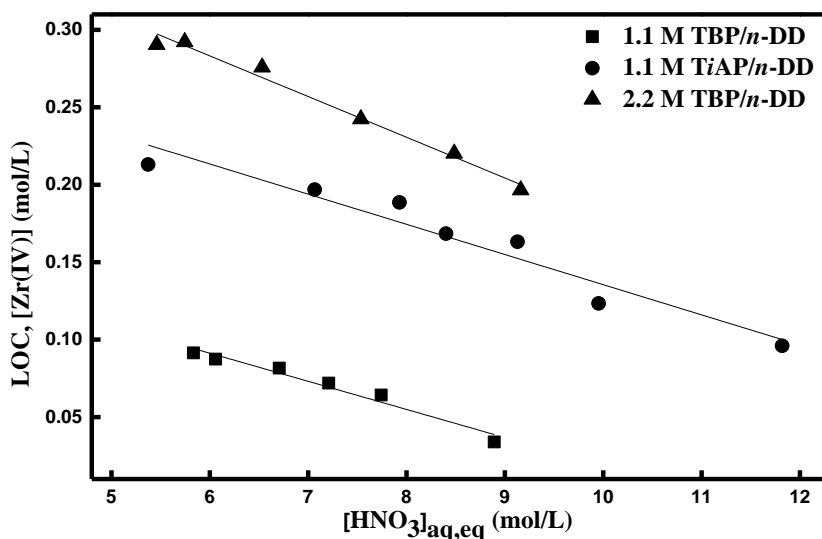


**Fig. 7.2:** Variation of LOC, in the extraction of Zr(IV) by solutions of TiAP and TBP in *n*-DD from Zr(NO<sub>3</sub>)<sub>4</sub> solutions in nitric acid media as a function of  $[\text{HNO}_3]_{\text{aq,eq}}$  at 303 K.

The results also indicate that under identical conditions, TiAP based solvent can load higher concentration of Zr(IV) without phase splitting as compared to TBP based solvent. For instance, 2.2 M TBP/*n*-DD forms the TP with 7.12 M HNO<sub>3</sub> at 303 K. However, 2.2 M TiAP/*n*-DD does not form third phase at this HNO<sub>3</sub> concentration and the maximum organic concentration is 0.521 mol/L of Zr(IV). The corresponding saturated [Zr(IV)]<sub>aq,eq</sub> is 0.736 mol/L. In general, the third phase formation limits are lower for TBP/*n*-DD - Zr(NO<sub>3</sub>)<sub>4</sub>/HNO<sub>3</sub> system as compared to TiAP/*n*-DD - Zr(NO<sub>3</sub>)<sub>4</sub>/HNO<sub>3</sub> system under identical conditions. The reason for higher third phase formation tendency of TBP based solvents is due to the higher attractive interaction among the organic phase species which has been explained based on SANS results in a later Chapter.

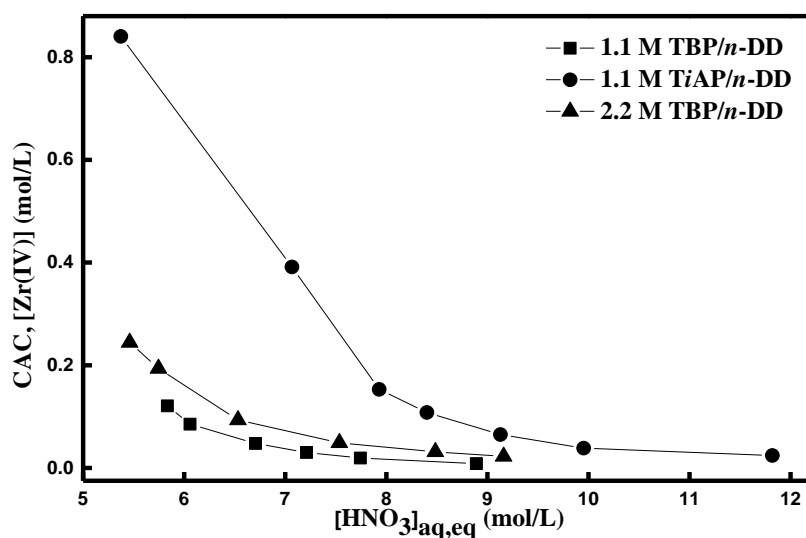


**Fig. 7.3:** Variation of CAC, in the extraction of Zr(IV) by solutions of TiAP and TBP in *n*-DD from Zr(NO<sub>3</sub>)<sub>4</sub> solutions in nitric acid media as a function of [HNO<sub>3</sub>]<sub>aq,eq</sub> at 303 K.

#### 7.4 Composition of organic phases before and after third phase formation with Zr(IV)

The nature of the constituents of the organic phase affects the limits of the organic phase splitting and hence the information about the composition of the organic phases after

Zr(IV) loading is essential to understand their influence on phase splitting behaviour of the TalPs. In this context, the concentrations of Zr(IV), HNO<sub>3</sub>, water and TalP present in the organic and the corresponding aqueous phases which are in equilibrium with each other have been estimated at a particular [Zr(IV)]<sub>aq,eq</sub> in biphasic as well as triphasic regions.

In order to compare the third phase formation behaviour of 1.1 M TiAP/*n*-DD and 1.1 M TBP/*n*-DD as a function of [Zr(IV)]<sub>aq,eq</sub>, the metal loaded organic phases have been prepared under three different conditions (with low, moderate and high Zr(IV) concentrations). At low Zr(IV) concentrations, both TiAP and TBP phases do not undergo phase splitting; at moderate Zr(IV) concentrations, only TBP system undergoes phase splitting and TiAP phase does not split; and at higher concentrations, both the organic phases undergo phase splitting. A plot of [Zr(IV)]<sub>org,eq</sub> vs [Zr(IV)]<sub>aq,eq</sub> shown in Fig. 7.4 depicts a schematic representation of various organic phase samples of TiAP and TBP based solvents prepared during third phase formation studies at 298 K. All S<sub>AD</sub> samples (“A” stands for TiAP and “D” stands for dodecane) represent TiAP-dodecane system and S<sub>BD</sub> samples (“B” stands for TBP) represent TBP-dodecane system. For example, S<sub>AD-1</sub> and S<sub>BD-1</sub> are TiAP and TBP samples which are in equilibrium with aqueous phase with similar Zr(IV) concentration in the biphasic regions of TiAP and TBP systems, respectively. Details about the other samples are shown in Fig. 7.4 and Table 7.1. The samples were chosen at various regions of equilibrated organic-aqueous phase fields in such a way that TiAP and TBP can be compared under the above mentioned conditions. The other parameters such as temperature, [HNO<sub>3</sub>]<sub>aq,eq</sub>, concentration of TalP and diluent-chain length which influence the extraction profile were kept constant.

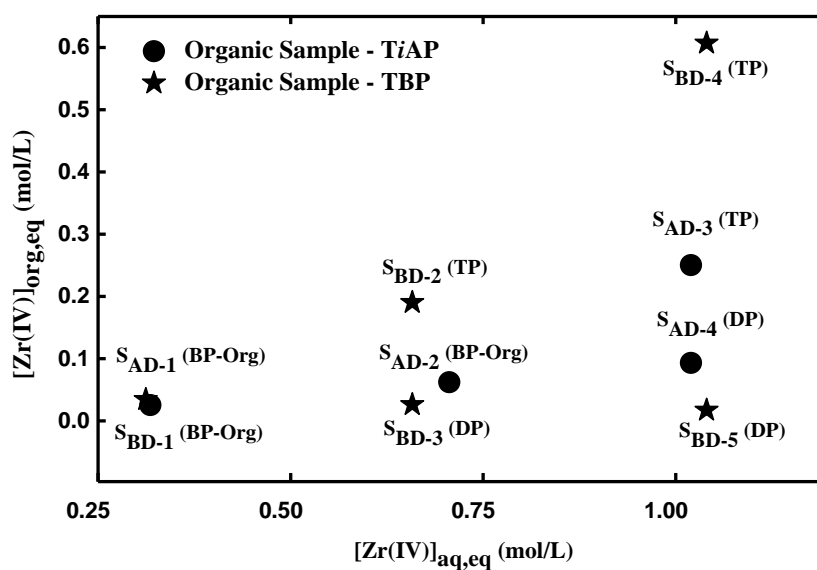


**Fig. 7.4:** Schematic representation of samples taken for the estimation of constituents of organic phases (biphasic organic, third and diluent-rich phases) in the extraction of Zr(IV) from its solution in nitric acid media (nominal acidity = 4 M HNO<sub>3</sub>) by 1.1 M solutions of TiAP and TBP in *n*-DD at 298 K.

Data shown in Table 7.1 indicate the accumulation of Zr(IV), HNO<sub>3</sub>, water and TalP in the TP leaving a major fraction of diluent in the DP. When [Zr(IV)]<sub>aq,eq</sub> increases the phase splitting tendency of the loaded organic phase also increases thereby accumulating more extractant in the TP with a negligible extractant concentration in the DP. It is established that Zr(IV) gets extracted into the organic phase as a co-ordination complex along with HNO<sub>3</sub> and water. After phase splitting, these polar solutes are always associated with the extractant. This leads to the accumulation of Zr(IV), HNO<sub>3</sub> and water in the TP rather than the DP. However, in the biphasic region, with increase in [Zr(IV)]<sub>aq,eq</sub> the extraction of Zr(IV) by organic phase increases and HNO<sub>3</sub> decreases. As Zr(IV) and HNO<sub>3</sub> form disolvate and monosolvate complexes with TalP [187,161], respectively, when Zr(NO<sub>3</sub>)<sub>4</sub> is transferred into a TalP based organic phase which is saturated with HNO<sub>3</sub>, one mole of TalP-Zr(IV) complex is formed at

the expense of dissociation of two moles of TalP-HNO<sub>3</sub> adduct. Hence, an increase in metal ion concentration in the organic phase leads to a decrease in HNO<sub>3</sub> concentration.

**Table 7.1: Equilibrium concentrations of Zr(IV), HNO<sub>3</sub>, TalP and H<sub>2</sub>O in organic (org) and aqueous (aq) phases in the extraction of Zr(IV) by 1.1 M TalP/*n*-DD from its solution in nitric acid media (nominal acidity = 4 M HNO<sub>3</sub>) as a function of [Zr(IV)]<sub>aq,eq</sub> at 298 K.**

Org Sample <sup>a</sup>	[Zr(IV)] (mol/L)		[HNO <sub>3</sub> ] (mol/L)		[TalP] <sub>org</sub> (mol/L)	[H <sub>2</sub> O] <sub>org</sub> (mol/L)
	Aq	Org	Aq	Org		
S <sub>AD-1</sub> (BP-Org)	0.318 ± 0.003	0.025 ± 0.001	4.27 ± 0.04	0.908 ± 0.009	1.10 ± 0.01	0.184 ± 0.009
S <sub>AD-2</sub> (BP-Org)	0.706 ± 0.007	0.062 ± 0.001	4.11 ± 0.04	0.898 ± 0.009	1.10 ± 0.01	0.128 ± 0.006
S <sub>AD-3</sub> (TP)	1.02 ± 0.01	0.250 ± 0.002	4.62 ± 0.05	1.25 ± 0.01	1.78 ± 0.02	0.24 ± 0.01
S <sub>AD-4</sub> (DP)	1.02 ± 0.01	0.093 ± 0.001	4.62 ± 0.05	0.586 ± 0.006	1.05 ± 0.01	0.045 ± 0.002
S <sub>BD-1</sub> (BP-Org)	0.312 ± 0.003	0.034 ± 0.001	4.24 ± 0.04	0.872 ± 0.009	1.10 ± 0.01	0.22 ± 0.01
S <sub>BD-2</sub> (TP)	0.658 ± 0.007	0.190 ± 0.002	4.14 ± 0.04	1.84 ± 0.02	2.77 ± 0.03	0.34 ± 0.02
S <sub>BD-3</sub> (DP)	0.658 ± 0.007	0.026 ± 0.001	4.14 ± 0.04	0.418 ± 0.004	0.574 ± 0.006	0.061 ± 0.003
S <sub>BD-4</sub> (TP)	1.04 ± 0.01	0.607 ± 0.006	4.61 ± 0.05	2.17 ± 0.02	3.20 ± 0.03	0.41 ± 0.02
S <sub>BD-5</sub> (DP)	1.04 ± 0.01	0.017 ± 0.001	4.61 ± 0.05	0.146 ± 0.001	0.187 ± 0.002	0.017 ± 0.001

<sup>a</sup> S<sub>AD-1</sub> (BP-Org) = TiAP/*n*-DD - Biphasic Organic Phase - Low Zr(IV);

S<sub>AD-2</sub> (BP-Org) = TiAP/*n*-DD - Biphasic Organic Phase - Moderate Zr(IV);

S<sub>AD-3</sub> (TP) = TiAP/*n*-DD - Third Phase - High Zr(IV);

S<sub>AD-4</sub> (DP) = TiAP/*n*-DD - Diluent-rich Phase - High Zr(IV);

S<sub>BD-1</sub> (BP-Org) = TBP/*n*-DD - Biphasic Organic Phase- Low Zr(IV);

S<sub>BD-2</sub> (TP) = TBP/*n*-DD - Third Phase - Moderate Zr(IV);

S<sub>BD-3</sub> (DP) = TBP/*n*-DD - Diluent-rich Phase - Moderate Zr(IV);

S<sub>BD-4</sub> (TP) = TBP/*n*-DD - Third Phase - High Zr(IV);

S<sub>BD-5</sub> (DP) = TBP/*n*-DD - Diluent-rich Phase - High Zr(IV)

Table 7.1 shows that the concentrations of Zr(IV), HNO<sub>3</sub>, TalP and water in the TP are higher for TBP system than TiAP system and in the DP their concentrations are lower for TBP system than TiAP system. This particular trend is observed due to the lesser solubility of TBP-solute complexes in *n*-DD as compared to TiAP-solute complexes. For TBP solvent

system, with increase in  $[Zr(IV)]_{aq,eq}$ , the concentration of TBP-solute complexes increases and when the concentration of these complexes exceeds the solubility limit they get accumulated in the TP leaving behind most of the *n*-DD in the DP. As compared to TBP-solute complexes, the *TiAP*-solute complexes are soluble in *n*-DD and therefore, even after organic phase splitting, considerable amount of *TiAP*-solute complexes are present in the DP and hence these complexes are accumulated in less quantity in the TP. Earlier studies in this laboratory have shown that the extraction of water by *TiAP* is lesser than TBP [155]. Table 7.1 illustrates a similar trend in the extraction of water by 1.1 M *TalP/n*-DD.

Studies on third phase formation using various techniques such as SANS, SAXS, DLS etc., reveal that the splitting of organic phase loaded with metal ions and acid is caused by the formation of reverse micelles due to the reorganization of extracted species and the associated interactions between them in the organic phase [121,122,129,139]. This kind of micellar reorganization of constituents of the organic phase stabilizes the polar species in a non-polar medium. However, when the attractive energy of the reverse micelles overcomes their thermal energy, most of the metal-extractant complexes separate out from diluent as third phase.

The higher third phase formation tendency of TBP as compared to *TiAP* can be explained based on this reverse micelle formation concept. A *TiAP* molecule additionally possesses three  $-CH_2-$  groups as compared to a TBP molecule. Accordingly, the size of the non-polar region of the reverse micelles formed by the aggregation of *TiAP*-metal complex is larger than TBP-metal complex. This increases the distance between the core of the reverse micelles and thereby reduces the effective attraction between the reverse micelles. As the attractive energy between the reverse micelles formed by *TiAP* is lower than TBP, the organic phase splitting tendency of *TiAP* is also lesser than TBP.

**Table 7.2: Equilibrium concentrations of Zr(IV), HNO<sub>3</sub>, TalP and H<sub>2</sub>O in organic (org) and aqueous (aq) phases in the extraction of Zr(IV) by 1.1 M TalP/*n*-TD from its solution in nitric acid media (nominal acidity = 4 M HNO<sub>3</sub>) as a function of [Zr(IV)]<sub>aq,eq</sub> at 298 K.**

Org Sample <sup>b</sup>	[Zr(IV)] (mol/L)		[HNO <sub>3</sub> ] (mol/L)		[TalP] <sub>org</sub> (mol/L)	[H <sub>2</sub> O] <sub>org</sub> (mol/L)
	Aq	Org	Aq	Org		
S <sub>AT</sub> (TP)	1.08 ± 0.01	0.341 ± 0.003	4.09 ± 0.04	1.61 ± 0.02	2.22 ± 0.02	0.28 ± 0.01
S <sub>AT</sub> (DP)	1.08 ± 0.01	0.057 ± 0.001	4.09 ± 0.04	0.352 ± 0.004	0.446 ± 0.004	0.038 ± 0.003
S <sub>BT</sub> (TP)	1.01 ± 0.01	0.785 ± 0.008	3.95 ± 0.04	2.23 ± 0.02	3.18 ± 0.03	0.49 ± 0.02
S <sub>BT</sub> (DP)	1.01 ± 0.01	0.008 ± 0.001	3.95 ± 0.04	0.135 ± 0.001	0.148 ± 0.001	0.007 ± 0.001

<sup>b</sup> S<sub>AT</sub> (TP) = TiAP/*n*-TD - Third Phase - High Zr(IV);

S<sub>AT</sub> (DP) = TiAP/*n*-TD - Diluent-rich Phase - High Zr(IV)

S<sub>BT</sub> (TP) = TBP/*n*-TD - Third Phase - High Zr(IV);

S<sub>BT</sub> (DP) = TBP/*n*-TD - Diluent-rich Phase - High Zr(IV);

In order to have a better understanding about the effect of diluent chain length on Zr(IV) third phase formation, the TP and the DP samples of 1.1 M solutions of TiAP and TBP in *n*-TD loaded with Zr(IV) at 1 M [Zr(IV)]<sub>aq,eq</sub> in nitric acid media were prepared at 298 K. S<sub>AT</sub> and S<sub>BT</sub> samples (“T” stands for tetradecane) represent TiAP-tetradecane and TBP-tetradecane systems, respectively. The data on the concentration of constituents of organic and aqueous phases for 1.1 M TalP/*n*-TD – Zr(NO<sub>3</sub>)<sub>4</sub>/HNO<sub>3</sub> systems are shown in Table 7.2. Comparison of the data shown in Tables 7.1 and 7.2 indicates that in general Zr(IV), HNO<sub>3</sub>, water and TalP concentrations are higher in the TP of 1.1 M TalP/*n*-TD system as compared to the TP of 1.1 M TalP/*n*-DD system. Similar results were observed for 1.1 M TalP/*n*-alkane - Th(NO<sub>3</sub>)<sub>4</sub>/HNO<sub>3</sub> systems as mentioned in the Chapter 4 and hence, it is confirmed that the third phase formation tendency of TalPs increase with increase in diluent chain length.

### 7.5 SANS studies on 1.1 M TiAP/*n*-DD - Zr(NO<sub>3</sub>)<sub>4</sub>/HNO<sub>3</sub> and 1.1 M TBP/*n*-DD - Zr(NO<sub>3</sub>)<sub>4</sub>/HNO<sub>3</sub> extraction systems

SANS studies have been performed with 1.1 M TiAP/*n*-C<sub>12</sub>D<sub>26</sub> – Zr(NO<sub>3</sub>)<sub>4</sub>/HNO<sub>3</sub> and 1.1 M TBP/*n*-C<sub>12</sub>D<sub>26</sub> – Zr(NO<sub>3</sub>)<sub>4</sub>/HNO<sub>3</sub> solvent extraction systems. Samples labeled with “A” represent TiAP system and samples labeled with “B” represent TBP system. For example, A1 and B1 are TiAP and TBP samples, respectively, which are in equilibrium with aqueous phase with similar Zr(IV) concentration in biphasic regions. Similarly, A2 and B2 represent third phase samples and A3 and B3 represent diluent-rich phase samples of TiAP and TBP in triphasic regions.

**Table 7.3: Equilibrium concentrations of Zr(IV) and HNO<sub>3</sub> in organic (org) and aqueous (aq) phases in the extraction of Zr(IV) by 1.1 M TalP/*n*-DD (Deuterated) from its solution in nitric acid media (nominal acidity = 4 M HNO<sub>3</sub>) as a function of [Zr(IV)]<sub>aq,eq</sub> at 298 K.**

Sample <sup>c</sup>	[Zr(IV)] (mol/L)		[HNO <sub>3</sub> ] (mol/L)	
	Aq	Org	aq	Org
A1 (BP-Org)	0.335 ± 0.003	0.044 ± 0.001	4.41 ± 0.04	0.846 ± 0.008
A2 (TP)	1.09 ± 0.01	0.324 ± 0.003	4.14 ± 0.04	1.14 ± 0.01
A3 (DP)	1.09 ± 0.01	0.132 ± 0.001	4.14 ± 0.04	0.560 ± 0.006
B1 (BP-Org)	0.324 ± 0.003	0.057 ± 0.001	4.34 ± 0.04	0.859 ± 0.009
B2 (TP)	1.05 ± 0.01	0.646 ± 0.006	4.06 ± 0.04	1.83 ± 0.02
B3 (DP)	1.05 ± 0.01	0.016 ± 0.001	4.06 ± 0.04	0.166 ± 0.002

<sup>c</sup> A1 (BP-Org) = TiAP - Biphasic Organic Phase - Low Zr(IV);

A2 (TP) = TiAP - Third Phase - High Zr(IV);

A3 (DP) = TiAP - Diluent-rich Phase - High Zr(IV);

B1 (BP-Org) = TBP - Biphasic Organic - Low Zr(IV);

B2 (TP) = TBP - Third Phase - High Zr(IV);

B3 (DP) = TBP - Diluent-rich Phase - High Zr(IV)

Concentrations of solutes (Zr(IV) and HNO<sub>3</sub>) in organic phases (biphasic organic phase, third phase and diluent-rich phase) for the extraction of Zr(IV) from its solutions in nitric acid media (4.06 – 4.41 M HNO<sub>3</sub>) by 1.1 M TBP/*n*-C<sub>12</sub>D<sub>26</sub> and 1.1 M TiAP/*n*-C<sub>12</sub>D<sub>26</sub>

solvents at 298 K are shown in Table 7.3. It is clear from Table 7.3 that for both the solvent systems, the concentrations of Zr(IV) and HNO<sub>3</sub> are higher in TP samples as compared to DP samples and the organic samples collected from biphasic regions. Also, it can be seen that concentration of Zr(IV) in B1 is higher than that of B3, whereas the concentration of Zr(IV) in A3 is higher than that of A1. Comparison of concentrations shown in Tables 7.1 and 7.3 indicates that the results obtained are comparable.

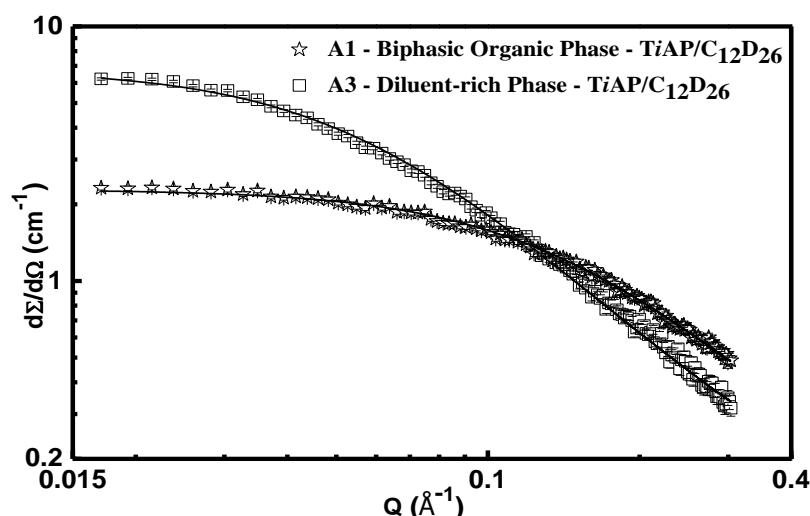


**Fig. 7.5:** SANS data obtained from the 1.1 M TiAP/*n*-C<sub>12</sub>D<sub>26</sub> - Zr(NO<sub>3</sub>)<sub>4</sub>/HNO<sub>3</sub> system.

The variation of differential scattering cross-section per unit volume ( $d\Sigma/d\Omega$ ) as a function of scattering vector ( $Q$ ) for the organic phase (biphasic region) and the diluent-rich phase (triphasic region) samples loaded with solutes for 1.1 M solutions of TiAP and TBP in *n*-C<sub>12</sub>D<sub>26</sub> are shown in Figs. 7.5 and 7.6, respectively. A comparison of above referred figures shows that the scattering intensity of the biphasic organic (BP-Org) sample of TBP is significantly higher than that of TiAP. A higher scattering intensity is expected for the aggregates that interact strongly [213]. This further confirms that under identical extraction conditions, TBP species aggregate into reverse micelles that interact strongly to form a third phase. Scattering data in Fig. 7.6 show that the neutron scattering intensity of the BP-Org sample of TBP (B1) is much higher than the diluent-rich phase sample of TBP (B3) for all

the Q values. However, Fig. 7.5 shows that the scattering intensity is marginally higher for the BP-Org sample of TiAP (A1) than the diluent-rich phase sample of TiAP (A3) in high Q values and a reversal in the scattering intensity is observed at low Q values. This observation indicates the possibility of either higher aggregation or interaction of species in the diluent-rich phase of TiAP. This is due to high concentration of Zr(IV) metal ion in the DP of TiAP as compared to organic phase of TiAP in the biphasic region. These data have been modeled using spherical reverse micelles for the calculation of P(Q) and S(Q), which give information about the size and the attractive interaction of the reverse micelles, respectively.

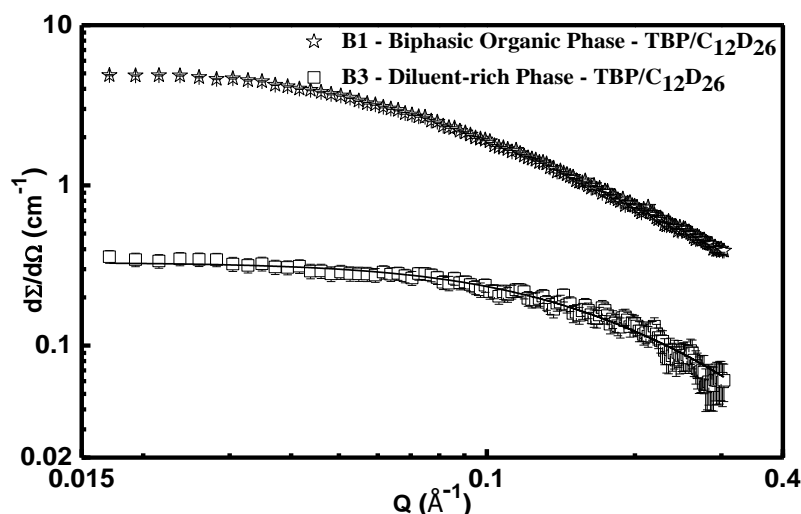


*Fig. 7.6: SANS data obtained from the 1.1 M TBP/n-C<sub>12</sub>D<sub>26</sub> - Zr(NO<sub>3</sub>)<sub>4</sub>/HNO<sub>3</sub> system.*

The variation of  $d\Sigma/d\Omega$  as a function of Q for the third phase samples of both TiAP and TBP were also measured and are depicted in Fig. 7.7. The SANS data of the third phase sample of TBP do not show any measurable Q dependent profile in the present Q range of measurements. This indicates the existence of larger aggregates in the third phase, especially in the case of TBP. However, comparison of Figs. 7.5 and 7.7 indicates that the SANS data of the third phase sample of TiAP shows quite similar features to that of the diluent-rich phase. In the case of TiAP, the concentration of  $[\text{Zr(IV)}]_{\text{aq,eq}}$  is only marginally higher than the CAC

(i.e. third phase formation limit) and hence a similar SANS data profile is observed for both the third phase and the diluent-rich phase samples of TiAP.

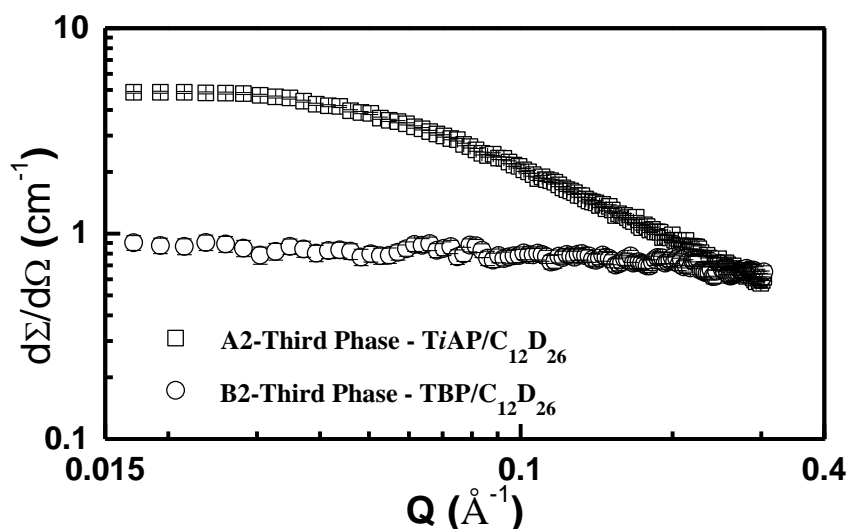


*Fig. 7.7: SANS data of the third phase sample of the 1.1 M TalP/n-C<sub>12</sub>D<sub>26</sub> - Zr(NO<sub>3</sub>)<sub>4</sub>/HNO<sub>3</sub> systems.*

The fitted parameters of SANS data using Eq. (2.6) are given in Table 7.4. The aggregation number of TiAP and TBP in the biphasic organic phase and the diluent-rich phase is 2. The volume fraction of TiAP in the organic phase is higher than TBP (for the same molar concentration used) in the organic phase because of the differences in their molecular weight. However, the volume fraction of B3 (diluent-rich phase of TBP) is drastically lesser than the corresponding TiAP sample (A3). The higher values of stickiness parameter and potential energy also support the stronger interaction among the aggregates of TBP species and higher third phase formation tendency of TBP. The overall results of SANS experiments reveal the presence of reverse micelles and lower stickiness (attractive interaction) between them which is responsible for lesser third phase formation tendency of TiAP based solvents as compared to TBP based solvents.

**Table 7.4: The fitted parameters of SANS data for the biphasic organic (BP-Org) and the diluent-rich phase (DP) samples of TiAP and TBP solvents.**

Sample <sup>d</sup>	Aggregate Diameter ( $\sigma$ ) Å	Aggregation Number (N)	Stickiness Parameter ( $1/\tau$ ) $k_B T$	Potential Energy ( $U_0$ ) $k_B T$	Volume Fraction of Aggregates ( $\phi$ )
A1 (BP-Org)	12.8	2	7.3	-1.16	0.35
A3 (DP)	12.8	2	9.3	-1.41	0.25
B1 (BP-Org)	12.0	2	9.7	-1.40	0.30
B3 (DP)	12.0	2	11.6	-1.58	0.035

<sup>d</sup>A1 (BP-Org) = TiAP - Biphasic Organic - Low Zr(IV);

A3 (DP) = TiAP - Diluent-rich Phase - High Zr(IV);

B1 (BP-Org) = TBP - Biphasic Organic - Low Zr(IV);

B3 (DP) = TBP - Diluent-rich Phase - High Zr(IV)

### 7.6 Third phase formation of TiAP and TBP systems with Zr(IV)-Hf(IV) solution

The third phase formation behaviour of TiAP and TBP for the extraction from an aqueous solution containing Zr(IV) and Hf(IV) have been compared. The feed solutions were prepared in such a way that the ratio of concentration of Zr(IV) to Hf(IV) is within the range of the ratio of concentration of Zr(IV) to Hf(IV) generally encountered in Zr(IV)-Hf(IV) feed solutions in the processing plants [98]. The concentrations of Zr(IV), Hf(IV) and HNO<sub>3</sub> in the concentrated (near-saturation) and dilute feed solutions which have been used to investigate third phase formation behaviour of 1.1 M solutions of TiAP and TBP in *n*-DD are shown in Table 7.5. Equal volumes of the organic phases and the feed solutions were equilibrated at 303 K and the phases were allowed to settle to identify any third phase formed after the metal ion extraction.

It has been observed that 1.1 M TBP/*n*-DD forms third phase with concentrated feed solution (near-saturation) and 1.1 M TiAP/*n*-DD does not form third phase with both concentrated and dilute feed solutions. Therefore, these results indicate that highly

concentrated feed solutions can be used for the separation of Zr(IV) and Hf(IV) using TiAP based solvents. In the case of TBP, the feed concentration has to be reduced to avoid third phase formation and hence the loading of Zr(IV) in the organic phase decreases. This favours the extraction of Hf(IV) into the organic phase due to higher free extractant concentration and reduces the  $\beta_{\text{Zr(IV)/Hf(IV)}}$ . In the case of TiAP based solvents, the extraction of Zr(IV) can attain higher loading which reduces the extraction of Hf(IV) and thereby improves the  $\beta_{\text{Zr(IV)/Hf(IV)}}$  as well as throughput.

**Table 7.5: Concentrations of Zr(IV), Hf(IV) and HNO<sub>3</sub> in concentrated and dilute feed solutions used for their extraction by 1.1 M TalP/n-DD at 303 K.**

Feed Solution	[Zr(IV)] (mol/L)	[Hf(IV)] (mol/L)	[HNO <sub>3</sub> ] (mol/L)
High Concentration	0.811 ± 0.008	0.012 ± 0.001	4.72 ± 0.05
Low Concentration	0.477 ± 0.005	0.007 ± 0.001	4.42 ± 0.04

## 7.7 Conclusions

The trends in the variations of  $D_{\text{Zr(IV)}}$  and  $D_{\text{Hf(IV)}}$  for their extraction by TiAP and TBP as a function of  $[\text{HNO}_3]_{\text{aq,eq}}$  are comparable under identical experimental conditions. The LOC and the CAC values for third phase formation in the extraction of Zr(IV) increase with an increase in the extractant concentration but decrease with HNO<sub>3</sub> concentration. The constituents of organic phase such as extractant, Zr(IV), HNO<sub>3</sub> and water are found to be concentrated in the third phase of TBP as compared to the third phase of TiAP. SANS studies confirm the higher aggregation in TBP solvent system as compared to TiAP system. The potential energy of attraction and stickiness parameter of the reverse micelles are higher for TBP based solvents as compared to TiAP system. Our studies confirm that the third phase formation occurs at much higher  $[\text{Zr(IV)}]_{\text{aq,eq}}$  in TiAP system as compared to TBP system,

which is a very favourable situation for the extraction of  $Zr(NO_3)_4$  and therefore flow sheets can be designed with TiAP based solvents for the extraction of  $Zr(NO_3)_4$  under high solvent loading conditions.



# Chapter 8



**“A discovery is said to be an accident meeting a prepared mind”**

*-Albert Szent-Gyorgyi*

## CONCLUSIONS

---

This chapter summarizes the results of the work explained in the thesis. The principal objective of this thesis is to explore the potential of TiAP based solvents for various solvent extraction processes in nuclear industry. The conclusions drawn based on several investigations that are centralized around this objective are elaborated in Chapter 8. This Chapter also provides a glimpse of potential research avenues opened up by the present study.

### **8.1 Extraction and stripping behaviour of TiAP and TBP with U(VI) in nitric acid media**

Determination of free acidity in U(VI) solutions is challenging as U(VI) undergoes hydrolysis and in this regard the method reported for the estimation of free acidity of U(VI) solutions by acid-base titration using oxalate-fluoride as dual complexing agent has been studied in detail over a wide ratio of U(VI):HNO<sub>3</sub>. The results showed that this method can be adopted for the determination of free acidity in U(VI) solutions over a range of U(VI):HNO<sub>3</sub> mole ratios from 1:1 to 100:1. Data on the extraction of U(VI) by 1.1 M TiAP/*n*-DD from U(VI) solutions in various concentrations of nitric acid reported in the thesis can be utilized for the development of flow sheets for the extraction of U(VI) by TiAP based solvents for spent nuclear fuel reprocessing. Extraction, scrubbing and stripping behaviour of both 1.1 M TiAP/*n*-DD as well as 1.1 M TBP/*n*-DD solvents loaded with U(VI) under high solvent loading conditions are comparable. The degradation of both the solvents loaded with U(VI) and HNO<sub>3</sub> are also comparable and it increases with increase in time.

### **8.2 Third phase formation behaviour of TiAP and TBP in the extraction of Th(NO<sub>3</sub>)<sub>4</sub>**

The comparable  $D_{\text{Th(IV)}}$  values for the macro-level extraction of Th(IV) by 1.1 M TiAP/*n*-alkane and 1.1 M TBP/*n*-alkane show the independency of extraction of Th(IV) with

respect to diluent chain length and extractant in trialkyl phosphate system. However, these parameters greatly influence the third phase formation behaviour during the extraction of Th(IV) in nitric acid media. Comparative studies on the organic phase splitting of 1.1 M TiAP/*n*-alkane and 1.1 M TBP/*n*-alkane as a function of parameters such as  $[\text{Th(IV)}]_{\text{aq,eq}}$ ,  $[\text{HNO}_3]_{\text{aq,eq}}$  and diluent chain length revealed the higher third phase formation tendency of TBP as compared to TiAP. The phase splitting tendency of both the solvents increases with increase in  $[\text{Th(IV)}]_{\text{aq,eq}}$ ,  $[\text{HNO}_3]_{\text{aq,eq}}$  and diluent chain length. This has been reflected as the preferential accumulation of solutes in the TP leaving behind the DP containing a major fraction of diluent with increase in these parameters. Moreover, the nature of the DP becomes close to diluent with increase in phase splitting tendency of the trialkyl phosphates. In general, trends in the variation of densities of organic phases in biphasic and triphasic regions parallel with the variation of Th(IV) concentrations in the corresponding organic phases. Therefore, the formation of TP in a solvent extraction system can be monitored by detecting the drastic variation in the density of organic phase.

### 8.3 Methods for the estimation of extractant concentration after organic phase splitting

Physical properties such as density and refractive index can be used for the determination of extractant concentration after organic phase splitting. These methods for the estimation of extractant have been validated by using conventional nitric acid equilibration method. The results on the determination of concentration of the extractant under various conditions confirm the accumulation of extractant in the TP leaving behind the DP with increase in  $[\text{Th(IV)}]_{\text{aq,eq}}$  and diluent chain length. The model developed to predict the extractant concentration in the organic phases after third phase formation is well-behaved for Th(IV) extraction from near-saturated aqueous solutions. However, this model deviates in predicting the extractant concentration at low Th(IV) concentrations, as the model requires

some correction for the free extractant available in the organic phase under such low concentrations.

#### **8.4 Separation of U(VI) and Th(IV) from Nd(III) by cross-current solvent extraction mode using TiAP**

The credibility of the analytical methods employed for the estimation of U(VI), Th(IV) and Nd(III) in the presence of each other has been confirmed by the analysis of these metal ions with known concentrations in the presence of other metal ions. Batch extraction studies have been conducted to examine the feasibility of using TiAP based solvents for the separation of U(VI) and Th(IV) from Nd(III) in nitric acid media. Studies showed that the extraction of U(VI) from concentrated monazite feed solution (near-saturation) can be achieved by using 0.183 M TiAP/*n*-DD without third phase formation. Even though 1.47 M TiAP/*n*-DD formed the TP in the extraction of Th(IV) from concentrated feed solution of Th(IV) and Nd(III) in nitric acid media, the CAC values obtained are very close to saturation limits and hence, slight dilution of feed solution is sufficient to avoid third phase formation with 1.47 M TiAP/*n*-DD. As the metal loading in the organic phase can attain theoretical loading without third phase formation, the separation factor for Th(IV) with respect to rare earths can be improved by using TiAP as the extractant by adopting flow sheets with high Th(IV) loading. The separation factor can also be improved by performing Th(IV) extraction with feed solution in 8 M HNO<sub>3</sub>. All these preliminary results show that TiAP can very well be an alternate extractant to TBP for monazite ore processing.

#### **8.5 Extraction and third phase formation behaviour of TiAP and TBP with Zr(IV) and Hf(IV)**

The  $D_{Zr(IV)}$  and the  $D_{Hf(IV)}$  values for the extraction of Zr(IV) and Hf(IV) by 1.1 M solutions of TiAP and TBP in *n*-DD measured as a function of  $[HNO_3]_{aq,eq}$  revealed the analogous extraction chemistry of both these extractants towards Zr(IV) and Hf(IV) metal

ions. The LOC and the CAC values for the extraction of Zr(IV) by *TiAP* and TBP based solvents investigated as a function of  $[\text{HNO}_3]_{\text{aq,eq}}$  revealed the lesser third phase formation tendency of *TiAP* towards Zr(IV) metal ion. Therefore, the feasibility of using *TiAP* as an alternate extractant to TBP for the separation of Zr(IV) from Hf(IV) was investigated with concentrated feed solution containing Zr(IV) and Hf(IV). These studies indicated that in contrast to TBP based solvents, highly concentrated feed solutions can be used in the case of *TiAP* based solvents. As a consequence, the Zr/Hf separation factor can be improved due to the reduction in the Hf(IV) extraction as free extractant available for complexation is less at the high loadings which can be achieved with *TiAP* based solvents.

In general, the constituents of organic phases such as solutes, water and *TalP* accumulate in the TP as compared to the DP. Also, the third phase formation tendency increases with increase in diluent chain length. The aggregation behaviour of *TiAP* and TBP in the extraction of Zr(IV) from its solution in nitric acid media by SANS confirmed the severity in organic phase splitting by TBP as compared to *TiAP*. The attractive energy and stickiness parameter between the reverse micelles are higher for TBP solvent as compared to *TiAP* solvent.

## 8.6 Future Perspectives

Although the investigations in this thesis favour the application of *TiAP* based solvents for monazite ore processing and Zr/Hf separation, further studies have to be performed prior to the large scale deployment of this extractant in process plants. Also, the results obtained in the present study have shown prospects for future work. Some of them are listed as follows.

In addition to uranium, thorium and rare earth metal ions, monazite feed solution also contain several elements such as magnesium, calcium, aluminium, lead, silicon and iron as well as phosphates. Similarly, the feed solutions used for Zr/Hf separation also possess these

constituents. As some of these constituents are extractable in minor quantities, it may affect the efficiency of the solvent extraction process. Apart from that, silicon interferes in the solvent extraction process by forming gelatinous precipitate. Therefore, it is essential to study the influence of these constituents on the extraction behaviour of *TiAP* based solvents. This objective can be accomplished by performing extraction and stripping studies with actual feed solutions that are used for the monazite ore processing and the Zr/Hf separation.

It might be convenient to carry out batch studies of various metal ions as a function of various parameters in cross-current mode. However, the actual process plants employ several litres of solutions for solvent extraction processes in counter-current mode. Hence, it is necessary to perform pilot plant studies with equipment in counter-current mode using the actual feed solutions employed in process plants.

The monazite ore concentrate solution and the Zr-Hf feed solution used for monazite processing and Zr/Hf separation, respectively, are prepared in nitric acid media which induce chemical degradation of *TiAP*. Besides, *TiAP* can also undergo radiation degradation. Consequently, these chemical and radiation degradation products of *TiAP* influence the extraction and third phase formation characteristics of *TiAP* based solvents. Hence, the effects of chemical and radiation degradation of *TiAP* based solvents on the extraction and third phase formation behaviour must be investigated under various conditions followed in process plants.

Physical properties of solvents such as interfacial tension, density, viscosity and phase disengagement time are essential to control the hydrodynamics of solvent extraction processes in large scale equipment like mixer-settlers, centrifugal extractors etc. Data on the variations of these properties under the extraction conditions followed in process plants are essential to develop flow sheet for solvent extraction processes with maximum efficiency. Therefore, the measurement of such properties of *TiAP* based solvent systems under process

conditions could be helpful for the development of solvent extraction flow sheets with these solvents.

Undiluted TBP finds applications in the extraction of vanadium, scandium, iron, etc and hence there is a scope for the investigation of *TiAP* based solvents for the extraction of above metal ions. It is well known that TBP (100%) is employed for the separation of Y(III) from Sr(II), where the pure  $^{90}\text{Sr}$  isolated from irradiated yttrium targets is used for the synthesis of bone palliative drugs. The efficiency of Y(III)/Sr(II) separation process can be fine tuned by diluting TBP with a diluent. As a binary solution of TBP in *n*-alkane has high tendency to form the TP with Y(III), the enhancement of selectivity by using TBP/*n*-alkane solutions is practically not feasible. Therefore, in view of lesser third phase formation tendency of *TiAP*, it can be investigated for Y(III)/Sr(II) separation processes.

Models that correlate the extraction of metal ions with structure of an extractant are necessary to comprehend the extraction mechanism. Such models allow predicting the extractability and third phase formation tendency of new extractants with respect to a particular metal ion of interest. Thereby proper choice of extractant and operation conditions can be made that ensure flawless function of process plants. It will be instructive to study the extraction and third phase formation behaviour with trialkyl phosphates of differing carbon chain length, with branched carbon chains, asymmetry in carbon chains etc., to evolve such predictive models. For example, it is of interest to know whether the third phase formation tendency is mainly dependent on the total number of carbon atoms in the molecule, by comparing the behaviour of *TiAP* with an extractant such as a trialkyl phosphate containing 2 butyl and one heptyl group in place of three amyl groups.

Mitigation of third phase formation becomes complicated unless there is an understanding about this phenomenon at the molecular level. In general, techniques like SANS, SAXS, DLS etc., are used as tools to probe the aggregation in solvent systems to

understand the mechanism of this phenomenon. SANS and SAXS techniques provide information on energy of interaction, stickiness parameter, size and shape of the particles in the organic solutions. NMR and EXAFS techniques provide information on the chemical environment around the molecules. Infra red spectroscopy gives details regarding the bonding in these molecules. Extraction and third phase formation investigations in the present study showed lesser third phase formation behaviour of TiAP based solvents towards Th(IV) and Zr(IV) metal ions. Metal loaded TiAP based solvents prepared under various conditions can be investigated with aforementioned instrumental techniques to understand the reason behind the lesser third phase tendency of TiAP.

Even though the TP is mostly observed in the extraction of tetravalent metal ions by TBP, it is possible to induce the TP in the extraction of hexavalent and trivalent metal ions such as U(VI) and Y(III), respectively by adjusting the extraction conditions. Therefore, investigations on the organic phase splitting can be extended to various metal ions as third phase formation is a universal phenomenon. Several aspects of third phase formation are yet to be understood well. For instance, the reason for unusual increase in the LOC of Pu(IV) after attaining a minimum value for the extraction of Pu(IV) by 1.1 M TBP/*n*-alkane as a function of nitric acid concentration is yet to be unequivocally established. Similarly, it has been reported that the change in the LOC of a metal ion for a small change in temperature is enormous as compared to the change in other parameters like diluent chain length, nitric acid concentration etc. These aspects need further study and scattering based techniques can be of much value in such investigations.

Theoretical studies based on density functional theory have been reported for various solvent extraction systems to understand the extraction mechanism. One of the assumptions in these kinds of modelling studies is that the metal-extractant complexes are in isolated gas phase. However, in the actual scenario with respect to solvent extraction, these metal-

extractant complexes are not in isolation and they are present in a matrix of diluent and can also undergo inter-molecular interactions. Therefore, new approaches have to be used to consider the inter-molecular interactions in solution phase. The modelling approaches which take into account of inter-molecular interactions will be able to provide the actual structure of metal species present in the organic phase and can also explain third phase formation phenomenon theoretically.

## REFERENCES

---

1. R.B. Grover; S. Chandra; Scenario for growth of electricity in India. *Energy Policy* 34, (2006) 2834-2847.
2. P. Garg; Energy scenario and vision 2020 in India. *J. Sustainable Energy Environ.* 3, (2012) 7-17.
3. J.P. Dorian; H.T. Franssen; D.R. Simbeck; MD; Global challenges in energy. *Energy Policy* 34, (2006) 1984-1991.
4. K. Singh; India's emissions in a climate constrained world. *Energy Policy* 39, (2011) 3476-3482.
5. M. Eisenbud; H.G. Petrow; Radioactivity in the atmospheric effluents of power plants that use fossil fuels. *Science* 144 (3616), (1964) 288-289.
6. R.B. Grover; Green growth and role of nuclear power: A perspective from India. *Energy Strategy Rev.* 1, (2013) 255-260.
7. A. Ramachandran; J. Gururaja; Perspectives on energy in India. *Annu. Rev. Energy* 2, (1977) 365-386.
8. S. Shafiee; E. Topal; When will fossil fuel reserves be diminished? *Energy Policy* 37, (2009) 181-189.
9. N. Armaroli; V. Balzani; The Future of energy supply: Challenges and opportunities. *Angew. Chem. Int. Ed.* 46, (2007) 52-66.
10. J. Parikh; K. Parikh; India's energy needs and low carbon options. *Energy* 36, (2011) 3650-3658.
11. A.D. Sahin; Progress and recent trends in wind energy. *Prog. Energy Combust. Sci.* 30, (2004)

- 501-543.
12. R. Ramanna; Inevitability of nuclear energy. *Curr. Sci.* 73 (4), (1997) 319-325.
  13. B. Zwaan; The role of nuclear power in mitigating emissions from electricity generation. *Energy Strategy Rev.* 1, (2013) 296-301.
  14. A. Adamantiades; I. Kessides; Nuclear power for sustainable development: Current status and future prospects. *Energy Policy* 37, (2009) 5149-5166.
  15. C. Karakosta; C. Pappas; V. Marinakis; J. Psarras; Renewable energy and nuclear power towards sustainable development: Characteristics and prospects. *Renewable and Sustainable Energy Rev.* 22, (2013) 187-197.
  16. Status of minor actinide fuel development. International Atomic Energy Agency (IAEA) Nuclear energy series No. NF-T-4.6, IAEA, Vienna, Austria, 2009.
  17. M. Salvatores; Nuclear fuel cycle strategies including partitioning and transmutation. *Nucl. Eng. Des.* 235, (2005) 805-816.
  18. J.N. Mathur; M.S. Murali; K.L. Nash; Actinide partitioning - A review. 19 (3), (2001) 357-390.
  19. Z. Kolarik; Complexation and separation of lanthanides(III) and actinides(III) by heterocyclic N-donors in solutions. *Chem. Rev.* 108, (2008) 4208-4252.
  20. I.W. Donald; B.L. Metcalfe; R.N.J. Taylor; The immobilization of high level radioactive wastes using ceramics and glasses. *J. Mater. Sci.* 32, (1997) 5851-5887.
  21. K. Raj; K.K. Prasad; N.K Bansal; Radioactive waste management practices in India. *Nucl. Eng. Des.* 236, (2006) 914-930.
  22. M.M. Curtis; India's worsening uranium shortage. Pacific Northwest National Laboratory Report, PNNL-16348, Jan. 2007.
  23. S. Fareeduddin; Status report from India; In *Panel proceedings series*, Processing of low-grade

- uranium ores, IAEA, Vienna, Austria, 1967, 27-31.
24. A. Gopalakrishnan; Evolution of the Indian nuclear power program. *Annu. Rev. Energy Environ.* 27, (2002) 369-95.
  25. R. Chidambaram; C. Ganguly; Plutonium and thorium in the Indian nuclear programme. *Curr. Sci.* 70 (1), (1996) 21-35.
  26. S.C. Chetal; P. Chellapandi; P. Puthiyavinayagam; S. Raghupathy; V. Balasubramaniyan; P. Selvaraj; P. Mohanakrishnan; B. Raj; Current status of fast reactors and future plans in India. *Energy Procedia* 7, (2011) 64-73.
  27. B. Raj; H.S. Kamath; R. Natarajan; P.R. Vasudeva Rao; A perspective on fast reactor fuel cycle in India. *Prog. Nucl. Energy* 47 (1-4), (2005) 369-379.
  28. H.S. Kamath; Recycle fuel fabrication for closed fuel cycle in India. *Energy Procedia* 7, (2011) 110-119.
  29. Country nuclear fuel cycle profiles; Technical reports series no. 425, Second Edn., IAEA, Vienna, Austria, 2005.
  30. Status and developments in the back end of the fast reactor fuel cycle. IAEA Nuclear energy series No. NF-T-4.2, IAEA, Vienna, Austria, 2011.
  31. P. Maestro; D. Huguenin; Industrial applications of rare earths: Which way for the end of the century? *J. Alloys Compd.* 225, (1995) 520-528.
  32. M.P. Lowe; MRI contrast agents: The next generation. *Aust. J. Chem.* 55, (2002) 551-556.
  33. V.W. Yam; K.K. Lo; Recent advances in utilization of transition metal complexes and lanthanides as diagnostic tools. *Coord. Chem. Rev.* 184, (1998) 157-240.
  34. R. Sessoli; A.K. Powell; Strategies towards single molecule magnets based on lanthanide ions. *Coord. Chem. Rev.* 253, (2009) 2328-2341.

35. S. Cotton; Lanthanide and actinide chemistry, John Wiley and Sons Ltd., West Sussex, England, 2006.
36. I.G. Tananaev; M.V. Nikonov; B.F. Myasoedov; D.L. Clark; Plutonium in higher oxidation states in alkaline media. *J. Alloys Compd.* 444-445, (2007) 668-672.
37. L.I. Katzin; D.C. Sonnenberger; Thorium; In *The chemistry of the actinide elements*, Vol. 1, Second Edn., J.J. Katz; G.T. Seaborg; L.R. Morss (Eds.); Chapman and Hall Ltd., London, Great Britain, 1986, 41-101.
38. I. Kimura; Review of cooperative research on thorium fuel cycle as a promising energy source in the next century. *Prog. Nucl. Energy* 29, (1995) 445-452.
39. S. David; E. Huffer; H. Nifenecker; Revisiting the thorium-uranium nuclear fuel cycle. *europhysicsnews* 38 (2), 24-27, (DOI: 10.1051/EPN:2007007).
40. T.K. Basu; M. Srinivasan; Thorium fuel cycle development activities in India. Bhabha Atomic Research Centre (BARC) report, BARC-1532, Dec. 1990.
41. M. Lung; O. Gremm; Perspectives of the thorium fuel cycle. *Nucl. Eng. Des.* 180, (1988) 133-146.
42. K. Anantharaman; V. Shivakumar; D. Saha; Utilisation of thorium in reactors. *J. Nucl. Mater.* 383, (2008) 119-121.
43. Thorium fuel cycle - Potential benefits and challenges. IAEA-TECDOC-1450, IAEA, Vienna, Austria, 2005.
44. Y. Jiyang; W. Kan; Y.S.J. Baoshan; S. Shifei; S. Gong; Thorium fuel cycle of a thorium-based advanced nuclear energy system. *Prog. Nucl. Energy* 45 (1), (2004) 71-84.
45. I. Ursu; Physics and technology of nuclear materials. First Edn., Pergamon press, Oxford, England, 1985.

46. F. Weigel; Uranium; In *The chemistry of the actinide elements*, Vol. 1, Second Edn., J.J. Katz; G.T. Seaborg; L.R. Morss (Eds.); Chapman and Hall Ltd, London, Great Britain, 1986, 169-442.
47. G.R. Choppin; Solution chemistry of the actinides. *Radiochim. Acta* 32, (1983) 43-53.
48. J.A. Fahey; Plutonium; In *The chemistry of the actinide elements*, Vol. 1, Second Edn., J.J. Katz; G.T. Seaborg; L.R. Morss (Eds.); Chapman and Hall Ltd, London, Great Britain, 1986, 499-886.
49. Safe handling and storage of plutonium. Safety reports series No. 9, IAEA, Vienna, Austria, 1998.
50. J.M. Cleveland; The chemistry of plutonium, American nuclear society, Gordon and Breach Science Publishers, New York, USA, 1969.
51. G.R. Choppin; K.L. Nash; Actinide separation science. *Radiochim. Acta* 70-71, (1995) 225-236.
52. R. Knopp; V. Neck, J.I. Kim; Solubility, hydrolysis and colloid formation of plutonium(IV). *Radiochim. Acta* 86, (1999) 101-108.
53. A.K. Mukherji; Analytical chemistry of zirconium and hafnium, First Edn., Pergamon Press Ltd., London, England, 1970.
54. P.L. Brown; E. Curti; B. Grambow; C. Ekberg; Chemical thermodynamics of zirconium, Vol. 8, Elsevier, Amsterdam, Netherland, 2005.
55. C.F. Baes; R.E. Mesmer; The hydrolysis of cations, John Wiley and Sons, New York, USA, 1976.
56. J.C. Mailen; D.E. Horner; S.E. Dorris; N. Pih; S.M. Robinson; R.G. Yates; Solvent extraction chemistry and kinetics of zirconium. *Sep. Sci. Technol.* 15 (4), (1980) 959-973.

57. H.Y. Aboul-Enein; R. Stefan; G. Baiulescu; Quality and reliability in analytical chemistry, CRC press, Florida, USA, 2000.
58. R. Pribil; Contributions to the basic problems of complexometry - I: The blocking of indicators and its elimination. *Talanta* 3, (1959) 91-94.
59. P. Kumar; P.G. Jaison; V.M. Telmore; S. Paul; S.K. Aggarwal; Determination of lanthanides, thorium, uranium and plutonium in irradiated (Th,Pu)O<sub>2</sub> by liquid chromatography using  $\alpha$ -Hydroxyisobutyric acid ( $\alpha$ -HIBA). *Int. J. Anal. Mass Spectrom. Chromatogr.* 1, (2013) 72-80.
60. R. Pribil; Present state of complexometry - I: Determination of quadrivalent and trivalent metals. *Talanta* 12, (1965) 925-939.
61. S.B. Savvin; Analytical use of Arsenazo - III: Determination of thorium, zirconium, uranium and rare earth elements. *Talanta* 8, (1961) 673-685.
62. W.D. Shults; Applications of controlled-potential coulometry to the determination of plutonium. *Talanta* 10, (1963) 833-849.
63. W. Davies; W. Gray; A rapid and specific titrimetric method for the precise determination of uranium using iron(II) sulphate as reductant. *Talanta* 11, (1964) 1203-1211.
64. E. Celon; S. Degetto; G. Marangoni; L. Baracco; Rapid determination of milligram amounts of uranium in organic complexes with pyridine-2,6-dicarboxylic acid as titrant and arsenazo-I as indicator after oxygen-flask combustion. *Talanta* 26, (1979), 160-162.
65. D.I. Ryabchikov; E.K. Gol'braikh; Translated by A.D. Norris; Translation edited by R Belcher; L. Gordon; Analytical chemistry of thorium, Pergamon Press, London, England, 1963.
66. Z. Karpas; Analytical chemistry of uranium - Environmental, forensic, nuclear and toxicological applications, CRC press, Florida, USA, 2014.
67. T.G. Srinivasan; P.R. Vasudeva Rao; Free acidity measurement - A review. *Talanta* 118,

- (2014) 162-171.
68. J.L. Ryan; G.H. Bryan; M.C. Burt; D.A. Costanzo; Preparation of acid standards for and determination of free acid in concentrated plutonium-uranium solutions. *Anal. Chem.* 57, (1985) 1423-1427.
69. P. Pakalns; Potentiometric titration of free acid in salt solutions after addition of potassium oxalate as a complexing agent. *Anal. Chim. Acta* 127, (1981) 263-269.
70. R.A. Schneider; M.J. Rasmussen. HW-53368, 1959.
71. M.K. Ahmed; D.S. Suryanarayana; K.N. Sabharwal; N.L. Sreenivasan; Potentiometric determination of free acidity in uranium(VI) and plutonium(IV) solutions and a sequential determination of uranium. *Anal. Chem.* 57 (12), (1985) 2358-2360.
72. N.C. Li; A. Lindenbaum; J.M. White; Some metal complexes of citric and tricarballic acids. *J. Inorg. Nucl. Chem.* 12 (1-2), (1959) 122-128.
73. R.P. Graham; Determination of acid in the presence of aluminium. *Ind. Eng. Chem.* 18 (8), (1946) 472-474.
74. J. Rydberg; G.R. Choppin; C. Musikas; T. Sekine; Solvent extraction equilibria; In *Principles and practices of solvent extraction*, J. Rydberg; M. Cox; C. Musikas; G.R. Choppin (Eds.); Marcel Dekker, Inc., New York, USA, 1992, 413-447.
75. D.A. Orth; R.M. Wallance; D.G. Karraker; Solvent extraction reactions and mechanisms. In *Science and technology of tributyl phosphate (Synthesis, properties, reactions and analysis)*, Vol. 1, W.W. Schulz; J.D. Navratil; A.E. Talbot (Eds.); CRC Press, Inc., Florida, USA, 1984, 161-219.
76. H.A.C. McKay; J.H. Miles; J.L. Swanson; The purex process; In *Science and technology of tributyl phosphate*, Vol. 3, W.W. Schulz; L.L. Burger; J.D. Navratil; K.P. Bender (Eds.); CRC

- Press, Florida, USA, 1990, 1-9.
77. M. Cox; J. Rydberg; Introduction to solvent extraction; In *Principles and practices of solvent extraction*, J. Rydberg; M. Cox; C. Musikas; G.R. Choppin (Eds.); Marcel Dekker, Inc., New York, USA, 1992, 1-25.
  78. H.A.C. McKay; Introduction; In *Science and technology of tributyl phosphate*, Vol. 1, W.W. Schulz; J.D. Navratil (Eds.); CRC Press, Florida, USA, 1984, 1-14.
  79. Grinbaum; Integrated methods for extraction processes; In *Ion exchange and solvent extraction*; Vol. 15, Chap. 7, Y. Marcus; A.K. Sengupta (Eds.); CRC Press, Florida, USA, 2001, 13.
  80. G.F. Vandegrift; Diluents for TBP extraction systems; In *Science and technology of tributyl phosphate*, W.W. Schulz; J.D. Navratil; Eds., Vol. 1, CRC Press, Florida, USA, 1984, 69-136.
  81. C.K. Gupta; Hydrometallurgy. In: *Chemical metallurgy - Principles and practice*, Wiley-VCH Verlag GmbH and Co. KGaA, Weinheim, Germany, 2003, 459.
  82. M. Cox; Solvent extraction in hydrometallurgy; In *Principles and practices of solvent extraction*, J. Rydberg; C. Musikas; G.R. Choppin (Eds.); Marcel Dekker, Inc., New York, USA, 1992, 357-407.
  83. J.D. Navratil; Solvent extraction in nuclear technology. *Pure Appl. Chem.* 58 (6), (1986) 885-888.
  84. H. Singh; C.K. Gupta; Solvent extraction in production and processing of uranium and thorium. *Miner. Process. Extr. Metall. Rev.* 21, (2000) 307-349.
  85. J.H. Miles; Separation of plutonium and uranium; In *Science and technology of tributyl phosphate*, Vol. 3, W.W. Schulz; L.L. Burger; J.D. Navratil; K.P. Bender (Eds.); CRC Press, Florida, USA, 1990, 11-54.

86. A. Ramanujam; An introduction to the PUREX Process, In *Nuclear Fuel Reprocessing*, IANCAS Bulletin, BARC, 14 (2), (1998) 11-20.
87. D.D. Sood; S.K. Patil; Chemistry of nuclear fuel reprocessing: Current status. J. Radioanal. Nucl. Chem. 203 (2), (1996) 547-573.
88. J.L. Swanson; Purex process flowsheets; In *Science and technology of tributyl phosphate*, Vol. 3, W.W. Schulz; L.L. Burger; J.D. Navratil; K.P. Bender (Eds.); CRC Press, Florida, USA, 1990, 55-79.
89. W.D. Bond; The thorex process; In *Science and technology of tributyl phosphate*, Vol. 3, W.W. Schulz; L.L. Burger; J.D. Navratil; K.P. Bender (Eds.); CRC Press, Florida, USA, 1990, 225-247.
90. N. Srinivasan; G.R. Balasubramanian; R.T. Chitnis; S. Venkateswaran; R.T. Kulkarni; Laboratory studies on acid THOREX process, BARC report, BARC-681, 1973.
91. S. Muthuchamy; V.R. Nair; L.N. Maharana; Application of solvent extraction technique for the separation of rare earths, thorium and uranium. Proceedings of the International symposium on solvent extraction, V.N. Misra; S.C. Das; K.S. Rao (Eds.), Sept. 26-27, 2002; 511-523.
92. F. Habashi; Extractive metallurgy of rare earths. Can. Metall. Q. 52 (3), (2013) 224-233.
93. C.K. Gupta, N. Krishnamurthy; Extractive metallurgy of rare earths. Int. Mater. Rev. 37 (5), (1992) 197-248.
94. J.C. Warf; Extraction of cerium(IV) nitrate by butyl phosphate. J. Am. Chem. Soc. 71, (1949) 3257.
95. G.R. Balasubramanian; R.T. Chitnis; A. Ramanujam; M. Venkatesan; Laboratory studies on the recovery of uranium 233 from irradiated thorium by solvent extraction using 5% TBP shell sol-T as solvent. BARC report, BARC-940, 1977.

96. J.H. Cavendish; Recovery and purification of uranium and thorium from ore concentrates; In *Science and technology of tributyl phosphate (Selected technical and industrial use)*, Vol. 2, Part A, W.W. Schulz; J.D. Navratil; T. Bess (Eds.); CRC Press, Florida, USA, 1987, 1-41.
97. G.M. Ritcey; G. Pouskouleli; Nonnuclear hydrometallurgical applications. In *Science and technology of tributyl phosphate (Selected technical and industrial use)*, Vol. 2, Part A, W.W. Schulz; J.D. Navratil; T. Bess (Eds.); CRC Press, Florida, USA, 1987, 65-121.
98. G.M. Ritcey; Use of TBP to separate zirconium from hafnium; In *Science and technology of tributyl phosphate (Selected technical and industrial use)*, Vol. 2, Part A, W.W. Schulz; J.D. Navratil; T. Bess (Eds.); CRC Press, Florida, USA, 1987, 43-64.
99. M. Benedict; T.H. Pigford; H.W. Levi; Nuclear chemical engineering, Second Edn., McGraw-Hill, New York, USA, 1981.
100. L.L. Burger; Physical properties; In *Science and technology of tributyl phosphate (Synthesis, properties, reactions and analysis)*, Vol. 1, W.W. Schulz; J.D. Navratil; A.E. Talbot (Eds.); CRC Press, Inc., Florida, USA, 1984, 25-67.
101. T.G. Srinivasan; P.R. Vasudeva Rao; Red oil excursions: A review. *Sep. Sci. Technol.* 49, (2014) 2315–2329.
102. G.S. Barney; T.D. Cooper; The chemistry of tributyl phosphate at elevated temperature in the plutonium finishing plant process vessels. WHC-EP-0737, Washington, USA, 1994.
103. Y. Hou; E.K. Barefield; D.W. Tedder; S.I. Abdel-Khalik; Thermal decomposition of nitrated tributyl phosphate. Westinghouse Savannah River Company (WSRC) Report, WSRC-RP-95-259, 1995.
104. W. Davis; Radiolytic behavior; In *Science and technology of tributyl phosphate (Synthesis, properties, reactions and analysis)*, Vol. 1, W.W. Schulz; J.D. Navratil; A.E. Talbot (Eds.);

- CRC Press, Inc., Florida, USA, 1984, 221-265.
105. S.C. Tripathi; A. Ramanujam; K.K. Gupta; P. Bindu; Studies on the identification of harmful radiolytic products of 30% TBP-N-Dodecane-HNO<sub>3</sub> by gas-liquid chromatography. II. Formation and characterization of high molecular weight organophosphates. *Sep. Sci. Technology* 36 (13), (2001) 2863-2883.
  106. R.R. Shoun; M.C. Thompson; Chemical properties and reactions; In *Science and technology of tributyl phosphate (Synthesis, properties, reactions and analysis)*, Vol. 1, W.W. Schulz; J.D. Navratil; A.E. Talbot (Eds.); CRC Press, Inc., Florida, USA, 1984, 137-160.
  107. S.C. Tripathi; A. Ramanujam; Effect of radiation-induced physicochemical transformations on density and viscosity of 30% TBP-n-Dodecane-HNO<sub>3</sub> system. *Sep. Sci. Technol.* 38 (10), (2003) 2307-2326.
  108. Z. Kolarik; The formation of a third phase in the extraction of Pu(IV), U(IV) and Th(IV) nitrates with tributyl phosphate in alkane diluents. *Proceedings of the International Solvent Extraction Conference (ISEC-77)*, Toronto, Canada, 1977; B.H. Lucas; G.M. Ritcey; H.W. Smith (Eds.); Vol. 2 (21), *Can. Inst. Mining Metallurgy* 1979, 178-182.
  109. T.G. Srinivasan; M.K. Ahmed; A.M. Shakila; R. Dhamodaran; P.R. Vasudeva Rao; C.K. Mathews; Third phase formation in the extraction of plutonium by tri-*n*-butyl phosphate. *Radiochim. Acta* 40, (1986) 151-154.
  110. A.S. Kertes; The chemistry of the formation and elimination of a third phase in organophosphorous and amine extraction systems; In *Solvent extraction chemistry of metals*, H.A.C. McKay; T.V. Healy; I.L. Jenkins; A. Naylor (Eds.); McMillan, London, England, 1965, 377-400.
  111. P.R. Vasudeva Rao; Z. Kolarik; A review of third phase formation in extraction of actinides by

- neutral organophosphorous extractants. *Solvent Extr. Ion Exch.* 14 (6), (1996) 955-993.
112. P.R. Vasudeva Rao; Fast reactor fuel reprocessing: A challenge for solvent extraction chemist. In *Solvent extraction new perspectives*. IANCAS Bulletin, 10 (2), 1994, 16-19.
113. R. Dhamodaran; T.G. Srinivasan; P.R. Vasudeva Rao; Effect of alcohols on third phase formation in extraction of Th(IV) by tributyl phosphate. Proceedings of Nuclear and Radiochemistry Symposium, Kalpakkam, India, S.G. Kulkarni; S.B. Manohar; D.D. Sood (Eds.), 1995; 126–127.
114. P.R. Vasudeva Rao; R. Dhamodaran; T.G. Srinivasan; C.K. Mathews; The effect of diluent on third phase formation in thorium nitrate - TBP system: Some novel empirical correlations. *Solvent Extr. Ion Exch.* 11 (4), (1993) 645-662.
115. A. Suresh; T.G. Srinivasan; P.R. Vasudeva Rao; Extraction of U(VI), Pu(IV) and Th(IV) by some trialkyl phosphates. *Solvent Extr. Ion Exch.* 12 (4), (1994) 727-744.
116. A. Suresh; T.G. Srinivasan; P.R. Vasudeva Rao; Parameters influencing third-phase formation in the extraction of Th(NO<sub>3</sub>)<sub>4</sub> by some trialkyl phosphates. *Solvent Extr. Ion Exch.* 27, (2009) 132-158.
117. K. Osseo-Asare; Aggregation, reversed micelles and microemulsions in liquid-liquid extraction: The tri-*n*-butyl phosphate-diluent-water-electrolyte system. *Adv. Colloid Interface Sci.* 37, (1991) 123-173.
118. K. Osseo-Asare; Third phase formation in solvent extraction: A microemulsion model; In *Metal Separation Technologies Beyond 2000: Integrating Novel Chemistry with Processing*; K.C. Liddell; D.J. Chaiko (Eds.); The Minerals, Metals and Materials Society, 1999, 339-346.
119. K. Osseo-Asare; Microemulsions and third phase formation. Proceeding of International Solvent Extraction Conference (ISEC-2002), K.C. Sole; P.M. Cole; J.S. Preston; D.J. Robinson

- (Eds.); 118-124.
120. L. Lefrancois; F. Belnet; D. Noel; C. Tondre; An attempt to theoretically predict third-phase formation in the dimethyldibutyltetradecylmalonamide (DMDBTDMA)/dodecane/water/ nitric acid extraction system. *Sep. Sci. Technol.* 34, (1999) 755-770.
  121. R. Chiarizia; M.P. Jensen; M. Borkowski; P. Thiyagarajan; K.C. Littrell; Interpretation of third phase formation in the Th(IV)-HNO<sub>3</sub>, TBP-*n*-octane system with baxter's sticky spheres model. *Solvent Extr. Ion Exch.* 22 (3), (2004) 325-351.
  122. R. Chiarizia; M.P. Jensen; P.G. Rickert; Z. Kolarik; M. Borkowski; P. Thiyagarajan; Extraction of zirconium nitrate by TBP in *n*-octane: Influence of cation type on third phase formation according to the sticky sphere model, *Langmuir* 20 (25), (2004) 10798-10808.
  123. R. Chiarizia; K.L. Nash; M.P. Jensen; P. Thiyagarajan; K.C. Littrell; Application of the Baxter model for hard spheres with surface adhesion to SANS data for the U(VI)-HNO<sub>3</sub>, TBP-*n*-dodecane system. *Langmuir* 19, (2003) 9592-9599.
  124. J. Plaue; A. Gelis; K. Czerwinski; P. Thiyagarajan; R. Chiarizia; Small-angle neutron scattering study of plutonium third phase formation in 30% TBP/HNO<sub>3</sub>/alkane diluent systems. *Solvent Extr. Ion Exch.* 24, (2006) 283-298.
  125. R.J. Ellis; Critical Exponents for Solvent Extraction Resolved Using SAXS. *J. Phys. chem. B* 118, (2014) 315-322.
  126. C. Erlinger; L. Belloni; Th. Zemb; C. Madic; Attractive interactions between reverse aggregates and phase separation in concentrated malonamide extractant solutions. *Langmuir* 15 (7), 1999, 2290-2300.
  127. R.J. Ellis; T.L. Anderson; M.R. Antonio; A. Braatz; M. Nilsson; A SAXS study of aggregation in the synergistic TBP-HDBP solvent extraction system. *J. Phys. chem. B* 117, (2013) 5916-

- 5924.
128. C. Dejugnat; L. Berthon; V. Dubois; Y. Meridiano; S. Dourdain; D. Guillaumont; S. Pellet-Rostaing; T. Zemb; Liquid-liquid extraction of acids and water by a malonamide: I - Anion specific effects on the polar core microstructure of the aggregated malonamide. *Solvent Extr. Ion Exch.* 32, (2014) 601-619.
129. F. Testard; P. Bauduin; Th. Zemb; L. Berthon; Third phase formation in liquid/liquid extraction: A colloidal approach. In *Ion Exchange and Solvent Extraction: A Series of Advances*, Vol. 19, Chap. 7, B.A. Moyer (Ed.); CRC Press, Florida, USA, 2010, 381-428.
130. C. Erlinger; D. Gazeau; T. Zemb; C. Madic; L. Lefrancois; M. Hebrant; C. Tondre; Effect of nitric acid extraction on phase behavior, microstructure and interaction between primary aggregates in the system dimethyldibutyltetradecylmalonamide (DMDBTDMA)/n-Dodecane/Water: A phase analysis and small angle x-ray scattering (SAXS) characterisation study. *Solvent Extr. Ion Exch.* 16, (1998) 707-738.
131. J.R. Ferraro; M. Borkowski; R. Chiarizia; D.R. McAlister; FT-IR spectroscopy of nitric acid in TBP/octane solution. *Solv. Extr. Ion Exch.* 19 (6), (2001) 981-992.
132. Y. Meridiano; L. Berthon; X. Crozes; C. Sorel; P. Dannus; M. R. Antonio; R. Chiarizia; T. Zemb; Aggregation in organic solutions of malonamides: Consequences for water extraction; *Solvent Extr. Ion Exch.* 27, (2009) 607-637.
133. T.L. Anderson; A. Braatz; R.J. Ellis; M.R. Antonio; M. Nilsson; Synergistic extraction of dysprosium and aggregate formation in solvent extraction systems combining TBP and HDBP. *Solvent Extr. Ion Exch.* 31, (2013) 617-633.
134. P.K. Verma; P.N. Pathak; P.K. Mohapatra; V.K. Aswal; B. Sadhu; M. Sundararajan; An insight into third-phase formation during the extraction of thorium nitrate: Evidence for

- aggregate formation from small-angle neutron scattering and validation by computational studies. *J. Phys. Chem. B* 117, (2013) 9821-9828.
135. J. Jiang; W. Li; H. Gao; J. Wu; Extraction of inorganic acids with neutral phosphorus extractants based on a reverse micelle/microemulsion mechanism. *J. Colloid Interface Sci.* 268, (2003) 208-214.
136. P.K. Verma; P.N. Pathak; T. Jayasekharan; R.K. Vatsa; P.K. Mohapatra; Characterization of the species formed during the extraction of thorium employing tri-*n*-butyl phosphate and *N,N*-dihexyl octanamide as extractants by laser desorption/ionization time-of-flight mass spectrometry. *Eur. J. Mass Spectrom.* 19, (2013) 275-283.
137. L. Berthon; L. Martinet; F. Testard; C. Madic; Th. Zemb; Solvent penetration and sterical stabilization of reverse aggregates based on the DIAMEX process extracting molecules: Consequences for the third phase formation. *Solvent Extr. Ion Exch.* 25, (2007) 545-576.
138. L. Lefrancois; J. Delpuech; M. Hebrant; J. Chrisment; C. Tondre; Aggregation and protonation phenomena in third phase formation: An NMR study of the quaternary malonamide/dodecane/nitric acid/water system. *J. Phys. Chem. B* 105, (2001) 2551-2564.
139. M. Borkowski; R. Chiarizia; M.P. Jensen; J.R. Ferraro; P. Thiyagarajan; K.C. Littrell; SANS study of third phase formation in the Th(IV)-HNO<sub>3</sub>/TBP-*n*-octane system. *Sep. Sci. Technol.* 38, (2003) 3333-3351.
140. P.K. Verma; N. Kumari; P.N. Pathak; B. Sadhu; M. Sundararajan; V.K. Aswal; P.K. Mohapatra; Investigations on preferential Pu(IV) extraction over U(VI) by *N,N*-Dihexyloctanamide versus tri-*n*-butyl phosphate: Evidence through small angle neutron scattering and DFT studies. *J. Phys. Chem A* 118, (2014) 3996-4004.
141. R. Chiarizia; M.P. Jensen; M. Borkowski; J.R. Ferraro; P.C. Thiyagarajan; K.C. Littrell; Third

- phase formation revisited: The U(VI), HNO<sub>3</sub>-TBP, *n*-dodecane system. *Solvent Extr. Ion Exch.* 21 (1), (2003) 1-27.
142. R.J. Baxter; Percus-Yevick equation for hard spheres with surface adhesion. *J. Chem. Phys.* 49, (1968) 2770-2774.
143. T.H. Siddall; The effects of altering the alkyl substituents in trialkyl phosphates on the extraction of actinides. *J. Inorg. Nucl. Chem.* 13, (1960) 151-155.
144. T.H. Siddall; Trialkyl phosphates and dialkyl alkylphosphonates in uranium and thorium extraction. *Ind. Eng. Chem.* 51 (1), (1959) 41-44.
145. L.L. Burger; Uranium and plutonium extraction by organophosphorus compounds. *J. Phys. Chem.* 62, (1958) 590-593.
146. L.L. Burger; The neutral organophosphorus compounds as extractants. *Nucl. Sci. Eng.* 16, (1963) 428-439.
147. T.V. Healy; J. Kennedy; The extraction of nitrates by phosphorylated reagents-I. *J. Inorg. Nucl. Chem.* 10, (1959) 128-136.
148. T.V. Healy; J. Kennedy; The extraction of nitrates by phosphorylated reagents-II. *J. Inorg. Nucl. Chem.* 10, (1959) 137-147.
149. C.V.S.B. Rao; A. Suresh; T.G. Srinivasan; P.R. Vasudeva Rao; Tricyclohexylphosphate - A Unique Member in the Neutral Organophosphate Family. *Solvent Extr. Ion Exch.* 21 (2), (2003) 221-238.
150. C. Musikas; Potentiality of non organophosphorus extractants in chemical separations of actinides. *Sep. Sci. Technol.* 23 (12-13), (1988) 1211-1226.
151. G.M. Gasparini; G. Grossi; Long chain disubstituted aliphatic amides as extracting agents in industrial applications of solvent extraction. *Solvent Extr. Ion Exch.* 4 (6), (1986) 1233-1271.

152. P.N. Pathak; L.B. Kumbare; V.K. Manchanda; Structural effects in N,N-Dialkyl amides on their extraction behaviour toward uranium and thorium. *Solvent Extr. Ion. Exch.* 19 (1), (2001) 105-126.
153. R.K. Jha; K.K. Gupta; P.G. Kulkarni; P.B. Gurba; P. Janardan; R.D. Changarani; P.K. Dey; P.N. Pathak; V.K. Manchanda; Third phase formation studies in the extraction of Th(IV) and U(VI) by N,N-dialkyl aliphatic amides. *Desalination* 232, (2008) 225-233.
154. V.K. Manchanda; P.B. Ruikar; S. Sriram; M.S. Nagar; P.N. Pathak; Distribution behavior of U(VI), Pu(IV), Am(III), and Zr(IV) with N,N-Dihexyl octanamide under uranium loading conditions. *Nucl. Technol.* 134, (2001) 231-240.
155. A. Suresh; T.G. Srinivasan; P.R. Vasudeva Rao; The effect of the structure of trialkyl phosphates on their physicochemical properties and extraction behavior. *Solvent Extr. Ion Exch.*, 27, (2009) 258-294.
156. P.R. Vasudeva Rao; Extraction of actinides by trialkyl phosphates. *Miner. Process. Extr. Metall. Rev.* 18 (3-4), (1998) 309-331.
157. F.C. Whitmore; J.H. Olewine; The separation of primary active amyl alcohol from fusel oil by distillation. *J. Am. Chem. Soc.* 60 (11), (1938) 2569-2570.
158. A.D. Webb; J.L. Ingraham; Fusel oil. In *Advances in Applied Microbiology*, Vol. 5, W.W. Umbreit (Ed.); Academic Press, London, England, 1963, 317-354.
159. G.V. Kostikova; N.A. Danilov; Y.S. Krylov; G.V. Korpusov; E.V. Salnikova; Extraction of scandium from various media with triisoamyl phosphate: 1. Extraction of Sc and impurity metals from aqueous nitric acid solutions. *Radiochemistry* 47 (2), (2005) 181-185.
160. G.V. Kostikova; N.A. Danilov; Y.S. Krylov; G.V. Korpusov; E.V. Salnikova; Extraction of Sc from various media with triisoamyl phosphate: 2. Extraction of Sc from aqueous perchloric and

- hydrochloric acid solutions. *Radiochemistry* 48 (2), (2006) 181-185.
161. R. Prasanna; A. Suresh; T.G. Srinivasan; P.R. Vasudeva Rao; Extraction of nitric acid by some trialkyl phosphates. *J. Radioanal. Nucl. Chem.* 222 (1-2), (1997) 231-234.
162. S.H. Hasan; J.P. Shukla; Tri-iso-amyl phosphate (TAP): An alternative extractant to tri-butyl phosphate (TBP) for reactor fuel reprocessing. *J. Radioanal. Nucl. Chem.* 258 (3), (2003) 563-573.
163. T.K. Sahoo; T.G. Srinivasan; Effect of temperature on the extraction of uranium by TiAP/*n*-dodecane. *Desalination Water Treat.* 12 (1-3), (2009) 40-44.
164. T.K. Sahoo; K. Chandran; P. Muralidaran; V. Ganesan; T.G. Srinivasan; Calorimetric studies on thermal decomposition of tri-iso-amyl phosphate–nitric acid systems. *Thermochim. Acta* 534, (2012) 9-16.
165. T.K. Sahoo; T.G. Srinivasan; P.R. Vasudeva Rao; Note: Effect of Temperature in the Extraction of Uranium and Plutonium by Triisoamyl Phosphate. *Solvent Extr. Ion Exch.* 29, (2011) 260-269.
166. F. Kong; J. Liao; S. Ding; Y. Yang; H. Huang; J. Yang; J. Tang; N. Liu; Extraction and thermodynamic behavior of U(VI) and Th(IV) from nitric acid solution with tri-isoamyl phosphate. *J. Radioanal. Nucl. Chem.* 298, (2013) 651-656.
167. T.G. Srinivasan; P.R. Vasudeva Rao; D.D. Sood; Diluent and extractant effects on the enthalpy of extraction of uranium(VI) and americium(III) nitrates by trialkyl phosphates. *Solvent Extr. Ion Exch.* 16 (6), (1998) 1369-1387.
168. B. Das; S. Kumar; P. Mondal; U.K. Mudali; R. Natarajan; Synthesis and characterization of red-oil from tri-iso-amyl phosphate/*n*-dodecane/nitric acid mixtures at elevated temperature. *J. Radioanal. Nucl. Chem.* 292, (2012) 1161-1171.

169. M. Balamurugan; S. Kumar; U.K. Mudali; R. Natarajan; Measurement of dispersion numbers for 36 and 100% tri-isoamyl phosphate solvents equilibrated with aqueous nitric acid solutions. *J. Radioanal. Nucl. Chem.* 289, (2011) 507-510.
170. M.L. Singh; S.C. Tripathi; M. Lokhande; P.M. Gandhi ; V.G. Gaikar; Density, viscosity, and interfacial tension of binary mixture of tri-iso-amyl phosphate (TiAP) and n-dodecane: Effect of compositions and gamma absorbed doses. *J. Chem. Eng. Data* 59, (2014) 1130-1139.
171. M. Muthukumar; S. Kumar; P. K. Sinha; U.K. Mudali; R. Natarajan; Estimation of PVT properties and vapour pressure of alternate PUREX/UREX extractant tri-*iso*-amyl phosphate. *J. Radioanal. Nucl. Chem.* 288 (3), (2011) 819-821.
172. B. Sreenivasulu; A. Suresh; N. Sivaraman; P.R. Vasudeva Rao; Solvent extraction studies with some fission product elements from nitric acid media employing tri-*iso*-amyl phosphate and tri-*n*-butyl phosphate as extractants. *J. Radioanal. Nucl. Chem.* 303, (2015) 2165-2172.
173. J.P. Shukla; M.M. Gautam; C.S. Kedari; S.H. Hasan; D.C. Rupainwar; Extraction of uranium(VI), plutonium(IV) and some fission products by tri-iso-amyl phosphate. *J. Radioanal. Nucl. Chem.* 219 (1), (1997) 61-67.
174. A.S. Nikiforov; B. Zakharin; V. Renard; A.M. Rozen; Y. Smetanin; Reprocessing of high burn-up (100 GWd/t) short cooled fuel. Proceedings of International Conference, Actinides-89, Tashkent, USSR, Sept. 24-29, 1989; 20-21.
175. B. Sreenivasulu; A. Suresh; S. Subramaniam; K.N. Sabharwal; N. Sivaraman; K. Nagarajan; T.G. Srinivasan; P.R. Vasudeva Rao; Separation of U(VI) and Pu(IV) from Am(III) and trivalent lanthanides with tri-iso-amyl phosphate (TiAP) as the extractant by using an ejector mixer-settler. *Solvent Extr. Ion Exch.* 33, (2015) 120-133.
176. A. Suresh; B. Sreenivasulu; S. Jayalakshmi; S. Subramaniam; K.N. Sabharwal; N. Sivaraman;

- K. Nagarajan; T.G. Srinivasan; P.R. Vasudeva Rao; Mixer-settler runs for the evaluation of tri-*iso*-amyl phosphate (TiAP) as an alternate extractant to tri-*n*-butyl phosphate (TBP) for reprocessing applications. *Radiochim. Acta* 103 (2), (2015) 101-108.
177. V.K. Aswal; P.S. Goyal (2000) Small-angle neutron scattering diffractometer at Dhruva reactor. *Curr. Sci.* 79, (2000) 947-953.
178. K.L. Cheng; Analytical applications of xylenol orange-III: Spectrophotometric study on the hafnium-xylenol orange complex. *Talanta* 3, (1959) 81-90.
179. A.K. Gupta, J.E. Powell. Successive determination of thorium and rare earths by complexometric titrations. *Talanta* 11, (1964) 1339-1342.
180. P.C. Mayankutty; S. Ravi; M.N. Nadkarni; Determination of free acidity in uranyl nitrate solutions. *J. Radioanal. Chem.* 68 (1-2), (1982), 145-150.
181. A. Suresh; D.K. Patre; T.G. Srinivasan; P.R. Vasudeva Rao; A new procedure for the spectrophotometric determination of uranium(VI) in the presence of a large excess of throrium(IV). *Spectrochim. Acta, Part A* 58, (2002) 341-347.
182. K.L. Cheng; Analytical applications of xylenol orange-I: Determination of traces of zirconium. *Talanta* 2, (1959) 61-66.
183. E. Scholz; Karl Fischer titration - Determination of water, *Chemical laboratory practice*, Springer-Verlag, Berlin, Germany, 1984.
184. J. Plaue; A. Gelis ; K. Czerwinski; Plutonium third phase formation in the 30% TBP/Nitric acid/Hydrogenated polypropylene tetramer system. *Solvent Extr. Ion Exch.* 24, (2006) 271-282.
185. G. Petrich; Z. Kolarik; Distribution of U(VI), Pu(IV) and nitric acid in the system uranyl nitrate - plutonium (IV) nitrate - nitric acid - water/30% TBP in aliphatic diluents: A compilation and

- critical evaluation of equilibrium Data. Kernforschungszentrum Karlsruhe (KfK) report, KfK-2536, 1977.
186. G. Petrich; Z. Kolarik; The 1981 purex distribution data index. KfK-3080, 1981.
187. D.J. Pruett; Extraction chemistry of fission products; In *Science and technology of tributyl phosphate*, Vol. 3, W.W. Schulz; L.L. Burger; J.D. Navratil; K.P. Bender (Eds.); CRC Press, Florida, USA, 1990, 81-121.
188. T.G. Srinivasan; A. Suresh; R. Prasanna; N. Jayanthi; P.R. Vasudeva Rao; Metal-solvate stoichiometry evaluation in extractions by solvating type neutral extractants - A novel approach. *Solvent Extr. Ion Exch.* 14 (3), (1996) 443-458.
189. T.V. Healy; H.A.C. McKay; N. Hackerman; N.H. Simpson; The extraction of nitrates by tri-*n*-butyl phosphate (TBP) Part 2 - The nature of the TBP phase. *Trans. Faraday Soc.* 52, (1956) 633-642.
190. S. Mallick; A. Suresh; T.G. Srinivasan; P.R. Vasudeva Rao; Comparative studies on third-phase formation in the extraction of thorium nitrate by tri-*n*-butyl phosphate and tri-*n*-amyl phosphate in straight chain alkane diluents. *Solvent Extr. Ion Exch.* 28 (4), (2010) 459-481.
191. Y. Sze; D.P. Archambault; Studies of thorium nitrate complexation in aqueous solutions by a liquid-liquid extraction method - Application to the calculation of thorium distribution in the thorex processes. *Solvent Extr. Ion Exch.* 3 (6), (1985) 785-805.
192. M. Borkowski; New approach for third phase investigation in solvent extraction system. *Ars Separatoria Acta*, 6, (2008) 31-40.
193. B. Sreenivasulu; A. Suresh; N. Sivaraman; P.R. Vasudeva Rao; Co-extraction and co-stripping of U(VI) and Pu(IV) using tri-iso-amyl phosphate and tri-*n*-butyl phosphate in *n*-dodecane from nitric acid media under high loading conditions. *Radiochim. Acta* 104 (4), (2016) 227-

- 237.
194. W. David; J.D. Navratil; A. Zaszity; Z. Horvath; The analytical methods. In *Science and technology of tributyl phosphate (Synthesis, properties, reactions and analysis)*, Vol. 1, W.W. Schulz; J.D. Navratil; A.E. Talbot (Eds.); CRC Press, Inc., Florida, USA, 1984, 267-327.
195. M.M. Villalba; K.J. McKeegan; D.H. Vaughan; M.F. Cardosi; J. Davis; Bioelectroanalytical determination of phosphate: A review. *J. Mol. Catal. B: Enzym.* 59, (2009) 1-8.
196. C. Rivasseau; L. Lando; F. Rey-Gaurez; I. Bisel; D. Sans; M. Faucon; J.M. Adnet; Direct determination of phosphate esters in concentrated nitrate media by capillary zone electrophoresis. *J. Chromatogr. A* 1015, (2003) 219-231.
197. P.B. Ruikar; M.S. Nagar; M.S. Subramanian; Quantitative analysis of some extractants by infrared spectrometry. *J. Radioanal. Nucl. Chem. Lett.* 155 (6), (1991) 371-376.
198. M.A. Ali; A.M. Al-ani; Gas chromatographic determination of tributyl phosphate, dibutyl phosphate and butyl phosphate in kerosene solutions. *Analyst* 116, (1991) 1067-1069.
199. G. Becker; A. Colmsjo; C. Ostman; Elemental composition determination of organophosphorus compounds using gas chromatography and atomic emission spectrometric detection. *Anal. Chim. Acta* 340, (1997) 181-189.
200. M. Shoji; T. Toshiaki; T. Kyoji. Spectrophotometric determination of phosphate in river waters with molybdate and malachite green. *Analyst* 108, (1983) 361-367.
201. A.W. Ashbrook; On the role of analytical chemistry in solvent extraction processing. *Talanta* 22, (1975) 327-343.
202. E.A. Costner; B.K. Long; C. Navar; S. Jockusch; X. Lei; P. Zimmerman; A. Campion; N.J. Turro; C.G. Willson; Fundamental optical properties of linear and cyclic alkanes: VUV

- absorbance and index of refraction. *J. Phys. Chem. A* 113, (2009) 9337-9347.
203. T.M. Aminabhavi; V.B. Patil; M.I. Aralaguppi; H.T.S. Phayde; Density, viscosity, and refractive index of the binary mixtures of cyclohexane with hexane, heptane, octane, nonane and decane at (298.15, 303.15, and 308.15) K. *J. Chem. Eng. Data* 41, (1996) 521-525.
204. M.N. Hossain; M.M.H. Rocky; S. Akhtar; Density, refractive index, and sound velocity for the binary mixtures of tri-*n*-butyl phosphate and *n*-butanol between 303.15 K and 323.15 K. *J. Chem. Eng. Data* (DOI: 10.1021/acs.jced.5b00343).
205. S.C. Bhatia; N. Tripathi; G.P. Dubey; Refractive indices of binary liquid mixtures of (decane + benzene) and (hexadecane + benzene, or + hexane) at 303.15, 308.15 and 313.15 K. *Indian J. Chem.* 41A, (2002) 266-269.
206. Q. Tian; H. Liu; Densities and viscosities of binary mixtures of tributyl phosphate with hexane and dodecane from (298.15 to 328.15) K. *J. Chem. Eng. Data* 52, (2007) 892-897.
207. A.J. Queimada; S.E. Quinones-Cisneros; I.M. Marrucho; J.A.P. Coutinho E.H. Stenby; Viscosity and liquid density of asymmetric hydrocarbon mixtures. *Int. J. Thermophys.* 24 (5), (2003) 1221-1239.
208. T. Unak; What is the potential use of thorium in the future energy production technology? *Prog. Nucl. Energy* 37 (1-4), (2000) 137-144.
209. C.K. Gupta; H. Singh; Uranium from minor secondary resources, Springer-Verlag, Berlin, Germany, 2003.
210. T.K. Mukherjee, Processing of Indian monazite for the recovery of thorium and uranium values; In *Characterization and quality control of nuclear fuels*, C. Ganguly; R.N. Jayaraj (Eds.); Allied publishers pvt. ltd., New Delhi, India, 187-195.
211. J. Barghusen Jr; M. Smutz; Processing of monazite sands, *Ind. Eng. Chem.* 50 (12), (1958)

1754-1755.

212. R. Pribil, Present state of complexometry-IV - Determination of rare earths. *Talanta* 14, (1967)

619-627.

213. L.A. Feigin; D.I. Svergun; Structure analysis by small-angle x-ray and neutron scattering.

G.W. Taylor (Ed.), Springer, New York, USA, 1987.